LUND UNIVERSITY

Peripheral Nerve Regeneration after Injury, Repair and Reconstruction in Experimental Diabetes

Stenberg, Lena

2018

Document Version:
Publisher's PDF, also known as Version of record

Link to publication

Citation for published version (APA):
Stenberg, L. (2018). *Peripheral Nerve Regeneration after Injury, Repair and Reconstruction in Experimental Diabetes*. [Doctoral Thesis (compilation), Department of Translational Medicine]. Lund University: Faculty of Medicine.

Total number of authors:
1

General rights
Unless other specific re-use rights are stated the following general rights apply:
Copyright and moral rights for the publications made accessible in the public portal are retained by the authors and/or other copyright owners and it is a condition of accessing publications that users recognise and abide by the legal requirements associated with these rights.
• Users may download and print one copy of any publication from the public portal for the purpose of private study or research.
• You may not further distribute the material or use it for any profit-making activity or commercial gain
• You may freely distribute the URL identifying the publication in the public portal

Read more about Creative commons licenses: https://creativecommons.org/licenses/

Take down policy
If you believe that this document breaches copyright please contact us providing details, and we will remove access to the work immediately and investigate your claim.

LUND UNIVERSITY

PO Box 117
221 00 Lund
+46 46-222 00 00

Peripheral Nerve Regeneration after Injury, Repair and Reconstruction in Experimental Diabetes

Peripheral Nerve Regeneration after Injury, Repair and Reconstruction in Experimental Diabetes

Lena Stenberg

LUND
UNIVERSITY

DOCTORAL DISSERTATION

By permission of the Faculty of Medicine, Lund University, Sweden.
To be defended at 13.00 on April 3rd, 2018 in Lilla Aulan, Medicinskt Forskningscentrum, Skåne University Hospital, Malmö, Sweden

Faculty opponent
Associate Professor Lev N. Novikov
Department of Integrative Medical Biology,
Umeå University, Umeå, Sweden.

Organization
LUND UNIVERSITY

Department of Translational Medicine, Hand Surgery, Malmö, Sweden

Author Lena Stenberg

Document name
DOCTORAL DISSERTATION

Date of issue
2018-04-03

Sponsoring organization
Lund University

Title and subtitle

Peripheral Nerve Regeneration after Nerve Injury, Repair and Reconstruction in Experimental Diabetes

Abstract

Peripheral nerve injury and disease represent a global problem and affect both men and women at different ages. Trauma is not the sole cause of nerve injury; the problems that arise can sometimes also be due to, or exacerbated by, a disease, such as diabetes. The outcome after surgery for traumatic nerve injuries still varies widely, despite the use of modern repair and reconstruction techniques. Improved knowledge concerning nerve regeneration mechanisms is crucial for the development of new surgical strategies. In this respect, I believe that the influence of gender and diabetes should also be considered.

The aim of the current thesis was to investigate nerve regeneration in rats after a sciatic nerve injury and subsequent direct repair or reconstruction. The injured nerves were reconstructed, and regeneration was compared after bridging the nerve defects with either autologous nerve grafts or novel chitosan nerve conduits, with different acetylation degrees, in short- and long-term experiments. Nerve regeneration was also compared between healthy and diabetic rats of both genders using two different diabetic models - BioBreeding (BB, resembling type 1 diabetes) and Goto-Kakizaki (GK, resembling type 2 diabetes).

The BB and healthy rats did not differ regarding short-term axonal outgrowth, although activated and apoptotic Schwann cells were more numerous in the former. Differences were found after direct nerve repair in the short-term nerve regeneration process, with improved axonal outgrowth in males compared to females and in healthy compared to diabetic GK rats. A regenerative matrix, correlating to axonal outgrowth, was formed in chitosan conduits with successful short- and long-term nerve regeneration across a 10 mm long nerve defect. We also established that medium acetylation of chitosan was optimal in conduits for nerve reconstruction. Short–term nerve regeneration was, however, better in autologous nerve grafts than in chitosan conduits. I also found that short-term nerve regeneration was improved in the diabetic GK rats compared to the healthy rats, both when using autologous nerve grafts and chitosan conduits to bridge a 10 mm long nerve defect. Both short- and long-term nerve regeneration and functional recovery were improved after reconstruction of 15 mm long nerve defects with enhanced (membrane inserted) chitosan conduits. This result was obtained in both healthy and GK rats, particularly for those conduits which were equipped with inserted perforated membranes, where axonal outgrowth reached almost the same levels as for autologous nerve grafts.

The present thesis reveals differences in nerve regeneration after nerve repair and reconstruction in healthy and diabetic male and female rats; results which are relevant when developing new treatment strategies after nerve injury. Using novel chitosan conduits resulted in nerve regeneration and functional recovery after reconstruction of nerve defects in both healthy and diabetic rats.

Key words: Nerve injury, Nerve regeneration, Diabetes, Nerve repair, Nerve reconstruction, Schwann cells, Axons

Classification system and/or index terms (if any)

Supplementary bibliographical information
Lund University, Faculty of Medicine Doctoral Dissertation Series 2018:30

Language
English

ISSN and key title 1652-8220

ISBN 978-91-7619-597-0

Recipient's notes

Number of pages 84

Price

Security classification

I, the undersigned, being the copyright owner of the abstract of the above-mentioned dissertation, hereby grant to all reference sources permission to publish and disseminate the abstract of the above-mentioned dissertation.

Signature

Date 2018-02-21

Peripheral Nerve Regeneration after Injury, Repair and Reconstruction in Experimental Diabetes

Lena Stenberg

Faculty of Medicine

Department of Translational Medicine, Hand Surgery, Lund University, Malmö, Sweden

Front cover image taken by Lena Stenberg: *Cultured Schwann cells*.

Copyright Lena Stenberg

Department of Translational Medicine

Lund University, Faculty of Medicine
Doctoral Dissertation 2018:30

ISBN 978-91-7619-597-0
ISSN 1652-8220

Printed in Sweden by Media-Tryck, Lund University
Lund 2018

MADE IN SWEDEN

Media-Tryck is an environmentally certified and ISO 14001 certified provider of printed material. Read more about our environmental work at www.mediatryck.lu.se

To Isabelle and Filip

Table of Contents

Abstract 11
List of papers 13
Abbreviations 15
Thesis at a glance 17
Introduction 21
Background 23
The central and peripheral nervous systems and the neurons 23
The peripheral nerve 23
Peripheral nerve injury and regeneration 24
Signal transduction, factors and nerve regeneration 26
Peripheral nerve repair and reconstruction 27
Nerve sutures and nerve grafts 27
Nerve conduits 29
Chitosan conduits 29
Diabetes and peripheral nerves 30
Diabetic animal models 31
Aims 33
Methods and surgery 35
Surgery 35
Chitosan conduits 37
Immunohistochemistry and histological methods 39
Immunohistochemistry 39
Histo-morphometry 39
Functional evaluation 41
Static sciatic index 41
von Frey test 42
Electrophysiology 42
Muscle weight ratio 42
Chitosan material evaluation 43
Nuclear magnetic resonance spectroscopy (NMR) 43
Gel permeation chromatograph (GPC) 43
In vitro cytotoxicity test 43
Molecular and biochemical evaluation 43

Quantitative RT-PCR 43
Western Blot 44
In vitro study - cell culture 44
Macroscopic investigation 44
Visual investigation 44
Image analysis 44
Statistical analyses 45
Results 47
Paper I 47
Paper II 48
Paper III 49
Paper IV 51
Paper V 51
Discussion 55
Diabetes and gender affect nerve regeneration 56
Reconstruction of the injured sciatic nerve using chitosan conduits 59
Selection of chitosan conduits 59
Functional recovery after reconstruction using chitosan conduits 62
Nerve regeneration in chitosan conduits and autologous nerve grafts .63
Nerve regeneration and influence of diabetes after nerve reconstruction 63
Modification of the chitosan conduits and addition of Schwann cells .64
Conclusions 67
Sammanfattning/Summary in Swedish 69
Acknowledgements 71
References 73

Abstract

Peripheral nerve injury and disease represent a global problem and affect both men and women at different ages. Trauma is not the sole cause of nerve injury; the problems that arise can sometimes also be due to, or exacerbated by, a disease, such as diabetes. The outcome after surgery for traumatic nerve injuries still varies widely, despite the use of modern repair and reconstruction techniques. Improved knowledge concerning nerve regeneration mechanisms is crucial for the development of new surgical strategies. In this respect, I believe that the influence of gender and diabetes should also be considered.

The aim of the current thesis was to investigate nerve regeneration in rats after a sciatic nerve injury and subsequent direct repair or reconstruction. The injured nerves were reconstructed, and regeneration was compared after bridging the nerve defects with either autologous nerve grafts or novel chitosan nerve conduits, with different acetylation degrees, in short- and long-term experiments. Nerve regeneration was also compared between healthy and diabetic rats of both genders using two different diabetic models - BioBreeding (BB, resembling type 1 diabetes) and Goto-Kakizaki (GK, resembling type 2 diabetes).

The BB and healthy rats did not differ regarding short-term axonal outgrowth, although activated and apoptotic Schwann cells were more numerous in the former. Differences were found after direct nerve repair in the short-term nerve regeneration process, with improved axonal outgrowth in males compared to females and in healthy compared to diabetic GK rats. A regenerative matrix, correlating to axonal outgrowth, was formed in chitosan conduits with successful short- and long-term nerve regeneration across a 10 mm long nerve defect. We also established that medium acetylation of chitosan was optimal in conduits for nerve reconstruction. Short–term nerve regeneration was, however, better in autologous nerve grafts than in chitosan conduits. I also found that short-term nerve regeneration was improved in the diabetic GK rats compared to the healthy rats, both when using autologous nerve grafts and chitosan conduits to bridge a 10 mm long nerve defect. Both short- and long-term nerve regeneration and functional recovery were improved after reconstruction of 15 mm long nerve defects with enhanced (membrane inserted) chitosan conduits. This result was obtained in both healthy and GK rats, particularly for those conduits which were equipped with inserted perforated membranes, where axonal outgrowth reached almost the same levels as for autologous nerve grafts.

The present thesis reveals differences in nerve regeneration after nerve repair and reconstruction in healthy and diabetic male and female rats; results which are relevant when developing new treatment strategies after nerve injury. Using novel chitosan conduits resulted in nerve regeneration and functional recovery after reconstruction of nerve defects in both healthy and diabetic rats.

List of papers

This thesis is based on the following papers, which will be referred to in the text by their Roman numerals:

Paper I: **Expression of Activating Transcription Factor-3 (ATF-3) and caspase-3 in Schwann cells and axonal outgrowth after sciatic nerve repair in diabetic BB-rats.** Stenberg L, Kanje M, Dolezal K, Dahlin LB. Neurosci Lett. 2012, 25;515(1): 34-8.

Paper II: **Gender differences in nerve regeneration after sciatic nerve injury and repair in healthy and in type 2 diabetic Goto-Kakizaki rats.** Stenberg L, Dahlin LB. BMC Neurosci. 2014, 13;15:107.

Paper III: **Chitosan tubes of varying degrees of acetylation for bridging peripheral nerve defects.** Haastert-Talini K, Geuna S, Dahlin LB, Meyer C, Stenberg L, Freier T, Heimann C, Barwig C, Pinto LF, Raimondo S, Gambarotta G, Samy SR, Sousa N, Salgado AJ, Ratzka A, Wrobel S, Grothe C. Biomaterials. 2013, 34(38):9886-904.

Paper IV: **Nerve regeneration in chitosan conduit and in autologous nerve grafts in healthy and diabetic Goto-Kakizaki rats.** Stenberg L, Kodama A, Lindwall-Blom C, Dahlin LB. Eur J Neurosci. 2016, 43(3): 463-73.

Paper V: **Chitosan- film enhanced chitosan nerve guides for long-distance regeneration of peripheral nerves.** Meyer C, Stenberg L, Gonzales-Perez F, Wrobel S, Ronchini G, Udina E, Suganuma S, Geuna S, Navarro X, Dahlin LB, Heimann C, Grothe C, Haastert-Talini K. Biomaterials. 2016, 76:33-51.

Permission to reprint the published articles has been granted by the publishers.

Abbreviations

ATF-3	Activating transcription factor 3
ANG	Autologous nerve graft
ANOVA	Analysis of variance
BB rats	Biobreeding rats
BDNF	Brain-derived neurotrophic factor
BSA	Bovine serum albumin
Chat	Choline acetyltransferase
CMAP	Compound muscle action potential
CNS	Central nervous system
CREB	cAMP response element binding protein
DA	Degree of acetylation
DAPI	4',6 -diamidino-2-phenylindole
DRG	Dorsal root ganglia
ERK	Extracellular signal-regulated kinas
FGF-2	Fibroblast growth factor-2
GA	Gastrocnemius muscle
GAP-43	Growth associated protein-43
GDNF	Glial cell–derived neurotrophic factor
GK rats	Goto-Kakizaki rats
GPC	Gel permeation chromatograph
HA	Hyaluronic acid
HE	Hematoxylin eosin
HSP27	Heat shock protein 27
IGF	Insulin-like growth factor
IHC	Immunohistochemistry
JNK	Jun N-terminal kinase
MAPK	Mitogen-activated protein kinase
MCG	Multinucleated giant cell
m-RNA	Messenger ribonucleic acid
NCV	Nerve conduction velocity
NF	Neurofilament
NGF	Nerve growth factor
NeoSC	Neonatal Schwann cell
NMR	Nuclear magnetic resonance spectroscopy
NTF	Neurotrophic factor

NVR	Non-volatile residue
PBS	Phosphate buffer saline
PL	Plantar interosseous muscle
PNI	Peripheral nerve injury
PNS	Peripheral nervous system
qRT-PCR	Quantitative real-time polymerase chain reaction
RBMSC	Rat bone marrow mesenchymal stromal cell
SAPK	Stress activating protein kinase family
SSI	Static sciatic index
STZ	Streptozotocin
TA	Tibialis anterior muscle
TrkB	Tyrosine kinase receptor B

Thesis at a glance

Paper I. Expression of Activating Transcription Factor 3 (ATF-3) and cleaved caspase-3 in Schwann cells and axonal outgrowth after sciatic nerve repair in diabetic BB rats.

Aim: To investigate and compare short-term axonal outgrowth, as well as activated and apoptotic Schwann cells, after sciatic nerve transection and repair in healthy versus diabetic Bio-Breeding BB rats (resembling human type 1 diabetes).

Method: Examination and quantification of neurofilament (NF) length (axonal outgrowth), activated (ATF-3 stained) and apoptotic (cleaved caspase-3 stained) Schwann cells at six days after transection and repair of the sciatic nerve in healthy and BB rats.

Results and conclusion: No significant differences were found between healthy and diabetic rats regarding axonal outgrowth and no correlation was found between axonal outgrowth and activated or apoptotic Schwann cells in either healthy or BB rats. However, compared to healthy rats, the diabetic rat sciatic nerve contained larger numbers of ATF-3 and cleaved caspase-3 stained Schwann cells, both at the lesion site and in the nerve segment distal to the injury site. Thus, the Schwann cell response differs between healthy and BB rats, but axonal outgrowth does not appear to be affected by this or by the diabetic conditions. Nonetheless, the differences in the Schwann cell response to injury stresses the importance of evaluating nerve regeneration after nerve injury in diabetic models, and should be considered in future experiments.

Paper II. Gender differences in nerve regeneration after sciatic nerve injury and repair in healthy and in type 2 diabetic Goto-Kakizaki rats.

Aim: To evaluate and explore gender and disease differences after nerve injury in short-term sciatic nerve regeneration by comparing healthy and genetically developed diabetic GK rats.

Method: Analyses and comparison of axonal outgrowth and number of activated and apoptotic stained Schwann cells after nerve transection followed by immediate repair in healthy and diabetic GK rats of both genders.

Results and conclusion: Longer axonal outgrowth was detected in male compared to female rats in both healthy and diabetic rats. A greater number of activated ATF-3 stained Schwann cells was found at the site of the lesion in the healthy and

diabetic male rats compared to healthy and GK female rats. No gender differences were observed, however, regarding the numbers of apoptotic Schwann cells either at the lesion site or in the distal nerve segment. On the other hand, GK rats had more apoptotic Schwann cells than healthy rats both at the lesion site and in the distal nerve segment. These results emphasise the importance of evaluating and comparing nerve regeneration in both genders after nerve injury in experimental diabetes studies.

Paper III. Chitosan tubes of varying degrees of acetylation for bridging peripheral nerve defects.

Aim: To examine and investigate the material chitin in short- and long-term nerve regeneration using novel hollow chitosan conduits with different degrees of acetylation (DAs) to bridge a 10 mm short nerve defect inflicted on the sciatic nerve of healthy rats.

Method: Various structural and functional tests were used to analyse nerve regeneration within hollow chitosan conduits and in autologous nerve grafts for up to 90 days after repair.

Results and conclusion: A regenerative matrix was formed in all three DA models of chitosan conduits, with no apparent differences between the various degrees of acetylation, when comparing axonal outgrowth or early immunological reactions. Chitosan conduits with a low (DAI) and high (DAIII) degree of acetylation were, however, limited in terms of supporting nerve regeneration. For this reason, the chitosan conduit with a medium degree of acetylation (DAII) was considered the most appropriate conduit for nerve regeneration and was therefore used for all future experiments.

Paper IV. Nerve regeneration in chitosan conduits and in autologous nerve grafts in healthy and in diabetic Goto-Kakizaki rats.

Aim: To evaluate short-term nerve regeneration in hollow chitosan conduits and compare this to regeneration in autologous nerve grafts when bridging a 10 mm long sciatic nerve defect in healthy and diabetic GK rats.

Method: Nerve regeneration was examined at 21 days after reconstruction through analysis of stained neurofilaments, and of activated and apoptotic Schwann cells.

Results and conclusion: In all rats, a matrix had been formed within the conduits at 21 days, although it was thicker in diabetic rats than in the healthy rats. Notably, axonal outgrowth positively correlated with the diameter of the matrix formed in the chitosan conduits both in healthy and GK rats. In addition, the axonal outgrowth was longer in the GK rats than in the healthy rats in both reconstruction techniques used. Short-term nerve regeneration was better in autologous nerve grafts than in the chitosan conduits. These results indicate that autologous nerve

grafts are superior to chitosan conduits when reconstructing a shorter nerve defect. Surprisingly, axonal outgrowth after nerve reconstruction improved in rats with diabetic conditions compared to healthy rats, revealing the presence of a complex process that needs further investigation.

Paper V. Chitosan–film enhanced chitosan nerve guides for long distance regeneration of peripheral nerves.

Aim: To evaluate short- and long-term nerve regeneration after reconstruction of 15 mm long nerve defects with "enhanced" chitosan nerve conduits or autologous nerve grafts in healthy and diabetic GK rats.

Method: Long-term functional and morphological tests were performed after bridging a nerve defect with either hollow chitosan conduits, "enhanced" chitosan nerve conduits (inserts of membrane with or without perforations within the conduits) or with autologous nerve grafts in healthy rats. Immunohistological methods were used to evaluate the short-term regenerative matrix after reconstruction of 15 mm long nerve defects with "enhanced" chitosan nerve conduits in healthy and GK rats.

Results and conclusion: An improvement in morphological and functional nerve regeneration was observed after the injury was repaired with chitosan nerve conduits "enhanced" with an inserted membrane. Notably, both functional and morphological regeneration was further extended in the chitosan nerve conduits with an insertion of perforated membranes as compared to regular chitosan nerve conduits, both in healthy and diabetic rats. Enrichment with FGF-2^{18kDa} overexpressing Schwann cells did not, however, further improve functional nerve regeneration. Morphological analysis of the DRGs on the injury side revealed that sensory neurons expressed ATF-3 and HSP27 in healthy rats, and an even more pronounced expression of both of these molecules was observed in the GK rats. Regarding long-term regeneration, the outcome when chitosan nerve conduits with inserts (perforated membranes) were used for nerve reconstruction reached levels that were almost similar to the outcomes for autologous nerve grafts. Modification of chitosan nerve conduits with membrane inserts improved nerve regeneration in both healthy and diabetic rats after nerve reconstruction in terms of short- and long-term recovery. The implication of this is that "enhanced" chitosan nerve conduits should be considered a good possibility for use in future experiments in nerve reconstruction.

Introduction

Peripheral nerve injuries are common and may affect anyone [1-5] although they are more frequently observed in men than in women [6]. Few experimental studies have examined and compared the nerve regeneration process in male and female subjects in order to elucidate gender differences. Such information could, however, potentially extend our knowledge of the complicated nerve regeneration process. A complete nerve injury, with or without a nerve defect, requires surgical attention with a direct nerve repair using sutures, or a nerve reconstruction using conventional autologous nerve grafts. Whether the nerve is repaired or reconstructed, the outcome is still, generally, unsatisfactory with subsequent residual problems severely affecting the patient and leading to high costs for society [4, 7-11].

If repair and reconstruction procedures after nerve injury are to be improved, understanding the mechanisms behind nerve regeneration is crucial. Our current knowledge stems from experimental studies, where the results, when successful, including the introduction of novel techniques, could be incorporated into clinical settings [7, 12]. The outcome of peripheral nerve injuries and subsequent repair can be followed in randomized clinical trials. However, there are limitations when studying nerve regeneration in patients due, for instance, to insufficient numbers of patients, the effects of concomitant disease, time aspects (i.e. short- and long-term studies), different types of injuries, as well as variations in delay prior to carrying out the nerve reconstruction procedures [11, 13, 14]. In the clinic, the currently preferred method for repairing a severed nerve, when it has been completely transected, is to use sutures, while a nerve defect is best bridged by an autologous nerve graft [15]. However, the lack of graft material and sometimes a need to bridge both shorter and longer nerve defects without a nerve graft, have led to the introduction of alternative methods for reconstructing a nerve injury [16]. Various biological and artificial alternatives for use in reconstructing a nerve gap have been developed and used in clinical practice, but problems have been encountered related to the use of artificial materials [17, 18]. For this reason, chitosan, made of a chitin derivative from shrimp shells, which appear to be more tissue-friendly than other types of materials, may provide a promising alternative in manufacturing conduits [19, 20].

Patients with a concomitant disease, such as type 1 or type 2 diabetes, can also sustain a traumatic nerve injury that requires surgical attention. Both types of

diabetes generally display complications involving the peripheral nervous system [21]. The number of subjects with diabetes is expected to increase globally, due both to an increase in the incidence of type 1 diabetes and to a greater proportion of elderly people with type 2 diabetes. Worldwide, approximately 642 million people may suffer from the disease by 2040, according to the International Diabetes Federation [22]. The mechanisms behind the detrimental effects of diabetes on the peripheral nerves are not known in detail, despite extensive experimental and clinical research over many years. Furthermore, very few studies have evaluated nerve regeneration in experimental diabetes, and in particular very few have included and compared animals of both genders. In addition, most studies performed to examine how diabetes affects the peripheral nerves and their functions have used experimental diabetic models, such as the streptozotocin (STZ)-induced diabetes model, which may not be clinically relevant [23, 24]. Thus, there is a clear need to study traumatic nerve injuries and subsequent nerve repair/reconstruction techniques in experimental diabetic models. Similarly, investigating nerve injury and nerve regeneration processes in other experimental diabetic rat models, such as Biobreeding, BB, rats with high blood glucose levels, or Goto-Kakizaki, GK, rats with moderate blood glucose levels, is needed [24-26]. Furthermore, investigation of specific mechanisms, such as injury-induced cell signalling, which is involved in the nerve regeneration process, is also relevant when novel repair and reconstruction techniques are developed for surgical procedures in both genders [12].

Background

The central and peripheral nervous systems and the neurons

The nervous system comprises the brain and the spinal cord, which belong to the central nervous system (CNS), as well as sensory and motor neurons with their extended processes, axons. The latter are assembled into peripheral nerve trunks, which comprise the peripheral nervous system (PNS). Motor neurons control the function of the muscles in the extremities, whereas sensory neurons convey impulses from various touch, heat, and pain receptors in the periphery to the CNS [27, 28].

The motor neuron cell bodies are located in the ventral horn of the spinal cord while the sensory neuron cell bodies are located just outside the spinal cord in structures called dorsal root ganglia (DRG). The rat DRG comprise the cell bodies of different sized neurons that extend axons of specific diameters. In this thesis, we used the 3rd (L3), 4th (L4) and the 5th (L5) lumbar DRG, which all have axons that run through the sciatic nerve. In addition to sensory neurons, two types of glial cells, the Schwann cells and satellite cells, exist both in the DRG and in the sciatic nerve.

Structural components are transported from the neuronal cell body along the axons to specific targets by anterograde axonal transport. Transport in the opposite direction, retrograde transport, provides the nerve cell body with important information from the periphery [27].

The peripheral nerve

The axons of the peripheral nerves are insulated by a myelin sheath, formed by Schwann cells, which wrap themselves around, and are positioned continuously, along the length of the axon. A peripheral nerve, such as the rat sciatic nerve, comprises both myelinated and unmyelinated axons. Axons are classified according to their size/diameter into three different groups - A, B and C fibres, where the conduction velocity depends on the diameter of the axon and the degree

of myelination. The unmyelinated nerve fibres (small diameter C fibres) are thinner than the large myelinated (A fibres) and the medium myelinated (B fibres) nerve fibres. Thus, the large A fibres have the fastest conduction velocity, whereas the smallest C fibres display the slowest conduction velocity [27]. Uncovered axon segments, minute separations between Schwann cells, called nodes of Ranvier, contain ion channels which contribute to the high velocity of nerve impulses. The Schwann cells, however, are not only insulators but also important communicators, particularly after nerve injury and during regeneration. Interactions between the Schwann cells and the neurons are complex and several cell-signalling systems are involved [12, 27, 28].

Several bundles of axons, together with the protective layer around each bundle, i.e. the perineurium, are termed fascicles. The outermost, loose connective tissue layer, in which several bundles of fascicles are embedded, is called the epineurium. The term endoneurium refers to connective tissue components located inside the fascicles [27, 29]. The space between the nerve fibres within the fascicles holds an extracellular matrix (ECM), which contains components involved in cell differentiation, cell migration and cell proliferation, and which also plays an important role in intracellular communication. The ECM contains collagen, laminin, fibronectin and many other components, and contributes to the guiding of the axonal outgrowth after nerve injury [30].

Peripheral nerve injury and regeneration

A clinical nerve injury is defined by the extent of damage to the nerve, which can be classified into three stages: 1) neurapraxia – a temporary interruption of function, but with the axons still in continuity; 2) axonotmesis - the axonal continuity is broken, but the epineurium, the perineurium and endoneurial tubes are still intact and 3) neurotmesis - a total disruption of the entire nerve trunk; the axonal continuity is broken and so are all the connective tissue components. In the first two conditions, the function can be restored without surgery, while in the third, where the whole nerve trunk is transected or lacerated, either surgical repair or reconstruction is required, depending on the length of the nerve defect [31, 32]. When the nerve is repaired or reconstructed, the age of the patient and the extension of the nerve injury are critical factors for outcome and functional recovery [10, 14, 33].

A nerve injury influences the integrity of the neuron and in turn affects the Schwann cells that surround the injured distal axon segments. A number of processes are subsequently initiated in the neurons and also in the affected Schwann cells in order to begin and maintain a regenerative process throughout

the restoration of function. On the distal side of the injury, Wallerian degeneration, a slow cleaning process aided by Schwann cells and invading macrophages, is important in preparing for the regeneration of the axons. During this process, the degenerating axons and the disintegrated myelin sheaths are removed. Generally, after 3-6 weeks, all cellular debris will have been eliminated through phagocytosis. Similar processes occur at the site of the lesion, with the same purpose [16, 34].

Peripheral nerve regeneration involves many distinctive and diverse processes and, in contrast to in the CNS, regrowth of the injured axons is made possible by the complex processes taking place in the regrowth environment, including production of local factors that influence regeneration. In this respect, the highly specialized Schwann cells are crucial for nerve regeneration, and shortly after an injury, these cells start to proliferate and form columns, called "the bands of Büngner", in the distal nerve segment. At the site of the lesion, a matrix is formed, which prepares the environment for the sprouting axons that emerge from the injured axon. If the matrix is disorganized, it will influence outgrowth of the axons negatively [30]. In this context, the Schwann cells are important for guiding the growing edge, the growth cone, of the sprouting axon, which extends through the lesion site into the distal nerve segment and, if successful, finally to the target tissue. The axons grow at a speed of approximately 1 mm/day after transection and repair or reconstruction [34-36].

Both motor and sensory neurons are affected by a peripheral nerve injury and, obviously, the prerequisite for regeneration is neuronal survival. Up to 50% of the sensory neurons in DRG survive after a severe sciatic nerve injury in rats; thus, sensory neurons are much more sensitive to injury than spinal motor neurons, where between 0-10% die after nerve injury. Motor neurons are not destroyed unless a more severe proximal injury, such as a ventral root avulsion, takes place in the CNS [37-39]. In addition, an increased number of sensory neurons die and functional recovery is impaired if the repair or reconstruction of the injured nerve is delayed [40, 41].

In this thesis, I focused on investigating complete nerve injuries, either a complete transection of the rat sciatic nerve, an injury model which is suitable for direct nerve repair, or a nerve injury where a nerve defect of 10 mm (smaller nerve defect) or 15 mm (longer nerve defect), was created and where there is a need for surgery.

Signal transduction, factors and nerve regeneration

After a nerve injury, intracellular mechanisms are initiated to optimize conditions for nerve regeneration. These mechanisms are important for the process by which the motor and sensory neurons change their status from “transmitting” to “regenerating” and cell “death” mode, where survival, apoptosis, and regeneration are balanced among the affected neurons [42, 43]. Similar processes are also initiated in Schwann cells, which begin to proliferate, but only to a certain extent, since proliferation has to be balanced against cell death. It is the connection between activated and apoptotic conditions, which includes both intra- and extra-cellular cascade-signalling pathways, that determines whether the Schwann cells will proliferate, become activated and start to repair, or whether they will die, after a nerve injury [42-44].

A cascade of intracellular mechanisms takes place in the injured nerve cells in order to ensure successful regeneration [45]. Early in vitro studies have shown that retrograde transport (i.e. molecules transported from the injury site to the cell body) translocates activated mitogen-activated protein kinase (MAPK) pathway members, i.e. extracellular signal-regulated kinase (ERK), mitogen associated protein kinase, 38kDa (p38), or Jun N-terminal Kinase (JNK) to the cell body [12, 46]. The p38 and JNK pathways are involved in apoptosis. The ERK signalling is upregulated and ERK is activated after nerve injury [47]. ERK systems 1 and 2 are involved in neurite outgrowth, proliferation and cell survival after nerve injury [12, 48]. The MAPK family members activate the signalling cascades, which stimulate transcription factors, such as c-jun, and Activating Transcription Factor 3 (ATF-3). These trigger cell survival, proliferation and regeneration in both Schwann cells and in the cell body [49-51]. ATF-3 is a member of the ATF/CREB family (activating transcription factor/cAMP response element binding protein family) and is activated when nerve injury occurs [52-54].

The up-regulation of ERK1/2 takes place quickly after nerve injury, i.e. within 30 minutes, both in the proximal and in the distal nerve ends in axons and in the Schwann cells. This activation is a prerequisite for Schwann cell proliferation and axonal outgrow [48, 55]. In the STZ-induced and BB diabetic rat models, activation of ERK1/2 is not as pronounced as in healthy rats after nerve injury [26], indicating impaired nerve regeneration. Growth factors, such as nerve growth factor (NGF), brain-derived neurotrophic factor (BDNF), glial cell-derived neurotrophic factor (GDNF) and insulin-like growth factor 1, (IGF-1), are also upregulated in injured neurons and in the supporting cells. These growth factors stimulate axonal outgrowth, prevent apoptosis, and support the formation of neurites and production of local factors, which in turn guide the axon after nerve injury [56, 57].

Heat Shock Protein 27 (HSP27) is a small protein that belongs to the heat shock family of proteins and which plays an important part in both survival and protection of neurons [58]. HSP27 is activated by the p38 MAPK signalling pathway and has been shown to play an essential role in combatting cellular stress and inhibiting apoptotic signalling in neurons, in both healthy and diabetic conditions. A lower activation of HSP27 in a neuron may pose a potential risk in subjects with diabetes of developing peripheral neuropathy and could therefore be a future possible method for discovering peripheral neuropathy in the clinic [58-60].

Studies have shown that a defect between the nerve ends, after suturing the nerve under tension, results in unsatisfactory axonal outgrowth [61]. Thus, if the nerve injury results in a nerve defect, tension in the nerve can be alleviated by using a nerve graft to bridge the defect and to allow axonal outgrowth (Figure 1). Four different experimental nerve graft models can be used for tension-free reconstruction – nerve allograft (i.e. a non-identical donor of the same species); nerve autograft or autologous nerve grafts, (i.e. the subject's own graft material); nerve isograft (i.e. graft material from another genetically compatible donor); and nerve xenograft (i.e. graft material from a different species [27, 62]. Clinically, the standard model used to bridge nerve defects is autologous nerve grafts, but extracted nerve allografts, i.e. a graft in which all resident cells have been removed, are now also available [62-64].

Peripheral nerve repair and reconstruction

Nerve sutures and nerve grafts

Different types of nerve injuries require different procedures for restoring nerve function. In simple nerve transection injuries, where direct coaptation of the proximal and distal nerve ends is possible, sutures are used to maintain the end-to-end coaptation (Figure 1).

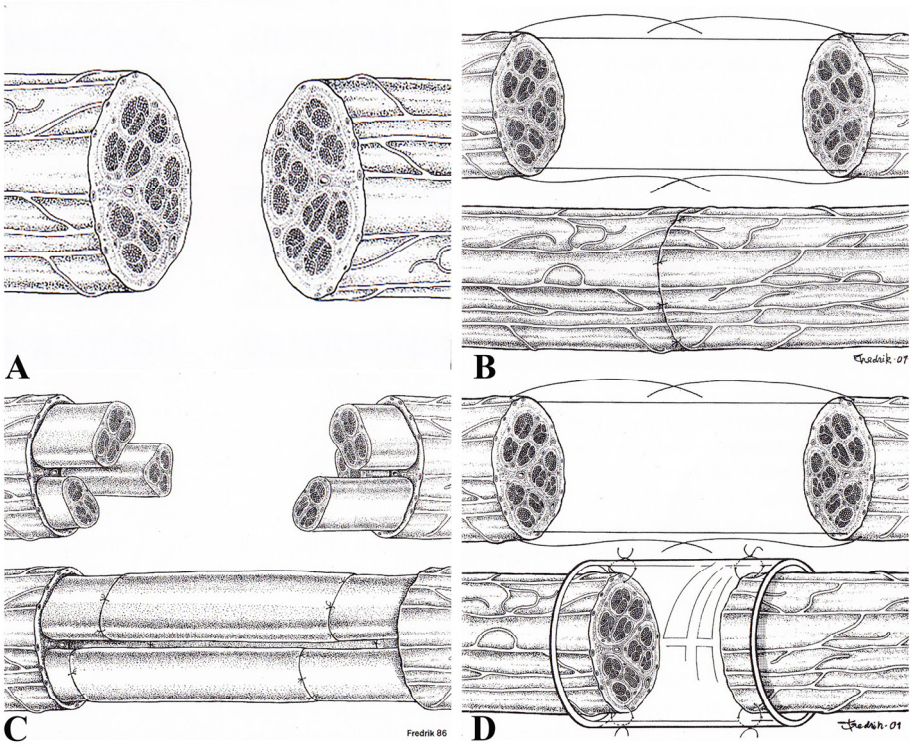

Figure 1.
Illustration of different procedures for repairing or reconstructing a peripheral nerve injury. Nerve transection (A). End-to-end nerve repair with sutures (B). Nerve reconstruction using nerve grafts (C). Nerve reconstruction using a conduit (D). Reproduced by kind permission of Dahlin and Lundborg, Neurosurgery Clinics of North America 2001 as well as Lundborg, Nerve Injury and Repair: Regeneration, reconstruction and cortical remodelling. Elsevier – Churchill Livingstone 2004.

Some of the clinical results of such reconstruction strategies have been presented in the RANGER study (Registry of Avance Nerve Graft Evaluating Utilization and Outcomes for the Reconstruction of Peripheral Nerve Discontinuities), an active database, started in 2012, which contains data from nerve reconstruction cases from 18 clinical centres in the USA [65, 66]. However, all the above-mentioned strategies have limitations, and if there is a lack of suitable donor material and none of the four described graft models above is suitable, it may be necessary to reconstruct the nerve defect using a bioartificial conduit [17, 67, 68] (Figure 1). The prerequisite for axonal outgrowth when using such conduits is that a matrix can be formed inside the conduit between the proximal and distal nerve ends through which the regenerated axons are able to grow [69].

Nerve conduits

Research is being performed to identify the most appropriate conduits for nerve reconstruction. There are studies investigating conduit characteristics, such as porosity, flexibility, material swelling and degradation ability [70, 71]. Conduits made of biological materials, such as collagen, and artificial materials, like silicone tubes (i.e. non-biodegradable), as well as biodegradable polymers have been evaluated. Some of these strategies have been tested clinically [72]. The use of conduits made of collagen (Neura-Gen™), which is the major ingredient in the ECM and therefore a tissue-compatible material, has produced good results in human studies when bridging small nerve defects (less than 2 cm). Another successful conduit, made of the suture material polyglycolic acid (PGA), is the Neurotube™ [73]. Other commercial conduits are also available, such as poly-DL-lactide-co-caprolactone (PLCL) and polycaprolactone (PCL) [68, 73, 74]. These conduits are, however, expensive and, due to their fast degradability, less suitable for reconstructing longer nerve defects [17, 70]. Despite the availability of a number of conduits made of a variety of materials, the best way to reconstruct longer nerve defects (e.g. more than 3 cm) seemingly remains the autologous nerve graft [75].

Chitosan conduits

In recent years, the polysaccharide chitosan has attracted attention as a conduit material [20]. Chitosan consists of chitin [chitin is a polymer of B (1-4) linked 2-acetamido-2-deoxy-D-glucopyranose], which is a primary and natural homopolymer that can be extracted from, for example, the shells of pandalus borealius shrimp and crab and fungi cell walls [20]. Once in the body, chitosan degenerates; the degree of degradation can vary from 0% to 60%. Chitosan degradation is the result of the hydrolysis of the connection between D-glucosamine and N-acetyl-D-glucosamine carried out by the enzyme lysozyme which occurs naturally in the human body [19, 76]. The degradation of chitosan, therefore, correlates to the degree of acetylation (DA) where a higher degree of DA results in faster degradation [77].

Chitosan has been investigated for various kinds of biomedical applications, not only because of its inherent ability to degrade in the human body, but also because it is non-toxic and biocompatible. These features make chitosan a promising material for improving axonal outgrowth after a peripheral nerve injury [19]. As with several other conduits, the chitosan conduits can be modified with, for instance, the insertion of membranes and nanofibers, as well as gels, such as NVR (non-volatile residue) comprised of hyaluronic acid (HA) and laminin. HA is a non-sulphated glycosaminoglycan which is a disaccharide that exists ubiquitously

in the human body [78]. The NVR gel is able to stabilize the matrix formed with the aim of improving nerve regeneration [74, 76, 78, 79].

Diabetes and peripheral nerves

Diabetes has long been known to negatively affect the peripheral nerve system. Type 1 diabetes is a complex autoimmune disease in which ß-cells in the pancreatic islets of Langerhans are completely destroyed, leading to a lack of insulin production. Type 2 diabetes is a disease involving insulin resistance and insulin deficiency, but with functioning ß-cells. Diabetes induces complications in a number of organ systems in the body. In both types 1 and 2, as many as 30-50 % of patients suffer from PNS complications, including peripheral and autonomic neuropathy [80], although the pathophysiological mechanisms probably differ in the two diseases [81].

The PNS complications experienced by diabetic patients include loss of sensory and motor function, sometimes with accompanying pain, i.e. polyneuropathy. Long nerves, such as the sciatic nerve, are particularly susceptible to diabetes, which explains why legs and feet are sensitive to neuropathy and so frequently affected in this disease [82]. Later aspects of the disease include risks of impaired wound healing, particularly in the lower extremities with reduced quality of life, and of limb amputations. Notably, male patients seem to develop neuropathy earlier than female patients [83]. Most experimental in vivo studies on nerve regeneration use either male or female animals and do not specifically analyse gender differences. Thus, evaluation of nerve regeneration in healthy male and female animals, as well as diabetic males and females, after nerve injury and following repair or reconstruction is of the utmost relevance [84, 85]. This aspect is one of the focuses in the present studies.

The entire PNS is affected by diabetes, which causes both demyelination and axonal degeneration in the peripheral nerve trunks. The disease also causes impaired nerve regeneration [86, 87]. However, the detailed mechanisms of these processes under the influence of diabetes are not known, but it is suggested that activation of MAPK is involved in the development of diabetic neuropathy [88, 89]. Unfortunately, no cure is available for diabetic neuropathy, only treatments that alleviate the symptoms [21, 90-92]. Neuropathy in diabetes comprises not only of the polyneuropathy mentioned, which affects several nerves in the body, but can also affect individual or specific nerves in the body, i.e. mononeuropathy. Mononeuropathy includes nerve compression lesions that can generally be treated with surgery, such as carpal tunnel syndrome, which is more common in patients with diabetes [93, 94]. There seems to be a predisposition towards nerve

compression lesions in diabetes, which may be due to various neurobiological events, such as nerve fibre and microvascular pathology [67, 94-96].

Diabetic animal models

Most experimental studies that evaluate how the peripheral nervous system is affected by diabetes are based on animal models using streptozotocin (STZ)-induced diabetes [89, 97]. In this model, the ß-cells are destroyed by the toxic effect of Streptomyces achromogenes, a chemotherapeutic drug [98]. There has, however, been criticism of this model, since it does not appear to be relevant to either type 1 or type 2 diabetes in humans. In this model, there is still some production of insulin, and therefore the symptoms are not completely insulin-dependent [90]. Nonetheless, in the STZ-induced diabetes model, impaired nerve regeneration has been described in both short- and long-term experiments [23]. In the current thesis, I used two other diabetic models, the BB rat and the GK rat models [24, 99, 100]. The former is a genetic model, in which the rats spontaneously develop diabetes with blood glucose values around 18-32 mmol/l. At these glucose levels this model resembles untreated type 1 diabetes in humans. The GK rats, also spontaneously develop diabetes and this model is therefore considered to be related more to human type 2 diabetes with blood glucose levels of between 7-12 mmol/l [25]. Both the BB and the GK rat models involve structural damage to the peripheral nervous system, including demyelination, altered nerve conduction velocity, and impaired axonal transport [90, 100]. Unfortunately, the BB rats do not survive for long periods without insulin treatment, which make them less suitable for use in studies of nerve regeneration after nerve injury in long-term. If BB rats are treated with insulin, there may be a potential influence on the regeneration process from the insulin, as well as from the substantial variation in the blood glucose levels caused by the daily insulin injections [85, 101]. Thus, only very short-term experiments are possible and therefore GK rats are more suitable for long-term experiments and in the experiments described in this thesis mainly used this model.

Aims

The overall aim of the present thesis was to evaluate techniques that could be used to improve nerve regeneration after a sciatic nerve injury. For this purpose, the severed nerve was repaired or reconstructed using chitosan conduits or autologous nerve grafts in healthy and diabetic rat models of both genders.

The specific aims were:

- To investigate and compare nerve regeneration shortly after a sciatic nerve transection and instant nerve repair in a diabetes type 1 rat model (BB rats) and healthy female Wistar rats (Paper I).
- To evaluate possible short-term gender differences in healthy Wistar and diabetic GK rats after sciatic nerve injury and repair, (i.e. animal model of type 2 diabetes) (Paper II).
- To examine short- and long-term nerve regeneration in healthy Wistar rats after sciatic nerve reconstruction of a 10 mm long nerve defect using hollow chitosan conduits with different degrees of acetylation (Paper III).
- To compare short-term nerve regeneration after reconstruction of a 10 mm long nerve defect with either a hollow chitosan conduit or an autologous nerve graft in healthy Wistar and diabetic GK rats (Paper IV).
- To investigate short- and long-term nerve regeneration in healthy Wistar and diabetic GK rats after bridging a 15 mm long sciatic nerve defect with 1) hollow chitosan nerve conduits or 2) chitosan conduits modified with membrane inserts with, or without, perforations or 3) chitosan conduits with a perforated membrane also containing FGF-2 overexpressing Schwann cells (Paper V).

Methods and surgery

A summary of the methods and surgery is presented here; the reader is referred to individual papers for more specific details.

All animal experiments were approved by the ethics committee for the Malmö and Lund region (Ethic No. M347-11 and M131-14) as well as at the respective universities in the Biohybrid consortium. The rats weighed approximately 200 g in all experiments. In Papers I-V, Wistar rats were used as healthy rats (Taconic, Denmark and Hannover; Germany, Barcelona; Spain). BB rats were used in Paper I (kindly provided by Professor Åke Lernmark and Dr Lina Åkesson, Department of Endocrinology, Lund University). For Papers II-V, GK rats, kindly provided by Malin Fex, Lund University, Sweden, were used.

Surgery

Animal care, including anaesthesia and analgesia, followed approved standard protocols. All animals were observed daily. Before surgery, blood glucose was obtained from the tail vein in all rats and measured in a blood glucose unit [Ascensia contour TM (Bio Healthcare, USA, Bio Diagnostics Europe) and LT (Bayer AB, Diabetes Care, Solna, Sweden); test slips (Microfil TM (Bio Healthcare Diabetes Care, USA]. Only diabetic GK rats with a blood glucose level above 6.5 mmol/l were included in the studies. The surgeries were performed in three different laboratories; Lund University, Sweden, Hannover Medical School, Germany, and Barcelona University, Spain.

In all papers, the sciatic nerve was unilaterally transected at mid-thigh level. In Papers I and II, the nerves were then immediately repaired with 9-0 ethilon sutures. In Papers III and IV, a sciatic nerve defect was created by removing a 5 mm piece of the nerve, creating a nerve defect 10 mm long, which was bridged by a chitosan conduit. For control experiments in Papers III-V, an autologous nerve graft reconstruction was performed by the removal of a 10 or 15 mm long nerve segment, which was then rotated (180 degrees) and sutured into the defect as an autologous nerve graft on the ipsilateral side (Figure 2).

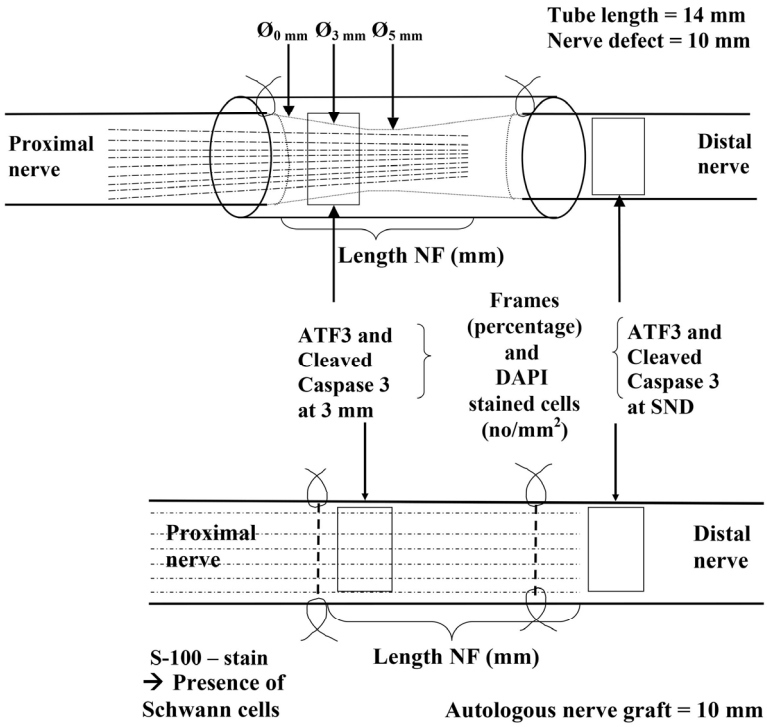

Figure 2.
Overview of the subspecimens in the autologous nerve grafts and in the hollow chitosan conduits analysed 21 days after surgery. Reproduced by kind permission from Stenberg et al, European Journal of Neuroscience 2016.

In the control rats in Paper III, the sciatic nerve was transected and a 5 mm nerve segment was removed. The proximal and distal nerve ends were folded over and sutured. The last paper (V) was divided into three separate studies, where a 15 mm nerve defect was bridged by; a) insertion of a hollow chitosan conduit with or without a membrane, b) insertion of a hollow chitosan conduit with or without a *perforated* membrane, and c) with a hollow chitosan conduit with or without a *perforated* membrane; the former either with or without overexpressing Schwann cells (neoSchwann cells). At selected time points, the rats were sacrificed and the repaired or reconstructed sciatic nerve and adjacent nerve ends, including the matrix formed inside the chitosan conduits, were dissected and analysed. In Papers III and V, dorsal root ganglia (DRG) were also harvested and analysed.

Chitosan conduits

Chitosan material was produced by Altakin S.A (Lisbon, Portugal) following required ISO 13485 approval. The chitosan conduits in Papers III, IV and V, and also the chitosan membrane (film) in Paper V, were then further modified by Medovent GmbH (Mainz, Germany), with all necessary permits, regarding the ISO standard 13485 protocol. Chitosan conduits in Papers III, IV and V had an inner diameter of 2.1 mm and a wall thickness of 0.3 mm. In Paper III, hollow chitosan conduits were evaluated to find the acetylation most suitable to support axonal outgrowth after nerve injury (Figure 3). Different acetylation degrees: DAI 2% (low), DAII 5% (medium) and DAIII 20% (high), were investigated. In Papers IV and V, conduits with medium acetylation (DAII) were used for all experiments. In Papers III and IV the chitosan conduits were 14 mm long and the nerve defects were 10 mm. In Paper V, the conduits were 19 mm long and the nerve defects were 15 mm. Various time points after surgery were evaluated in Papers III, IV and V. In Papers III-V, the surgery was performed with hollow chitosan conduits. In Paper V, chitosan nerve conduits with a membrane, which was perforated or not perforated, were also used. In this paper, the effects on nerve regeneration were also examined by placing genetically modified Schwann cells on both sides of the perforated membrane inside the chitosan conduits as described above.

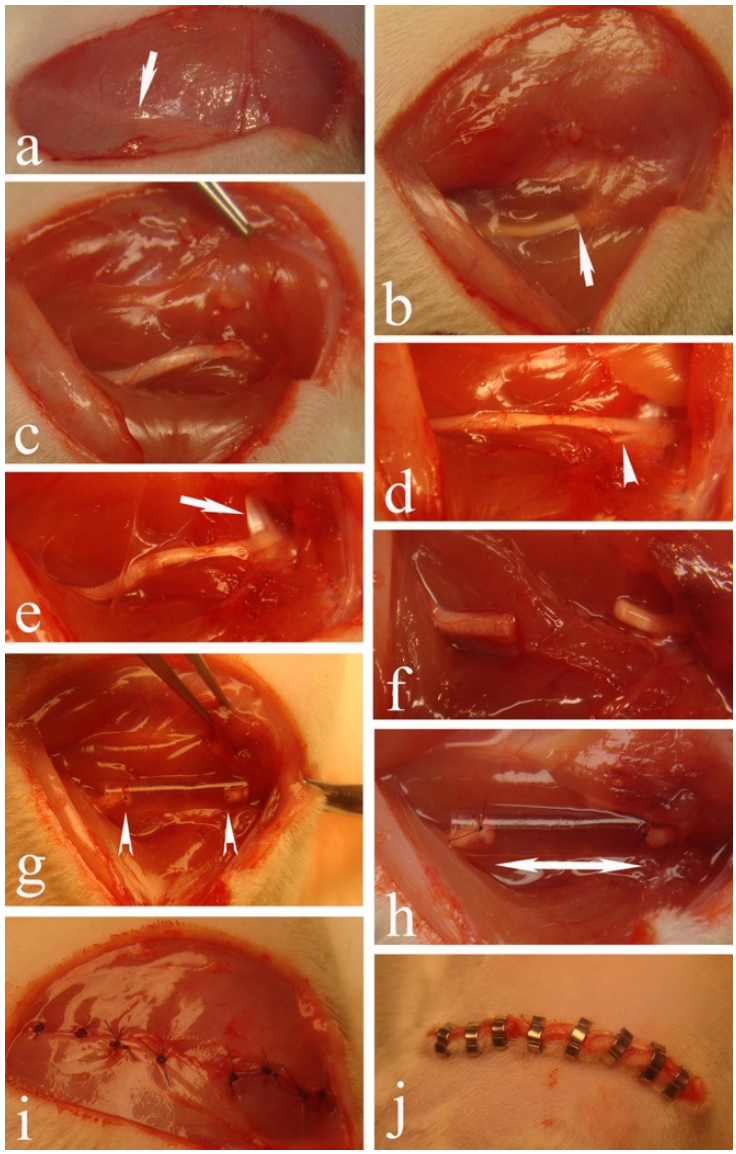

Figure 3.
The figure illustrates the surgical nerve reconstruction procedure using a chitosan conduit after nerve transection: a) thigh muscle incision; b) sciatic nerve identification; c) nerve exposure; d and e) identification of small nerve branch and tendon aponeurosis; f) nerve transection and removal of small nerve segment; g) hollow chitosan conduit insertion; h) measurement of nerve defect in conduit; i) sutures to adapt muscles; j) skin clips.

Immunohistochemistry and histological methods

Immunohistochemistry

Nerve samples were collected from all rats and were either frozen or embedded in paraffin and sectioned. For staining of specific antigens, the sections were incubated with primary antibodies (Table 1) diluted in different blocking solutions for various antibodies (Table 2). After washing in phosphate buffered saline (PBS, pH 7.2), the slides were incubated with secondary antibodies diluted in PBS (Table 3), washed again, and finally stained with a nuclear counterstain 4´,6´-diamidino-2-phenylindole (DAPI) and mounted with a coverslip. The neurofilament (NF), ATF-3 and Cleaved Caspase-3 staining, as well as total numbers of DAPI stained cells, were quantified in all experiments. Double staining using an S-100 antibody was performed to ascertain Schwann cell identity in all Papers. In Paper III, double staining was also performed after 13 weeks to evaluate ED1 and neurofilaments (Table 1) in the regenerated tissue. In Paper III, the total numbers of activated macrophages (ED1) within the connective tissue were also quantified on removal of the chitosan conduits. In Paper V, ATF-3 stained sensory neurons and the intensity of HSP27 were also quantified within the DRGs. In Paper V, genetically modified Schwann cells (neoSC), which had been developed in accordance with a previous study [78], were stained with primary antibody α-S-100 or anti-flag (Table 1) and secondary antibodies (Table 3) to ascertain viability by cell counting of the Schwann cells before placing them on the membranes. In Paper V, we also double stained for Choline acetyltransferase (ChAt) to identify the presence of motor axons inside the conduits. All immunohistochemical analyses were performed blind.

Histo-morphometry

In Paper III, the connective tissue, surrounding the conduits, was also investigated. After sectioning, the connective tissue was stained with haematoxylin-eosin in order to examine multinucleated giant cells (MGC) as an eventual reaction on the chitosan conduits. This was done after 18 days and 13 weeks of investigation. In Paper V, all nerve material from the conduits was sectioned and stained with haematoxylin-eosin (HE) and trichrome staining for investigation of collagen expression.

Table 1.
Primary antibodies.

Primary antibodies	Company	Dilution	Analysis
NF-L (70 kDa) Monoclonal mouse	DAKO, Denmark	1:80	IHC
ATF- 3 Polyclonal rabbit	Santa Cruz Biotechnology, USA	1:200	IHC
Cleaved caspase-3 Polyclonal rabbit	BioNordika, Sweden	1:200	IHC
S-100 α/β chain Monoclonal mouse	Santa Cruz Biotechnology, USA	1:200	IHC
ED 1 Monoclonal mouse	Serotec, United Kingdom	1:1000	IHC Histology
BDNF Polyclonal rabbit	Santa Cruz Biotechnology, USA	1:1000	Western Blot
NGF Polyclonal rabbit	Abcam, United Kingdom	1:2000	Western Blot
NF-H (200 kDa) Polyclonal rabbit	Sigma-Aldrich, Germany	1:200	Histology
HSP27 Polyclonal goat	Santa Cruz Biotechnology, USA	1:200	IHC
ChAT Polyclonal goat	Millipore, Germany	1:50	IHC
S100 α- chain Monoclonal mouse	Dako, Denmark	1:200	IHC
Anti-FLAG Monoclonal rabbit	Sigma – Aldrich, Germany	1:200	IHC

Table 2.
Blocking solution.

Blocking solution	Antibody	Paper
Rabbit serum 5% in PBS	ED 1	III
Bovine serum albumin (BSA) 0.25% and Triton-X-100 0.25% in PBS.	NF-L, ATF-3, Cleaved caspase-3, HSP27, S-100 α/β chain	I,II,III,IV,V
Dry milk 5% and Triton-X-100 0.5% in 0.5M Trisaline buffer.	NF-H	III
Horse serum 5% in PBS.	ChAT	V
Triton-X-100 0.3% and BSA 5% in PBS.	S100 α chain, anti-FLAG	V
Dry milk 3% and Triton-X-100 0.5% in PBS.	NF-H	V

Table 3.
Secondary antibodies.

Secondary antibodies	Company	Dilution	Analysis
Alexa fluor 594 goat anti-mouse	Molecular probes, USA	1:500	IHC
Alexa fluor 488 goat-anti rabbit	Molecular probes, USA	1:500, 1:1000	IHC, Histolgy
Alexa fluor 555 goat anti-mouse	Invitrogen, Germany	1:500	IHC
Alexa fluor 555 donkey anti-goat	Invitrogen, Germany	1:500	IHC
Alexa fluor 488 donkey anti-goat	Molecular probes, USA	1:500	IHC

The nerve samples for evaluation of morphometry in Papers III and V were stained using the same conventional histological methods (see papers for details). In Papers III and V, after removing the chitosan conduits, the distal nerve ends were taken out bilaterally from the healthy rats and prepared for morphometry. In Paper III, total numbers of myelinated fibres, axon diameter, fibre diameter, myelin thickness and the g-ratio (axon diameter/fibre diameter) were evaluated in all chitosan conduits and ANG as well as in the control nerves. In Paper V, the total number of myelinated fibres, cross sectional area, nerve fibre density, axon diameter, fibre diameter, myelin thickness and the g-ratio were evaluated.

Functional evaluation

Static sciatic index

In Paper III, the Static sciatic index (SSI) test was performed to evaluate motor recovery after nerve reconstruction. The SSI test is based on changes in the rat toe spreading after nerve injury from before surgery to after 1, 4, 9, or 12 weeks following surgery. For these measurements, the rats were placed in a box on a glass table with a camera connected to a computer beneath it to capture images of the toe positions. The images were then used to measure the distance between toes 1-5; toe spread (TS) and toes 2-4; intermediate toe spread (ITS) in both the lesioned (L) and non-lesioned (N) hind paws. The SSI test result [102] was then calculated according to the intermediate toe-spread factor (ITSF) and the toe-spread factor (TSF):

TSF=(LTS-NTS)/NTS
ITFS=(LITS-NITS)/NITS
SSI=(108.44*TSF) + (31,85*ITFS)-5.49.

von Frey test

The von Frey test was used in Papers III and V to determine the mechanical pain threshold at different times in order to define sensory recovery after nerve reconstruction. For this test, the rats were placed in plastic boxes connected to a von Frey algesimeter with a blunt needle used to stimulate the injured and non-injured site of the hind paw. The pressure of the needle was increased successively until the rats responded by withdrawing the hind paw. The tibial and sural nerves were evaluated bilaterally. The three steadiest values were selected from a total of five recordings from each side for further calculation of a mean value and used for statistical analysis.

Electrophysiology

Evaluation of motor function recovery in Papers III and V was performed using an electrodiagnostic device to measure the compound muscle action potentials (CMAPs). The recordings were made bilaterally in the plantar interosseous muscles (PL) and tibialis anterior (TA) muscles (i.e. on both the experimental and control sides). All the serial non-invasive tests were performed one week before reconstruction and then at different times after surgery and finally as invasive before the rats were sacrificed. The nerve conduction velocity (NCV) ratio was calculated from the recorded values between the controls and the experimental sides of the rats.

Muscle weight ratio

After sacrificing the rats at 13 weeks post-surgery in Paper III and 120 days post-surgery in Paper V, the tibialis anterior (TA) and gastrocnemius (GA) muscles were harvested and weighed. The muscle weight ratio was calculated in both the experimental and contralateral sides of the rats.

Chitosan material evaluation

Nuclear magnetic resonance spectroscopy (NMR)

In Paper III, the degree of acetylation (DA) of the chitosan material before the manufacturing of the chitosan conduits was confirmed through NMR analysis.

Gel permeation chromatograph (GPC)

In Paper III, the molecular weight of the chitosan samples was evaluated using GPC analysis before production of the chitosan conduits.

In vitro cytotoxicity test

In Paper III, rat bone marrow mesenchymal stromal cells (RBMSCs) were used for incubation with the different DAs to evaluate the biocompatibility and possible cytotoxicity within 24 h, 72 h, and seven days of incubation. Cell structure and cell viability were examined using MTS [3-(4,5-dimethylthiazol-2-yl)-5-(3carboxymethoxyphenyl)-2-(4-sulfophenyl)-2H-tetrazolium] proliferation assay test kit and the Minimum Essential Medium (MEM) extraction test.

Molecular and biochemical evaluation

Quantitative RT-PCR

In Paper III, DRG were collected on days 5 and 18 from both the rats reconstructed using chitosan conduits and the control rats. The DRG from the experimental and the control side of the rats were harvested and immediately frozen in liquid nitrogen. The samples were prepared for quantitative real-time polymerase chain reaction (qRT-PCR) analysis to investigate the level of mRNA expression for the BDNF, FGF-2, NGF, IL-6, trkB and GAP-43 genes.

Western Blot

In Paper III the content of the chitosan conduits was collected on days 5 and 18 after nerve reconstruction, to verify the presence of BDNF. Since a former study has shown that BDNF accumulates in the proximal site after nerve injury, which acts as a protection, we thought that it could be important to evaluate the BDNF levels within the matrix [103]. The samples were prepared and analysed as described earlier [104].

In vitro study - cell culture

Sciatic nerves were harvested from rat pups to produce neonatal Schwann cells (neoSC). The cells were genetically modified by introducing the non-viral plasmid encoding FGF-2^{18kDA} (pCAGGS-FGF-2-18 kDa-Flag, NCBI GenBank accession NM_019305.2, 533e994 bp). In Paper V the modified Schwann cells were placed on both sides of the perforated membranes inside the chitosan nerve conduits, as described in a previous study [78].

Macroscopic investigation

Visual investigation

In Papers III and V, macroscopic investigation was performed directly after sacrificing the rats. This included visual evaluation of the short- and long-term formation of the matrix/cables. The chitosan conduits were then removed and further evaluated visually before fixation of the tissue and continued analysis.

Image analysis

In all papers, a fluorescence microscope (Nikon 80i) connected to a digital camera and software NIS elements (Nikon, Japan) was used. In Papers III and V, a DM4000B microscope equipped with a DFC320 digital camera and an IM50 image manager system (Leica Microsystems, Germany) was used for nerve morphometry. In Papers III and V, BX53 and BX51 (Olympus, Germany) light microscopes with CellSense Dimension and CellSense Entry (Olympus, Germany) software were used. In Papers III and V, fluorescence microscopes IX70

(Olympus, Denmark) and BX60 (Olympus, Germany), respectively, with CellP software (Olympus, Germany) were used.

Statistical analyses

All data was processed using Statview (Paper I), IBM SPSS statistics (versions 17.0, 20.0, 22.0; Papers II-V) or GraphPad InStat software (versions 5.03.0 and 6.00; GraphPad Software, USA; Papers III-V). The non-parametric Kruskal-Wallis test or two-way ANOVA (Analysis of Variance) were used to calculate differences between test groups in the individual papers. The Mann-Whitney, Dunn's test, Tukey's test, or Bonferroni test were used to evaluate differences between individual groups. The p-value was calculated using the specific Fisher's test [105] for independent samples based on the Chi-Square test for separate p-values (Papers II, IV and V). The statistical values regarding nerve regeneration in Papers II-V are presented as median values with 25 to 75 percentiles, and in Paper I as median values with min-max. The Spearman test was used for the correlation evaluation in Papers I-IV. In Paper V, the differences between the experimental and control sides of the DRG were evaluated using the Wilcoxon signed rank test. A p-value of less than 0.05 was considered significant in all papers.

Results

A summary of the results is presented here; the reader is referred to individual papers for more specific details.

Paper I. Expression of Activating Transcription Factor 3 (ATF-3) and cleaved caspase-3 after sciatic nerve repair in diabetic BB rats

Nerve regeneration in diabetic BB rats and healthy Wistar rats was investigated and compared. As expected, fasting blood glucose values were significantly higher in the diabetic BB rats than in to healthy Wistar rats. There were, however, no differences in length of axonal outgrowth as assessed by means of neurofilament staining in sections of the repaired nerve between the diabetic BB and the healthy Wistar rats. However, significant differences were observed between diabetic and healthy rats regarding the number of ATF-3 and cleaved caspase-3 stained Schwann cells at the site of the nerve lesion, with increased numbers of both in the BB rats. The same was true for the distal nerve segment, where a higher number of ATF-3 and cleaved caspase-3 Schwann cells was found in the BB rats compared to in the Wistar rats. There was, however, no significant correlation, in either the Wistar or the BB rats, between axonal outgrowth and the number of activated ATF-3 stained or apoptotic cleaved caspase-3 stained Schwann cells, either at the site of lesion or in the distal nerve end. Furthermore, there was no correlation between activated and apoptotic Schwann cells at the two investigated sites in either of the two models.

Paper II. Gender differences in nerve regeneration after sciatic nerve injury and repair in healthy and in type 2 diabetic Goto-Kakizaki rats

Differences in nerve regeneration between males and females were evaluated in healthy Wistar rats and diabetic GK rats. The blood glucose levels were higher in the diabetic rats than in the healthy rats, and also significantly higher in male diabetic rats compared to in female diabetic rats. There were also statistical differences between the groups, regardless of gender, with longer axonal outgrowth in the healthy Wistar rats than in the diabetic GK rats. Furthermore, axonal outgrowth was improved in male rats compared to in females in both healthy and diabetic GK rats.

Generally, there were also differences in the number of activated and apoptotic Schwann cells at the lesion site between the GK rats and the Wistar rats. Increased numbers of ATF-3 stained Schwann cells were observed in the male GK rats compared to in the female GK rats. In the distal nerve segment, we observed a higher number of activated ATF-3 stained Schwann cells in the Wistar rats than in the GK rats. The apoptotic Schwann cells were significantly higher in the GK rats than in the Wistar rats, both in males and females, but no statistical differences were observed between male and female rats, either at the lesion site or in the distal nerve end.

When the results from all groups of rats were pooled, the Spearman's test revealed a positive correlation between activated ATF-3 stained Schwann cells and the length of axonal outgrowth. There was also a positive correlation between preoperative blood glucose levels and number of apoptotic Schwann cells at the lesion site. In the distal nerve segment, preoperative blood glucose levels also positively correlated with the numbers of apoptotic Schwann cells, but not with the activated ATF-3 stained Schwann cells.

When diabetic rats were analysed individually and tested for correlations at the lesion site, a positive correlation was found between preoperative blood glucose level and axonal outgrowth as well as with the number of ATF-3 Schwann cells. A positive correlation at the lesion site was also observed between the numbers of ATF-3 and cleaved caspase-3 stained Schwann cells. In the distal nerve segment, a positive correlation was observed between preoperative blood glucose levels and activated ATF-3 stained Schwann cells. Finally, in healthy rats, blood glucose levels positively correlated with axonal outgrowth.

Paper III. Chitosan tubes of varying degrees of acetylation for bridging peripheral nerve defects

Regeneration was investigated both in vivo and in vitro using hollow chitosan conduits with three different DAs to reconstruct a 10 mm long nerve defect in healthy Wistar rats. Time points selected for observation were 5 days, 18 days, 21 days, and 3 months after reconstruction.

The in vitro test revealed no differences and no negative effects on the metabolic activity in the RBMSCs when using extracts from chitosan conduits of different acetylation (DAI, DAII and DAIII) compared to the positive control, which was ordinary culturing medium.

After 5 and 18 days of reconstruction with the chitosan conduits the qRT-PCR method was performed to evaluate mRNA levels of NGF, FGF-2, BDNF, the cytokine IL-6, the BDNF receptor TrkB and GAP-43 in the DRG. No significant differences were found in the mRNA levels when comparing the three models of chitosan conduits.To summarize, the three models of chitosan conduits have no effect on up-regulation of neurotrophic factors in the DRG after nerve injury. The conduit contents were also analysed, using Western blot, after 5 and 18 days to evaluate levels of BDNF protein. The protein was detected in all chitosan conduits, but no differences were found in the levels of BDNF protein when comparing the three models of chitosan conduits. In addition, no significant differences between the three chitosan conduits were observed when evaluating MGCs and ED 1 in the surrounding connective tissue at 18 days and 13 weeks after reconstruction.

The macroscopic evaluation of the nerve 5 days after reconstruction revealed no apparent degradation of any of the DA chitosan conduits. However, degradation had started at 18 days in the DAIII conduits and was even more pronounced after 3 months with clear traces of different types of damage in the DAIII conduits compared to the other two groups of conduits, which showed very little signs of degradation.

After 21 days, we found that a matrix had formed in all three types of chitosan conduits without any apparent differences in matrix formation or axonal outgrowth. The presence of the matrix was also evaluated at earlier time points, i.e. after 10, 14 and 18 days, but at these time points we observed no fully formed matrix between the nerve ends. A similar, but limited, number of activated ATF-3 stained Schwann cells was observed in the matrix in the various chitosan conduits. However, in the distal nerve segment, a higher number of ATF-3 stained Schwann cells was observed in the DAIIIs compared to the other two types of chitosan conduits. An increased number of apoptotic Schwann cells was also observed in

the matrix formed in the DAIII group compared to the other groups. A positive correlation was observed between the thickness of the matrix formed in DAI and DAIII conduits and the length of axonal outgrowth.

Motor recovery was evaluated using the SSI test at 1, 4, 9 and 12 weeks after repair, but no significant differences were detected between the three different models of chitosan conduits. The electrophysiological test CMAP was used in the TA and PL muscles at 4, 9, and 12 weeks after reconstruction. No signs of CMAPs were detected at 4 weeks after reconstruction, but after 9 weeks, in the rats where the nerve had been reconstructed with an autologous nerve graft, a CMAP was found in the TA and PL muscles. However, such CMAPs were less pronounced in rats where the nerve had been reconstructed with chitosan conduits. At the final invasive test, 12 weeks after reconstruction, several rats, where the sciatic nerve had been reconstructed with a chitosan conduit, reached the same CMAP levels in both TA and PL muscles as did the rats where the sciatic nerve had been reconstructed with an autologous nerve graft. The nerve conduction velocity (NCV) and the NCV ratio, based on the CMAP recordings, showed no significant differences between the test groups. The muscle weight ratio also did not differ significantly between groups.

The morphological analysis revealed differences between the experimental and healthy nerves regarding the total number of myelinated fibres. Only the DAI chitosan conduits group, however, displayed a larger number of myelinated fibres compared to the ANG group of rats. No significant differences were observed when comparing the groups of chitosan conduits with regard to axon diameter, fibre diameter, myelin thickness and g-ratio in the distal nerve segment.

A significant increase in the number of ED1 stained macrophages was observed in the formed matrix of the DAIII chitosan conduits compared to the DAI and DAII groups, whereas in all three DA groups, a lower number of macrophages was observed compared to the ANG group. In addition, the perineurium in the distal nerve end in the nerves reconstructed with DAIII chitosan conduits was significantly thicker than that in the ANG group. There were, however, no significant differences in the area or the thickness of the connective tissue between the DA groups at 18 days and at 3 months, but the optical density of the surrounding tissue was significantly increased in the DAIII group compared to DAI and DAII groups.

Paper IV. Nerve regeneration in chitosan conduits and in autologous nerve grafts in healthy and in diabetic Goto-Kakizaki rats

In this study, we compared the effect of bridging a 10 mm long sciatic nerve defect with either hollow chitosan conduits (DAII) or autologous nerve grafts in healthy and diabetic GK rats. At 21 days after reconstruction with chitosan conduits, a thicker matrix and longer axonal outgrowth were observed in the GK rats compared to the Wistar rats. Longer axonal outgrowth was also found in the GK rats than in the Wistar rats reconstructed using autologous nerve grafts. The number of ATF-3 stained Schwann cells differed at 3 mm distal to the proximal suture line between the healthy rats and the diabetic rats with an increased number of ATF-3 stained cells observed in the healthy rats, where the sciatic nerve was reconstructed with autologous nerve grafts, compared to diabetic rats, where the nerve had been reconstructed in the same way. Differences were also observed between all groups of rats in the distal nerve end, with a higher number of activated ATF-3 stained Schwann cells in the Wistar rats compared to in the GK rats when the severed nerves in both groups had been reconstructed with autologous nerve grafts. An increased number of apoptotic Schwann cells was found at the lesion site in both Wistar and the GK rats when autologous nerve grafts were used in reconstruction than when chitosan conduits were used. In the distal nerve end, an increased number of apoptotic Schwann cells was observed in the Wistar rats than in the GK rats reconstructed with chitosan conduits.

When all data was pooled between the diabetic/healthy rats and chitosan conduits/autologous nerve grafts, correlation, evaluated using the Spearman's test, was positive between axonal outgrowth length and number of activated ATF-3 and apoptotic cleaved caspase-3 stained Schwann cells. The number of activated ATF-3 stained Schwann cells also positively correlated with the number of apoptotic Schwann cells both at 3 mm and in the distal nerve end.

Paper V. Chitosan–film enhanced chitosan nerve guides for long-distance regeneration of peripheral nerves

The last study was divided into three parts, where a 15 mm long sciatic nerve defect was reconstructed with chitosan conduits that had been modified in different ways; with an inserted membrane perforated or without holes and, in another set of experiments, containing genetically modified Schwann cells. The

nerve specimens were harvested at 56 days (short-term; healthy and diabetic GK rats) or for up to 120 days (long-term; healthy rats only) after reconstruction (Table 4).

Short-term evaluation

The short-term evaluation (study 2) of the hollow chitosan conduits (referred to as guides in the original paper) revealed one cable, which is a completely formed matrix between the proximal and distal nerve ends, in 75 % of the group of rats with hCNG-II^{healthy} and 50 % with hCNG-II^{diabetic} chitosan nerve conduits (see Table 4 for abbreviations). In the chitosan nerve conduits with a perforated membrane insert, two cables were found in 75 % of CFeCNG$^{2nd\text{-}healthy}$ and 88 % CFeCNG$^{2nd\text{-}diabetic}$ of the rats. In the other rats, no complete matrix/cable between the nerve ends was observed.

It was not possible to measure the exact length of outgrowing axons at 56 days because of the very thinly formed cables/matrix inside the chitosan conduits. Instead, we chose to evaluate whether axons existed at different levels in the formed matrix. We found that outgrowing axons were present in the centre of the matrix in 75 % of the rats in hCNG-II^{healthy} and hCNG-II^{diabetic} groups. In the groups of CFeCNG$^{2nd\text{-}healthy}$ and CFeCNG$^{2nd\text{-}diabetic}$, 100 % of rats had axons in the centre of the matrix; i.e. there were no differences between the groups.

Table 4.
Summary of the various models of chitosan conduits in Paper V.

Study	Experimental period	Identification of various chitosan conduits in Paper V	Number of animals (n)
1	120 days	hCNG-I = hollow chitosan conduit. CFeCNG^{1st} = 1st generation enhanced chitosan conduits with insert of membrane (film).	10 7
2	56 days	hCNG-II^{healthy} = hollow chitosan neve conduit. hCNG-II^{diabetic} = hollow chitosan nerve conduit in diabetic rats. CFeCNG$^{2nd\text{-}healthy}$ = chitosan nerve conduit with insert of perforated membrane (film) in healthy rats. CFeCNG$^{2nd\text{-}diabetic}$ = chitosan nerve conduit with insert of perforated membrane (film) in diabetic rats.	8 8 8 8
3	120 days	ANG = autologous nerve graft. hCNG-III = hollow chitosan nerve conduit. CFeCNG^{2nd} = chitosan nerve conduit with insert of perforated membrane. CFeCNG^{2nd}-SC-FGF-2^{18kDa} = second generation chitosan nerve conduit with insert of perforated membrane coated with FGF-2 overexpressing Schwann cells.	8 8 8 8

In contrast, we found differences within the distal nerve segment between the hCNG-II and CFeCNG^{2nd} groups, but not when comparing healthy with diabetic rats. We also observed axons in the distal nerve segment in 38 % of the rats reconstructed with hCNG-II^{healthy}, in 50 % of the rats with hCNG-II^{diabetic} conduits and 100 % in the rats with the CFeCNG$^{2nd\text{-}healthy}$ and CFeCNG$^{2nd\text{-}diabetic}$ chitosan nerve conduit groups. Thus, the "enhanced" chitosan conduits with perforated membrane inserts appeared to result in an improved axonal outgrowth compared to when nerves were repaired with hollow chitosan conduits.

There were significant differences at all three sites, i.e. at 3 mm, within the chitosan nerve conduit, and in the distal nerve segment, with more activated ATF-3 stained Schwann cells in the CFeCNG^{2nd} group compared to the hCNG-II group. Increased numbers of ATF-3 stained Schwann cells in the diabetic rats compared to the healthy rats, apart from at the 3 mm site, were observed. Differences were also found for all the chitosan conduit groups, with a higher number of apoptotic Schwann cells in the diabetic rats than in the healthy rats. No differences, however, were found between hCNG-II and CFeCNG^{2nd} groups in the centre of the chitosan conduits, but the diabetic rats had more apoptotic Schwann cells than the healthy rats. There were also more apoptotic Schwann cells in the healthy rats than in the diabetic rats in the distal nerve segment of the hCNG-II conduit group. The same results were found in the CFeCNG^{2nd} conduit group with more apoptotic Schwann cells in the healthy than in the diabetic rats.

When analysing the sensory neurons in the DRG, a higher number of activated ATF-3 stained sensory neurons were observed on the experimental side of the diabetic rats reconstructed with CFeCNG^{2nd} conduits than in healthy rats reconstructed with the same conduits. The HSP27 expression was also higher in the diabetic rats than in the healthy rats, but there were no differences between hCNG-II and CFeCNG^{2nd} conduits. The HSP27 ratio was significantly higher between healthy and diabetic rats as well as between the hCNG-II and CFeCNG^{2nd} conduits, with higher values in the group of CFeCNG$^{2nd\text{-}diabetic}$ chitosan nerve conduits.

Long-term evaluation

Macroscopic investigation of the chitosan nerve conduits after bridging a 15 mm nerve defect revealed that two cables within the chitosan nerve conduits were connected through the holes made in the membranes in the CFeCNG^{2nd} and CFeCNG^{2nd}-SC-FGF-2^{18kDa} groups of rats. Fifty percent of the rats with hCNG-I and 57 % of those with hCNG-III conduits had one cable. In 71 % of the rats with CFeCNG^{1st} and in 100 % of the rats with CFeCNG^{2nd}, the conduits contained two cables. Finally, in the CFeCNG^{2nd}-SC-FGF-2^{18kDa} group, two cables were observed in 86 % of the rats after long-term regeneration.

Motor recovery was assessed by electrophysiological tests and compared between the groups of rats, where the sciatic nerves had been reconstructed with the different chitosan nerve conduits. Assessment was made for up to 120 days after nerve reconstruction in studies 1 and 3. In study 1, we found that motor recovery in the PL muscle was improved after 60, 90, and finally 120 days in the hCNG-I and CFeCNG^{1st} groups of rats. The number of rats with improved motor function increased in CFeCNG^{1st} group particularly after 90 and 120 days. In study 3, all rats in the ANG group had noticeable motor reinnervation in the PL muscle after 60, 90 and 120 days. Improved PL muscle reinnervation was observed after 90 and 120 days in the hCNG-III, CFeCNG^{2nd} and CFeCNG^{2nd}-SC-FGF-2^{18kDa} groups of rats. Improvements were particularly noticeable in the CFeCNG^{2nd} group and several rats displayed better motor recovery than those in the other groups.

In study 1, the TA muscle motor function was improved at 60, 90, and 120 days in the hCNG-I and CFeCNG^{1st} group of rats. In study 3, the ANG group showed improved motor recovery in the TA muscle at all three time points. At 60 and 90 days, however, the hCNG-III and the CFeCNG^{2nd} groups of rats also displayed improved motor function, particularly the CFeCNG^{2nd} group, where almost the same number of rats as in the ANG group displayed full motor function. Unfortunately, the group of rats with CFeCNG^{2nd}-SC-FGF-2^{18kDa} chitosan nerve conduits did not display any kind of motor recovery at any time point. In study 3, the weight ratio analysis was performed for the TA and GA muscles. We found that the CFeCNG^{2nd} and ANG groups had similar results compared to the other groups, although the ANG group of rats had the highest weight ratio.

All groups of rats, regardless of type of reconstruction, responded to the von Frey test (sensory recovery) at 90 and 120 days in studies 1 and 3. The CFeCNG^{2nd} chitosan nerve conduit group of rats reached control levels after 120 days of reconstruction. There were no significant differences between the rats reconstructed with ANG and with the hCNG-III conduits, and the CFeCNG^{2nd}-SC-FGF-2^{18kDa} group of rats did not reach full sensory recovery even after 120 days.

The morphometric evaluation revealed significant differences between the healthy nerves and experimental groups concerning axon diameter, fibre diameter, g-ratio and myelin thickness, but no differences were observed among the experimental groups.

Discussion

Even though the development of techniques and methods for nerve repair and reconstruction, as well as the rehabilitation, have improved over the recent years, peripheral nerve injuries still give rise to short- and long-term consequences that pose a global clinical problem. From a functional perspective, the outcome after a peripheral nerve injury is still unsatisfactory [15, 36, 75, 106]. In the present thesis, the aim was to explore and evaluate experimental peripheral nerve regeneration after nerve injury inflicted on healthy and diabetic rats in order to enhance our understanding of how the regenerative process differs between healthy and diabetic conditions. The diabetic rat models used were selected specifically for their resemblance to human type 1 and type 2 diabetes (I, II, IV, V), and our studies were conducted using rats of both genders (II). We also used a variety of repair and reconstruction techniques, including common autologous nerve grafts but also hollow or modified chitosan conduits (III-V). Furthermore, in order to evaluate the regeneration process in detail, cell-signalling pathways induced by nerve injury, regeneration, and reconstruction, including those that activate or induce apoptosis in affected Schwann cells, were investigated (I-V).

Severed axons in the peripheral nervous system have the ability to regenerate after nerve injury and extend into the distal nerve end. However, when a disease, such as diabetes, is present this process may be impaired. Earlier studies have shown that Wallerian degeneration in experimental diabetes, such as in STZ-induced diabetes, can be delayed after nerve injury [23, 86]. The process of Wallerian degeneration is highly relevant for axonal outgrowth after a nerve injury and its delay impedes regeneration [107-109]. Diabetes affects both neurons and Schwann cells in the peripheral nervous system, which can be observed as a reduced amplitude and a slower conduction velocity of the nerve signals [108, 110]. Diabetes is also related to a reduced neurofilament expression, which is relevant for the nerve regeneration process [107, 108, 111]. Nerve regeneration is complex and several intracellular processes within neurons and Schwann cells, as well as extracellular processes, are generated to ensure regeneration and restoration of function after a peripheral nerve injury [12, 112]. Following a nerve injury, the affected Schwann cells usually dedifferentiate, upregulate specific substances and start to proliferate in order to support regeneration of the axons. Nonetheless, some sensory neurons still enter into apoptosis without the possibility of regeneration [43, 113]. Resident and recruited macrophages may also play an important role in

the regeneration process, since they enter the lesion site and migrate into the distal nerve end after the injury [7, 10].

Neuroma formation is the term used for the scarring of nervous tissue, which is often a consequence of nerve transection. To avoid neuroma formation, which may cause severe pain [114], the regenerating axons require some kind of guidance to be able to grow into the distal end of the injured nerve [115]. Biodegradable conduits, bridging the proximal and distal nerve ends, allow axon regrowth into a matrix formed within the conduit, and such conduits may therefore be useful in reconstructing shorter nerve defects [28, 73]. However, autologous nerve grafts still function as the gold standard in reconstruction, particularly when bridging longer nerve defects (III-V). To be able to introduce novel conduits into clinical practice, it is relevant to evaluate their efficacy in experimental animal models, examining not only healthy individuals, but also taking into account diseases, such as diabetes, and subject gender. The purpose of this thesis was to obtain such detailed information in relation to various nerve repair techniques.

Diabetes and gender affect nerve regeneration

It is important to understand and clarify how diabetes affects the peripheral nervous system after nerve injury. Most studies published to date have investigated STZ-induced diabetes in various animal models but mainly using male animals [23, 97]. In this thesis, we used genetically modified rats of both genders with symptoms that resemble type 1 or type 2 human diabetes. In Paper I, we used diabetic BB rats, which resemble human type 1 diabetes with symptomatic neuropathy [116]. To our surprise, these rats did not display any significant differences regarding axonal outgrowth compared to healthy rats. In contrast, previous studies, usually carried out with longer evaluation times, have shown reduced axonal outgrowth in this diabetic rat model compared to healthy rats, but the short evaluation time in our study (six days) may explain this discrepancy [107, 117]. The health status of the BB rats in our study did not allow any longer evaluation times without insulin treatment. Another possible explanation for the discrepancy in nerve regeneration in this BB model between previous studies and ours could be the age of the rats, considering the time factor for developing diabetes [118, 119]. At least at the start of the nerve regeneration process, there is a possibility that some functional ß-cells may remain in this rat model and, therefore, may still maintain the insulin pathway, which could affect nerve regeneration positively. A recently published study indicated that BB rats develop diabetes between 8 and 16 weeks of age and that at least 20 % of the ß-cells may still be active at the time of diagnosis [118, 119]. In our study, we used

7-week-old rats, so a possible explanation for the similarities in axonal outgrowth between the BB and healthy rats in Paper I, is that the BB rats could still have had active ß-cells. Nonetheless, the BB rats in our study displayed clinical signs of diabetes, including high blood glucose values.

Genetically modified rat models are uncommon in studies of nerve regeneration. Most previous in vivo studies have used rats with STZ-induced diabetes, often with a long evaluation time after nerve injury and repair [23, 86]. STZ-induced diabetes in rats may not, however, be optimal for extrapolation of nerve injury results to human subjects with type 1 or type 2 diabetes, as insulin is probably still produced in this model [99]. In addition, since insulin can act as a growth factor in the MAPK pathway, which has been linked to Schwann cell proliferation, it may indirectly affect axonal outgrowth [23, 81, 120, 121]. An interesting finding in our studies of Schwann cells was an increase in both the number of activated ATF-3 stained and apoptotic cleaved caspase-3 stained Schwann cells at the lesion site in the diabetic BB rats compared to the healthy rats at six days after nerve injury and repair. This result may indicate a more pronounced injury process in the diabetic BB rats with a more extensive up-regulation of Schwann cells to compensate for the injury, which may be necessary for axonal outgrowth. This finding could then also explain the observed similarities in axonal outgrowth between healthy and diabetic BB rats [122]. However, the diabetic environment in the BB rats may also induce oxidative stress, which is a disruption in the balance between reactive oxygen species (called free radicals) and antioxidant defensive structures [123]. Interestingly, an earlier study shows that treatment with antioxidants reduced the symptoms of diabetic neuropathy [124]. Indeed, oxidative stress imposed on Schwann cells, as well as the development of Schwann cell apoptosis, may lead to degeneration of the nerve [125, 126]. In the distal part of the sciatic nerve in the diabetic BB rats, a pattern similar to that observed at the lesion site was noted, with higher numbers of activated and apoptotic Schwann cells than in the healthy rats (I). There is probably a delicate balance between activated and apoptotic Schwann cells that is essential for axonal outgrowth [43, 44]. This is also indicated in the present studies using GK rats. On the other hand, this result could indicate that the high number of activated Schwann cells in the BB rats is due to an ongoing repair process, as has been described in other studies [52, 127].

Another diabetic animal model, probably better suited for diabetes studies than the BB rats, is the genetically modified GK rat, with milder diabetic symptoms and lower levels of blood glucose compared to the BB rats. The GK rats have activated insulin-producing ß-cells, and therefore survive for longer periods of time without insulin treatment, making this a more appropriate model for extrapolating results to human diabetes. For this reason, this model was selected for experiments in most of the papers in this thesis (II, IV, V). Another advantage of this model is that the blood glucose values remain stable for a longer period [25, 128], making

behavioural studies possible. It also enables long-term evaluation of the effects of nerve repair and reconstruction, even in delayed nerve procedures.

In Paper II, we observed differences between male and female diabetic GK rats regarding the length of the axonal outgrowth. After direct nerve repair and evaluation at six days, we found longer axonal outgrowth in the males than in the females. The same results were found in healthy rats, where longer axonal outgrowth, as assessed by neurofilament staining, was observed in the males than in the females. We found more activated and apoptotic Schwann cells, both at the lesion site and in the distal part of the nerve, in the GK rats compared to the healthy rats, which may contribute to the observed differences in axonal outgrowth. The insulin production in the GK rats, with modest blood glucose values, may also exert an influence on axonal outgrowth, but this probably differs in male and female rats. Previous clinical findings imply that there are also gender differences in humans, with higher insulin secretion in females [129]. Furthermore, in Paper II, the number of ATF-3 and cleaved caspase-3 stained Schwann cells at the lesion site correlated positively with blood glucose values in the GK rats, possibly indicating that blood glucose regulates the balance between activated and apoptotic Schwann cells after nerve injury influenced by diabetes.

One limitation in Papers I and II is the time aspect, making only short-term nerve regeneration possible. However, investigating short-term regeneration under the influence of hyperglycaemia was indeed the aim of the study. Most previously published studies have analysed the regeneration processes for longer periods of time and they have shown more pronounced differences between healthy and diabetic animals, with less axonal outgrowth in the diabetic animals than in the healthy animals. Hence, the time factor appears to be important for both the degeneration and regeneration processes under diabetic conditions [127, 130]. In our case, longer periods of observation were not possible for the diabetic BB rats since they were not treated with insulin and would therefore not have survived.

Only a few studies in the field have evaluated the influence of gender on nerve injury and regeneration and most of the experimental studies have used either male or female rats [131, 132]. Interestingly, a recently published study in the field of gender differences describes the importance of using both female and male animals in experimental studies with regard to a number of parameters [133]. This is in agreement with the aim of this thesis, where we decided to use healthy and diabetic rats of both genders. Furthermore, clinical studies show that male subjects with diabetes are more likely to develop peripheral neuropathy than female subjects, a fact that has not yet been explained [83, 134]. Remarkably, gender differences were indeed revealed in the present thesis, with longer axonal outgrowth in male than in female rats. One reason for the improved nerve regeneration in the male rats could be the impact of the neuroactive male hormone

testosterone, as it affects the peripheral nervous system by influencing Schwann cell proliferation and also by regulating specific transcription factors [135]. Sex hormones, such as testosterone in males and progesterone in females, could therefore be of potential value in treatment for diabetic neuropathy [136]. Conversely, diabetes affects the levels of the neuroactive hormones negatively, which could have a negative impact on the process of nerve regeneration [83, 137].

Reconstruction of the injured sciatic nerve using chitosan conduits

Selection of chitosan conduits

Chitosan is an interesting material for nerve repair and regeneration of tissue and because of its possible application in humans [20, 73]. One advantage of using chitosan conduits for reconstruction is that the original material, chitosan, is already manufactured to approved ISO-standard protocols for medical units - a necessary prerequisite for commercialization and access to the clinical market. After successful in vivo and in vitro studies, chitosan conduits have recently been approved for clinical application in Europe (CE mark, Reaxon®Nerve guide). Hollow chitosan conduits of three different degrees of acetylation (DAs) were tested in Paper III to identify a conduit that could appropriately be used to reconstruct a 10 mm long nerve defect. Based on a number of variables, the DAII chitosan conduit was found to be the best alternative and was therefore selected for the continuing studies of reconstruction and nerve regeneration. We also selected a minimum of three weeks for nerve regeneration, since this was the point at which the conduits contained a completely formed and sufficient matrix between the nerve ends. Paper III contains results from both in vivo and in vitro analyses. We evaluated the effect of reconstruction with chitosan conduits at different time points, and compared hollow chitosan conduits with autologous nerve grafts. In clinical reconstruction of a nerve injury with a defect, i.e. when suturing of the nerve ends is prohibited, the autologous nerve graft is “the gold standard” model [36, 62, 75]. Reconstruction with other available conduits remains limited, despite considerable advances in the development in various artificial nerve conduits, since few nerve defects can be bridged and the functional outcome is not satisfactory. For this reason they are less frequently used in clinical practice [74].

Several measurable parameters were interesting in this study, including investigation of the chitosan material itself and comparison of the three levels of

chitosan acetylation to enable selection of the most appropriate conduit. These parameters were evaluated by measurements of material degradation time, matrix formation, cellular reactions and axonal outgrowth observed by immunohistochemistry and histology as well as functional evaluation. Previously, silicone conduits have been used for reconstruction of smaller nerve defects (about 10 mm) in rats, but the material is non-degradable and is not suitable for reconstruction of longer nerve defects [138]. Any conduits made of material foreign to the body are required to degrade within a suitable time after nerve reconstruction to avoid adverse biological reactions, which would require a second operation to remove the conduits [74]. In this respect, numerous commercial conduits made of different materials have been tested over the years with varying results. It has been particularly difficult to reconstruct longer nerve defects (more than 30 mm) [74]. The three most widely described, and also most clinically used, conduits are made of collagen (NeuraGen™), polyglycolic acid (Neurotube™; PGA), or polylactide caprolactone (Neurolac™; PCL). These conduits have, however, only been tested in reconstructions of nerve defects shorter than 30 mm [139, 140]. An earlier study revealed that nerve regeneration failed in a number of patients after nerve reconstruction with NeuraGen™ conduits, which proved unable to provide the necessary scaffold for more than 6 months. This type of conduit is therefore not a good alternative for reconstruction of longer nerve defects [141]. A similar problem has been noted with the use of Neurotube™ conduits, which were found to have degraded completely after 9 months leaving a nerve defect between the nerve ends [142]. Another study describes fragmentation, massive swelling, and inflammation at 24 months after reconstruction with Neurolac™ conduits [143], which also makes it unsuitable for reconstructing nerves after injury.

Macroscopically, degradation of the DAI and DAII (low and medium acetylation degrees) chitosan conduits did not differ at 13 weeks, but the conduit with the highest degree of acetylation (DAIII) already started to degrade at 18 days and was almost completely degraded at 13 weeks. This finding corroborates results from a previous study [144], where the authors found that the degradation of low (1 %) and medium (5 %) DA was insignificant and there were no signs of degradation after 13 weeks. The criteria for producing an appropriate artificial conduit for both shorter and longer nerve defects should be as follows: the material must be able to provide a structure for the axons to grow in the appropriate direction; it must be able to avoid misdirection of axons; and it must be able to support sufficient axonal outgrowth to lead to functional recovery. Furthermore, to meet grafting requirements, the material needs to be 1) biocompatible, 2) non-toxic, 3) degradable within a suitable time frame, 4) transparent, which is important for correct positioning of the conduit after nerve reconstruction, 5) elastic, 6) easy to handle and 7) produced in a reasonable time at reasonable cost [74, 145].

Implantation with the three types of chitosan conduits had similar effects on investigated mRNA levels in the corresponding DRG at 5 and 18 days after nerve reconstruction. The data revealed an up-regulation of the neurotrophic factors (i.e. BDNF, FGF-2, and NGF), as well as the cytokine IL-6, and GAP-43 at both 5 and 18 days. An exception was the Trk-B receptor, which remained stable in all groups of chitosan conduits as well in the control DRG group. Generally, mRNA levels for the investigated neurotrophic factors, the cytokine receptor and GAP-43, were found to increase between 1 and 4 days after nerve injury, they then plateaued and started to decrease again around 7 to 14 days [146, 147]. We found that bridging a 10 mm nerve defect with chitosan conduits had no effect on these molecular processes, indicating that the chitosan material does not appear to exert negative effects on nerve reconstruction. In addition, a complete matrix was found to be formed between the proximal and the distal nerve ends of the transected sciatic nerve in all three DA groups of chitosan conduits. The thickness of the matrix was similar at all measured levels, and in all the three DA, and it resulted in similar axonal outgrowth. The matrix formed within the conduits has previously been described as crucial for axonal outgrowth and for successful nerve regeneration [72, 148]. We therefore investigated the number of activated and apoptotic Schwann cells within the matrix. The results, which are detailed in Paper III, revealed no differences in the numbers of activated Schwann cells in the matrix between the three DA groups of chitosan conduits at 21 days after nerve reconstruction. However, a significant increase in apoptotic Schwann cells was found in the matrix of the DAIII chitosan conduits. In the distal nerve end, we found more activated Schwann cells when using the DAIII chitosan conduits, and fewer activated Schwann cells after using the DAI conduits, both compared to the DAII conduits at the same level. No differences in cleaved caspase-3 stained Schwann cells in the distal nerve were observed among the three groups.

Taken together, these findings were not sufficient to allow selection of a specific group of chitosan conduits for continued use. Nonetheless, the importance of specific biomaterials for encouraging Schwann cell viability, proliferation and cell adhesion has been described in previous in vitro studies and such parameters could be crucial for successful nerve regeneration after nerve reconstruction with conduits [149]. For instance, Schwann cell proliferation and its importance for axonal outgrowth has been reported to be dependent on the degree of acetylation of the chitosan conduit [150]. Early in vitro studies suggest that the degree of acetylation should be between 5-10% for the optimal spread and proliferation of Schwann cells [150, 151]. Our data revealed no differences in number of ED1 stained macrophages after 18 days or at 13 weeks between the various types of chitosan conduits. The inflammatory reaction with ED1 macrophages was observed to be lower over time; although with no differences between the chitosan conduits. This result was expected, since an inflammatory process is required for

dealing with axonal debris. However, since an inflammatory process was still observed at 13 weeks, even within the DAIII conduits, this could pose a potential risk for degradation of the formed matrix (III). We, therefore, decided to exclude this group of conduits from our further studies. In the DAI group of chitosan conduits, we found increased sprouting after nerve reconstruction. Since a higher degree of sprouting may cause re-innervation of undesired targets, we decided that this group was also less suitable for further use [152].

Functional recovery after reconstruction using chitosan conduits

Clinically, the functional outcome when reconstructing severed nerves using conduits of different materials, has often been inadequate [68]. This could be related to the length of the nerve defect as well as the nerve injury itself, where the endoneurial tube of the distal nerve end is damaged to such an extent that it cannot provide outgrowing axons with proper guidance to reach the correct target [75]. In Paper III, the results of the SSI test revealed no improvement over time, whereas the electrophysiological recordings showed a significant improvement. These contradictory results have been reported previously and need to be considered in future studies [153], but the improvement in electrophysiological variables could be due to a maturation process [154]. Nevertheless, electrophysiological tests, together with morphological tests, are still important for evaluating nerve regeneration after nerve repair or reconstruction in rats [155]. The electrophysiology tests, the measuring of CMAP levels in Paper III, revealed almost full reinnervation in TA (62 %) and PL (80 %) muscles after reconstruction with autologous nerve grafts compared to reconstruction with chitosan conduits (6-29 % in TA and 33-50 % in PL muscles). At the last measurement (at 12 weeks), complete reinnervation was observed with reconstructions using any group of chitosan conduits and the results attained levels similar to those where autologous nerve grafts were used. A previous study has stressed the presence of misguided directional axons, which prevents other axons from reaching their target, and which may instead allow a single axon to reinnervate several muscles via branches [155]. Such increased sprouting may, however, lead to disturbed reinnervation and improper motor coordination [155]; however, it is even more important in sensory nerve regeneration, where misdirection is deleterious for functional recovery.

To conclude, the results of the studies conducted and described in Paper III, show that regeneration when using the DAII group of chitosan conduits (i.e. medium acetylation) was accompanied by less sprouting and a shorter degradation time compared to when DAI and DAIII chitosan conduits were used. Therefore, DAII chitosan conduits were selected for further investigation of nerve regeneration in

longer nerve defects (15 mm; Paper V) after primary and delayed nerve reconstruction [156].

Nerve regeneration in chitosan conduits and autologous nerve grafts

When comparing the effect of chitosan conduits and autologous nerve grafts in healthy and diabetic GK rats, an improved axonal outgrowth was observed in the autologous nerve grafts in both healthy and diabetic rats (IV). Surprisingly, axonal outgrowth was improved in the diabetic GK rats compared to in the healthy rats, when reconstructed both with chitosan conduits and autologous nerve grafts (IV). These results appear to contradict the findings in Paper II, where short-term nerve regeneration was studied after direct nerve repair, and where we observed an improved axonal outgrowth in the healthy rats compared to the diabetic GK rats. A possible explanation for this discrepancy could be that in Paper II the axons, after transection and direct nerve repair, grow directly into the distal nerve end *that* has an appropriate vascularized environment with all the benefits still available for nerve regeneration [157]. In Paper IV, the sciatic nerve was transected, the nerve segment rotated and then re-sutured back into the sciatic nerve defect resulting in a non-vascularized path encountered by the axons before they reached the vascularized distal nerve segment. Thus, the Schwann cells in the autologous nerve grafts in Paper IV depend on diffusion of oxygen from surrounding tissue in order to survive before microcirculation before microcirculation recovers within the graft. Such revascularization starts approximately 3 days after nerve repair in autologous nerve grafts [157]. Wallerian degeneration starts immediately after injury, but the speed can be affected by the condition of the microcirculation with subsequent delayed axonal outgrowth due to the tissue niche [157-160].

Nerve regeneration and influence of diabetes after nerve reconstruction

The hollow DAII chitosan conduits were found to be suitable for reconstruction of a 10 mm long nerve defect in healthy and diabetic GK rats (IV). In these experiments, we found that a matrix successfully formed inside all chitosan conduits in both healthy and diabetic GK rats. However, and as expected, better axonal outgrowth was observed in the autologous grafts than in the chitosan conduits (IV). More activated Schwann cells were observed in the autologous nerve grafts than in the chitosan conduits, which may explain the longer axonal outgrowth in the autologous graft. The higher number of activated Schwann cells was accompanied by an increased number of apoptotic Schwann cells, indicating a balance between activated and apoptotic Schwann cells. The longer axonal

outgrowth also positively correlated with blood glucose values in the diabetic GK rats after both reconstruction methods. A similar correlation was found in Paper II using a different treatment after nerve injury; i.e. direct nerve repair. In Paper I on the other hand, where the nerve injury in the BB rats, which displayed higher blood glucose values, was also directly repaired with sutures, these values did not correlate to length of axonal outgrowth. Since the results differed between BB and GK rats, these findings may indicate that the levels of blood glucose are important for axonal outgrowth and there is a substantial risk that high blood glucose is detrimental to the regeneration process. The effect of blood glucose on axonal outgrowth after nerve reconstruction of a minor nerve defect has been demonstrated in an earlier study [161]. In that study, there was an incompletely formed matrix between the nerve ends after the nerve injury in STZ-induced diabetic rats with higher blood glucose values, i.e. around 30 mmol/l [161]. These results are very different from the findings in the GK rats used in Papers II, IV and V, with modest blood glucose values and a completely formed matrix but still with the same evaluation time (21 days).

Modification of the chitosan conduits and addition of Schwann cells

Even in the diabetic GK rat model, a complete matrix, which is a prerequisite for axonal outgrow and functional recovery, was observed bridging a short nerve defect, 10 mm, within the chitosan conduit. This could indicate that the environment in the diabetic GK rat model may play the main part in nerve regeneration. To investigate longer nerve defects, nerve regeneration after reconstruction of a longer nerve defect (15 mm) was studied using “enhanced” chitosan nerve conduits, where a chitosan membrane with or without perforations (V) was introduced and compared to hollow chitosan nerve conduits in healthy and diabetic GK rats. In the macroscopic evaluation of the groups of $CFeCNG^{2nd}$ (inserted perforated membranes) and $CFeCNG^{1st}$ (inserted membranes) chitosan nerve conduits, we found extended cables (i.e. matrices; two cables instead of one) in both the healthy and the diabetic GK rats after short periods of time (56 days). These extended cables are probably the cause of the longer axonal outgrowth with visible axons in the distal part of the nerve. In addition, in some of the experiments the inserted perforated membrane was seeded with genetically modified Schwann cells (i.e. $CFeCNG^{2nd}$-SC-FGF-2^{18kDa}) with the aim of improving nerve regeneration over extended (15 mm) nerve defects in healthy Wistar rats. Previous in vitro studies show a positive effect of chitosan, both regarding cell-adhesion and Schwann cell proliferation [68, 149]. Furthermore, in vivo and in vitro studies indicate that nerve regeneration can be improved after nerve reconstruction using modified Schwann cells inserted in chitosan conduits [162-164]. However, the results in Paper V revealed no improvement of the nerve regeneration process or

functional recovery after nerve reconstruction in the long-term (after 120 days) with the perforated membrane insert with genetically modified Schwann cells (i.e. CFeCNG^{2nd}-SC-FGF-2^{18kDa}), compared to nerve conduits without such cells in healthy rats. It is possible that insufficient modified Schwann cells survived inside the chitosan nerve conduits in our study and that they were therefore not available to support axonal outgrowth.

Another interesting result was obtained in Paper V, where axonal outgrowth was improved when the healthy and GK rat sciatic nerve was reconstructed with chitosan nerve conduits equipped with a perforated membrane (CFeCNG^{2nd}). Prior to the analysis of the formed matrix/cables in Paper V, the neovascularization was investigated by means of visual observation in all experimental groups (both short- and long-term). Thin blood vessels were observed in the matrix/cables which in turn were connected to the membrane insert, especially in the diabetic GK and healthy Wistar rats where the nerve had been reconstructed with "enhanced" chitosan nerve conduits (CFeCNG^{2nd}). An increased neovascularization is necessary after nerve reconstruction and probably affects the axonal outgrowth positively by providing cells with proper nutrition and oxygen [159].

The improvement of muscle innervation in Paper V was noted in all groups of chitosan conduits after 120 days in both PL and TL muscle. The sciatic nerves reconstructed with conduits containing perforated membranes (CFeCNG^{2nd}) had the best recovery compared to the hollow conduits (hCNG-II) and the conduits with inserted non-perforated membranes (CFeCNG^{1st}). The von Frey test also indicated the same results, with almost normal values in the sensory recovery after nerve reconstruction with the CFeCNG^{2nd} conduits at long-term evaluation.

Early clinical studies reveal that increased levels of HSP27 are coupled to neuroprotection after nerve injury in patients with diabetes, which partially protect them from insufficient nerve function and are therefore an important factor in patients with diabetes [165, 166]. In Paper V, the HSP27 levels were higher in the sensory neurons in the diabetic GK rats than in the healthy Wistar rats. This finding is in line with the results from previous clinical studies investigating peripheral neuropathy [60, 165]. A recently published paper also confirms these results, although the authors had investigated delayed nerve reconstruction [156]. Nonetheless, high intensity of HSP27 was observed and a concomitant higher degree of neuroprotection was found in the diabetic GK rats after nerve injury and reconstruction. In Paper V the diabetic GK rats had more activated sensory neurons, especially in the group of CFeCNG^{2nd}chitosan nerve conduits, than the healthy rats reconstructed using the same conduit, in the short term. Thus, this may be a compensatory and protective mechanism. However, when all results were processed and validated in Paper V, we could conclude that the "enhanced" chitosan conduit CFeCNG^{2nd}group, both in healthy and diabetic GK rats in the

short and long term, provided the optimal nerve regeneration. This result is promising for further studies in the field of nerve reconstruction using modified chitosan nerve conduits.

Conclusions

- There are no differences, short term, in axonal outgrowth between diabetic BB rats and healthy rats, despite increased numbers of activated and apoptotic Schwann cells in the BB rats after nerve injury and repair.
- After short-term evaluation, gender differences are found in nerve regeneration following a sciatic nerve injury and repair in healthy and GK diabetic rats, with improved axonal outgrowth in healthy rats. Axonal outgrowth is increased in male rats with more activated Schwann cells compared to female rats, particularly in diabetic conditions, in which apoptotic Schwann cells are also more numerous after short-term evaluation.
- Hollow chitosan conduits can support both short- and long-term nerve regeneration through the formation of a regenerative matrix after a sciatic nerve reconstruction of a 10 mm long defect in healthy rats. Any differences between the activated or apoptotic Schwann cells inside the matrix or in the distal part of the nerve have no real impact on axonal outgrowth. Conduits with medium acetylation appear to be the most appropriate of the three different conduits tested.
- Nerve regeneration is superior in autologous nerve grafts compared to hollow chitosan conduits when reconstructing a 10 mm long sciatic nerve defect in both healthy and GK rats after short-term evaluation. Axonal outgrowth is also improved in diabetic GK rats after nerve reconstruction using autologous nerve grafts and hollow chitosan conduits in the short-term. There are higher numbers of activated and apoptotic Schwann cells after reconstruction with autologous nerve grafts. The thickness of the matrix, formed between the proximal and distal nerve ends in the chitosan conduits, influences axonal outgrowth in both GK and healthy rats.
- Functional and morphological recovery is improved after reconstruction of 15 mm long sciatic nerve defects using chitosan nerve conduits modified with a perforated membrane insert compared to when hollow chitosan conduits are used, both in healthy and in GK rats after short- and long-term evaluations. Addition of FGF-2 overexpressing Schwann cells did not further improve regeneration.

Sammanfattning/Summary in Swedish

Perifera nerver förmedlar känsel- och smärtsignaler från bland annat huden till ryggmärg och hjärna, liksom impulser till muskler i bl.a. armar och ben. Skador på dessa nerver kan ge varierande grader av känsel- och muskelbortfall. Kirurgisk behandling av nervskador med komplett kontinuitetsavbrott resulterar oftast i bristande återhämtning hos vuxna, vilket kan utgöra ett stort problem för individen.

Diabetes är en sjukdom som påverkar såväl funktionen i perifera nerver som nervläkningen efter skada. Sjukdomen medför därutöver risk för nervkomplikationer som förefaller uppkomma tidigare hos män än hos kvinnor. Kunskap om läkning och läkningsmekanismer hos båda könen efter nervskador med kontinuitetsavbrott är ofullständig, både vad gäller friska individer och patienter med diabetes.

Efter en perifer nervskada med kontinuitetsavbrott förstörs (degenererar) nervtrådarna (axonerna) bortom skadan, medan de stödjeceller (Schwann celler) som omger nervtrådarna bibehålls. Dessa celler reagerar på skadan och ”städar” upp i nerven bortom skadan, samt hjälper till att stimulera nervtrådarnas återväxt ut till känselkroppar och muskler (målorgan). Vid behandling av en nervskada repareras eller rekonstrueras (överbryggas) denna beroende på hur stort eller litet mellanrummet är mellan nervändarna. Antingen kan skadan sys ihop direkt (sutur) eller – om defekten är mer omfattande – överbryggas med en mindre viktig nerv som ”offras”, ett s.k. nervgraft. Meningen är att de skadade nervtrådarna skall kunna växa ut till målorganen igen genom att utnyttja nervgraftet som en bro.

I en del fall där nervgraft inte är möjliga, eller mindre lämpliga, kan de ersättas med konstgjorda material. Dessa material kan även vara tillämpliga vid kirurgisk behandling av nervskador med kontinuitetsavbrott på patienter med diabetes, men här är kunskapen om läkningsprocessen bristfällig. Vid utveckling av nya material måste man därför beakta att de även skall kunna användas på individer med diabetes.

I den här avhandlingen beskriver jag studier utförda på friska och diabetiska hon- och hanråttors nervtrådar och deras stödjeceller, samt hur läkningsmekanismerna efter en nervskada med komplett kontinuitetsavbrott påverkas efter sutur eller rekonstruktion med ett nervgraft eller ett konstgjort material. Två modeller av råttor med diabetes och olika blodsockernivåer, BB (Biobreeding; liknar mer s.k.

typ 1 diabetes) och GK (Goto-Kakizaki; liknar mer s.k. typ 2 diabetes; har lägre blodsockernivåer än BB-råttor), har använts och jämförts med friska råttor.

Utväxten av nervtrådarna och antalet stödjeceller har studerats i friska och diabetiska hon- och hanråttor. Jag har även utvärderat en ny sorts konstgjord nervtub tillverkad av kitin, som är ett naturligt material, ursprungligen från kräftdjur. Genom en specifik process tillverkas en kitosan-nervtub som är vävnadsvänlig, vilken kroppen inte reagerar negativt på.

En rekonstruktion av en nervdefekt med denna nervtub gjordes i friska och diabetiska råttor för att se hur nervtrådarna växte ut i jämförelse vid användning av ett nervgraft. Jag undersökte om stödjecellerna kring nervtrådarna ökar eller minskar i antal efter sutur eller rekonstruktion av nervskadan i de olika modellerna. Möjligheten att påskynda nervtrådarnas utväxt vid en längre nervdefekt undersöktes också genom att modifiera nervtuben med insättning av membran och stödjeceller.

Någon skillnad i längden på de utväxta nervtrådarna mellan de friska och de diabetiska BB-råttorna efter direktsutur kunde inte påvisas, medan det däremot förelåg en skillnad i antalet stödjeceller. Efter sutur av nervskadan hos friska och diabetiska GK-råttor noterades en bättre utväxt av nervtrådarna hos hanarna jämfört med hos honorna både i de friska och i de diabetiska råttorna.

Vid rekonstruktion av nervskada med en mindre substansdefekt understödde den tomma tuben av kitosan läkningen i både friska och diabetiska råttor, men nervgraft gav ett bättre resultat. Intressant nog var utväxten av nervtrådarna efter rekonstruktion med nervgraft eller tom nervtub bättre i de diabetiska GK-råttorna än hos de friska råttorna. Även antalet stödjeceller skiljde sig. Rekonstruktion av en längre nervdefekt med en modifierad nervtub, innehållande membran, gav ett bättre resultat jämfört med en helt tom nervtub. Tillägg av extra stödjeceller hade ingen effekt.

Sammanfattningsvis har avhandlingen påvisat skillnader i läknings-mekanismer mellan friska och diabetiska råttor – beroende på diabetesmodell – samt mellan han- och honråttor efter såväl reparation som rekonstruktion av en komplett skada på en perifer nerv. En nyutvecklad nervtub (s.k. kitosantub), särskilt när den modifierats med membran, kan användas för att rekonstruera nervskador och kan även tillämpas på patienter med diabetes. Nervtuben har genom våra och andra studier godkänts för användning i kliniska försök i Europa.

Acknowledgements

I would like to thank all those who supported this project financially: the Swedish Research Council (Medicine), Lund University, Region Skåne and Skåne University Hospital (Malmö-Lund), Sydvästra Skånes Diabetesförening, the Swedish Diabetes Foundation, and European Community's Seventh Framework Programme (FP7-HEALTH-2011) under grant agreement n°278612 (BIOHYBRID). I gratefully acknowledge the supply of the chitosan raw material by Altakitin S.A., Portugal, and the making of chitosan conduits by Medovent GmbH, Germany.

Lars Dahlin, my supervisor, Department of Translational Medicine, Hand Surgery, Malmö, thank you for your superb knowledge in the field of hand surgery and peripheral nerve regeneration. You are an extraordinary and excellent researcher and clinician. Without your help, this work would neither have been possible nor completed. Thank you for all the hours and efforts you put into it.

Martin Kanje, my first co-supervisor, Department of Biology, Lund, who sadly passed away in March 2013. Martin was an important source of knowledge for the design of the present project, but unfortunately he was not able to see it finalized. Martin should be remembered as an outstanding scientist in the field of peripheral nerve regeneration and he will continue to be an inspiration in my research.

Charlotta Blom, my second co-supervisor, Synergon AB Göteborg, thank you for your kindness and for believing in me. For all your outstanding knowledge in the field of neuroscience, for your writing skills, but also for your patience, excellent advice and your time.

Tina Folker, research administrator, Department of Translational Medicine, Hand Surgery, Malmö. Firstly I am grateful to you for your friendship and all the "bio" visits after eating cakes at Hollandia and secondly, for always helping me (with a smile) with different, important and essential administrative things over the years. Last, but not least, for your unfailing support, encouragement and belief in me! You are such a good person!

Jonas Björk, Department of Epidemiology Lund, thank you for the statistical advice.

Thanks to **Claudia Grothe** and **Kirsten Haastert-Talini** from the Institute of Neuroanatomy, Hannover Medical School for your invaluable cooperation.

Thanks to the whole **BIOHYBRID** - consortium of outstanding researchers with immense knowledge, some of whom were also co-authors in two of my papers.

I would also like to express my gratitude to **Silke Fischer**, **Natascha Heidrich**, **Jennifer Metzen**, **Hildegard Streich**, **Maike Wesemann** (all from the Institute of Neuroanatomy, Hannover Medical School) for their technical support.

Camilla Orbjörn, **Bodil Roth**, **Marcus Ljunqvist**, **Nina Schultz**, **Elin Byman**, **Malin Wennström**, my colleagues and friends at the Wallenberg Laboratory, Malmö. You all contribute to the friendly and inspiring atmosphere at lab.

Hanna Frost, Department of Translational Medicine, Hand Surgery, Malmö, thanks for all your support.

Gerry Jönsson, Clinical Research Center (CRC), Malmö, for always being helpful and engaged. I also want to thank the rest of the staff at CRC animal facilities, for their very professional care of the animals.

A big thank you to all my dear **Friends** for your understanding and positive support.

Finally, my heartfelt thanks to my **Family,** the most important people in my life. Thank you for endless love, support and encouragement during this time.

References

1. Krivickas LS, Wilbourn AJ: Peripheral nerve injuries in athletes: a case series of over 200 injuries. Semin Neurol 2000, 20(2):225-232.
2. Bekelis K, Missios S, Spinner RJ: Restraints and peripheral nerve injuries in adult victims of motor vehicle crashes. J Neurotrauma 2014, 31(12):1077-1082.
3. Lohmeyer JA, Hulsemann W, Mann M, Schmauss D, Machens HG, Habenicht R: [Return of sensitivity after digital nerve reconstruction in children: how does age affect outcome?]. Handchir Mikrochir Plast Chir 2013, 45(5):265-270.
4. Thorsen F, Rosberg HE, Steen Carlsson K, Dahlin LB: Digital nerve injuries: epidemiology, results, costs, and impact on daily life. J Plast Surg Hand Surg 2012, 46(3-4):184-190.
5. Bekelis K, Missios S, Spinner RJ: Falls and peripheral nerve injuries: an age-dependent relationship. J Neurosurg 2015, 123(5):1223-1229.
6. Ciaramitaro P, Mondelli M, Logullo F, Grimaldi S, Battiston B, Sard A, Scarinzi C, Migliaretti G, Faccani G, Cocito D *et al*: Traumatic peripheral nerve injuries: epidemiological findings, neuropathic pain and quality of life in 158 patients. J Peripher Nerv Syst 2010, 15(2):120-127.
7. Dahlin LB: Nerve injuries. Current Orthopaedics 2008, 22:9-16.
8. Chemnitz A, Bjorkman A, Dahlin LB, Rosen B: Functional outcome thirty years after median and ulnar nerve repair in childhood and adolescence. J Bone Joint Surg Am 2013, 95(4):329-337.
9. Rosberg HE, Carlsson KS, Cederlund RI, Ramel E, Dahlin LB: Costs and outcome for serious hand and arm injuries during the first year after trauma - a prospective study. BMC Public Health 2013, 13:501.
10. Fex Svennigsen A, Dahlin LB: Repair of the Peripheral Nerve-Remyelination that Works. Brain Sci 2013, 3(3):1182-1197.
11. Palispis WA, Gupta R: Surgical repair in humans after traumatic nerve injury provides limited functional neural regeneration in adults. Exp Neurol 2017, 290:106-114.
12. Raivich G, Makwana M: The making of successful axonal regeneration: genes, molecules and signal transduction pathways. Brain Res Rev 2007, 53(2):287-311.
13. Grinsell D, Keating CP: Peripheral nerve reconstruction after injury: a review of clinical and experimental therapies. Biomed Res Int 2014, 2014:698256.
14. Jonsson S, Wiberg R, McGrath AM, Novikov LN, Wiberg M, Novikova LN, Kingham PJ: Effect of delayed peripheral nerve repair on nerve regeneration, Schwann cell function and target muscle recovery. PLoS One 2013, 8(2):e56484.
15. Isaacs J: Treatment of acute peripheral nerve injuries: current concepts. J Hand Surg Am 2010, 35(3):491-497; quiz 498.

16. Campbell WW: Evaluation and management of peripheral nerve injury. Clin Neurophysiol 2008, 119(9):1951-1965.
17. Ichihara S, Inada Y, Nakamura T: Artificial nerve tubes and their application for repair of peripheral nerve injury: an update of current concepts. Injury 2008, 39 Suppl 4:29-39.
18. de Ruiter GC, Spinner RJ, Yaszemski MJ, Windebank AJ, Malessy MJ: Nerve tubes for peripheral nerve repair. Neurosurg Clin N Am 2009, 20(1):91-105, vii.
19. Freier T, Koh HS, Kazazian K, Shoichet MS: Controlling cell adhesion and degradation of chitosan films by N-acetylation. Biomaterials 2005, 26(29):5872-5878.
20. Freier T, Montenegro R, Shan Koh H, Shoichet MS: Chitin-based tubes for tissue engineering in the nervous system. Biomaterials 2005, 26(22):4624-4632.
21. Obrosova IG: Diabetes and the peripheral nerve. Biochim Biophys Acta 2009, 1792(10):931-940.
22. Ogurtsova K, da Rocha Fernandes JD, Huang Y, Linnenkamp U, Guariguata L, Cho NH, Cavan D, Shaw JE, Makaroff LE: IDF Diabetes Atlas: Global estimates for the prevalence of diabetes for 2015 and 2040. Diabetes Res Clin Pract 2017, 128:40-50.
23. Nishida N, Yamagishi S, Mizukami H, Yagihashi S: Impaired nerve fiber regeneration in axotomized peripheral nerves in streptozotocin-diabetic rats. J Diabetes Investig 2013, 4(6):533-539.
24. Srinivasan K, Ramarao P: Animal models in type 2 diabetes research: an overview. Indian J Med Res 2007, 125(3):451-472.
25. Portha B, Lacraz G, Kergoat M, Homo-Delarche F, Giroix MH, Bailbe D, Gangnerau MN, Dolz M, Tourrel-Cuzin C, Movassat J: The GK rat beta-cell: a prototype for the diseased human beta-cell in type 2 diabetes? Mol Cell Endocrinol 2009, 297(1-2):73-85.
26. Stenberg L, Kanje M, Martensson L, Dahlin LB: Injury-induced activation of ERK 1/2 in the sciatic nerve of healthy and diabetic rats. Neuroreport 2011, 22(2):73-77.
27. Brushart T: Nerve repair. New York: Oxford University Press Inc; 2011.
28. Johnson EO, Zoubos AB, Soucacos PN: Regeneration and repair of peripheral nerves. Injury 2005, 36 Suppl 4:S24-29.
29. Lundborg G: Nerve injury and repair. Regeneration, reconstruction and cortical remodelling, 2nd edn. Philadelphia: Elsevier; 2004.
30. Gonzalez-Perez F, Udina E, Navarro X: Extracellular matrix components in peripheral nerve regeneration. Int Rev Neurobiol 2013, 108:257-275.
31. Seddon H: Three types of nerve injury. Brain 1943, 66:237-288.
32. Sunderland S: The anatomy and physiology of nerve injury. Muscle Nerve 1990, 13(9):771-784.
33. Dahlin LB: The role of timing in nerve reconstruction. Int Rev Neurobiol 2013, 109:151-164.
34. Stoll G, Muller HW: Nerve injury, axonal degeneration and neural regeneration: basic insights. Brain Pathol 1999, 9(2):313-325.

35. Stoll G, Jander S, Myers RR: Degeneration and regeneration of the peripheral nervous system: from Augustus Waller's observations to neuroinflammation. J Peripher Nerv Syst 2002, 7(1):13-27.
36. Lundborg G: A 25-year perspective of peripheral nerve surgery: Evolving neuroscientific concepts and clinical significance. J Hand Surg 2000, 25A:391-414.
37. Navarro X, Vivo M, Valero-Cabre A: Neural plasticity after peripheral nerve injury and regeneration. Prog Neurobiol 2007, 82(4):163-201.
38. Welin D, Novikova LN, Wiberg M, Kellerth JO, Novikov LN: Survival and regeneration of cutaneous and muscular afferent neurons after peripheral nerve injury in adult rats. Exp Brain Res 2008, 186(2):315-323.
39. Swanberg M, Harnesk K, Strom M, Diez M, Lidman O, Piehl F: Fine mapping of gene regions regulating neurodegeneration. PLoS One 2009, 4(6):e5906.
40. Jivan S, Novikova LN, Wiberg M, Novikov LN: The effects of delayed nerve repair on neuronal survival and axonal regeneration after seventh cervical spinal nerve axotomy in adult rats. Exp Brain Res 2006, 170(2):245-254.
41. Jivan S, Kumar N, Wiberg M, Kay S: The influence of pre-surgical delay on functional outcome after reconstruction of brachial plexus injuries. J Plast Reconstr Aesthet Surg 2009, 62(4):472-479.
42. Jessen KR, Mirsky R: The repair Schwann cell and its function in regenerating nerves. J Physiol 2016, 594(13):3521-3531.
43. Terenghi G, Hart A, Wiberg M: The nerve injury and the dying neurons: diagnosis and prevention. J Hand Surg Eur Vol 2011, 36(9):730-734.
44. Nunez G, del Peso L: Linking extracellular survival signals and the apoptotic machinery. Curr Opin Neurobiol 1998, 8(5):613-618.
45. Makwana M, Raivich G: Molecular mechanisms in successful peripheral regeneration. FEBS J 2005, 272(11):2628-2638.
46. Lindwall C, Kanje M: Retrograde axonal transport of JNK signaling molecules influence injury induced nuclear changes in p-c-Jun and ATF3 in adult rat sensory neurons. Mol Cell Neurosci 2005, 29(2):269-282.
47. Wada T, Penninger JM: Mitogen-activated protein kinases in apoptosis regulation. Oncogene 2004, 23(16):2838-2849.
48. Agthong S, Kaewsema A, Tanomsridejchai N, Chentanez V: Activation of MAPK ERK in peripheral nerve after injury. BMC Neurosci 2006, 7:45.
49. Raivich G, Bohatschek M, Da Costa C, Iwata O, Galiano M, Hristova M, Nateri AS, Makwana M, Riera-Sans L, Wolfer DP *et al*: The AP-1 transcription factor c-Jun is required for efficient axonal regeneration. Neuron 2004, 43(1):57-67.
50. Lindwall C, Kanje M: The role of p-c-Jun in survival and outgrowth of developing sensory neurons. Neuroreport 2005, 16(15):1655-1659.
51. Patodia S, Raivich G: Role of transcription factors in peripheral nerve regeneration. Front Mol Neurosci 2012, 5:8.
52. Hunt D, Hossain-Ibrahim K, Mason MR, Coffin RS, Lieberman AR, Winterbottom J, Anderson PN: ATF3 upregulation in glia during Wallerian degeneration: differential expression in peripheral nerves and CNS white matter. BMC Neurosci 2004, 5:9.

53. Lonze BE, Ginty DD: Function and regulation of CREB family transcription factors in the nervous system. Neuron 2002, 35(4):605-623.
54. Lindwall C, Dahlin L, Lundborg G, Kanje M: Inhibition of c-Jun phosphorylation reduces axonal outgrowth of adult rat nodose ganglia and dorsal root ganglia sensory neurons. Mol Cell Neurosci 2004, 27(3):267-279.
55. Martensson L, Gustavsson P, Dahlin LB, Kanje M: Activation of extracellular-signal-regulated kinase-1/2 precedes and is required for injury-induced Schwann cell proliferation. Neuroreport 2007, 18(10):957-961.
56. Barde YA: Trophic factors and neuronal survival. Neuron 1989, 2(6):1525-1534.
57. Boyd JG, Gordon T: Neurotrophic factors and their receptors in axonal regeneration and functional recovery after peripheral nerve injury. Mol Neurobiol 2003, 27(3):277-324.
58. Vidyasagar A, Wilson NA, Djamali A: Heat shock protein 27 (HSP27): biomarker of disease and therapeutic target. Fibrogenesis Tissue Repair 2012, 5(1):7.
59. Dodge ME, Wang J, Guy C, Rankin S, Rahimtula M, Mearow KM: Stress-induced heat shock protein 27 expression and its role in dorsal root ganglion neuronal survival. Brain Res 2006, 1068(1):34-48.
60. Pourhamidi K, Dahlin LB, Englund E, Rolandsson O: Evaluation of clinical tools and their diagnostic use in distal symmetric polyneuropathy. Prim Care Diabetes 2014, 8(1):77-84.
61. Yi C, Dahlin LB: Impaired nerve regeneration and Schwann cell activation after repair with tension. Neuroreport 2010, 21(14):958-962.
62. Millesi H: Nerve grafts: Indications, techniques, and prognosis. In: Management of peripheral nerve problems. edn. Edited by Omer GEJ, Spinner M. Philadelphia: W.B. Saunders; 1980: 410-430.
63. Kvist M, Sondell M, Kanje M, Dahlin LB: Regeneration in, and properties of, extracted peripheral nerve allografts and xenografts. J Plast Surg Hand Surg 2011, 45(3):122-128.
64. Sondell M, Lundborg G, Kanje M: Regeneration of the rat sciatic nerve into allografts made acellular through chemical extraction. Brain Res 1998, 795:44-54.
65. Rinker BD, Ingari JV, Greenberg JA, Thayer WP, Safa B, Buncke GM: Outcomes of short-gap sensory nerve injuries reconstructed with processed nerve allografts from a multicenter registry study. J Reconstr Microsurg 2015, 31(5):384-390.
66. Rinker B, Zoldos J, Weber RV, Ko J, Thayer W, Greenberg J, Leversedge FJ, Safa B, Buncke G: Use of Processed Nerve Allografts to Repair Nerve Injuries Greater Than 25 mm in the Hand. Ann Plast Surg 2017, 78(6S Suppl 5):S292-S295.
67. Dahlin LB: Techniques of peripheral nerve repair. Scand J Surg 2008, 97(4):310-316.
68. Daly W, Yao L, Zeugolis D, Windebank A, Pandit A: A biomaterials approach to peripheral nerve regeneration: bridging the peripheral nerve gap and enhancing functional recovery. J R Soc Interface 2012, 9(67):202-221.
69. Lundborg G, Dahlin LB, Danielsen NP, Hansson HA, Larsson K: Reorganization and orientation of regenerating nerve fibres, perineurium and epineurium in

preformed mesothelial tubes – an experimental study on the sciatic nerve of rats. J Neurosci Res 1981, 6:265-281.
70. Muheremu A, Ao Q: Past, Present, and Future of Nerve Conduits in the Treatment of Peripheral Nerve Injury. Biomed Res Int 2015, 2015:237507.
71. Konofaos P, Ver Halen JP: Nerve repair by means of tubulization: past, present, future. J Reconstr Microsurg 2013, 29(3):149-164.
72. Dahlin LB, Lundborg G: Use of tubes in peripheral nerve repair. Neurosurg Clin N Am 2001, 12(2):341-352.
73. Nectow AR, Marra KG, Kaplan DL: Biomaterials for the development of peripheral nerve guidance conduits. Tissue Eng Part B Rev 2012, 18(1):40-50.
74. Bell JH, Haycock JW: Next generation nerve guides: materials, fabrication, growth factors, and cell delivery. Tissue Eng Part B Rev 2012, 18(2):116-128.
75. Dahlin LB, Wiberg M: Nerve injuries of the upper extremity and hand. EFORT Open Rev 2017, 2(5):158-170.
76. Duarte ML, Ferreira MC, Marvao MR, Rocha J: Determination of the degree of acetylation of chitin materials by 13C CP/MAS NMR spectroscopy. Int J Biol Macromol 2001, 28(5):359-363.
77. Kean T, Thanou M: Biodegradation, biodistribution and toxicity of chitosan. Adv Drug Deliv Rev 2010, 62(1):3-11.
78. Meyer C, Wrobel S, Raimondo S, Rochkind S, Heimann C, Shahar A, Ziv-Polat O, Geuna S, Grothe C, Haastert-Talini K: Peripheral Nerve Regeneration Through Hydrogel-Enriched Chitosan Conduits Containing Engineered Schwann Cells for Drug Delivery. Cell Transplant 2016, 25(1):159-182.
79. Morano M, Wrobel S, Fregnan F, Ziv-Polat O, Shahar A, Ratzka A, Grothe C, Geuna S, Haastert-Talini K: Nanotechnology versus stem cell engineering: in vitro comparison of neurite inductive potentials. Int J Nanomedicine 2014, 9:5289-5306.
80. Tomlinson DR, Gardiner NJ: Diabetic neuropathies: components of etiology. J Peripher Nerv Syst 2008, 13(2):112-121.
81. Callaghan BC, Hur J, Feldman EL: Diabetic neuropathy: one disease or two? Curr Opin Neurol 2012, 25(5):536-541.
82. Zochodne DW: Diabetic neuropathies: features and mechanisms. Brain Pathol 1999, 9(2):369-391.
83. Aaberg ML, Burch DM, Hud ZR, Zacharias MP: Gender differences in the onset of diabetic neuropathy. J Diabetes Complications 2008, 22(2):83-87.
84. Vacca V, Marinelli S, Pieroni L, Urbani A, Luvisetto S, Pavone F: Higher pain perception and lack of recovery from neuropathic pain in females: a behavioural, immunohistochemical, and proteomic investigation on sex-related differences in mice. Pain 2014, 155(2):388-402.
85. de la Hoz CL, Cheng C, Fernyhough P, Zochodne DW: A model of chronic diabetic polyneuropathy: benefits from intranasal insulin are modified by sex and RAGE deletion. Am J Physiol Endocrinol Metab 2017, 312(5):E407-E419.
86. Kennedy JM, Zochodne DW: Impaired peripheral nerve regeneration in diabetes mellitus. J Peripher Nerv Syst 2005, 10(2):144-157.

87. Mohseni S, Badii M, Kylhammar A, Thomsen NOB, Eriksson KF, Malik RA, Rosen I, Dahlin LB: Longitudinal study of neuropathy, microangiopathy, and autophagy in sural nerve: Implications for diabetic neuropathy. Brain Behav 2017, 7(8):e00763.
88. Price SA, Agthong S, Middlemas AB, Tomlinson DR: Mitogen-activated protein kinase p38 mediates reduced nerve conduction velocity in experimental diabetic neuropathy: interactions with aldose reductase. Diabetes 2004, 53(7):1851-1856.
89. Agthong S, Tomlinson DR: Inhibition of p38 MAP kinase corrects biochemical and neurological deficits in experimental diabetic neuropathy. Ann N Y Acad Sci 2002, 973:359-362.
90. Sima AA, Sugimoto K: Experimental diabetic neuropathy: an update. Diabetologia 1999, 42(7):773-788.
91. Edwards JL, Vincent AM, Cheng HT, Feldman EL: Diabetic neuropathy: mechanisms to management. Pharmacol Ther 2008, 120(1):1-34.
92. Yasuda H, Terada M, Maeda K, Kogawa S, Sanada M, Haneda M, Kashiwagi A, Kikkawa R: Diabetic neuropathy and nerve regeneration. Prog Neurobiol 2003, 69(4):229-285.
93. Thomsen NO, Cederlund R, Rosen I, Bjork J, Dahlin LB: Clinical outcomes of surgical release among diabetic patients with carpal tunnel syndrome: prospective follow-up with matched controls. J Hand Surg Am 2009, 34(7):1177-1187.
94. Osman AA, Dahlin LB, Thomsen NO, Mohseni S: Autophagy in the posterior interosseous nerve of patients with type 1 and type 2 diabetes mellitus: an ultrastructural study. Diabetologia 2015, 58(3):625-632.
95. Thomsen NO, Mojaddidi M, Malik RA, Dahlin LB: Reduced myelinated nerve fibre and endoneurial capillary densities in the forearm of diabetic and non-diabetic patients with carpal tunnel syndrome. Acta Neuropathol 2009, 118(6):785-791.
96. Mojaddidi MA, Ahmed MS, Ali R, Jeziorska M, Al-Sunni A, Thomsen NO, Dahlin LB, Malik RA: Molecular and pathological studies in the posterior interosseous nerve of diabetic and non-diabetic patients with carpal tunnel syndrome. Diabetologia 2014, 57(8):1711-1719.
97. Tomlinson DR, Townsend J, Fretten P: Prevention of defective axonal transport in streptozotocin-diabetic rats by treatment with "Statil" (ICI 128 436), an aldose reductase inhibitor. Diabetes 1985, 34:970-972.
98. Graham ML, Janecek JL, Kittredge JA, Hering BJ, Schuurman HJ: The streptozotocin-induced diabetic nude mouse model: differences between animals from different sources. Comp Med 2011, 61(4):356-360.
99. Yono M, Pouresmail M, Takahashi W, Flanagan JF, Weiss RM, Latifpour J: Effect of insulin treatment on tissue size of the genitourinary tract in BB rats with spontaneously developed and streptozotocin-induced diabetes. Naunyn Schmiedebergs Arch Pharmacol 2005, 372(3):251-255.
100. Sima AA, Hay K: Functional aspects and pathogenetic considerations of the neuropathy in the spontaneously diabetic BB-Wistar rat. Neuropathol Appl Neurobiol 1981, 7(5):341-350.

101. Brussee V, Cunningham FA, Zochodne DW: Direct insulin signaling of neurons reverses diabetic neuropathy. Diabetes 2004, 53(7):1824-1830.
102. Bervar M: Effect of weak, interrupted sinusoidal low frequency magnetic field on neural regeneration in rats: functional evaluation. Bioelectromagnetics 2005, 26(5):351-356.
103. Tonra JR, Curtis R, Wong V, Cliffer KD, Park JS, Timmes A, Nguyen T, Lindsay RM, Acheson A, DiStefano PS: Axotomy upregulates the anterograde transport and expression of brain-derived neurotrophic factor by sensory neurons. J Neurosci 1998, 18(11):4374-4383.
104. Ratzka A, Kalve I, Ozer M, Nobre A, Wesemann M, Jungnickel J, Koster-Patzlaff C, Baron O, Grothe C: The colayer method as an efficient way to genetically modify mesencephalic progenitor cells transplanted into 6-OHDA rat model of Parkinson's disease. Cell Transplant 2012, 21(4):749-762.
105. Fisher RA: Combining independent tests of significance. American Statistician 1948, 2(5):30.
106. Bassilios Habre S, Bond G, Jing XL, Kostopoulos E, Wallace RD, Konofaos P: The Surgical Management of Nerve Gaps: Present and Future. Ann Plast Surg 2017.
107. Kamijo M, Merry AC, Akdas G, Cherian PV, Sima AA: Nerve fiber regeneration following axotomy in the diabetic biobreeding Worcester rat: the effect of ARI treatment. J Diabetes Complications 1996, 10(4):183-191.
108. Pierson CR, Zhang W, Murakawa Y, Sima AA: Insulin deficiency rather than hyperglycemia accounts for impaired neurotrophic responses and nerve fiber regeneration in type 1 diabetic neuropathy. J Neuropathol Exp Neurol 2003, 62(3):260-271.
109. Terada M, Yasuda H, Kikkawa R: Delayed Wallerian degeneration and increased neurofilament phosphorylation in sciatic nerves of rats with streptozocin-induced diabetes. J Neurol Sci 1998, 155(1):23-30.
110. Cashman CR, Hoke A: Mechanisms of distal axonal degeneration in peripheral neuropathies. Neurosci Lett 2015, 596:33-50.
111. Hoke A: Animal models of peripheral neuropathies. Neurotherapeutics 2012, 9(2):262-269.
112. Patodia S, Raivich G: Downstream effector molecules in successful peripheral nerve regeneration. Cell Tissue Res 2012, 349(1):15-26.
113. Reid AJ, Welin D, Wiberg M, Terenghi G, Novikov LN: Peripherin and ATF3 genes are differentially regulated in regenerating and non-regenerating primary sensory neurons. Brain Res 2010, 1310:1-7.
114. Alant JD, Kemp SW, Khu KJ, Kumar R, Webb AA, Midha R: Traumatic neuroma in continuity injury model in rodents. J Neurotrauma 2012, 29(8):1691-1703.
115. Danielsen N, Lundborg G, Frizell M: Nerve repair and axonal transport: Outgrowth delay and regeneration rate after transection and repair of rabbit hypoglossal nerve. Brain Res 1986, 376:125-132.

116. Zhang W, Kamiya H, Ekberg K, Wahren J, Sima AA: C-peptide improves neuropathy in type 1 diabetic BB/Wor-rats. Diabetes Metab Res Rev 2007, 23(1):63-70.
117. Sima AA, Zhang W, Sugimoto K, Henry D, Li Z, Wahren J, Grunberger G: C-peptide prevents and improves chronic Type I diabetic polyneuropathy in the BB/Wor rat. Diabetologia 2001, 44(7):889-897.
118. Cnop M, Welsh N, Jonas JC, Jorns A, Lenzen S, Eizirik DL: Mechanisms of pancreatic beta-cell death in type 1 and type 2 diabetes: many differences, few similarities. Diabetes 2005, 54 Suppl 2:S97-107.
119. Al-Awar A, Kupai K, Veszelka M, Szucs G, Attieh Z, Murlasits Z, Torok S, Posa A, Varga C: Experimental Diabetes Mellitus in Different Animal Models. J Diabetes Res 2016, 2016:9051426.
120. Dey I, Midha N, Singh G, Forsyth A, Walsh SK, Singh B, Kumar R, Toth C, Midha R: Diabetic Schwann cells suffer from nerve growth factor and neurotrophin-3 underproduction and poor associability with axons. Glia 2013, 61(12):1990-1999.
121. Kennedy PR, Bakay RA, Moore MM, Adams K, Goldwaithe J: Direct control of a computer from the human central nervous system. IEEE Trans Rehabil Eng 2000, 8(2):198-202.
122. Seijffers R, Allchorne AJ, Woolf CJ: The transcription factor ATF-3 promotes neurite outgrowth. Mol Cell Neurosci 2006, 32(1-2):143-154.
123. Maritim AC, Sanders RA, Watkins JB, 3rd: Diabetes, oxidative stress, and antioxidants: a review. J Biochem Mol Toxicol 2003, 17(1):24-38.
124. Ziegler D, Hanefeld M, Ruhnau KJ, Meissner HP, Lobisch M, Schutte K, Gries FA: Treatment of symptomatic diabetic peripheral neuropathy with the anti-oxidant alpha-lipoic acid. A 3-week multicentre randomized controlled trial (ALADIN Study). Diabetologia 1995, 38(12):1425-1433.
125. Vincent AM, Brownlee M, Russell JW: Oxidative stress and programmed cell death in diabetic neuropathy. Ann N Y Acad Sci 2002, 959:368-383.
126. Sima AA: New insights into the metabolic and molecular basis for diabetic neuropathy. Cell Mol Life Sci 2003, 60(11):2445-2464.
127. Eckersley L, Ansselin AD, Tomlinson DR: Effects of experimental diabetes on axonal and Schwann cell changes in sciatic nerve isografts. Brain Res Mol Brain Res 2001, 92(1-2):128-137.
128. Portha B, Giroix MH, Tourrel-Cuzin C, Le-Stunff H, Movassat J: The GK rat: a prototype for the study of non-overweight type 2 diabetes. Methods Mol Biol 2012, 933:125-159.
129. Hall E, Volkov P, Dayeh T, Esguerra JL, Salo S, Eliasson L, Ronn T, Bacos K, Ling C: Sex differences in the genome-wide DNA methylation pattern and impact on gene expression, microRNA levels and insulin secretion in human pancreatic islets. Genome Biol 2014, 15(12):522.
130. Ariza L, Pages G, Garcia-Lareu B, Cobianchi S, Otaegui PJ, Ruberte J, Chillon M, Navarro X, Bosch A: Experimental diabetes in neonatal mice induces early peripheral sensorimotor neuropathy. Neuroscience 2014, 274:250-259.

131. Yu WH: Sex difference in the regeneration of the hypoglossal nerve in rats. Brain Res 1982, 238(2):404-406.
132. Yu WH, McGinnis MY: Androgen receptors in cranial nerve motor nuclei of male and female rats. J Neurobiol 2001, 46(1):1-10.
133. Karp NA, Mason J, Beaudet AL, Benjamini Y, Bower L, Braun RE, Brown SDM, Chesler EJ, Dickinson ME, Flenniken AM *et al*: Prevalence of sexual dimorphism in mammalian phenotypic traits. Nat Commun 2017, 8:15475.
134. Kamenov ZA, Parapunova RA, Georgieva RT: Earlier development of diabetic neuropathy in men than in women with type 2 diabetes mellitus. Gend Med 2010, 7(6):600-615.
135. Melcangi RC, Azcoitia I, Ballabio M, Cavarretta I, Gonzalez LC, Leonelli E, Magnaghi V, Veiga S, Garcia-Segura LM: Neuroactive steroids influence peripheral myelination: a promising opportunity for preventing or treating age-dependent dysfunctions of peripheral nerves. Prog Neurobiol 2003, 71(1):57-66.
136. Caruso D, Scurati S, Maschi O, De Angelis L, Roglio I, Giatti S, Garcia-Segura LM, Melcangi RC: Evaluation of neuroactive steroid levels by liquid chromatography-tandem mass spectrometry in central and peripheral nervous system: effect of diabetes. Neurochem Int 2008, 52(4-5):560-568.
137. Pesaresi M, Maschi O, Giatti S, Garcia-Segura LM, Caruso D, Melcangi RC: Sex differences in neuroactive steroid levels in the nervous system of diabetic and non-diabetic rats. Horm Behav 2010, 57(1):46-55.
138. Dahlin LB, Lundborg G: The use of tubes in peripheral nerve repair. In: Neurosurg Clin N Am. edn. Edited by Kliot M: Saunders Co; 2001.
139. Weber RA: A randomized prospective study of the use of polyglycolic acid conduits for nerve reconstraction in humans. In: American Society for Surgery of the Hand, 54th Annual Meeting: 1999; Boston: W.B. Saunders Company; 1999.
140. Archibald SJ, Krarup C, Shefner J, Li ST, Madison RD: A collagen-based nerve guide conduit for peripheral nerve repair: an electrophysiological study in rodents and non-human primates. J Comp Neurol 1991, 306:685-696.
141. Liodaki E, Bos I, Lohmeyer JA, Senyaman O, Mauss KL, Siemers F, Mailaender P, Stang F: Removal of collagen nerve conduits (NeuraGen) after unsuccessful implantation: focus on histological findings. J Reconstr Microsurg 2013, 29(8):517-522.
142. Moore AM, Kasukurthi R, Magill CK, Farhadi HF, Borschel GH, Mackinnon SE: Limitations of conduits in peripheral nerve repairs. Hand (N Y) 2009, 4(2):180-186.
143. Meek MF, Jansen K: Two years after in vivo implantation of poly(DL-lactide-epsilon-caprolactone) nerve guides: has the material finally resorbed? J Biomed Mater Res A 2009, 89(3):734-738.
144. Tomihata K, Ikada Y: In vitro and in vivo degradation of films of chitin and its deacetylated derivatives. Biomaterials 1997, 18(7):567-575.
145. Gaudin R, Knipfer C, Henningsen A, Smeets R, Heiland M, Hadlock T: Approaches to Peripheral Nerve Repair: Generations of Biomaterial Conduits Yielding to Replacing Autologous Nerve Grafts in Craniomaxillofacial Surgery. Biomed Res Int 2016, 2016:3856262.

146. Cobianchi S, Casals-Diaz L, Jaramillo J, Navarro X: Differential effects of activity dependent treatments on axonal regeneration and neuropathic pain after peripheral nerve injury. Exp Neurol 2013, 240:157-167.
147. Haastert-Talini K, Schmitte R, Korte N, Klode D, Ratzka A, Grothe C: Electrical stimulation accelerates axonal and functional peripheral nerve regeneration across long gaps. J Neurotrauma 2011, 28(4):661-674.
148. Zhao Q, Dahlin LB, Kanje M, Lundborg G: Repair of the transected rat sciatic nerve: Matrix formation within silicone tubes. Restor Neurol Neurosci 1993, 5:197-204.
149. Martinez-Campos E, Civantos A, Redondo JA, Guzman R, Perez-Perrino M, Gallardo A, Ramos V, Aranaz I: Cell Adhesion and Proliferation on Sulfonated and Non-Modified Chitosan Films. AAPS PharmSciTech 2017, 18(4):974-982.
150. Wenling C, Duohui J, Jiamou L, Yandao G, Nanming Z, Xiufang Z: Effects of the degree of deacetylation on the physicochemical properties and Schwann cell affinity of chitosan films. J Biomater Appl 2005, 20(2):157-177.
151. Wrobel S, Serra SC, Ribeiro-Samy S, Sousa N, Heimann C, Barwig C, Grothe C, Salgado AJ, Haastert-Talini K: In vitro evaluation of cell-seeded chitosan films for peripheral nerve tissue engineering. Tissue Eng Part A 2014, 20(17-18):2339-2349.
152. Streppel M, Azzolin N, Dohm S, Guntinas-Lichius O, Haas C, Grothe C, Wevers A, Neiss WF, Angelov DN: Focal application of neutralizing antibodies to soluble neurotrophic factors reduces collateral axonal branching after peripheral nerve lesion. Eur J Neurosci 2002, 15(8):1327-1342.
153. Korte N, Schenk HC, Grothe C, Tipold A, Haastert-Talini K: Evaluation of periodic electrodiagnostic measurements to monitor motor recovery after different peripheral nerve lesions in the rat. Muscle Nerve 2011, 44(1):63-73.
154. Lundborg G, Rosen B, Dahlin L, Holmberg J, Rosen I: Tubular repair of the median or ulnar nerve in the human forearm: a 5-year follow-up. J Hand Surg [Br] 2004, 29(2):100-107.
155. Navarro X, Udina E: Chapter 6: Methods and protocols in peripheral nerve regeneration experimental research: part III-electrophysiological evaluation. Int Rev Neurobiol 2009, 87:105-126.
156. Stenberg L, Stossel M, Ronchi G, Geuna S, Yin Y, Mommert S, Martensson L, Metzen J, Grothe C, Dahlin LB *et al*: Regeneration of long-distance peripheral nerve defects after delayed reconstruction in healthy and diabetic rats is supported by immunomodulatory chitosan nerve guides. BMC Neurosci 2017, 18(1):53.
157. Almgren KG: Revascularisation of free peripheral nerve grafts. An experimental study in the rabbit. Acta Orthop Scand 1974, Suppl 154:1-104.
158. Andersson-Sjoland A, Nihlberg K, Eriksson L, Bjermer L, Westergren-Thorsson G: Fibrocytes and the tissue niche in lung repair. Respir Res 2011, 12:76.
159. Penkert G, Bini W, Samii M: Revascularization of nerve grafts: an experimental study. J Reconstr Microsurg 1988, 4(4):319-325.
160. Almgren KG: Revascularization of free pheripheral nerve grafts. An experimental study in the rabbit. Acta Orthop Scand Suppl 1975, 154:1-104.

161. Zochodne DW, Guo GF, Magnowski B, Bangash M: Regenerative failure of diabetic nerves bridging transection injuries. Diabetes Metab Res Rev 2007, 23(6):490-496.
162. Bozkurt A, van Neerven SG, Claeys KG, O'Dey DM, Sudhoff A, Brook GA, Sellhaus B, Schulz JB, Weis J, Pallua N: The proximal medial sural nerve biopsy model: a standardised and reproducible baseline clinical model for the translational evaluation of bioengineered nerve guides. Biomed Res Int 2014, 2014:121452.
163. Sanen K, Martens W, Georgiou M, Ameloot M, Lambrichts I, Phillips J: Engineered neural tissue with Schwann cell differentiated human dental pulp stem cells: potential for peripheral nerve repair? J Tissue Eng Regen Med 2017, 11(12):3362-3372.
164. Haastert K, Lipokatic E, Fischer M, Timmer M, Grothe C: Differentially promoted peripheral nerve regeneration by grafted Schwann cells over-expressing different FGF-2 isoforms. Neurobiol Dis 2006, 21(1):138-153.
165. Pourhamidi K, Dahlin LB, Boman K, Rolandsson O: Heat shock protein 27 is associated with better nerve function and fewer signs of neuropathy. Diabetologia 2011, 54(12):3143-3149.
166. Pourhamidi K, Skarstrand H, Dahlin LB, Rolandsson O: HSP27 concentrations are lower in patients with type 1 diabetes and correlate with large nerve fiber dysfunction. Diabetes Care 2014, 37(3):e49-50.

Paper I

Neuroscience Letters 515 (2012) 34–38

Contents lists available at SciVerse ScienceDirect

Neuroscience Letters

journal homepage: www.elsevier.com/locate/neulet

Expression of Activating Transcription Factor 3 (ATF 3) and caspase 3 in Schwann cells and axonal outgrowth after sciatic nerve repair in diabetic BB rats

Lena Stenberg[a], Martin Kanje[b], Katarina Dolezal[a], Lars B. Dahlin[a,*]

[a] Hand Surgery/Department of Clinical Sciences, Lund University, Skåne University Hospital, SE-205 02 Malmö, Sweden
[b] Department of Functional Zoology, Lund University, SE-223 62 Lund, Sweden

ARTICLE INFO

Article history:
Received 31 October 2011
Received in revised form 4 March 2012
Accepted 5 March 2012

Keywords:
ATF3
Caspase 3
Schwann cell
Nerve regeneration
Diabetes
BB rat

ABSTRACT

The aim of this study was to evaluate nerve regeneration in relation to the transcription factor, Activating Transcription Factor 3 (ATF 3), and an apoptotic marker, caspase 3, in the Schwann cells of diabetic BB rats (i.e. display type 1 diabetes phenotype). Sciatic nerves in healthy Wistar rats and in diabetic BB rats were transected and immediately repaired. Axonal outgrowth (neurofilament staining) and expression of ATF 3 and caspase 3 were quantified by immunohistochemistry after six days. There was no difference in axonal outgrowth between healthy and diabetic rats. However, the sciatic nerve in the diabetic rats exhibited a larger number of ATF 3 expressing Schwann cells at the site of the lesion and also a higher number of caspase 3 expressing Schwann cells. Similar differences were observed in the distal nerve segment between the healthy and diabetic rats. There were no correlations between the number of Schwann cells expressing ATF 3 and caspase 3. Thus, diabetic BB rats display an increased activation of ATF 3 and also a rise in apoptotic caspase 3 expressing Schwann cells, but with no discrepancy in length of axonal outgrowth after nerve injury and repair at six days. Knowledge about signal transduction mechanisms in diabetes after stress may provide new insights into the development of diabetic neuropathy and neuropathic pain.

© 2012 Elsevier Ireland Ltd. All rights reserved.

1. Introduction

Neuropathy is a common complication to diabetes [10]. Furthermore, the prevalence of diabetic neuropathy is rising with the global burden of type 2 diabetes in an older population and an increase in type 1 diabetes [13]. There is a broad variety of diabetic neuropathies affecting single (mononeuropathy), several (mononeuropathy multiplex), or many nerves (polyneuropathy). Longer nerves are especially vulnerable; explaining why nerve-related problems in the extremities are most common in diabetes.

The pathophysiology of diabetic neuropathy is not fully understood, but may include vascular, metabolic and genetic factors [22]. In addition, neither the reaction of neurons nor Schwann cells in diabetes after a nerve injury has been clarified. Normally after a nerve injury, Schwann cells are rapidly activated and proliferate both at the site of the lesion and in the distal nerve segment with remodelling of the extracellular matrix [8,21]. Proliferation of Schwann cells is in turn important for outgrowth of axons [8]. The transcription factor Activating Transcription Factor 3 (ATF 3) is expressed in neurons and Schwann cells after nerve injury and repair [17]. The up-regulation is dependent on kinases from the stress-activating protein kinase-family (SAPK), which is activated by several stress inducers, such as trauma and even hyperglycaemia and oxidative stress [9]. Previous studies indicate that ATF 3 is obligatory for regeneration of axons after nerve injury in healthy rats [7]. Schwann cells may also express cleaved caspase 3 as a marker for programmed cell death (apoptosis), and this expression is inversely correlated to the expression of ATF 3 [18]. Most studies on nerve regeneration have been performed in rats made diabetic by injection of the beta-cell toxic streptozotocin [3,14], while studies on spontaneously diabetic rats [21] are less common. Such rats show signs of more prominent expression of ATF 3 in neurons and Schwann cells after a nerve compression lesion [2]. Therefore, this study aim was to evaluate the expression of ATF 3 and cleaved caspase 3 in Schwann cells in relation to axonal outgrowth after nerve injury and repair in diabetic BB and healthy rats.

2. Materials and methods

2.1. Rats and injury to the sciatic nerve

Two groups of female rats were included: spontaneously induced diabetic BB rats (Biobreeding, body weight around

* Corresponding author. Tel.: +46 40 3 67 69; fax: +46 40 92 88 55.
E-mail addresses: Lena.Stenberg@med.lu.se (L. Stenberg), Martin.Kanje@biol.lu.se (M. Kanje), katta21@lycos.com (K. Dolezal), Lars.Dahlin@med.lu.se (L.B. Dahlin).

0304-3940/$ – see front matter © 2012 Elsevier Ireland Ltd. All rights reserved.
doi:10.1016/j.neulet.2012.03.011

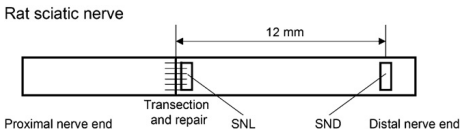

Fig. 1. Schematic drawing of the examined nerve and the two different locations that were used to analyze presence of DAPI, ATF 3 and caspase 3 stained Schwann cells [near site of lesion (SNL) and 12 mm more distally (SND)].

180 g), kindly provided by Professor Åke Lernmark and Dr Lina Åkesson, Department of Endocrinology, Malmö, Sweden, and healthy control rats (Wistar), with body weight approximately 200 g (obtained from Taconic, Denmark). The animal ethics committee in Malmö/Lund approved all animal experiments. The animals were kept in cages with a 12 h light/dark cycle. Food and water were changed daily. B-glucose, body weight and signs of diabetes (polydipsia) were observed daily in all rats. B-glucose was measured from a blood sample from a puncture of the tail vein [Ascensia contour (Bio Healthcare, USA, Bio Diagnostics Europe) and LT (Bayer AB, Diabetes Care, Solna, Sweden); test slip (Microfil TM; Bio Healthcare Diabetes Care, USA)].

The rats were anaesthetized with an intraperitoneal injection of a mixture of pentobarbital sodium (60 mg/ml, Apoteket, Malmö, Sweden) and sodium chloride in a 1:10 proportion. The sciatic nerves were unilaterally exposed, transected and immediately repaired using three 9–0 ethilon sutures (Ethicon®) in 7 rats in each group (Fig 1).

The skin was closed and the rats were allowed to recover. After six days, due to the hyperglycaemic state and the condition of the diabetic BB rats, the rats reanaesthetized and the sciatic nerves were harvested bilaterally. All animals were killed by an overdose of pentobarbital sodium (60 mg/ml).

The sciatic nerves were attached, and nailed on cork. They were fixed in Stefanini's fixative (2% paraformaldehyde and 1.9% picric acid in 0.1 M phosphate buffered, pH 7.2) overnight and then washed 3× 20 min in PBS (phosphate buffered saline, pH 7.2). The sciatic nerves were mounted in O.C.T. Compound (Tissue-tek®, Histolab products AB, Göteborg, Sweden), sectioned in a cryostat at a thickness of 10 μm, thaw-mounted on to Super Frost® plus slides (Menzel-Gläser, Germany) and allowed to air dry. After sectioning the slides were stored at −80 °C.

2.2. Immunohistochemistry

For the neurofilament staining, the sections were washed in PBS for 5 min. The sections were labelled with the monoclonal mouse anti-human neurofilament protein (Dako cytomation, Dako Denmark) diluted 1:80 in 0.25% Triton-X-100, 0.25% BSA in PBS overnight at 4 °C. After washing with PBS the sections were incubated with the Alexa Fluor 594 conjugated goat anti-mouse IgG (Invitrogen, Molecular Probes, Eugene, Oregon, USA) diluted 1:500 in PBS for 1 h at room temperature. Finally, the sections were washed 3× 5 min in PBS counterstained with 4′,6-diamino-2-phenylindole [DAPI; Vectashield®, Vector Laboratories, Inc. Burlingame, CA 94010] to visualise the nuclei, and then mounted and cover slipped. The length of axonal outgrowth was measured on the neurofilament stained and coded sections. The DAPI staining was used for counting and identification of nuclei.

For the staining with ATF 3, the sections were washed in PBS for 5 min. The sections were exposed to rabbit anti-ATF 3 polyclonal antibody (Santa Cruz Biotechnology, USA) 1:200 diluted in 0.25% Triton-X-100, 0.25% BSA in PBS overnight at 4 °C. After washing with PBS the sections were incubated with the secondary antibody, Alexa Fluor 488 conjugated goat anti-rabbit IgG (Invitrogen, Molecular Probes, Eugene, OR, USA) diluted 1:500 in PBS for 1 h at room temperature. Finally, the sections were washed 3× 5 min in PBS, mounted with DAPI as described for counting the total number of cells, cover slipped, coded and analysed as described below.

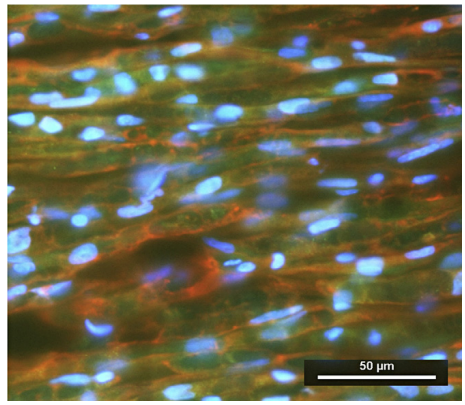

Fig. 2. Double staining with ATF 3 (green) and S-100 (red) antibodies in the distal nerve segment of an injured and repaired diabetic nerve. DAPI stained cells (blue) were used to visualize the cell nuclei (oval) of the Schwann cells. Length of bar = 50 μm.

For the visualisation of caspase3, the sections were washed in PBS for 5 min, and then incubated with an antibody to cleaved caspase 3 at a dilution of 1:200 (Invitrogen, Sweden AB Stockholm Sweden) diluted in 0.25% Triton-X-100, 0.25% BSA in PBS overnight at 4 °C. The sections were then washed 3× 5 min and incubated with the secondary Alexa Fluor goat-anti-rabbit antibody (1:500) (Invitrogen, Molecular Probes, Eugene, OR, USA) diluted in PBS for 1 h at room temperature. Finally, the sections were washed 3× 5 min in PBS, mounted with DAPI and analysed as described below.

2.3. Photography and image analysis

The sections were photographed using a fluorescence microscope (Nikon 80i) equipped with a digital system camera system (Digital sight DF-U1) connected to a computer. The digital photographs were analysed with NIS elements (Nikon, Japan).

The length of axonal outgrowth was measured and expressed in mm from a mean value of at least three analysed sections. From the sciatic nerve, three other sections were randomly selected (100–200 μm apart) and pictures (500 μm × 400 μm size) were taken. In these three pictures, 6 × 200 μm^2 areas were also randomly selected for counting of nuclei. By using this system, spaces without nerve tissue and artifacts could be excluded. Only the endoneurial space was analysed and other areas, such as epineurium/perineurium, large vessels, scar tissue and other non-neuronal tissues, were not included in the evaluation. In the randomly selected areas, ATF 3 and caspase 3 positive cells were identified and counted as Schwann cells based on the morphology and size of their nucleus and location within basal lamina tubes (DAPI staining). In addition, double staining of ATF 3 and S-100 was done (Fig. 2) in separate sections as previously described [8,23]. The total number of DAPI stained cells (including Schwann cells, perineurial cells, fibroblasts, endothelial cells, inflammatory cells and others) were also counted. In the nerve distal to the nerve sutures, pictures were taken and the cells were quantified (Fig. 1) at two locations: at the distal site adjacent to the sciatic nerve lesion (SNL)

close to the suture line and in the distal nerve segment (SND) 12 mm distal to the suture line.

2.4. Statistical methods

The results were expressed as median (minimum–maximum) values. To examine any significant differences between the groups the non-parametric method Mann–Whitney *U*-test was used with subsequent Spearman rank correlation to assess the relationship between two variables. A *p*-value less than 0.05 were considered as significant and the programme Stat View® was used for calculating.

3. Results

3.1. Fasting blood glucose and bodyweight

The preoperative body weight at the time of nerve injury and repair were not statistically different between the control (211 g, 172–220) and the BB rats (189 g, 158–194; $p = 0.12$) (Table 1). The preoperative fasting blood glucose level in the BB rats (28.1 mmol/l, 19.1–31.2) was significantly higher ($p = 0.002$) than the corresponding level measured in the control rats (4.3 mmol/l, 3.4–5.9; Table 1).

3.2. ATF 3 and caspase 3 positive cells and total number of DAPI positive cells at the site of the lesion

The number of ATF 3 positive cells at the site of the lesion just distal to the suture line, expressed as a percentage of the total number of DAPI positive cells (ATF 3 positive/total number of cells; %), was significantly higher ($p = 0.002$) in the diabetic BB rats than in the control rats (Fig. 3a and b and Table 1). The number of caspase 3 positive cells at the site of the lesion (caspase 3 positive/total number of cells; %) was also higher in the BB rat group ($p = 0.002$) (Fig. 3c and d and Table 1). The total number of DAPI positive cells (number/mm^2) was not different at the site of the lesion between the groups ($p = 0.90$).

3.3. ATF 3 and caspase 3 positive cells and total number of DAPI positive cells in the distal nerve segment

When the ATF 3 positive cells were expressed as a percentage of the total number of DAPI positive cells (ATF 3 positive/total number of cells; %) in the distal nerve segment 12 mm from the suture line, a statistical difference was seen ($p = 0.002$) between the diabetic BB and control rats (Table 1). The number of caspase 3 positive cells in the distal segment, expressed as a percentage of the total number of DAPI positive cells (caspase 3 positive/total number of cells; %), was again higher in the group with BB rats ($p = 0.002$) (Table 1). In contrast, the total number of DAPI positive cells (number/mm^2) in the distal nerve segment was higher in the control rats ($p = 0.002$).

3.4. Measurement of axonal outgrowth—neurofilament staining

The length of axonal outgrowth from the site of nerve repair into the distal nerve segment was judged by neurofilament staining. All operated nerves in the control rats and the BB rats exhibited axonal outgrowth detected by neurofilament staining. The lengths of the regenerating axons were 5635 μm (4987–6700) in the diabetic sciatic nerves and 6533 μm (5305–7235) in the healthy control rats with no statistical difference between the two groups ($p = 0.11$; Table 1).

3.5. Correlations

The Spearman correlation test was done to correlate between axonal outgrowth and ATF 3 positive cells and was shown to be not significant either at the site of the lesion (BB rats; $p = 0.12$ and control; $p = 0.93$) or in the distal nerve segment (BB rats; $p = 0.60$ and control; $p = 0.48$) in both groups. Correlation was also tested for axonal outgrowth and the apoptotic marker caspase 3, which again showed no significant difference for either group at the site of the lesion (BB rats; $p = 0.38$ and control; $p = 0.80$) or in the distal nerve segment (BB rats; $p = 0.48$ and control; $p = 0.60$). No correlations were found between ATF 3 and caspase 3 positive cells at the site of the lesion (BB rats; $p = 0.72$ and control $p = 0.86$) or in the distal nerve lesion (BB rats; $p = 0.38$ and control $p = 0.79$).

4. Discussion

Differences between healthy and diabetic BB rats with respect to activation of and apoptosis of Schwann cells after nerve injury and repair were noted. The diabetic BB (BioBreeding) rats, which have a type 1 diabetic phenotype, were used to evaluate axonal growth and Schwann cell activation and apoptosis at six days. This interval is shorter than we have previously used to evaluate axonal outgrowth [23,24], since the hyperglycaemic and clinical condition of the BB rats did not allow examination at later time points. The BB rats show similarities with the commonly used streptozotocin-induced diabetic rat model with respect to activation of Schwann cells, but also with respect to expression of the MAP kinase p-ERK 1/2 [21] and PDGF-B in transected sciatic nerves [12]. We observed an up-regulation of ATF 3 as well as the apoptotic marker, cleaved caspase 3, in the Schwann cells in both groups of rats although there were differences between the healthy- and the BB rats. The Schwann cells could be distinguished from other cells by examination of their nuclei and their location as well as by staining for S-100 in accordance with previous studies [17,18,23].

At the site of the lesion, where the nerve had been transected and immediately repaired, the diabetic rats had an augmented response to injury as compared to healthy rats. There were higher numbers of both ATF 3 positive cells and caspase 3 positive cells in the diabetic BB rats. Interestingly, in response to a less traumatic nerve

Table 1
Results of ATF 3 (% of total number of cells), caspase 3 (% of total number of cells), and DAPI stained cells (number/mm^2) at the site of the lesion (SNL) and in the distal nerve segment (SND) and axonal outgrowth (neurofilament staining) in diabetic and healthy control rats.

	Control ($n = 7$)	BB ($n = 7$)	*P*-values (Mann–Whitney *U*)
ATF 3 at the site of the lesion (SNL) (% of total)	13.9 (12.8–15.9)	21.1[a] (19.0–22.1)	0.002
ATF 3 in the distal nerve segment (% of total)	16.3 (15.1–17.0)	19.0[a] (17.6–19.9)	0.002
Total number of DAPI stained cells at the site of the lesion (no/mm^2)	1058 (1019–1080)	1048 (1009–1101)	0.90
Caspase 3 stained cells at the site of the lesion (SNL) (% of total)	2.9 (2.5–3.9)	17.7[a] (16.3–18.9)	0.002
Caspase 3 stained cells in the distal nerve segment (SND) (% of total)	2.5 (2.0–4.5)	11.4[a] (10.8–12.9)	0.002
Total number of DAPI stained cells in the distal nerve segment (SND) (no/mm^2)	1105 (1062–1147)	967[a] (875–1023)	0.002
Axonal outgrowth (neurofilament staining) (μm)	6533 (5305–7235)	5635 (4987–6700)	0.11

Values are median values (min – max).
[a] A significant difference from the corresponding values in the control rats.

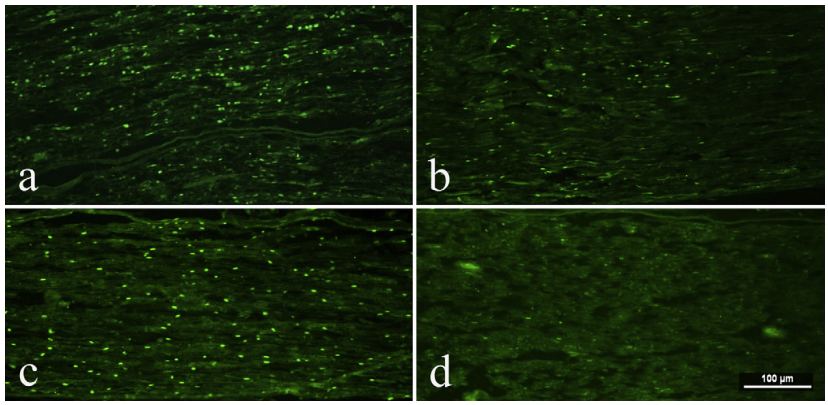

Fig. 3. Immunohistochemical staining with ATF 3 (a and b) and caspase 3 (c and d) antibodies of Schwann cells in injured and repaired sciatic nerves from diabetic (left) and healthy (right) rats. Length of bar = 100 μm.

injury than a transection injury, i.e. a compression injury, diabetic rat sciatic nerves also respond with an increased number of ATF 3 expressing Schwann cells [2] as compared to healthy rats. Thus, diabetic nerves show an increased susceptibility to injuries or stress as compared to normal nerves.

The novel finding of a higher number of both the survival and regenerative marker ATF 3 and the apoptotic death cell marker caspase 3 in the diabetic BB nerves is surprising. It has previously been shown that nerve transection followed by an immediate repair results in cleaved caspase 3 mediated Schwann cell apoptosis in healthy rats [18]. In such rats, using a regeneration period of 10 days, axonal outgrowth correlates positively with the number of ATF 3 positive cells and inversely with cleaved caspase 3 positive cells [17,23]. However, no such correlation between the number of ATF 3 and cleaved caspase 3 positive cells could be detected in the present study, where we used a six days evaluation period due to previously mentioned reasons. We believe that this indicates that the relations between cell survival, apoptotic cell death and axonal outgrowth are very complex. In the context of such intricate relations, analyses of signal transduction pathways, as a way to elucidate development of neuropathy and neuropathic pain, have been stressed [22].

We found an increased number of apoptotic Schwann cells both at the site of the lesion and in the distal nerve segment in the diabetic BB rats. It has been suggested from studies in streptozotocin-induced diabetes in rats in vitro and in vivo that oxidative stress leads to activation of programmed cell death through the caspase pathways both in sensory neurons and in Schwann cells [16]. We found a lower caspase mediated cell death in Schwann cells in the healthy than in the diabetic rats. If this can be related to oxidative stress remains to be determined. Anyhow, hyperglycaemia with the accompanying alterations in metabolic pathways, hypoxia and oxidative stress are believed to be the main causes of diabetic neuropathies [20]. Hyperglycaemia per se has been shown to induce apoptosis in cardiac myoblast cells in vitro [1]. In addition, hyperglycaemia has also been demonstrated to inhibit Schwann cell proliferation and migration as well as axonal outgrowth in cultured DRG [4]. In this context it is noteworthy that our in vivo model in BB rats, in contrast to an in vitro system, represents a complex model that more closely resembles the clinical situation [11,19]. Apoptotic stress to sensory neurons in diabetic BB/Worcester rats with hyperglycaemia, although partly balanced at 24 mmol/l with daily insulin injections and slightly lower than in the present BB rats, has been reported [6]. Such apoptotic stress is counterbalanced by e.g. antiapoptotic HSP27 in sensory neurons [6]. Thus, it is reasonable to assume that hyperglycaemia, with its consequences, is related to apoptotic cell death.

All studied rats exhibited successful axonal outgrowth, as detected by neurofilament staining, into the distal nerve segment. The outgrowth in the diabetic rats in the present study appeared to be perturbed, but not statistically significantly different from the healthy rats at the presently used evaluation point; i.e. six days. Previously, other authors have suggested that advanced glycation end products in extracellular matrix proteins in diabetic rats, like laminin and fibronectin, contribute to a reduced outgrowth of sensory neurites in diabetic rats [3]. However, earlier studies have also shown various results concerning regeneration in diabetic BB rats after both transection and compression injuries [5,15,25].

In conclusion, a more prominent activation and apoptotic cell death of Schwann cells, as detected by expression of ATF 3 and cleaved caspase 3, was observed in sciatic nerves of diabetic BB rats compared to healthy rats after nerve injury and repair. We could not see any difference in length of axonal outgrowth at six days between the groups, and there was no correlation between either ATF 3 or cleaved caspase 3, indicating complex mechanisms which have to been elucidated in the future. With respect to the increasing number of patients with diabetes globally, it is crucial to understand basic mechanisms of regeneration in diabetes, where MAPK activation may be linked to neuropathic pain [22]. Furthermore, when developing new techniques for repair and reconstruction of nerve injuries, like new conduits for bridging short and long nerve defects, they have to be applicable also in diabetes in which neuropathy occurs. Hyperglycaemia may be deleterious for the regeneration process for several reasons and via different mechanisms [22]. Thus, to study regenerative events and repair and reconstruction methods in diabetic models are therefore highly warranted.

Acknowledgements

The study was supported by the Swedish Research Council (Medicine), Region Skåne, and Skåne University Hospital (Malmö-Lund). The research leading to these results has received funding from the European Community's Seventh Framework Programme

(FP7-HEALTH-2011) under grant agreement no. 278612 (BIOHYBRID).

References

[1] L. Cai, W. Li, G. Wang, L. Guo, Y. Jiang, Y.J. Kang, Hyperglycemia-induced apoptosis in mouse myocardium: mitochondrial cytochrome C-mediated caspase-3 activation pathway, Diabetes 51 (2002) 1938–1948.
[2] L.B. Dahlin, L. Stenberg, H. Luthman, N.O. Thomsen, Nerve compression induces activating transcription factor 3 in neurons and Schwann cells in diabetic rats, Neuroreport 19 (2008) 987–990.
[3] B. Duran-Jimenez, D. Dobler, S. Moffatt, N. Rabbani, C.H. Streuli, P.J. Thornalley, D.R. Tomlinson, N.J. Gardiner, Advanced glycation end products in extracellular matrix proteins contribute to the failure of sensory nerve regeneration in diabetes, Diabetes 58 (2009) 2893–2903.
[4] L.F. Gumy, E.T. Bampton, A.M. Tolkovsky, Hyperglycaemia inhibits Schwann cell proliferation and migration and restricts regeneration of axons and Schwann cells from adult murine DRG, Mol. Cell. Neurosci. 37 (2008) 298–311.
[5] M. Kamijo, A.C. Merry, G. Akdas, P.V. Cherian, A.A. Sima, Nerve fiber regeneration following axotomy in the diabetic biobreeding Worcester rat: the effect of ARI treatment, J. Diabetes Complications 10 (1996) 183–191.
[6] H. Kamiya, W. Zhangm, A.A. Sima, Apoptotic stress is counterbalanced by survival elements preventing programmed cell death of dorsal root ganglions in subacute type 1 diabetic BB/Wor rats, Diabetes 54 (2005) 3288–3295.
[7] C. Lindwall, L. Dahlin, G. Lundborg, M. Kanje, Inhibition of c-Jun phosphorylation reduces axonal outgrowth of adult rat nodose ganglia and dorsal root ganglia sensory neurons, Mol. Cell. Neurosci. 27 (2004) 267–279.
[8] L. Martensson, P. Gustavsson, L.B. Dahlin, M. Kanje, Activation of extracellular-signal-regulated kinase-1/2 precedes and is required for injury-induced Schwann cell proliferation, Neuroreport 18 (2007) 957–961.
[9] A. Middlemas, J.D. Delcroix, N.M. Sayers, D.R. Tomlinson, P. Fernyhough, Enhanced activation of axonally transported stress-activated protein kinases in peripheral nerve in diabetic neuropathy is prevented by neurotrophin-3, Brain 126 (2003) 1671–1682.
[10] D.M. Nathan, Long-term complications of diabetes mellitus, N. Engl. J. Med. 328 (1993) 1676–1685.
[11] I.G. Obrosova, Diabetes and the peripheral nerve, Biochim. Biophys. Acta 1792 (2009) 931–940.
[12] T. Oya, Y.L. Zhao, K. Takagawa, M. Kawaguchi, K. Shirakawa, T. Yamauchi, M. Sasahara, Platelet-derived growth factor-b expression induced after rat peripheral nerve injuries, Glia 38 (2002) 303–312.
[13] C.C. Patterson, G.G. Dahlquist, E. Gyurus, A. Green, G. Soltesz, Incidence trends for childhood type 1 diabetes in Europe during 1989–2003 and predicted new cases 2005–20: a multicentre prospective registration study, Lancet 373 (2009) 2027–2033.
[14] E.J. Pawson, B. Duran-Jimenez, R. Surosky, H.E. Brooke, S.K. Spratt, D.R. Tomlinson, N.J. Gardiner, Engineered zinc finger protein-mediated VEGF—a activation restores deficient VEGF-a in sensory neurons in experimental diabetes, Diabetes 59 (2010) 509–518.
[15] C.R. Pierson, W. Zhang, Y. Murakawa, A.A. Sima, Insulin deficiency rather than hyperglycemia accounts for impaired neurotrophic responses and nerve fiber regeneration in type 1 diabetic neuropathy, J. Neuropathol. Exp. Neurol. 62 (2003) 260–271.
[16] J.W. Russell, K.A. Sullivan, A.J. Windebank, D.N. Herrmann, E.L. Feldman, Neurons undergo apoptosis in animal and cell culture models of diabetes, Neurobiol. Dis. 6 (1999) 347–363.
[17] H. Saito, L.B. Dahlin, Expression of ATF3 and axonal outgrowth are impaired after delayed nerve repair, BMC Neurosci. 9 (2008) 88.
[18] H. Saito, M. Kanje, L.B. Dahlin, Delayed nerve repair increases number of caspase 3 stained Schwann cells, Neurosci. Lett. 456 (2009) 30–33.
[19] K. Sango, H. Saito, M. Takano, A. Tokashiki, S. Inoue, H. Horie, Cultured adult animal neurons and schwann cells give us new insights into diabetic neuropathy, Curr. Diabetes Rev. 2 (2006) 169–183.
[20] A.A. Sima, New insights into the metabolic and molecular basis for diabetic neuropathy, Cell. Mol. Life Sci. 60 (2003) 2445–2464.
[21] L. Stenberg, M. Kanje, L. Martensson, L.B. Dahlin, Injury-induced activation of ERK 1/2 in the sciatic nerve of healthy and diabetic rats, Neuroreport 22 (2011) 73–77.
[22] D.R. Tomlinson, N.J. Gardiner, Diabetic neuropathies: components of etiology, J. Peripher. Nerv. Syst. 13 (2008) 112–121.
[23] Y. Tsuda, M. Kanje, L.B. Dahlin, Axonal outgrowth is associated with increased ERK 1/2 activation but decreased caspase 3 linked cell death in Schwann cells after immediate nerve repair in rats, BMC Neurosci. 12 (2011) 12.
[24] C. Yi, L.B. Dahlin, Impaired nerve regeneration and Schwann cell activation after repair with tension, Neuroreport 21 (2010) 958–962.
[25] W. Zhang, H. Kamiya, K. Ekberg, J. Wahren, A.A. Sima, C-peptide improves neuropathy in type 1 diabetic BB/Wor-rats, Diabetes Metab. Res. Rev. 23 (2007) 63–70.

Paper II

Stenberg and Dahlin *BMC Neuroscience* 2014, **15**:107
http://www.biomedcentral.com/1471-2202/15/107

BMC Neuroscience

RESEARCH ARTICLE Open Access

Gender differences in nerve regeneration after sciatic nerve injury and repair in healthy and in type 2 diabetic Goto-Kakizaki rats

Lena Stenberg* and Lars B Dahlin

Abstract

Background: In view of the global increase in diabetes, and the fact that recent findings indicate that diabetic neuropathy is more frequently seen in males, it is crucial to evaluate any gender differences in nerve regeneration in diabetes. Our aim was to evaluate in short-term experiments gender dissimilarities in axonal outgrowth in healthy and in genetically developed type 2 diabetic Goto-Kakizaki (GK) rats, and also to investigate the connection between activated (i.e. ATF-3, Activating Transcription Factor 3) and apoptotic (cleaved caspase 3) Schwann cells after sciatic nerve injury and repair. Female and male diabetic GK rats, spontaneously developing type 2 diabetes, were compared with corresponding healthy Wistar rats. The sciatic nerve was transected and instantly repaired. After six days the nerve was harvested to measure axonal outgrowth (i.e. neurofilament staining), and to quantify the number of ATF-3 (i.e. activated) and cleaved caspase 3 (i.e. apoptotic) stained Schwann cells using immunohistochemistry.

Results: Axonal outgrowth was generally longer in male than in female rats and also longer in healthy than in diabetic rats. Differences were observed in the number of activated Schwann cells both in the distal nerve segment and close to the lesion site. In particular the female diabetic rats had a lower number. There were no gender differences in number of cleaved caspase 3 stained Schwann cells, but rats with diabetes exhibited more (such cleaved caspase 3 stained Schwann) cells both at the lesion site and in the distal part of the sciatic nerve. Axonal outgrowth correlated with the number of ATF3 stained Schwann cells, but not with blood glucose levels or the cleaved caspase 3 stained Schwann cells. However, the number of cleaved caspase 3 stained Schwann cells correlated with the blood glucose level.

Conclusions: We conclude that there are gender differences in nerve regeneration in healthy rats and in type 2 diabetic GK rats.

Keywords: Nerve regeneration, Nerve repair, Neuropathy, Diabetes, Gender differences, Schwann cells

Background

Neuropathy, which is a general complication in both type 1 and type 2 diabetes, may cause serious problems for patients, particularly male patients with type 2 diabetes [1]. Male patients also seem to develop neuropathy earlier than female patients [1,2]. The mechanisms behind the development of neuropathy are complex and not fully understood, nor why male patients express neuronal complications earlier than female patients. The gender differences are also relevant in traumatic nerve injuries since such injuries more frequently affect males.

Earlier studies have shown that neuroactive hormones or steroids (affecting the nervous systems), such as testosterone and progesterone, play an active role in nerve regeneration and that the levels of neuroactive steroids differ in male and female rats, among both healthy and diabetic rats [3-5]. Recent findings indicate that axonal outgrowth six days after nerve injury and repair does not differ between healthy and diabetic BB (i.e. genetically developed and resembling type 1 diabetes; [6]) (female) rats. However, both numbers of activated and apoptotic Schwann cells, which are present in the distal nerve segment, were significantly higher in female diabetic BB rats

* Correspondence: Lena.Stenberg@med.lu.se
Department of Clinical Sciences - Hand Surgery, Lund University, Skane University Hospital, Malmö, Sweden

BioMed Central

© 2014 Stenberg and Dahlin; licensee BioMed Central Ltd. This is an Open Access article distributed under the terms of the Creative Commons Attribution License (http://creativecommons.org/licenses/by/4.0), which permits unrestricted use, distribution, and reproduction in any medium, provided the original work is properly credited. The Creative Commons Public Domain Dedication waiver (http://creativecommons.org/publicdomain/zero/1.0/) applies to the data made available in this article, unless otherwise stated.

than in female healthy rats [6]. Interestingly, a positive correlation between axonal outgrowth and Schwann cell activation (i.e. ATF 3 staining) has been reported, indicating the importance of Schwann cells for nerve regeneration and that the time point for nerve repair is crucial for axonal outgrowth [7-9]. Clarification of the nerve regeneration process from a gender perspective as well as in relation to a rat model with genetically developed diabetes similar to type 2, in contrast to the streptozotocin-induced diabetes model [10], is needed. This is relevant in view of the global increase in the number of patients with type 2 diabetes, where neuropathy is often present, and the fact that males are frequently affected by traumatic nerve injuries, particularly in the upper extremity, which require nerve repair or reconstruction. Thus, our aims were two-fold; to investigate any gender differences in nerve regeneration after nerve injury and repair in healthy rats from a short-term perspective and to explore whether the process is different in genetically developed type 2 Goto-Kakizaki diabetic rats. In conclusion, we observed differences between healthy and diabetic rats, using an appropriate diabetic animal model, as well as between male and female rats, with interesting correlations.

Results

Fasting blood glucose and weight increase

Pre- and post-operative blood glucose levels were significantly higher (Fisher's method; $p < 0.0001$) in diabetic than in healthy rats and were also significantly higher $p < 0.0001$) in male than in female rats (Table 1). There were no statistical differences between the groups concerning increase in weight during the regeneration period (Table 1).

Length of axonal outgrowth

Statistical differences were found between male and female rats ($p < 0.0001$; Fisher's test; Table 1) with longer outgrowth (Figure 1) in male rats ($p < 0.0001$ for both healthy and diabetic rats, MW). There were also distinctions between healthy and diabetic rats ($p = 0.02$; Fisher's test), where axonal outgrowth was much longer in female healthy rats than in female diabetic rats ($p = 0.004$, MW, Table 1), while no difference was observed between healthy and diabetic male rats ($p = 0.68$, MW).

ATF-3 stained Schwann cells at the site of lesion

Only those cells with a Schwann cell shape were counted as ATF-3 stained Schwann cells (Figure 2a,c-d). ATF-3 stained Schwann cells differed ($p = 0.0001$; KW) at the lesion site. The Fisher's test showed a statistical difference ($p = 0.0001$) between male and female rats and also between healthy and diabetic rats ($p = 0.001$). The number of ATF-3 stained Schwann cells was higher ($p = 0.001$ MW) in diabetic rats than in healthy male rats. The numbers were also higher ($p = 0.0001$, MW) in diabetic male rats than in diabetic female rats. On the contralateral side (i.e. uninjured side), only a few ATF-3 stained Schwann cells were found.

ATF-3 stained Schwann cells in the distal nerve segment

Again, only cells with the shape of a Schwann cell were counted as ATF-3 stained Schwann cells. ATF-3 stained Schwann cells differed ($p = 0.0001$; KW) in the distal segment. The Fisher's test demonstrated significant differences between male and female rats ($p = 0.0003$) as well as between healthy and diabetic rats ($p = 0.001$). Higher numbers of ATF-3 stained Schwann cells ($p = 0.0001$, MW) were

Table 1 Nerve regeneration after nerve injury and repair in healthy and diabetic rats

	Healthy male (n = 10)	Healthy female (n = 10)	Diabetes male (n = 10)	Diabetes female (n = 10)	p-values (KW[a])	Fisher's method[b]	
						Male/female	Healthy/ Diabetes
Axonal outgrowth (neurofilaments, mm)	7.0 (6.8-7.3)	6.3 (6.1-6.4)	6.9 (6.7-7.1)	5.8 (5.1-6.2)	**0.0001**	**<0.0001**	**0.02**
ATF-3 (% of total) SNL	17.8 (17.6-18.4)	17.6 (16.7-18.0)	19.8 (19.1-21.1)	16.4 (15.7-17.3)	**0.0001**	**0.0001**	**0.001**
ATF-3 (% of total) SND	19.2 (17.7-19.6)	19.5 (18.9-20.1)	18.7 (16.9-20.1)	15.2 (14.4-15.7)	**0.0001**	**0.0003**	**0.001**
Cleaved caspase-3 (% of total) SNL	5.2 (2.6-7.8)	3.1 (2.9-3.4)	9.6 (8.7-11.6)	7.0 (6.4-10.1)	**0.0001**	0.31	**<0.0001**
Cleaved caspase-3 (% of total) SND	2.7 (2.2-4.0)	2.5 (2.4-2.7)	6.4 (4.5-7.1)	5.8 (4.3-6.1)	**0.0001**	0.39	**<0.0001**
Total cell number (mm^2) SNL	1137 (1127-1142)	1050 (1027-1066)	1073 (1046-1103)	1089 (1059-1098)	**0.0001**	**0.0007**	**0.0001**
Total cell number (mm^2) SND	1137 (1122-1152)	1112 (1068-1147)	1053 (1019-1091)	1093 (1045-1102)	**0.0001**	0.07	**<0.0001**
Preoperative B-glucose (mmol/l)	4.6 (4.3-4.9)	3.90 (3.8-4.3)	15.0 (13.3-17.2)	10.3 (9.7-11.7)	**0.0001**	**<0.0001**	**<0.0001**
Weight increase (%)	2.2 (0.7-2.7)	2.4 (1.3-4.8)	2.0 (1.2-2.6)	2.6 (2.0-3.2)	0.34	-	-

Values are median 25th (Q1) -75th (Q3) percentiles. [a]KW = Kruskal-Wallis. [b]Fisher's method for independent samples based on the chi square distribution.
SNL = Lesion site. *SND* = Distal nerve segment. *Total cell* = DAPI stained cells. P-values in bold is significantly different at least at the 0.05 level.

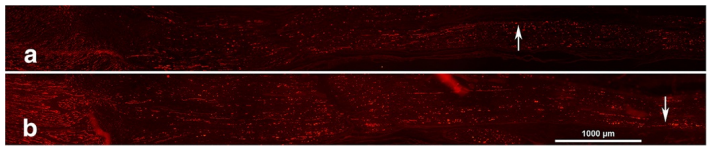

Figure 1 Immunohistochemistry of neurofilament staining. Immunohistochemistry of staining for neurofilament proteins in female **(a)** and male **(b)** GK rats. The arrow indicates tip of the outgrowing axons, where the nerve repairs are in the left part of the panel. Length of bar = 1000 µm.

found in diabetic male rats than in diabetic female rats and in healthy female rats than in diabetic female rats (p = 0.0001, MW). Again, few ATF-3 stained Schwann cells were found on the contralateral side.

Cleaved caspase-3 stained Schwann cells at the lesion site

Generally, there were differences (p = 0.0001; KW) regarding numbers of cleaved caspase 3 stained Schwann cells at the lesion site in the sciatic nerve (Figure 2b,e-f). There were mostly no gender differences in the number of cleaved caspase 3 stained Schwann cells at the lesion site (p = 0.31, Fisher's test) among male and female rats. However, a significant difference was found between healthy and diabetic rats (p < 0.0001, Fisher's test). The number of stained cleaved caspase 3 Schwann cells was statistically higher (p = 0.0001, MW) in diabetic male rats than in healthy male rats and also in diabetic female rats than in healthy female rats (p = 0.0001 MW). Single cleaved caspase 3 stained Schwann cells were found on the contralateral side.

Cleaved caspase 3 stained Schwann cells in the distal nerve segment

There were generally differences (p = 0.0001; KW) regarding cleaved caspase 3 stained Schwann cells in the distal nerve segment. Furthermore, Fisher's test showed no significant differences between male and female rats (p = 0.39), but a significant difference between healthy and diabetic

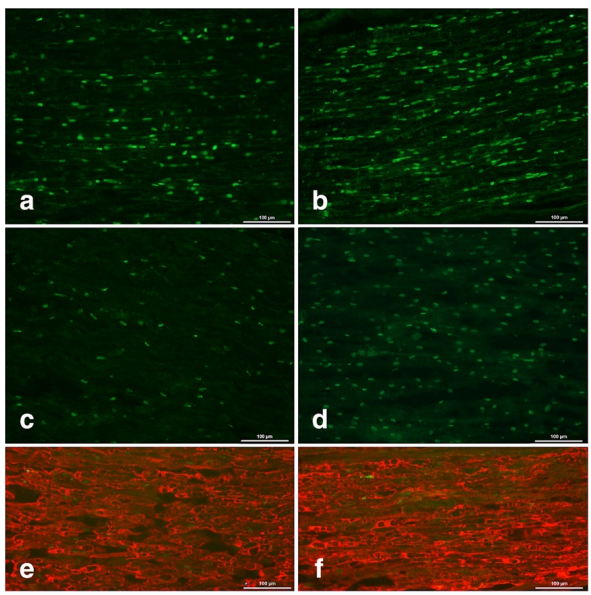

Figure 2 Immunohistochemistry of ATF3 and cleaved caspase 3 stained Schwann cells. Immunohistochemistry of ATF3 stained Schwann cells in Wistar **(a)** and GK **(b)** male rats as well as cleaved caspase 3 stained cells in Wistar **(c)** and GK **(d)** male rats; all at the lesion site. Double staining of ATF 3 and S-100 **(e)** as well as cleaved caspase 3 and S-100 **(f)**, at the lesion site in a male GK rat. Length of bar = 100 µm.

rats ($p < 0.0001$). A significantly higher number of cleaved caspase-3 stained Schwann cells ($P = 0.0001$, MW) was found in diabetic female rats than in healthy female rats. There were also significantly higher numbers in diabetic male rats ($p = 0.0001$, MW) than in healthy male rats. Again, single cleaved caspase 3 stained Schwann cells were found on the contralateral side.

Total number of DAPI stained cells at the lesion site

Kruskal-Wallis showed differences ($p = 0.0001$) with respect to total number of DAPI stained cells at the lesion site. There were significant differences in the total number of DAPI stained cells between male and female rats ($p = 0.0007$, Fisher's test; Table 1) and between healthy and diabetic rats ($p = 0.0001$). The total number of DAPI stained cells at the lesion site was higher in the healthy male rats than in healthy female rats ($p = 0.0001$, MW) and in healthy male rats than in diabetic male rats ($p = 0.0001$, MW).

Total number of DAPI stained cells in the distal nerve segment

Kruskal-Wallis showed differences ($p = 0.0001$) in the total number of DAPI stained cells in the distal nerve segment. Significant differences were observed between healthy and diabetic rats ($p < 0.0001$, Fisher's test), but not between male and female rats ($p = 0.07$; Fisher's test). There was a significantly higher number of total DAPI stained cells in healthy male rats than in diabetic male rats ($p = 0.0001$, MW).

Correlation

All rats pooled

The Spearman correlation test showed a significant positive correlation between numbers of ATF-3 stained Schwann cells at the lesion site and axonal outgrowth (rho = 0.59, $p = 0.0001$; Figure 3a), but blood glucose levels did not correlate with axonal outgrowth ($p = 0.39$) when all rats were pooled. Preoperative blood glucose level and cleaved caspase 3 stained Schwann cells at the lesion site were also tested for correlation and found to be positively correlated (rho = 0.69, $p = 0.0001$; Figure 3b). A weaker correlation (rho = 0.32, 0 = 0.046) was found between preoperative blood glucose and numbers of ATF-3 stained Schwann cells at the lesion site. While there was no significant correlation between the numbers of cleaved caspase 3 stained Schwann cells and axonal outgrowth ($p = 0.24$), they correlated weakly with the number of ATF-3 stained Schwann cells (rho = 0.40, $p = 0.01$).

In the distal nerve segment, when all rats were pooled, the preoperative blood glucose levels positively correlated with the number of cleaved caspase 3 stained Schwann cells (rho = 0.74, $p = 0.0001$, Figure 3c), but the blood glucose levels did not correlate with the numbers of ATF 3 stained Schwann cells ($p = 0.11$). The weight increase in the rats did not influence any of the variables.

Diabetic rats

If the diabetic animals were analysed separately, there was a positive correlation between preoperative blood glucose levels, and axonal outgrowth (rho = 0.60, $p = 0.005$; Figure 3d) and ATF-3 stained Schwann cells at the site of the lesion (rho = 0.67, $p = 0.001$) as well as between the number of ATF-3 and cleaved caspase 3 stained Schwann cells at the lesion site (rho = 0.51, $p = 0.02$; Figure 3e). Furthermore, in the diabetic rats the preoperative blood glucose levels positively correlated with the number of ATF-3 stained Schwann cells in the distal nerve segment (rho = 0.66, $p = 0.001$, Figure 3f).

Healthy rats

The blood glucose levels in healthy rats positively correlated with axonal outgrowth (rho = 0.60, $p = 0.005$).

Discussion

We examined whether any gender differences between female and male rats, regarding axonal outgrowth, were present. In particular, we analysed how a high blood glucose level in a diabetic GK rat model, resembling type 2 diabetes, influenced the axonal outgrowth. The published literature in the field of nerve regeneration in diabetes is limited and studies almost exclusively use streptozotocin-induced diabetes in rats in which blood glucose levels are high (see e.g. [11-14]). The ability of axons to regenerate in relation to the state of the Schwann cells may also be an important point in relation to moderate blood glucose levels and in view of the global increase of diabetes, particularly bearing in mind its most common complication, i.e. neuropathy. We used genetically developed diabetic GK rats as a model for type 2 diabetes, which is a valid model and also a gentle alternative to the diabetic BB (BioBreeding) rats [6] and the frequently used rats with streptozotocin-(STZ)induced diabetes. The similarity with human beta cells, compared to these cells in other rodent models, is an unique characteristic of GK rats [15] making the model valid also for studies of the peripheral nervous system. The relationship between ATF3 and cleaved caspase 3 stained Schwann cells and axonal outgrowth were evaluated in these rat models. The present nerve regeneration model utilizes the possibility of analysing ATF3 (i.e. activation) and cleaved caspase 3 (i.e. apoptosis) stained Schwann cells in relation to axonal outgrowth, where the cells at the lesion site (SNL) interact with the outgrowing axons, while the axons have not yet reached the analysis site in the distal nerve segment (SND; Figure 4; [9]).

Few studies have highlighted any gender differences or possible mechanisms in nerve regeneration (see e.g. [16-18]). Our results clearly show that there was a gender difference

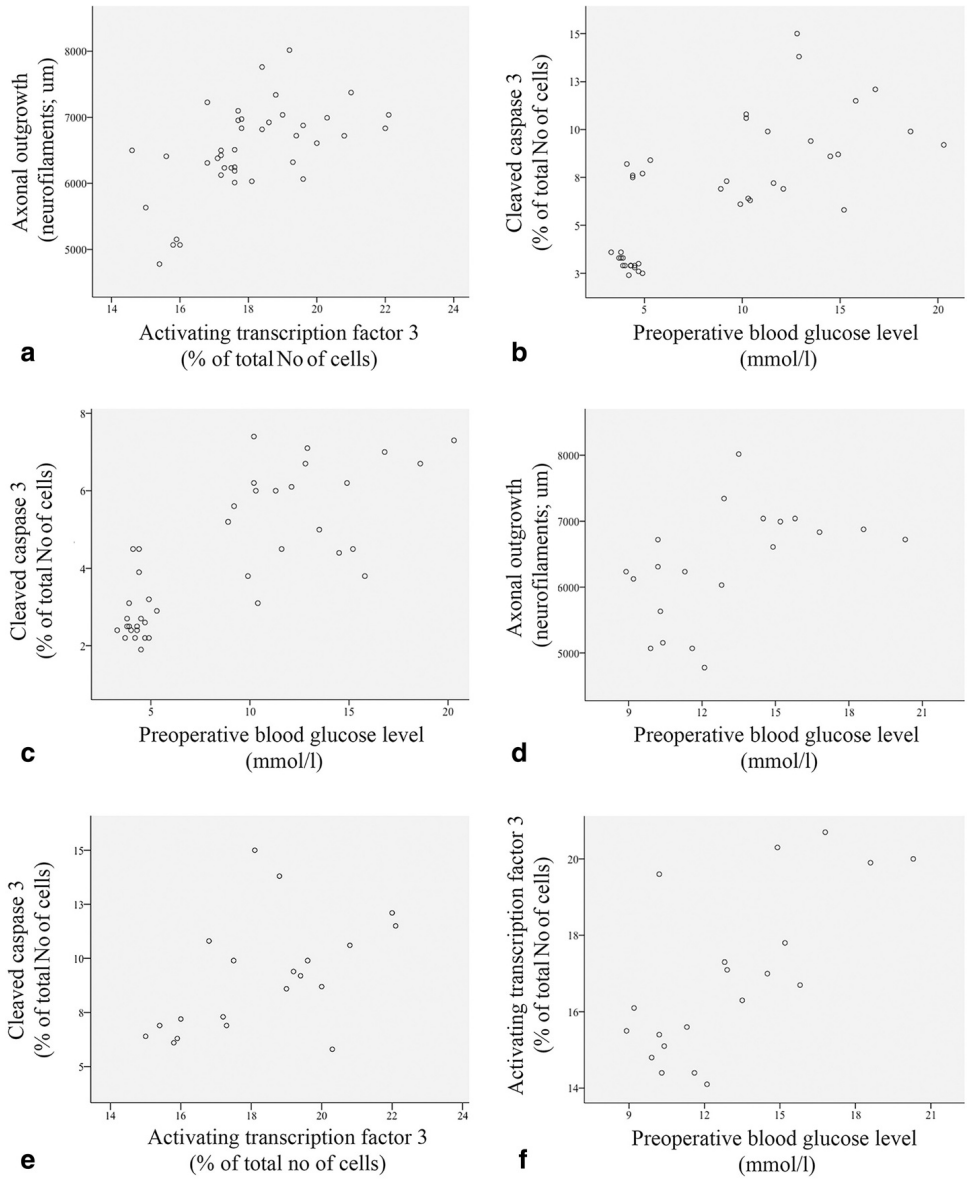

Figure 3 Scatter plots from all rats (a-c) and rats with diabetes (d-f). Scatter plots from all rats pooled **(a-c)** with numbers of ATF-3 stained cells (lesion site) and axonal outgrowth (**a**; rho = 0.59, p = 0.0001), preoperative blood glucose level and cleaved caspase 3 stained cells (**b**, lesion site; rho = 0.69, p = 0.0001; **c**. in distal nerve segment; rho = 0.74, p = 0.0001). Scatter plots from diabetic rats **(d-f)** with preoperative blood glucose levels and axonal outgrowth (d, rho = 0.60, p = 0.005; **d**), number of cleaved caspase 3 and ATF-3 stained cells (**e**, lesion site; rho = 0.51, p = 0.02) and preoperative blood glucose level and number of ATF-3 stained cells (**f**, distal nerve segment; rho = 0.66, p = 0.001).

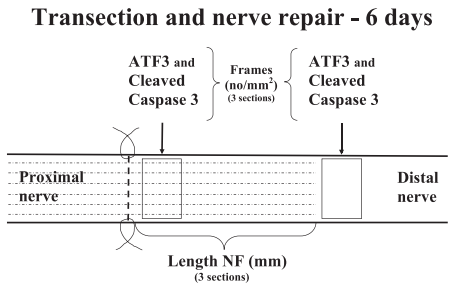

Figure 4 Schematic drawing of the experimental set up. The sciatic nerve was transected and immediately repaired. Axonal outgrowth was evaluated by measuring the length of neurofilaments (NF). The numbers of activated (Activating Transcription Factor 3; ATF3) and apoptotic (cleaved caspase 3) Schwann cells were measured just distal to the lesion site (i.e. axons presented) and in the distal nerve segment (distal to the most distal parts of the neurofilament stained axons).

in axonal outgrowth after nerve injury and repair, with a longer outgrowth in male rats. The weight increase in the rats, a possible factor in a difference in axonal outgrowth, did not differ between male and female or even between healthy and diabetic rats and did not correlate with any of the variables; thus it could not explain the difference. However, our results are in accordance with previous studies using a nerve crush injury, i.e. a clinically less important injury [19], showing that neuroactive steroids, such as pregnenolone and progesterone metabolites that interact with progesterone receptor, are protective. This is also relevant for myelin repair in different neurological disorders [20]. Progesterone has been considered as an autocrine signalling molecule [21]. Interestingly, progesterone-loaded chitosan prostheses have been used to successfully reconstruct nerve injuries [22]; chitosan conduits being a promising clinical material for nerve reconstruction [23]. Potential use of neuroactive steroids, such as progesterone and testosterone, for treatment of diabetic neuropathy has also been suggested [5,24], where differences between gender, diabetic state and a regional location, with request to neuroactive steroid levels, are reported [3,25]. The reason (s) male subjects with diabetes develop neuropathy earlier than female subjects [1,2] is not clear and may be complex, but factors such as testosterone deficiency, which is common in men with diabetes (i.e. leading to a pronounced deficit of neurosteroids), as well as lifestyle differences may contribute to the discrepancy in development, at least in type 2 diabetes in humans [26]. In addition, the mechanisms for the development of neuropathy in type 1 and 2 in humans may be different and particularly complex and multifactorial in type 2 diabetes [27,28] which the present GK rat model resembles.

In our short-term model (i.e. six days), the regeneration process, which showed longer regeneration distances in male rats, may depend on the level of blood glucose. Thus, a moderately higher short-term blood glucose level may be advantageous for axons, leading to longer axonal outgrowth, while the opposite may be present in humans where higher long-standing blood glucose levels may have deleterious effects on the neurons and Schwann cells. An even more complex situation exists in diabetic BB rats, who have even higher blood glucose levels and in which axonal outgrowth does not differ from healthy rats in a short-term regeneration model (i.e. six days), although an increased number of activated and apoptotic Schwann cells are present after injury and repair in such BB rats [6]. The diabetic rat model used is crucial and gender aspects should also be considered in nerve regeneration studies. In long-term (i.e. three months) streptozotocin-induced diabetes in rats, the level of neuroactive steroids is lower than in healthy rats [3,29,30], which may contribute to explaining the findings of a shorter axonal outgrowth in experimental diabetes in the present study [3]. However, the pattern of various neuroactive steroid levels in the sciatic nerve among the healthy and diabetic rats in a study by Pesaresi et al. [3], who used another diabetes model, cannot be related to our findings regarding length of axonal outgrowth and numbers of ATF3 and cleaved caspase 3 stained Schwann cells. Thus, the neuroactive steroid levels may not entirely explain the differences between genders and state of glucose levels, but we cannot rule out the influence of neuroactive steroids since we did not measure such steroids. Moreover, several essential factors for nerve regeneration may be in play simultaneously.

Progesterone also promotes myelination, which we did not specifically address in the short-term experiments, by activating transcription factors (Krox-20) and/or myelin proteins (P0, PMP22; [21]). However, we did see gender differences, with higher numbers of ATF3 stained Schwann cells at the lesion site as well as in the distal nerve segment in male rats, which was particularly evident in the diabetic rats. The number of ATF3 stained Schwann cells correlated with axonal outgrowth, suggesting ATF3 has a role in axonal outgrowth [9], and it may even be suggested that ATF3 acts through different mechanisms in healthy and diabetic GK rats. ATF3, a member of CREB family, is a marker for activated Schwann cells and ATF3 stained Schwann cells and neurons rapidly increase locally as well as in dorsal root ganglia and in the spinal cord, respectively, after a nerve injury; this is an indication of cell viability [31]. In contrast, cleaved caspase 3 staining is a marker for apoptosis, i.e. cell death [32]. The numbers of ATF3 and cleaved caspase 3 stained cells correlated positively. Thus, the number of cleaved caspase 3 stained cells seems to balance the number of ATF3 stained cells at the lesion site in various models of diabetes [6] and in healthy rats.

Such a mechanism has been suggested as a control function of Schwann cell proliferation, which is important [9,33], although not crucial [34], for nerve regeneration.

The axonal outgrowth correlated with blood glucose levels when healthy and diabetic rats were analysed separately, which can probably be explained by the higher blood glucose levels in both healthy and diabetic male rats. In contrast to the present diabetic rat model, axonal outgrowth after nerve repair does not differ between female diabetic BB rats, which have much higher blood glucose levels, and female healthy rats [6]. However, these diabetic female rats also have an increased number of activated and apoptotic Schwann cells. Interestingly, the blood glucose levels in the present study correlated positively with the number of ATF3 stained Schwann cells in all rats and particularly in diabetic GK rats. The present higher numbers of cleaved caspase 3 stained Schwann cells in the diabetic female rats agrees with findings in diabetic BB rats [6] despite their different blood glucose profiles and potentially other dissimilarities. The blood glucose levels in diabetic rats correlated with both the numbers of ATF3 and cleaved caspase 3 stained Schwann cells; the latter finding was not surprising [35]. Apoptosis of Schwann cells and neurons is reported to be induced in STZ-induced diabetes and by glucose infusion due to oxidative stress [35,36]. However, the diabetic BB model (i.e. female rats) had higher numbers of ATF3 stained cells, which contrasts with the present study, where female diabetic rats had fewer ATF3 stained cells than the healthy female rats [6]. There was also generally a lower number of DAPI stained cells in the distal nerve segment (Fisher $p < 0.0001$) in the diabetic rats, which agrees with findings in diabetic BB rats [6].

Not only is the blood glucose level per se relevant, but also the level of insulin, which may have a trophic support [37] making the use of different models relevant. In STZ-induced diabetes, the beta cells are destroyed by the toxic effect of STZ and in the BB rats autoimmune mechanisms that destroy beta cells are in action [38]. Any possible insulin effect is, therefore, mostly deleted in both such models, although there may be a lingering insulin production in STZ-induced diabetes [39], explaining why these rats survive without insulin supplementation over a period. In contrast, BB rats have no capacity to produce any insulin [39] and develop an insulin-dependent diabetes resembling that in humans. Such rats may also show symptoms similar to those of an autoimmune disease as well as pathological changes in the peripheral nervous system, which STZ-induced rats do not [40,41]. Interestingly, there is no significant difference in the concentration of insulin between GK and Wistar rats [42]. Therefore, it is unlikely that the insulin level per se will explain the present changes in nerve regeneration. The influence of blood glucose levels on the nerve regeneration process is complex, as is also discussed when considering the development of diabetic neuropathy, where vibrotactile sense (i.e. sign of neuropathy) in patients with diabetes is not affected by the long-term blood glucose level, i.e. HbA1c, levels [43-45]. Heat Shock Protein 27 (HSP27) has recently been described tentatively as an important factor in the preservation of nerve function in patients with type 2 diabetes [46]. Whether HSP 27 is relevant in the present model, and not only in STZ-induced diabetes [47] or in BB/Wor rats with diabetes [48], remains to be investigated.

One limitation of our studies on nerve regeneration in diabetic GK and BB rats is the short-term design, which should be considered when interpreting nerve regeneration in diabetes and in connection with gender aspects. However, our approach was to relate axonal outgrowth with possible activation and apoptotic events concerning the Schwann cells in relation to certain blood glucose levels in male and female rats, without interfering with the processes in the treatment of insulin, which would be required in long-term studies in BB rats. Finally, the nature of the nerve injury is also relevant in this context, since a nerve compression lesion in diabetic rats induces a different response in the nerve trunk with more ATF-3 stained Schwann cells in diabetic BB rats than in diabetic GK and healthy rats [49]. Taken together, in future studies of nerve regeneration and neuropathy in diabetes, one may have to consider the diabetic model, the injury model and the gender of the rats as well as determine e.g. the levels of blood glucose, insulin, neuroactive steroids and potential protective substances, such as HSP27.

Conclusions

Our study demonstrates gender differences in axonal outgrowth in diabetic GK and healthy rats after transection and repair after six days, with differences also detected in activation and apoptosis of Schwann cells in the sciatic nerve. This is interesting in view of the fact that males with diabetes have a higher frequency of neuropathy than females with diabetes and that males develop it more rapidly in humans [1,2], indicating that relevant experimental models are compulsory. We suggest that it is extremely important to take into account gender differences as well as type of experimental diabetic model when new strategies and techniques for treatment of nerve injuries are developed.

Methods

Animals and surgery

Four groups of rats (initial body weight 200 g) were included: healthy male (n = 10) and female (n = 10) Wistar rats with normal blood glucose were compared with male (n = 10) and female (n = 10) Goto-Kakizaki rats (GK) in

which a moderate increase in blood glucose is observed. Fasting blood glucose, body weight and polydipsia, as signs of diabetes, were measured and observed daily in all rats. Blood glucose was measured in a blood sample from the tail vein [Ascensia contour TM (Bio Healthcare, USA, Bio Diagnostics Europe) and LT (Bayer AB, Diabetes Care, Solna, Sweden); test slips (Microfil TM (Bio Healthcare Diabetes Care, USA)]. The rats had a 12 h day/night cycle in the cages and the GK rats were provided with extra water.

Before surgery the rats were anesthetized with intraperitoneal injection of a mixture of Rompun® (20 mg/ml; Bayer Health Care, Leverkusen, Germany) and Ketalar® (10 mg/ml, Pfizer, Helsinki, Finland) at a dose of a 1 ml Ketalar® and 0.25 ml Rompun® per 100 g body weight of the rat. Postoperatively, all rats were treated with Temgesic® 0.01-0.05 mg/kg (0.3 mg/ml; Schering-Plough Europe, Brussels, Belgien) to prevent pain. The sciatic nerve in the hind limb in each rat was unilaterally exposed, transected and instantly repaired with 9-0 ethilon (Ethicon®) epi/perineurial sutures (Figure 4). The muscles were secured with resorbable sutures, the skin was closed and the rats were allowed to recover.

Six days after surgery the rats were killed by an overdose of pure pentobarbitalnatrium (60 mg/ml; Apoteksbolaget, Malmö, Sweden). The sciatic nerve was harvested bilaterally. The samples were fixed in Stefanini solution [4% paraformaldehyde and 1.9% picric acid in 0.1 M phosphate buffer (PBS) pH 7.2] for 24 hours. After the fixation procedure the samples were washed (PBS × 3) and placed in 20% sucrose solution over night. Before cryostat sectioning the samples were placed in OCT Cry mount® (Histolab products AB, Gothenburg, Sweden) for embedding. After freezing the samples the nerves were sectioned longitudinally at thickness of 8 μm on superfrost plus glass (Thermo scientific, Braunschweig, Germany).

Immunohistochemistry

After washing (PBS 5 min) the sections were incubated with anti-human neurofilament protein (DAKO Glostrup, Denmark; dilution 1:80 in 0.25% Triton-X 100 and 0.25% BSA; bovine serum albumin) in PBS, over night at 4°C. On day two, after additional washing (PBS 3×5 min), the slides were incubated with the second antibody Alexa Fluor 594 conjugated goat anti-mouse IgG (Invitrogen, Molecular Probes, Eugene, Oregon, USA; 1:500 in PBS) for one hour, at room temperature. The slides were then washed (PBS 3×10 min), counterstained with 4',6'-diamino-2-phenylindole DAPI (Vectashield®, Vector Laboratories, Inc. Burlingame, CA 94010, USA) to visualize the nuclei (i.e. for counting the total number of cells) and then mounted and cover slipped.

Other sections were instead incubated with rabbit anti-ATF-3 polyclonal antibody (Santa Cruz Biotechnology, USA; dilution 1:200) as the primary antibody and Alexa Fluor 488 conjugated goat anti-rabbit IgG (Invitrogen, Molecular Probes, Eugene, Oregon, USA; dilution 1:500) as the secondary antibody.

In further sections the antibody against cleaved caspase 3 (BioNordica, Stockholm, Sweden, dilution 1:200) together with the secondary antibody Alexa Fluor 488 conjugated goat anti-rabbit IgG (Invitrogen, Molecular Probes, Eugene, Oregon, USA; dilution 1:500) was used to count the apoptotic cells.

Double immunohistochemical staining (S-100 and ATF-3) was done to ensure that only Schwann cells were counted. The slides were incubated day one with rabbit anti-ATF-3 polyclonal antibody (Santa Cruz Biotechnology, USA, dilution 1:200) and on day two with the secondary antibody Alexa Fluor 488 conjugated goat anti-rabbit IgG (Invitrogen, Molecular Probes, Eugene, Oregon, USA; dilution in 1:500). After one hour the slides were incubated with mouse monoclonal IgG anti-S100 antibody α/β chain (Santa Cruz Biotechnology, USA; dilution 1:200). On day three, the sections were incubated with Alexa Fluor 594 conjugated goat anti-mouse IgG (Invitrogen, Molecular Probes, Eugene, Oregon, USA; dilution1:500) and one hour later mounted with VECTASHIELD (Vectashield®, Vector Laboratories, Inc. Burlingame, CA 94010, USA) and cover slipped. A similar double immunohistochemistry procedure was used for staining of cleaved caspase 3 stained Schwann cells (i.e. S-100).

Photography and computer analysis

Sections from each nerve were blind coded before the analyses in the digital system. From the contralateral uninjured side only a few sections were analyzed, but not quantified, to see whether there was any difference between healthy female and male and GK diabetic female and male rats. The sections were photographed using a fluorescence microscope provided with a digital system camera (Nikon 80i) system connected to a computer. The digital images were analysed using the NIS elements computer program. The length of the stained neurofilament proteins was measured in three randomly selected sections (mean value from the three sections; Figure 4) from the lesion site to the front of the longest growing axons [6]. The stained cells for ATF-3 and cleaved caspase 3 stained cells were counted in three sections (image size 500 μm ×400 μm; mean values from three sections) from the sciatic nerve both at the lesion site (SNL) and in the distal nerve segment (SND) beyond the stained neurofilaments (i.e. at 8 mm from nerve lesion) [9]. At these locations, squares (6 × 100 μm^2) were randomly selected and examined for the presence of cleaved caspase 3 and ATF-3 stained Schwann cells (Figure 4). Exactly the same squares were also used to count the total number of DAPI stained cells.

Statistical methods

IBM SPSS Statistics version 20 was used for the statistical analysis. The results are presented as median values [with 25th - 75th percentiles] since the data were not considered to be normally distributed and thus required non-parametric tests for further analyses. To detect any significant values among the four groups, the non-parametric method Kruskal-Wallis (KW) was used and with the post hoc Mann-Whitney (MW) test to observe differences between the following groups: healthy/diabetic and male/female. Separate p-values for males and females were then combined in to an overall p-value by using the Fisher method for independent samples based on the chi square distribution [50] (http://en.wikipedia.org/wiki/Fisher's_method, courtesy of our statistician, Professor Jonas Björk, Lund University, Lund, Sweden). A p-value of less than 0.05 was regarded as significant.

Ethics

The animal ethics committees in Malmö and Lund approved all animal experiments (Lund University permit number: 347/2011). The study was carried out in strict accordance with the recommendations made by the Swedish Board of Agriculture and the European Union. All efforts were made to minimize suffering.

Abbreviations

BB: Biobreeding; ATF3: Activation Transcription Factor 3; GK: Goto-Kakizaki; PBS: Phosphate Buffered Saline; MW: Mann-Whitney; KW: Kruskal-Wallis; P0: Protein zero; PMP22: Peripheral Myelin Protein 22; CREB: CAMP Response Element Binding; STZ: Streptozotocin; HbA1c: Haemoglobin A1c; HSP27: Heat Shock Protein 27; BB/Wor: Biobreeding/Worchester.

Competing interests

The authors declare that they have no competing interests.

Authors' contributions

Both authors were involved with the conception and design of the work, acquisition of data, or analysis and interpretation of data, drafting the article or revising it critically for important intellectual content and gave their final approval of the version for publication.

Acknowledgements

We would like to acknowledge our close friend, colleague and mentor Professor Martin Kanje, PhD, Department of Biology, Lund University, Sweden, who died in March 2013. Martin was an important source of knowledge for the design of the present project, but he was not able to see it finalized. Martin should be remembered as an outstanding scientist in the field of peripheral nerve regeneration and will continue to be an inspiration in our research.

The project was supported by the Swedish Research Council (Medicine), European Community's Seventh Framework Programme (FP7-HEALTH-2011) under grant agreement no. 278612 (BIOHYBRID), Lund University, Sydvästra Skånes Diabetesförening and Region Skåne (Skåne University Malmö, Lund), Sweden. We would also like to thank Professor Jonas Björk for statistical advice.

Received: 3 April 2014 Accepted: 9 September 2014
Published: 13 September 2014

References

1. Aaberg ML, Burch DM, Hud ZR, Zacharias MP: **Gender differences in the onset of diabetic neuropathy.** *J Diabetes Complications* 2008, **22:**83–87.
2. Sima AA: **New insights into the metabolic and molecular basis for diabetic neuropathy.** *Cell Mol Life Sci* 2003, **60:**2445–2464.
3. Pesaresi M, Maschi O, Giatti S, Garcia-Segura LM, Caruso D, Melcangi RC: **Sex differences in neuroactive steroid levels in the nervous system of diabetic and non-diabetic rats.** *Horm Behav* 2010, **57:**46–55.
4. Sharma N, Marzo SJ, Jones KJ, Foecking EM: **Electrical stimulation and testosterone differentially enhance expression of regeneration-associated genes.** *Exp Neurol* 2010, **223:**183–191.
5. Melcangi RC, Giatti S, Pesaresi M, Calabrese D, Mitro N, Caruso D, Garcia-Segura LM: **Role of neuroactive steroids in the peripheral nervous system.** *Front Endocrinol (Lausanne)* 2011, **2:**104.
6. Stenberg L, Kanje M, Dolezal K, Dahlin LB: **Expression of activating transcription factor 3 (ATF 3) and caspase 3 in Schwann cells and axonal outgrowth after sciatic nerve repair in diabetic BB rats.** *Neurosci Lett* 2012, **515:**34–38.
7. Tsujino H, Kondo E, Fukuoka T, Dai Y, Tokunaga A, Miki K, Yonenobu K, Ochi T, Noguchi K: **Activating transcription factor 3 (ATF3) induction by axotomy in sensory and motoneurons: A novel neuronal marker of nerve injury.** *Mol Cell Neurosci* 2000, **15:**170–182.
8. Kataoka K, Kanje M, Dahlin LB: **Induction of activating transcription factor 3 after different sciatic nerve injuries in adult rats.** *Scand J Plast Reconstr Surg Hand Surg* 2007, **41:**158–166.
9. Saito H, Dahlin LB: **Expression of ATF3 and axonal outgrowth are impaired after delayed nerve repair.** *BMC Neurosci* 2008, **9:**88.
10. Stenberg L, Kanje M, Martensson L, Dahlin LB: **Injury-induced activation of ERK 1/2 in the sciatic nerve of healthy and diabetic rats.** *Neuroreport* 2011, **22:**73–77.
11. Nishida N, Yamagishi S, Mizukami H, Yagihashi S: **Impaired nerve fiber regeneration in axotomized peripheral nerves in streptozotocin-diabetic rats.** *J Diabetes Investig* 2013, **4:**533–539.
12. Dey I, Midha N, Singh G, Forsyth A, Walsh SK, Singh B, Kumar R, Toth C, Midha R: **Diabetic Schwann cells suffer from nerve growth factor and neurotrophin-3 underproduction and poor associability with axons.** *Glia* 2013, **61:**1990–1999.
13. Salles GS Jr, Faria JC, Busnardo FF, Gemperli R, Ferreira MC: **Evaluation of nerve regeneration in diabetic rats.** *Acta Cir Bras* 2013, **28:**509–517.
14. Yao CH, Chang RL, Chang SL, Tsai CC, Tsai FJ, Chen YS: **Electrical stimulation improves peripheral nerve regeneration in streptozotocin-induced diabetic rats.** *J Trauma Acute Care Surg* 2012, **72:**199–205.
15. Portha B, Lacraz G, Kergoat M, Homo-Delarche F, Giroix MH, Bailbe D, Gangnerau MN, Dolz M, Tourrel-Cuzin C, Movassat J: **The GK rat beta-cell: a prototype for the diseased human beta-cell in type 2 diabetes?** *Mol Cell Endocrinol* 2009, **297:**73–85.
16. Meek MF, Koning MA, Nicolai JP, Gramsbergen A: **Rehabilitation strategy using enhanced housing environment during neural regeneration.** *J Neurosci Methods* 2004, **136:**179–185.
17. Yu WH: **Sex difference in the regeneration of the hypoglossal nerve in rats.** *Brain Res* 1982, **238:**404–406.
18. Yu WH, McGinnis MY: **Androgen receptors in cranial nerve motor nuclei of male and female rats.** *J Neurobiol* 2001, **46:**1–10.
19. Roglio I, Bianchi R, Gotti S, Scurati S, Giatti S, Pesaresi M, Caruso D, Panzica GC, Melcangi RC: **Neuroprotective effects of dihydroprogesterone and progesterone in an experimental model of nerve crush injury.** *Neuroscience* 2008, **155:**673–685.
20. Schumacher M, Guennoun R, Stein DG, De Nicola AF: **Progesterone: therapeutic opportunities for neuroprotection and myelin repair.** *Pharmacol Ther* 2007, **116:**77–106.
21. Schumacher M, Guennoun R, Mercier G, Desarnaud F, Lacor P, Benavides J, Ferzaz B, Robert F, Baulieu EE: **Progesterone synthesis and myelin formation in peripheral nerves.** *Brain Res Brain Res Rev* 2001, **37:**343–359.
22. Chavez-Delgado ME, Gomez-Pinedo U, Feria-Velasco A, Huerta-Viera M, Castaneda SC, Toral FA, Parducz A, Anda SL, Mora-Galindo J, Garcia-Estrada J: **Ultrastructural analysis of guided nerve regeneration using progesterone- and pregnenolone-loaded chitosan prostheses.** *J Biomed Mater Res B Appl Biomater* 2005, **74:**589–600.
23. Haastert-Talini K, Geuna S, Dahlin LB, Meyer C, Stenberg L, Freier T, Heimann C, Barwig C, Pinto LF, Raimondo S, Gambarotta G, Samy SR, Sousa N, Salgado AJ, Ratzka A, Wrobel S, Grothe C: **Chitosan tubes of**

varying degrees of acetylation for bridging peripheral nerve defects. *Biomaterials* 2013, **34**:9886–9904.
24. Pesaresi M, Giatti S, Cavaletti G, Abbiati F, Calabrese D, Lombardi R, Bianchi R, Lauria G, Caruso D, Garcia-Segura LM, Melcangi RC: **Sex-dimorphic effects of dehydroepiandrosterone in diabetic neuropathy.** *Neuroscience* 2011, **199**:401–409.
25. Caruso D, Pesaresi M, Maschi O, Giatti S, Garcia-Segura LM, Melcangi RC: **Effect of short-and long-term gonadectomy on neuroactive steroid levels in the central and peripheral nervous system of male and female rats.** *J Neuroendocrinol* 2010, **22**:1137–1147.
26. Kamenov ZA, Parapunova RA, Georgieva RT: **Earlier development of diabetic neuropathy in men than in women with type 2 diabetes mellitus.** *Gend Med* 2010, **7**:600–615.
27. Callaghan B, Feldman E: **The metabolic syndrome and neuropathy: therapeutic challenges and opportunities.** *Ann Neurol* 2013, **74**:397–403.
28. Callaghan BC, Hur J, Feldman EL: **Diabetic neuropathy: one disease or two?** *Curr Opin Neurol* 2012, **25**:536–541.
29. Caruso D, Scurati S, Maschi O, De Angelis L, Roglio I, Giatti S, Garcia-Segura LM, Melcangi RC: **Evaluation of neuroactive steroid levels by liquid chromatography-tandem mass spectrometry in central and peripheral nervous system: effect of diabetes.** *Neurochem Int* 2008, **52**:560–568.
30. Leonelli E, Bianchi R, Cavaletti G, Caruso D, Crippa D, Garcia-Segura LM, Lauria G, Magnaghi V, Roglio I, Melcangi RC: **Progesterone and its derivatives are neuroprotective agents in experimental diabetic neuropathy: a multimodal analysis.** *Neuroscience* 2007, **144**:1293–1304.
31. Lindwall C, Dahlin L, Lundborg G, Kanje M: **Inhibition of c-Jun phosphorylation reduces axonal outgrowth of adult rat nodose ganglia and dorsal root ganglia sensory neurons.** *Mol Cell Neurosci* 2004, **27**:267–279.
32. Saito H, Kanje M, Dahlin LB: **Delayed nerve repair increases number of caspase 3 stained Schwann cells.** *Neurosci Lett* 2009, **456**:30–33.
33. Tsuda Y, Kanje M, Dahlin LB: **Axonal outgrowth is associated with increased ERK 1/2 activation but decreased caspase 3 linked cell death in Schwann cells after immediate nerve repair in rats.** *BMC Neurosci* 2011, **12**:12.
34. Yang DP, Zhang DP, Mak KS, Bonder DE, Pomeroy SL, Kim HA: **Schwann cell proliferation during Wallerian degeneration is not necessary for regeneration and remyelination of the peripheral nerves: axon-dependent removal of newly generated Schwann cells by apoptosis.** *Mol Cell Neurosci* 2008, **38**:80–88.
35. Russell JW, Sullivan KA, Windebank AJ, Herrmann DN, Feldman EL: **Neurons undergo apoptosis in animal and cell culture models of diabetes.** *Neurobiol Dis* 1999, **6**:347–363.
36. Vincent AM, Brownlee M, Russell JW: **Oxidative stress and programmed cell death in diabetic neuropathy.** *Ann N Y Acad Sci* 2002, **959**:368–383.
37. Singh B, Xu Y, McLaughlin T, Singh V, Martinez JA, Krishnan A, Zochodne DW: **Resistance to trophic neurite outgrowth of sensory neurons exposed to insulin.** *J Neurochem* 2012, **121**:263–276.
38. von Herrath M, Nepom GT: **Remodeling rodent models to mimic human type 1 diabetes.** *Eur J Immunol* 2009, **39**:2049–2054.
39. Yono M, Pouresmail M, Takahashi W, Flanagan JF, Weiss RM, Latifpour J: **Effect of insulin treatment on tissue size of the genitourinary tract in BB rats with spontaneously developed and streptozotocin-induced diabetes.** *Naunyn Schmiedebergs Arch Pharmacol* 2005, **372**:251–255.
40. Ramanathan S, Poussier P: **BB rat lyp mutation and Type 1 diabetes.** *Immunol Rev* 2001, **184**:161–171.
41. Sima AA, Sugimoto K: **Experimental diabetic neuropathy: an update.** *Diabetologia* 1999, **42**:773–788.
42. Batulevicius D, Frese T, Peschke E, Pauza DH, Batuleviciene V: **Remodelling of the intracardiac ganglia in diabetic Goto-Kakizaki rats: an anatomical study.** *Cardiovasc Diabetol* 2013, **12**:85.
43. Nelander J, Speidel T, Bjorkman A, Dahlin LB: **Vibration thresholds are increased at low frequencies in the sole of the foot in diabetes-a novel multi-frequency approach.** *Diabet Med* 2012, **29**:e449–e456.
44. Dahlin E, Ekholm E, Gottsater A, Speidel T, Dahlin LB: **Impaired vibrotactile sense at low frequencies in fingers in autoantibody positive and negative diabetes.** *Diabetes Res Clin Pract* 2013, **100**:e46–e50.
45. Dahlin LB, Granberg V, Rolandsson O, Rosen I, Dahlin E, Sundkvist G: **Disturbed vibrotactile sense in finger pulps in patients with Type 1 diabetes–correlations with glycaemic level, clinical examination and electrophysiology.** *Diabet Med* 2011, **28**:1045–1052.
46. Pourhamidi K, Dahlin LB, Boman K, Rolandsson O: **Heat shock protein 27 is associated with better nerve function and fewer signs of neuropathy.** *Diabetologia* 2011, **54**:3143–3149.
47. Korngut L, Ma CH, Martinez JA, Toth CC, Guo GF, Singh V, Woolf CJ, Zochodne DW: **Overexpression of human HSP27 protects sensory neurons from diabetes.** *Neurobiol Dis* 2012, **47**:436–443.
48. Kamiya H, Zhangm W, Sima AA: **Apoptotic stress is counterbalanced by survival elements preventing programmed cell death of dorsal root ganglions in subacute type 1 diabetic BB/Wor rats.** *Diabetes* 2005, **54**:3288–3295.
49. Dahlin LB, Stenberg L, Luthman H, Thomsen NO: **Nerve compression induces activating transcription factor 3 in neurons and Schwann cells in diabetic rats.** *Neuroreport* 2008, **19**:987–990.
50. Fisher RA: **Combining independent tests of significance.** *Am Stat* 1948, **2**:30.

doi:10.1186/1471-2202-15-107
Cite this article as: Stenberg and Dahlin: Gender differences in nerve regeneration after sciatic nerve injury and repair in healthy and in type 2 diabetic Goto-Kakizaki rats. *BMC Neuroscience* 2014 **15**:107.

Submit your next manuscript to BioMed Central and take full advantage of:

- **Convenient online submission**
- **Thorough peer review**
- **No space constraints or color figure charges**
- **Immediate publication on acceptance**
- **Inclusion in PubMed, CAS, Scopus and Google Scholar**
- **Research which is freely available for redistribution**

Submit your manuscript at
www.biomedcentral.com/submit

BioMed Central

Paper III

Biomaterials 34 (2013) 9886–9904

Contents lists available at ScienceDirect

Biomaterials

journal homepage: www.elsevier.com/locate/biomaterials

Chitosan tubes of varying degrees of acetylation for bridging peripheral nerve defects

Kirsten Haastert-Talini [a, b], Stefano Geuna [c], Lars B. Dahlin [d], Cora Meyer [a, b], Lena Stenberg [d], Thomas Freier [e], Claudia Heimann [e], Christina Barwig [e], Luis F.V. Pinto [f], Stefania Raimondo [c], Giovanna Gambarotta [c], Silvina Ribeiro Samy [g, h], Nuno Sousa [g, h], Antonio J. Salgado [g, h], Andreas Ratzka [a], Sandra Wrobel [a, b], Claudia Grothe [a, b, *]

[a] Institute of Neuroanatomy, Hannover Medical School, Hannover, Germany
[b] Center for Systems Neuroscience (ZSN), Hannover, Germany
[c] Department of Clinical and Biological Sciences, and Cavalieri Ottolenghi Neuroscience Institute, University of Turin, Turin, Italy
[d] Hand Surgery Department of Clinical Sciences Malmö – Hand Surgery, Skåne University Hospital, Lund University, Malmö, Sweden
[e] Medovent GmbH, Mainz, Germany
[f] Altakitin S.A., Portugal
[g] Life and Health Sciences Research Institute (ICVS), School of Health Sciences, University of Minho, Braga, Portugal
[h] ICVS/3B's, PT Government Associate Lab., Braga, Guimarães, Portugal

ARTICLE INFO

Article history:
Received 1 August 2013
Accepted 27 August 2013
Available online 17 September 2013

Keywords:
Chitosan
Nerve guide
Electrophysiology
Histomorphometry
Connective tissue
Degradation

ABSTRACT

Biosynthetic nerve grafts are desired as alternative to autologous nerve grafts in peripheral nerve reconstruction. Artificial nerve conduits still have their limitations and are not widely accepted in the clinical setting. Here we report an analysis of fine-tuned chitosan tubes used to reconstruct 10 mm nerve defects in the adult rat. The chitosan tubes displayed low, medium and high degrees of acetylation (DAI: ~2%, DA: ~5%, DAIII: ~20%) and therefore different degradability and microenvironments for the regenerating nerve tissue. Short and long term investigations were performed demonstrating that the chitosan tubes allowed functional and morphological nerve regeneration similar to autologous nerve grafts. Irrespective of the DA growth factor regulation demonstrated to be the same as in controls. Analyses of stereological parameters as well as the immunological tissue response at the implantation site and in the regenerated nerves, revealed that DAI and DAIII chitosan tubes displayed some limitations in the support of axonal regeneration and a high speed of degradation accompanied with low mechanical stability, respectively. The chitosan tubes combine several pre-requisites for a clinical acceptance and DAII chitosan tubes have to be judged as the most supportive for peripheral nerve regeneration.

© 2013 The Authors. Published by Elsevier Ltd. Open access under CC BY-NC-ND license.

1. Introduction

In general, peripheral nerves have the ability to regenerate following nerve lesion in contrast to the central nervous system. However, in cases of more complex injuries with substantial loss of nerve tissue and a subsequent defect between the nerve ends, the requirements for axonal regeneration are not sufficiently fulfilled. Such complex peripheral nerve injuries, which include 300,000 cases per year in Europe due to traumatic events, represent a major cause for morbidity and disability. During the last decades considerable efforts have been made to support and improve peripheral nerve regeneration across a nerve defect, but with limited and minor success [1]. Therefore, despite several shortcomings and limitations, such as misdirection of regenerating axons, neuronal cell death, and donor site morbidity, the gold standard for bridging a nerve defect remains grafting of an autologous nerve transplant to overcome such large defects [2]. The purpose is to apply an adequate substrate, including the provision of trophic and tropic factors, for the regrowing axons in order to restore the function after reconstruction of the nerve defect [3].

As a possible alternative for autologous nerve grafts, a variety of materials have been tested with regard to their suitability for fabrication of synthetic nerve conduits for bridging nerve defects [4]. In

* Corresponding author. Institute of Neuroanatomy, Hannover Medical School, Carl-Neuberg-Str. 1, 30625 Hannover, Germany. Fax: +49 511 532 2880.
E-mail address: Grothe.Claudia@mh-hannover.de (C. Grothe).

0142-9612 © 2013 The Authors. Published by Elsevier Ltd. Open access under CC BY-NC-ND license.
http://dx.doi.org/10.1016/j.biomaterials.2013.08.074

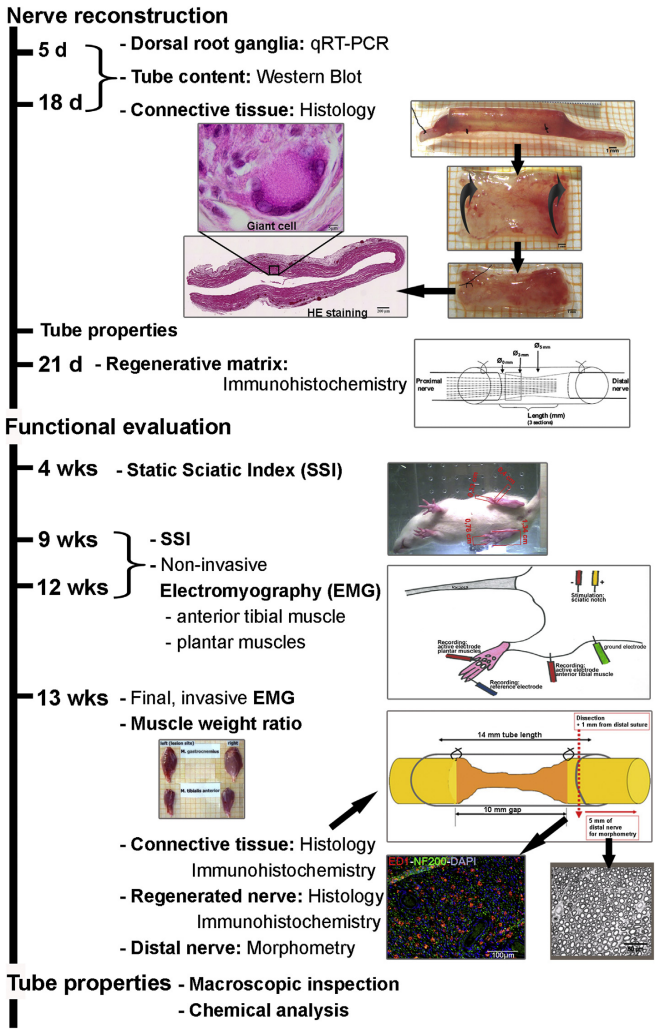

Fig. 1. Illustration of the various components of the comprehensive in vivo analysis of the new chitosan tubes with different degrees of acetylation as performed by several partners of the BIOHYBRID consortium. After the short terms of 5 and 18 days after nerve reconstruction, the connective tissue surrounding the chitosan tubes, the properties of the tubes, tube content as well as the proximal nerve ends and corresponding dorsal root ganglia were assessed with different methods, including RT-PCR, Western Blot, histology and immunohistochemistry. After 21 days in vivo, the newly formed regenerative matrix and the distal nerve segments were evaluated for matrix dimension, length of axonal outgrowth, and numbers of activated and apoptotic Schwann cells and total number of DAPI stained cells in the matrix and in the distal nerve segments. In long term observation, assessments of the motor regeneration were performed including the static sciatic index calculation, non-invasive and invasive electrodiagnostical measurements and muscle weight evaluation. Histological analyses were performed with the connective tissue and the regenerated nerve tissue. Finally, distal nerve morphometry and detailed analyses of the tube properties after nerve reconstruction and explantation were performed.

addition to non-degradable silicone tubes, which were earlier used clinically as an alternative for nerve repair [5,6] several biodegradable materials have been developed in animal experiments and applied for clinical investigation of nerve reconstruction devices [1,4]. Conduits, which are approved by the Food and Drug Administration (FDA) and authorized by the EC respectively, include Neurotube™ poly(glycolide) (PGA) tubes (successfully used in the clinical repair of digital nerves with defects of up to 3 cm in length [7]), Neura-Gen™ collagen nerve tubes [8,9], and Neurolac™ tubes [10,11]. Furthermore, processed, i.e. extracted, nerve allografts have

also been approved and applied to reconstruct nerve defects [12]. Although these off-the-shelve products have unlimited supply and avoid donor site morbidity, they have serious limitations in supporting peripheral nerve regeneration. Functional outcome after their use for nerve reconstruction is highly variable and only comparable to autologous nerve grafting when short defects in small diameter nerves are to be reconstructed [2,13]. Until today, no tubular or other type of biosynthetic nerve graft has shown strong potential to replace autologous nerve grafting for reconstruction of the substantial human nerves, such as the median or ulnar nerve trunks [14].

During the last years, the natural biopolymer chitosan – a derivative of chitin – has gained increasing interest in biomedical and tissue engineering applications. Chitosan displays biocompatibility, biodegradability, low toxicity, and structural similarity to natural glycosaminoglycans. Recent in vitro studies revealed the suitability of chitosan membranes as substrate for survival and oriented Schwann cell growth [12] as well as survival and differentiation of neuronal cells [15,16]. In addition, chitosan tubes alone or in combination with other biomaterials can efficiently bridge peripheral nerve defects [4,17]. However, improved technologies have been developed to overcome the poor mechanical strength of chitosan tubes, which was one of the main factors limiting the use of such tubes as nerve guidance channels for clinical applications until now [18]. Moreover, optimal biodegradation and cell compatibility, which are important features for tissue engineering, had to be adjusted by different degrees of acetylation of the chitosan [15].

The aim of the present study was to conduct in a multidisciplinary approach a comprehensive evaluation of chitosan tubes displaying different degrees of acetylation. The chitosan tubes were used to bridge a 10 mm defect in rat sciatic nerves. In addition to the fine-tuned manufacturing of the chitosan tubes and their evaluation with regard to biocompatibility, short and long term in vivo studies were performed and a battery of parameters were analysed. Thereby not only focussing on the effects on morphological and functional peripheral nerve regeneration, but also validating putative side effects, like Schwann cell survival and expression of transcription factors, neurotrophic factor regulation as well as immunological reaction. Finally, the properties of the non-implanted chitosan tubes were compared in structural and chemical analyses to tubes after explantation from the nerve reconstruction site.

2. Materials and methods

2.1. Manufacturing of chitosan

Medical grade chitosan supplied by Altakitin S.A. (Lisbon, Portugal) with a molecular weight (MW) of 260 kDa and degree of acetylation (DA) of 90% was obtained from *Pandalus borealis* shrimp shells using standard conditions for chitin extraction and deacetylation, following ISO 13485 requirements and specifications. The purification method consisted in homogeneous washing (liquid/liquid extraction) of chitosan with EDTA and SDS for heavy metals and protein removal. After the extractions, the product was washed with deionized water and neutralized prior to lyophilisation. The product was analysed using several methods and techniques to attest compliance with internal standards for degree of acetylation, molecular weight, heavy metal content, protein content, endotoxins, bioburden, pH, ash content and apparent viscosity.

2.2. Determination of the degree of acetylation by nuclear magnetic resonance (NMR) spectroscopy

The samples (approx. 5 mg) were dissolved in 2% DCl in D_2O (v/v, Sigma–Aldrich, Germany). The fid signal was acquired at 70 °C and suppressing the solvent signal (pulse program zgpr). Analysis and integrations were performed in MestReNova software according to Ref. [19].

2.3. Analysis of the molecular weight by gel permeation chromatography (GPC)

The samples (approx. 5 mg) were dissolved in 1 ml of eluent (AcOH/AcONa buffer pH 4.5, Panreac, Spain) and filtered through a 0.45 microns filter prior to injection (100 μl). The chromatographs were obtained at room temperature with a flow rate of 1 ml/min. A Varian PL aquagel-OH MIXED bed column (Varian, France) was used and a refractive index detector. Previously a calibration curve was obtained by using Varian pullulan polysaccharides certified standards in the same chromatographic conditions.

2.4. Production of chitosan tubes

Chitosan tubes were manufactured by Medovent GmbH (Mainz, Germany) under ISO 13485 conditions from chitin tubes made by a proprietary extrusion process, followed by distinctive washing and hydrolysis steps to adjust the required low, medium and high degree of acetylation (DA). Chitosan tubes have therefore been classified into DAI tubes (low DA, ~2%), DAII tubes (medium DA, ~5%) and DAIII tubes (high DA, ~20%). Tubes were finally cut into the required lengths and sterilized by electron beam.

2.5. In vitro cytotoxicity tests

In order to assess the short term cytotoxicity of the developed chitosan tubes, both the Minimum essential medium (MEM) extraction and the MTS cell viability tests were performed with 24 h, 72 h, and 7 days of extraction period following the guidelines described before [20]. In all tests the ratio material weight to extraction fluid was constant and equal to 0.2 g/ml for chitosan tubes (DAI: ~2%, DAII: ~5%, DAIII: ~20%), while for latex (negative control for cell viability) the ratio of material outer surface to extraction fluid was 2.5 cm^2/ml. After each period the extracts were filtered through a 0.45 μm pore size filter. These assays are particularly suitable for assessing the possible toxic effect of leachables extracted from biomedical polymers. With the MEM extraction test changes in cell morphology and growth inhibition are evaluated, whereas the metabolic cell viability is determined with the MTS test. In both cases, latex extracts (same extraction periods) were used as negative controls, while standard culture medium was used as positive control for cell death.

2.5.1. Cell culture

For the present experiment P1 rat bone marrow Mesenchymal Stromal Cells (RBMSCs) were used, which had been isolated according to the protocol described earlier [21]. Upon isolation cells were expanded in alpha-MEM (Gibco, USA), supplemented with 10% foetal bovine serum (FBS, Biochrome, Portugal) and 1% of an antibiotic–antimycotic mixture (Gibco). For the MTS test ($n = 5$, 2×10^4 cells/well) and the MEM extraction ($n = 3$, 2×10^4 cells), RBMSCs were seeded in a 24 well plate for 72 h at 37 °C, in a 5% (v/v) CO_2 cell culture incubator, prior to extract incubation.

2.5.2. MTS test

72 h after cell seeding, culture medium was removed from the wells and an identical volume (500 μl) of extraction fluid was added. Cultures were then incubated with the extracts for 72 h after which their metabolic viability was assessed through the MTS test. This is based on the bioreduction of [3-(4,5-dimethylthiazol-2-yl)-5-(3carboxymethoxyphenyl)-2-(4-sulfophenyl)-2H-tetrazolium] (MTS, Promega, USA), into a brown formazan product by dehydrogenase enzymes. After extracts, positive and negative controls were removed, a mixture of DMEM with MTS (5:1 ratio) was added to each well. Cells were then incubated for 3 h at 37 °C in a 5% CO_2 cell culture incubator after which the O.D. was determined at 490 nm using a 96 well plate reader (Tecan Sunrise, Männedorf, Switzerland).

2.5.3. MEM extraction test

72 h after cell seeding, culture medium was removed from the wells and an identical volume (500 μl) of extraction fluid was added. Cultures were then incubated with the extracts for 72 h after which a live/death assay by staining live cells with calcein-AM and non-viable cells with propidium iodide was performed. Cultures were observed in fluorescence microscopy.

2.6. Experimental design

In order to comprehensively analyse the performance of the newly designed chitosan tubes of different DA in vivo, short term and long term observation periods were chosen. As illustrated in Fig. 1, nerve reconstruction with chitosan tubes was performed and samples were collected for molecular and histological analysis after 5 and 18 days. The initially formed regenerative matrix was analysed 21 days after nerve reconstruction with chitosan tubes (short term). During the long term observation over 3 months the progress of sciatic nerve regeneration was periodically monitored with several functional tests. Finally, a comprehensive histomorphometrical analysis of the regenerated nerve tissue and further evaluation of the macroscopic and chemical tube properties were performed.

2.7. Animals and surgical procedure

The in vivo studies were performed in two different laboratories [Dahlin lab at Lund University (ULUND), Sweden, and Grothe lab at Hannover Medical School (MHH), Germany] with different animal breeders and regimes for anaesthesia and analgesia due to different local animal protection rules. All animal experiments were approved by the local animal protection committees (animal ethics committee in

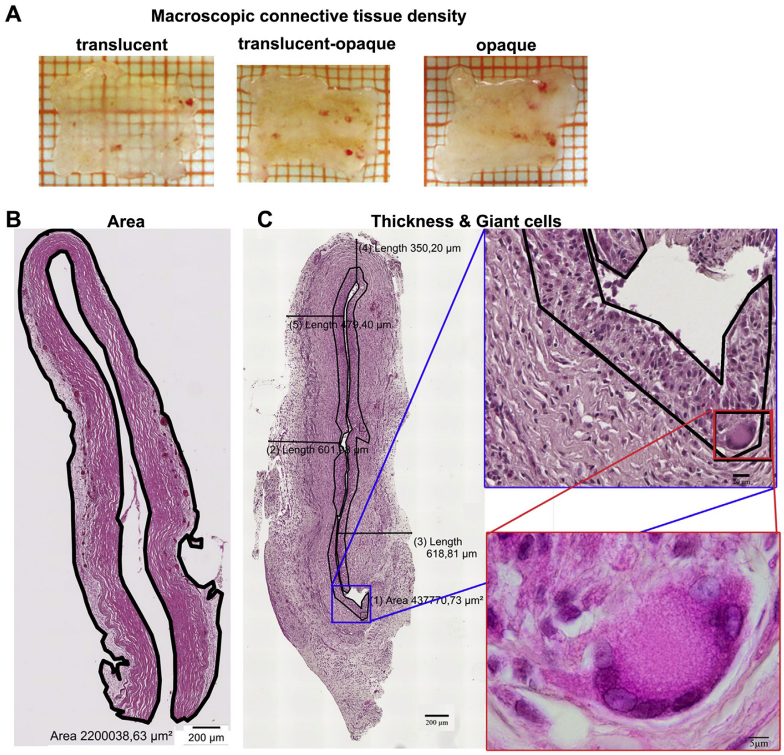

Fig. 2. Illustration of connective analysis. (A) Macroscopically three categories of optical density of the expanded connective tissue could be defined. (B) The area of sample connective tissue was determined in haematoxylin–eosin stained 7 µm paraffin cross sections. In these sections the inner surfaces of the connective tissue (contact area with chitosan tubes) are facing each other. (C) Within the contact area with the chitosan tubes the number of multinucleated giant cells (detail) was determined. Furthermore the thickness of sample connective tissue was evaluated at 5 randomly chosen locations.

Malmö/Lund, Sweden and animal care committee of Lower-Saxony, Germany). In common, female Wistar rats (225–250 g) were applied to the experiments and housed in groups of four animals under standard conditions (room temperature 22 ± 2 °C; humidity 55 ± 5%; light–dark-cycle 14-h/10-h [MHH] or 12-h/12-h [ULUND]) with food and water ad libitum.

For surgery, animals were anesthetized, sufficient analgesia induced and placed on a thermostatic blanket, to keep the body temperature stable, on the right side for surgery on the left sciatic nerves. After shaving the left hind leg the skin was disinfected, and aseptic techniques were used to ensure sterility. A skin incision was made with a surgical blade along the femur, and the gluteus and biceps femoris muscles were separated by sharp and blunt dissection to expose the sciatic nerve. The wound was kept open with the aid of small retractors. The sciatic nerve, exposed at the midthigh level, was transected with a single microscissors cut at a constant point (6 mm from the exit of the gluteus muscle). For tube transplantation 5 mm of the distal sciatic nerve end were removed and 14 mm long tubes were used to bridge a 10 mm nerve defect. Preparation of the tubes before nerve reconstruction included four washing steps in NaCl (4 × 30 min) as well as an overnight washing step. Four different observation periods were chosen after which the animals were finally examined and sacrificed prior to explantation of the implants and regenerated tissue: as short term periods 5 days (DAI, DAII, DAIII, $n = 6$ animals in each group), 18 days (DAI, DAII, DAIII, $n = 6$ animals in each group) and 21 days (DAI $n = 10$, DAII $n = 10$, DAIII $n = 9$); as long term period 3 months (13 weeks; DAI, DAII, DAIII, $n = 17$ animals in each group). Control animals for the long term investigations ($n = 17$) received an autologous nerve graft of 10 mm length, which was reversed (distal–proximal) and flipped 90° before three sutures (9-0, Ethilon) were placed 120° apart from each other. In control animals for the 5 days ($n = 4$) and 18 days ($n = 4$) short term investigations, the nerve defect was not reconstructed, but the proximal and distal nerve ends were folded over and sutured to themselves after removal of the 5 mm piece.

Anaesthesia at MHH was induced by chloral hydrate (370 mg/kg body weight, i.p., Sigma–Aldrich, Germany, MHH) combined with analgesia by buprenorphine (0.045 mg/kg body weight, Buprenovet, Germany). Anaesthesia at ULUND was induced by intraperitoneal injection of a mixture of Rompun (20 mg/ml; Bayer Health Care, Germany) and Ketalar (10 mg/ml, Pfizer, Finland). Postoperatively, all rats were treated with Temgesic (0.3 mg/ml; Schering-Plough Europe, Belgium) to prevent pain.

2.8. Quantitative RT-PCR

The ipsi- and contralateral dorsal root ganglia (DRGs) L3–L5 of animals subjected to the 5 and 18 days observation period were dissected and snap frozen in liquid nitrogen (5 days: DAI, DAII, DAIII $n = 3$ each, control $n = 4$; 18 days: DAI + DAIII $n = 3$ each, DAII + control $n = 4$ each). Tissue samples of each animal were homogenized and total RNA was extracted according to the manufacturer's instructions (RNeasy Plus Micro Kit, Qiagen, Germany). The eluate of 14 µl was used completely for cDNA synthesis using the iScript Kit (BioRad, Germany). Primer sequences were as previously stated for brain-derived neurotrophic factor (BDNF), growth-associated protein-43 (GAP-43) [22] and nerve growth factor (NGF) [23]. Further primer sequences were as follows: fibroblast growth factor-2 (FGF-2)-F: 5′-GAACCGGTACCTGGCTATGA-3′; FGF-2-R: 5′-CCAGGCGTTCAAAGAAGAAA-3′; interleukin 6 (IL6)-F: 5′-CGTTTCTACCTGGAGTTTGTGAAG-3′; IL6-R: 5′-GGAAGTTGGGG-TAGGAAGGAC-3′; tyrosine kinase receptor B (TrkB)-F: 5′-CCCAATTGTGGTCTGCCG-

3′; TrkB-R: 5′-CTTCCCTTCCTCCACCGTG-3′. Equal PCR efficiency was certified by serial cDNA dilutions and estimated to be 100%. Quantitative RT-PCR was performed with Power SYBR-Green PCR Master Mix (Applied Biosystems) on a StepOnePlus instrument (Applied Biosystems, Darmstadt, Germany) as described before [24]. Fold changes in mRNA levels are stated in comparison to the levels measured at the respective day on the contralateral side of the control animals. Calculation was done by using the $2(-\Delta\Delta Ct)$ method and normalized to the housekeeping gene peptidylprolyl isomerase A (Ppia)-F [24].

2.8.1. Western Blot

Tube contents were collected 5 and 18 days after nerve reconstruction with chitosan tubes and each pooled from 5 to 6 animals per DA. Samples were homogenized in 40 μl Radioimmunoprecipitation assay (RIPA) buffer (according to Ref. [25]). Samples were then boiled in Laemmli buffer (5 min) and separated by sodium dodecyl sulphate (SDS) polyacrylamide gel electrophoresis (PAGE) (12% gel) before being transferred (50 μg) electrophoretically to nitrocellulose membranes (Hybond ECL, Amersham) with 4 ng recombinant BDNF serving as positive control. Membranes were then probed with anti-BDNF (sc-546, 1:1000, rabbit, Santa Cruz, Germany) and anti-NGF (ab6199, 1:2000, abcam, UK) antibody and analysed following Ref. [25].

2.9. Assessment of the connective tissue

The connective tissue surrounding the tubes was macroscopically and histologically analysed. For the macroscopic evaluation, the connective tissue was dissected, spread on a scale paper glass plate and photographs taken of every sample. From the photographs, three classes of macroscopic connective tissue optical density were defined as translucent, translucent–opaque and opaque (Fig. 2A). Afterwards samples of the connective tissue ($n = 4$–6 per DA and evaluation time point), were folded and sutured at the proximal end such that the chitosan tubes contact surfaces were facing each other (Figs. 1 and 2B and C). The tissue was then fixed overnight in 4% paraformaldehyde (PFA) and paraffin embedded. For histological analysis blind-coded 7 μm paraffin sections were cut from the distal end of the connective tissue and subjected to haematoxylin–eosin (HE)-staining or immunohistochemistry for activated macrophages (see below) in the same sections. In 4–6 HE-stained sections per sample covering a distal–proximal distance of approximately 200 μm, the connective tissue area (Fig. 2B) and thickness (at 5 randomly chosen points, Fig. 2C) was determined. Furthermore, the number of multinucleated giant cells per mm^2 of the contact area with the chitosan tubes was manually quantified (Fig. 2C). Light microscopic evaluation (Olympus BX53 and Olympus BX51, Denmark) was aided by the programmes cellSense Dimensions and cellSense Entry (both Olympus; Denmark).

Immunohistochemistry was performed to estimate the number of ED1-stained cells, i.e. activated macrophages ($n = 4$–5/group). Therefore, two blind-coded 7 μm paraffin cross sections approximately 140 μm apart from each other were incubated in PBS + 5% rabbit serum as a blocking step prior to incubation with primary mouse anti-ED-1 antibody (1:1000; MCA 275R Serotec, UK) at 4 °C overnight. The next day sections were washed with PBS (3×) before being incubated with Alexa 555-conjugated secondary goat-anti-mouse antibody (1:1000; A21422, Invitrogen, Germany) for 1 h at room temperature (RT). Sections were finally counterstained with the nuclear dye 4′,6′-diamino-2-phenylindole (DAPI, 1:2000, Sigma, Germany) in PBS for 2 min at room temperature and then mounted with Moviol (Calbiochem, Germany, N° 475904). Two photomicrographs were each taken from an area with minimal and maximal ED1 signal per section (20× magnification) using an IX70 microscope (Olympus) and the cellP software (Olympus, Denmark) (Olympus). The number of ED1-+ cells was counted as number/mm^2 with the help of the ImageJ software (NIH, USA). The nuclear DAPI counterstaining was used to clearly identify ED1-immunopositive cells but not for further quantification in this case.

2.10. Analysis of regenerated matrix within the chitosan tubes at 21 days after nerve reconstruction

The sciatic nerve together with the chitosan tube and its content was harvested 21 days after surgery. The chitosan tube was removed, there after the tube content with proximal and distal nerve segments were fixed in Stefanini solution (4% paraformaldehyde and 1.9% picric acid in 0.1 M phosphate buffer pH 7.2) for 24 h. The samples were then washed in 0.01 M PBS pH 7.4 three times and stored in 20% sucrose solution overnight for cryoprotection. Before sectioning using a cryostat, the samples were embedded in OCT Compound (Tissue-Tek®, Histolab products AB, Gothenburg, Sweden) and frozen. The nerves sectioned longitudinally at 6 μm thickness were collected on Super Frost® plus glass slides (Menzel-Gläser, Germany).

2.10.1. Immunohistochemistry

Immunohistochemistry was performed for neurofilaments, activating transcription factor 3 (ATF3), and cleaved caspase 3 to evaluate axons, activated Schwann cells, and apoptotic Schwann cells, respectively, as described [26,27]. In short, the sections were washed in PBS for 5 min and incubated overnight at 4 °C with anti-human neurofilament protein (DAKO Glostrup, Denmark), diluted 1:80 in 0.25% Triton-X 100 and 0.25% BSA in PBS. The next day the slides were washed with PBS 3 × 5 min, then incubated for 1 h at room temperature with the secondary antibody ALEXA Fluor 594 conjugated goat anti-mouse IgG (Invitrogen, Molecular Probes, USA), diluted in 1:500 in PBS and coverslipped.

For ATF-3 immunohistochemistry, the sections were washed for 5 min in PBS and then incubated with rabbit anti-ATF-3 polyclonal antibody (1:200; Santa Cruz Biotechnology, USA), diluted 1:200 in 0.25% Triton-X 100 and 0.25% BSA in PBS, or with anti-cleaved caspase-3 antibody (1:200; Invitro Sweden AB, Stockholm, Sweden); both diluted in 0.25% Triton-X 100 and 0.25% BSA in PBS) overnight at 4 °C. The next day the slides were washed in PBS 3 × 5 min and then incubated with the secondary antibody Alexa Fluor 488 conjugated goat anti-rabbit IgG (Invitrogen, Molecular Probes, USA), diluted in 1:500 in PBS for 1 h at room temperature. Finally, the slides were washed 3 × 5 min in PBS, mounted with 4′,6′-diamino-2-phenylindole DAPI (Vectashield®, Vector Laboratories, Inc. Burlingame, USA) to visualize the oval shaped nuclei (i.e. for counting the total number of the cells) and then mounted and coverslipped.

The blind-coded sections were photomicrographed using a fluorescence microscope (Eclipse, Nikon, Tokyo, Japan) provided with a digital system camera (Nikon 80i) connected to a computer and the length of the outgrowing axons was measured from the site of lesion into the formed matrix in three randomly selected sections. The stained cells for cleaved caspase-3 and ATF-3 were also counted in one section (image size 500 × 400 μm) in the matrix 3 mm from the proximal nerve end (Fig. 1) and in the distal nerve segment as described [28]. The same squares were also used for counting the total number of DAPI stained cells. The images (20× magnification) were analysed with NIS elements (Nikon, Japan). Double staining for cleaved caspase 3 and S-100 was performed as described [27].

2.11. Functional evaluation

During the long term observation period of 3 months (13 weeks) after nerve reconstruction, the progress of functional motor recovery was monitored by calculation of the Static sciatic index, electrophysiological measurements (serial non-invasively and final invasively) and calculation of the lower limb muscle weight ratio. The investigators were blinded to the conditions of sciatic nerve reconstruction applied to the animals.

2.11.1. Static sciatic index (SSI)

The healthy SSI was determined 1 week prior to surgery and after surgery in weeks 1, 4, 9 and 12 as described before [29]. In brief, webcam images of the toe spreading of the right (contralateral) and left (ipsilateral) paw were acquired from the rats placed inside a plastic box located on a glass table. Using a freely available image-editing program (AxioVision, Zeiss, Jena, Germany), the distance between toe 1 and 5 (toe spread TS) as well as 2 and 4 (intermediate toe spread ITS) was measured for the lesioned (LTS; LITS) and non-lesioned (NTS; NITS) hind paws. The SSI was then calculated using the following equations (TSF = toe spread factor; ITSF = intermediate toe spread factor): $TSF = (LTS - NTS)/NTS$; $ITSF = (LITS - NITS)/NITS$; $SSI = (108.44 * TSF) + (31.85 * ITSF) - 5.49$.

2.11.2. Serial non-invasive electrodiagnostic recordings

For evaluation of ongoing muscle reinnervation in weeks 4, 9 and 12 after surgery a portable electrodiagnostic device (Keypoint Portable; Medtronic Functional Diagnostics A/S, Denmark) was used. Therefore, animals were anesthetized as described above and placed in a prone position and fixed with tape with the hindlimbs extended on a metal plate on top of a thermostatic blanket. Only during recordings the thermostatic blanket was turned off to avoid interfering signals. The sciatic nerve was stimulated with single electrical pulses (100 μs duration and supramaximal intensity) delivered by monopolar needles (30G, diameter 0.3 mm, length 10 mm; Alpine BioMed, Denmark) percutaneously placed either at the sciatic notch, proximal to the injury (proximal stimulation, cathode directly at sciatic notch, anode 1 cm more proximal) or in the popliteal fossa (distal stimulation). The compound muscle action potentials (CMAPs) of the tibialis anterior (TA) and plantar (PL) muscles were recorded by means of another pair of monopolar needles inserted across the skin on the muscle belly. To ensure reproducibility the recording needles were placed with the help of anatomical landmarks to secure the same placement on all animals. The active recording electrode is placed subcutaneously at the first third of the distance between knee and ankle on the TA muscle, and at the third metatarsal space for PL muscle recordings. The reference needle electrode was inserted at the distal phalange of the second or fourth toe. A ground needle electrode was inserted in the skin at the knee.

Taking into account the latency difference of the two stimulation points and the distance between them, the electrodiagnostic device calculated automatically the nerve conduction velocity (NCV). Furthermore, the signals amplitude and the area under the curve (AUC) of the negative CMAP peaks were recorded. Control values were obtained from the non-lesioned, right hindlimb.

2.11.3. Final invasive electrodiagnostic recordings

On the last day of observation (week 13) animals were once more anesthetized and the sciatic nerves were exposed consecutively on the lesioned and non-lesioned side. The recording electrodes were placed as described above. Using a bipolar steel

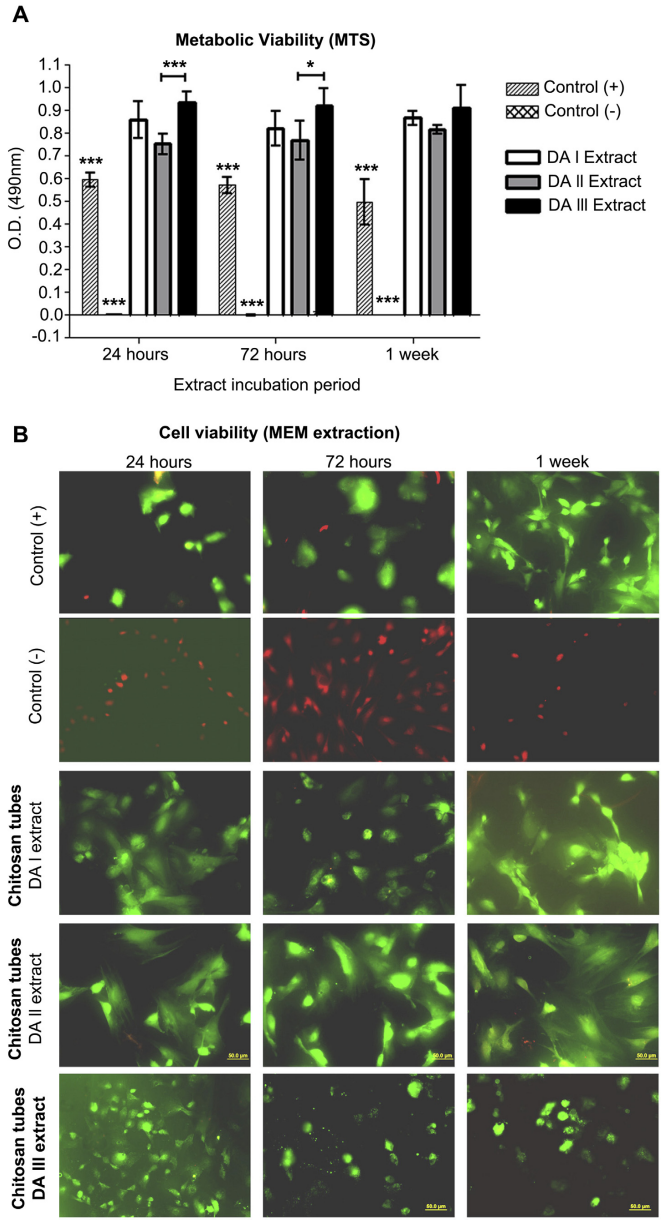

Fig. 3. (A) Metabolic activity of RBMSCs incubated with extracts from the chitosan tubes of different degrees of acetylation (DAI = ~2%; DAII = ~5%; DAIII = ~20%) for 72 h (MTS assay). No negative effect on the metabolic viability by any DA could be detected in comparison to the positive control. (B) Representative photomicrographs from the MEM extraction test. Incubation with the extracts from DAI-, DAII-, or DAIII-chitosan tubes did not negatively influence the cell density of cultured RBMSCs.

hook electrode the sciatic nerves were directly stimulated proximal and distal to the transplants [29]. Single electrical pulses (100 μs duration) with gradually increased intensity (not exceeding 8 mA) were applied in order to evaluate the threshold and maximal CMAP. Furthermore, the NCV was calculated by stimulating the sciatic nerve proximal and distal with a current intensity of 1 mA.

2.11.4. Muscle weight ratio

After completing the experiments the animals were sacrificed, the transplants with the adjacent nerve tissue were dissected and the gastrocnemius muscle and TA muscle of both hindlimbs were excised and weighted in order to determine the muscle weight ratio ($[g]_{ipsilateral}/[g]_{contralateral}$).

2.12. Histo-morphometrical assessment of the regenerated nerve tissue

The transplants with the adjacent nerve tissue were harvested and the regenerated nerve tissue extracted from the chitosan tubes. The regenerated nerve tissue was separated into a proximal and a distal part by a cut at 1 mm distal to the distal suture site (Fig. 1).

Five mm of the distal segment were then prepared for the stereological analysis (Fig. 1) by transferring the tissue into a fixative according to Karnovsky (2% PFA and 2.5% glutaraldehyde in 0.2 M sodium cacodylate buffer, pH 7.3) for 24 h, then rinsed three times with 0.1 M sodium cacodylate buffer containing 7.5% sucrose, prior to post-fixation in 1% OsO_4 for 2 h. Dehydration was performed in an ethyl alcohol row (5 × 5 min 25%, 5 × 5 min 50%, 5 × 5 min 75%). The samples were then shipped to the partner laboratory at the University in Turin for embedding in a mixture of Araldite resin (Sigma) following Glauerts' procedure [30].

The proximal regenerated nerve tissue was subjected to fixation in 4% PFA overnight at 4 °C. Afterwards Paraffin-embedding was performed in a Citadel tissue-embedding-automatic unit (Shandon Citadel 2000; USA) to prepare the tissue for HE-staining and immunohistochemical analysis.

2.12.1. Stereology/nerve morphometry

From each specimen of the distal nerve, 2.5 μm thick series of semi-thin transverse sections were cut using an Ultracut UCT ultramicrotome (Leica Microsystems, Germany). Finally, sections were stained using Toluidine blue and analysed with a DM4000B microscope equipped with a DFC320 digital camera and an IM50 image manager system (Leica Microsystems, Germany). Systematic random sampling and D-dissector were adopted, using a protocol previously described [31] in order to evaluate the total fibre number, fibre and axon diameter, myelin thickness and *g*-ratio.

2.12.2. Histology

Serial 7 μm-cross sections were obtained from the distal end of the regenerated nerve tissue and cut in proximal direction over a distance of approximately 1000 μm. Blind-coded sample sections (from $n = 5$ randomly chosen animals per group) taken from the distal end and 320 μm more proximal were processed in HE-staining in order to examine the number of multinucleated giant cells per mm^2 in the centre area as well as in the perineurium. Sections were examined in light microscopy (Olympus BX53; Denmark) software-aided with cellSense Dimensions (Olympus; Denmark). Overview photomicrographs were used for the measurements.

Additional blind-coded sample sections (from $n = 8$ randomly chosen animals per group) taken at defined distances in distal–proximal direction (0 μm (=1 mm in distal stump), 64 μm, 128 μm, 320 μm, 384 μm, 448 μm, 672 μm, 736 μm, 992 μm, 1056 μm (=distal end of former nerve defect)) were subjected to double-immunohistochemistry for activated macrophages (ED-1) and neurofilaments (NF-200). Blocking and ED-1-immunohistochemistry were performed as described above. After incubation with the secondary antibody the sections were further washed with PBS (3×) and a second blocking step with 0.5 M trisaline buffer (60.6 g tris + 9 g NaCl in 1.l H_2O; pH 7.4) containing 3% milk powder and 0.5% triton X-100 followed by overnight incubation (4 °C) with primary rabbit anti-NF-200 antibody (1:200; N4142, Sigma, Germany). After washing with trisaline buffer (3×), incubation with Alexa 488-conjugated secondary goat-anti rabbit antibody (1:1000, A11034, Invitrogen, Germany) was performed for 1 h at RT. Sections were finally counterstained with DAPI and mounted with Moviol. The nuclear DAPI counterstaining was used to clearly identify ED1-immunopositive cells but not for further quantification in this case.

For quantification of the number of activated ED1-immunopositive macrophages/mm^2, seven photomicrographs per section were randomly taken (20× magnification) in the outer area (4 photomicrographs) and in the centre area (3 photomicrographs) to examine approximately 32% of the complete section area. Finally, the thickness of the perineurium was evaluated on theses sections as well, therefore at three randomly chosen locations the thickness was determined and the mean calculated for each sample.

2.13. Analysis of tube properties after explantation

On day 5 and day 18 after nerve reconstruction the chitosan tubes were explanted. On day 18 a surrounding connective tissue could be dissected, macroscopically classified and processed for histological analysis. On day 5 and day 18 the tubes and their contents were stored for Western Blot analysis of the content. Therefore the middle parts of the tubes were harvested by cutting of the proximal and distal ends of the tubes at the suture sites. Also upon explantation in week 13 after nerve reconstruction (long term observation, 3 months), the tubes were explanted, dissected from surrounding connective tissue and stored in 0.9% NaCl solution for further analysis of biomaterial properties.

The properties of the tubes, the connective tissue as well as the macroscopic nerve cable peculiarities were then classified and connective tissue samples were processed for histological evaluation. Furthermore, tube samples (before and after nerve reconstruction) were analysed by Scanning electron microscopic (SEM) or biochemical tests ($n = 3$/group).

2.14. Statistics

In the different laboratories contributing to the presented study different statistical software was used, either the statistical package SPSS (version 17.0 or 20.0, IBM, USA) or GraphPad InStat software, version 5.0.3.0 & 6.00 for windows (Graphpad Software, CA, USA). A p value of <0.05 was taken as statistically significant. The statistical tests used for the different cytotoxical, functional and histological evaluations are stated in the respective results sections. For nerve stereology, the statistical analysis was performed using two or one-way ANOVA. If this analysis identified a significant difference the post-hoc HSD Tukey's test, or Bonferroni were applied for paired comparisons. Kruskal–Wallis, with subsequent Mann–Whitney as post-hoc, was used to detect differences between groups. Furthermore, the proportion of animals per group that displayed a predefined qualitative parameter (evocable CMAP) was calculated as percentage (0–100%) and analysed with the Chi-Square-test.

3. Results

3.1. In vitro cytotoxicity assays

In vitro cytotoxicity assays were performed to test the biocompatibility of the new chitosan tubes and the influence of the different degrees of acetylation (DA) on it. The MTS test revealed that the leachables and degradation products released by the chitosan tubes of different DA (i.e. DAI, DAII, DAIII) did not negatively affect the metabolic viability of RBMSCs when compared to the positive control (Fig. 3A). Similarly, the MEM extraction test revealed no negative influences on the cell densities (Fig. 3B). Therefore, the tested samples can be considered as non-cytotoxic, as the leachables and degradation products released by chitosan tubes tested with different DA did not induce any deleterious effects on RBMSCs.

3.2. In vivo evaluation after nerve reconstruction with chitosan tubes

Chitosan tubes of DAI, DAII, DAIII were implanted to bridge a 10 mm defect of lesioned sciatic nerves and compared with controls 5, 18, 21 days, and 3 months, respectively, after nerve reconstruction (Fig. 1).

3.2.1. Short term observation (5, 18 days)

Five and 18 days after nerve lesion and nerve reconstruction with chitosan tubes of different DAs, qRT-PCR for neurotrophic factors (NGF, FGF-2, BDNF), the cytokine IL-6, the BDNF-receptor TrkB and for GAP-43 were performed on DRGs (L3–L5). All data were normalized to the contralateral non-lesioned site of control animals in which the separated ipsilateral nerve ends were folded over and sutured to themselves. In accordance with the expression pattern in the DRGs of the control group, NGF, FGF-2, IL-6, BDNF and GAP-43 were up-regulated ($p \leq 0.05$, *t*-test) as well in the presence of the tubes, whereas TrkB remained unchanged in all experimental groups (Fig. 4A). In addition, there were no significant changes in the expression patterns of the respective neurotrophic factors between 5 and 18 days. It can be concluded that chitosan tubes do not influence the physiological up-regulation of neurotrophic factors following nerve injury.

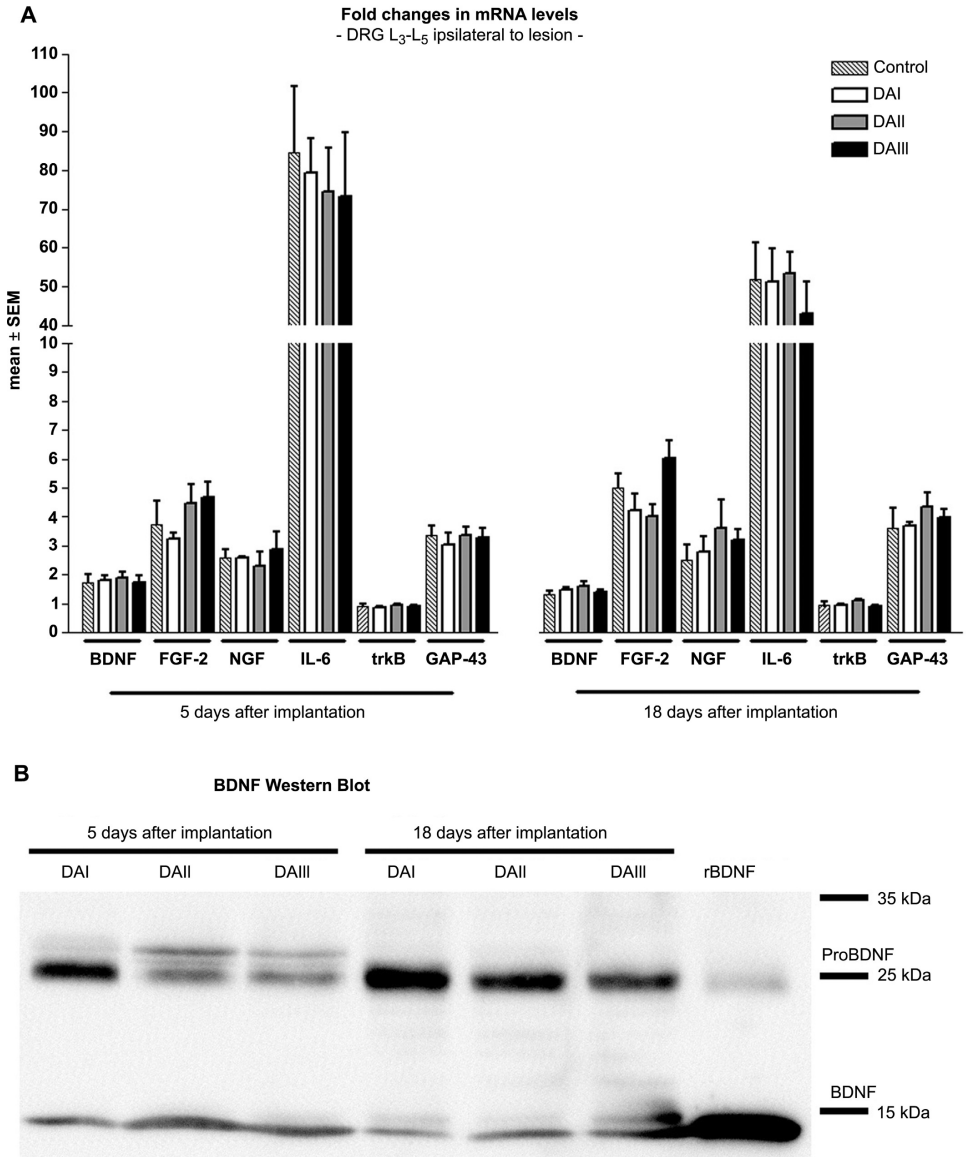

Fig. 4. (A) Regulation of mRNA levels of representative neurotrophic factors and regeneration associated proteins at the lesioned site, 5 and 18 days after nerve reconstruction with chitosan tubes or control surgery. Values were normalized to the non-lesioned site of the control group, DAI, DAII, DAIII, $n = 3$ each; control, $n = 4$. A representative Western Blot of pooled tube content ($n = 5–6$/group) is shown for BDNF (B). DAI = ~2%; DAII = ~5%; DAIII = ~20%.

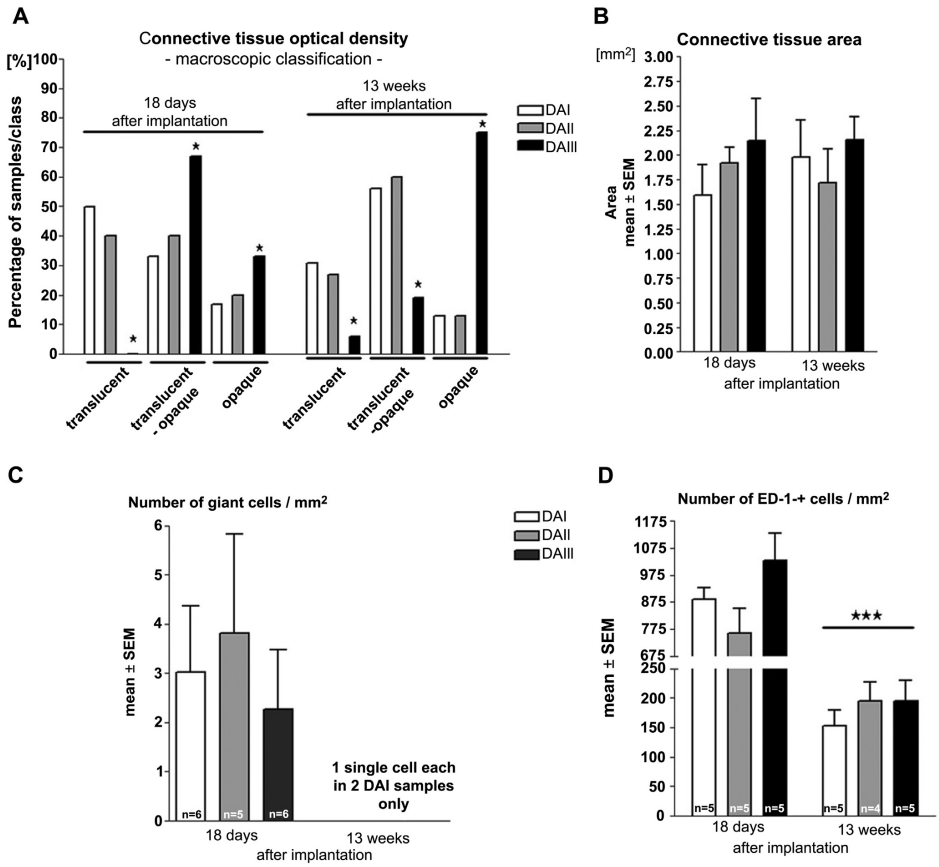

Fig. 5. Connective tissue developed around the chitosan tubes of different degree of acetylation was analysed for (A) its optical density and (B) its area [mm^2] as well as for (C) the number of multinucleated giant cells within the contact area to the chitosan tubes and (D) the number of activated macrophages (ED-1-immunopositive, ED1–+ cells). Significant changes were detectable between the short and the long term evaluation, but not among the connective tissue surrounding chitosan tubes of different degree of acetylation (DAI = ~2%; DAII = ~5%; DAIII = ~20%). Statistical tests used: (A) Chi-Square-test, asterix indicating differences between DAIII-tubes and others, $p < 0.05$; (C) Two way ANOVA, Tuckey's multiple comparison, asterix indicating difference to 18 days, $p < 0.001$.

Additionally, Western Blot analysis was performed from the tube content in order to detect the relative amounts of BDNF and NGF secreted into the chitosan tubes. Both, 5 and 18 days after nerve reconstruction pre-mature and mature BDNF and NGF (data not shown) were detectable in the pooled tube content with no difference between the DAs (Fig. 4B).

3.2.1.1. Connective tissue evaluation. Five days after nerve reconstruction with the chitosan tubes no surrounding connective tissue was detectable. At 18 days after nerve reconstruction, macroscopic evaluation revealed a significant shift to a higher optical tissue density for DAIII tubes (Fig. 5A). However, measurements of the connective tissue area (Fig. 5B) and thickness (data not shown) did not reveal any significant differences. The connective tissue contact area with the implanted tubes was further examined on HE-stained sections with regard to the presence of multinucleated giant cells and on ED1-immunopositive/DAPI counterstained sections with regard to activated macrophages, respectively. The quantification of giant cells, which are typically found in the environment of foreign materials, revealed no differences among the connective tissue in contact with DAI, DAII or DAIII chitosan tubes (Fig. 5C). Also the number of activated macrophages (ED1-immunopositive cells) was not altered among the different DAs (Fig. 5D).

3.2.2. Nerve regeneration, activation and apoptosis in short term (21 days)

3.2.2.1. The formed matrix. A matrix was formed in the chitosan tubes at 21 days. In separate experiments (results not shown), the content of the tube was examined at 10, 14 and 18 days, but there was not a sufficient and bridging matrix formed at these time

points. The thickness of the matrix in the different tubes was measured at three different sites (Fig. 6A; Table 1), and showed a somewhat hourglass shape, and with no statistical differences between the three types of acetylation tubes at any of the measured sites (Table 1).

3.2.2.2. Axonal outgrowth and Schwann cells. The immunohistochemical evaluation revealed a length of axonal outgrowth of about 7.9–8.6 mm in the three acetylation variants with no statistical difference present (Kruskal–Wallis $p = 0.28$), but with a tendency to shorter growth in the DAIII-tube group. S-100 staining revealed that Schwann cells were present in the matrix along the entire tube (Fig. 6B).

3.2.2.3. ATF3 stained Schwann cells. Few ATF3 stained cells were present in the matrix, but without any significant difference (Table 1) in the tubes, although DAPI stained cells were seen. However, a considerable number of ATF3 stained cells, with a significant difference between the three DAs (i.e. lowest in DAI- and highest in DAIII-tubes), was present in the distal nerve segment at 21 days (Table 1).

3.2.2.4. Cleaved caspase 3 stained Schwann cells. In contrast to ATF3 staining, cleaved caspase 3 stained cells were observed in the matrix along the entire length of the matrix in all three types of the chitosan tubes (Table 1, Fig. 6B). Significantly increasing higher cell numbers were detected in the formed matrix with increasing degree of acetylation of the tubes; i.e. with a low number in DAI tubes. There were extensive numbers of cleaved caspase 3 stained Schwann cells in the distal nerve segment, but with no difference between the tubes of different DAs.

3.2.2.5. Total number of DAPI-stained cells. DAPI-stained cells were present in the matrix of all tubes, but with no difference among the DAs. However, there was a significant difference in DAPI-stained cells in the distal nerve segment (Table 1).

3.2.2.6. Correlations. The thickness of the formed matrix correlated strongly with the length of the axonal outgrowth (rho-value up to 0.9; p-value < 0.02; Spearman), particularly in the DAI- ($\sim$2%) and DAIII- ($\sim$20%) tubes. The length of axonal outgrowth did only correlate with the number of cleaved caspase 3 stained Schwann cells in the distal nerve segment (rho 0.44, $p = 0.016$).

In the distal nerve segment, the number of cleaved caspase 3 stained Schwann cells negatively correlated (rho -0.53, $p = 0.003$) with the total number of DAPI stained cells, particularly in DAIII-tubes. No other relevant correlations were observed.

3.2.3. Long term observation (13 weeks) regeneration

3.2.3.1. Functional recovery. Long term regeneration was evaluated with regard to functional recovery analysing the SSI and non-invasive and invasive electrophysiology after different time points

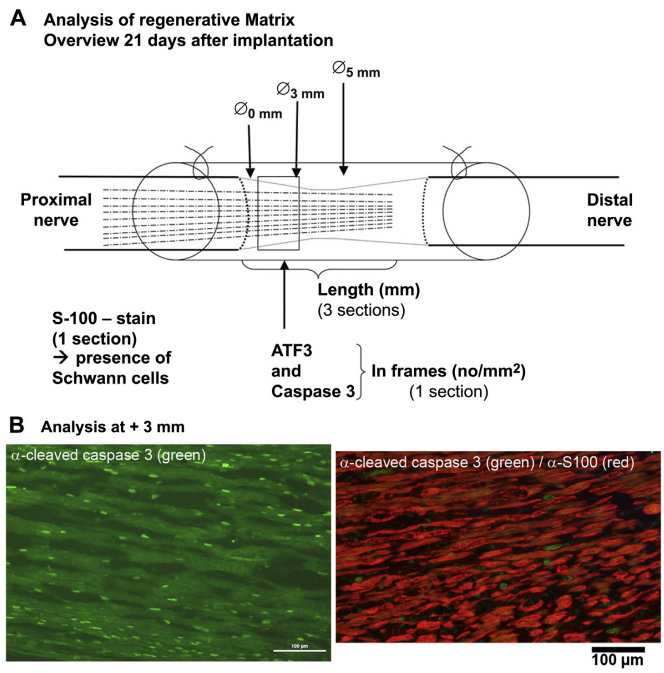

Fig. 6. (A) Overview of the quantification of matrix, axonal outgrowth, activated and apoptotic Schwann cells and total number of cells (DAPI) in the model. (B) Representative photomicrographs taken at +3 mm within the matrix in sections incubated with α-cleaved caspase 3 antibody (green, apoptotic cells; left panel) and α-S100 antibody (red, Schwann cells; double staining, right panel).

Table 1
Dimensions, length of axonal outgrowth, and numbers of activated and apoptotic Schwann cells and total number of DAPI stained cells in the matrix and in the distal nerve segments in rat sciatic nerve defects bridged by differentially acetylated chitosan tubes (DAI = ~2%; DAII = ~5%; DAIII = ~20%).

	DAI ($n = 10$)	DAII ($n = 10$)	DAIII ($n = 9$)	p-Values
Matrix diameter at 0 mm (μm)	317 [303–339]	313 [303–334]	303 [292–321]	0.36
Matrix diameter at 3 mm (μm)	242 [222–302]	250 [236–287]	232 [224–245]	0.29
Matrix diameter at 5 mm (μm)	242 [232–278]	248 [232–280]	237 [228–244]	0.54
Axonal outgrowth (mm)	8.61 [7.51–9.01]	8.64 [8.04–9.31]	7.91 [7.43–8.76]	0.28
ATF3 stained cells in the matrix (at 3 mm) (% of total)	0.4 [0–0.7]	0.4 [0–0.7]	0.3 [0–0.3]	0.39
ATF 3 stained cells in the distal nerve segment (% of total)	19.8 [18.6–21.6][c]	25.2 [20.2–28.3][b]	30.6 [27.9–35.3]	**0.0001**
Cleaved caspase 3 stained cells in the matrix (at 3 mm) (% of total)	4.7 [2.7–7.6][a]	15.3 [5.8–19.5][b]	20.5 [18.0–23.0]	**0.0001**
Cleaved caspase 3 stained cells in the distal nerve segment (% of total)	22.1 [20.5–28.3]	27.7 [22.9–34.9]	21.5 [20.4–22.9]	0.07
Total number of DAPI stained cells in the matrix (no/mm^2)	1010 [966–1046]	1057 [981–1080]	1011 [833–1030]	0.18
Total number of DAPI stained cells in the distal nerve segment (no/mm^2)	981 [914–1022][a]	888 [866–919][b]	1094 [1059–1142]	**0.0001**

Values are median [25th–75th percentiles]. p-Values based on Kruskal–Wallis-test.
Bold writing indicates statistical significance.
[a] Different from medium and high acetylation.
[b] Different from high acetylation.
[c] Different from high acetylation (Mann–Whitney-test).

(Fig. 1). Eventual changes from initial numbers of animals per group are indicated throughout and due to hamstring toe contractures or signs of autotomy, which excluded animals from certain tests at a certain time point. Additionally, few animals died over the long term observation period because of low tolerance to the repeated anaesthesia. Actual animal numbers are appropriately indicated in the graphs below.

3.2.3.2. Static sciatic index (SSI). With regard to the SSI a significant decrease from pre to post nerve defect and reconstruction was found which remained significantly decreased till the end of the observation period. Interestingly, the post-surgery performances of the different experimental groups revealed no significant differences, also when comparing the reconstruction of the nerve with hollow chitosan tubes to the autologous nerve graft (Fig. 7A). This suggests that the hollow chitosan tubes, independently of their DA, influence motor regeneration in the same extent as the gold standard.

3.2.3.3. Electrophysiological assessment. Compound muscle action potentials (CMAPs) were serially recorded from the tibialis anterior muscle (TA) and plantar muscles (PL) at 4, 9, and 12 weeks after nerve reconstruction. Additionally, a final invasive recording was performed on the last day of observation in week 13. Four weeks after nerve reconstruction no CMAPs were evocable for both locations. However, nine weeks after nerve reconstruction 62% of the animals treated with autologous nerve grafts demonstrated evoked CMAPs in the TA, while significantly less animals of the other groups showed these signs of reinnervation (6–29%, Table 2). Twelve weeks after nerve reconstruction the number of chitosan tubes treated animals with evoked CMAPs recordable from the TA muscle reached a level comparable to the autologous nerve grafted animals. When recordings were performed from the PL muscles, a similar development of motor recovery was detectable (Table 2). These data reveal that chitosan tubes of all degrees of acetylation allow functional recovery, which almost reaches the same distribution as after autologous nerve grafting.

Furthermore, the CMAPs were analysed in more detail, as was the nerve conduction velocity (NCV). No significant differences among the amplitudes of evocable CMAPs could be detected among the groups during the non-invasive and invasive measurements (data not shown). Also for the NCV-ratio (ipsilateral/contralateral), the TA and the PL muscles data revealed no significant differences in comparison with autologous nerve grafting and bridging of the nerve defects with chitosan hollow tubes or among the chitosan tubes with different degrees of acetylation (Fig. 7B).

3.2.3.4. Muscle weight ratio. After the final electrophysiological measurements, the muscle weight ratios (g_{ipsi}/g_{contra}) of the lower limb muscles were determined after harvest of the tibialis anterior and gastrocnemius muscles (Fig. 1) and revealed no differences among the experimental groups (Fig. 7C).

3.2.4. Histomorphological evaluation

3.2.4.1. Distal nerve stereology. The results of the stereological assessment of myelinated fibre number and axon diameter, fibre diameter, myelin thickness and g-ratio of all experimental groups are shown in Fig. 8. The total numbers of myelinated fibres (Fig. 8A) are significantly different in all groups towards the healthy nerve ($^{*}p \leq 0.05$; $^{**}p \leq 0.01$), but only the nerve distal to DAI-chitosan tubes is significantly different compared to the autologous nerve graft group ($\#p \leq 0.05$). With regard to axon and fibre diameters and myelin thickness (Fig. 8B), all the experimental groups differ from healthy nerves ($^{**}p \leq 0.01$) but no differences are seen among them. In Fig. 9 high-resolution representative images of semithin sections of regenerated sciatic nerves are shown in comparison to the contralateral healthy control (Fig. 9A: healthy contralateral nerve; Fig. 9B: autologous nerve graft; Fig. 9C: DAI; Fig. 9D: DAII; Fig. 9E: DAIII). Nerve fibre size distribution is also reported (Fig. 9F–J). The distribution is significantly different between healthy and regenerated nerves but again no significant differences in fibre size distribution could be detected among the experimental groups.

3.2.4.2. Immunological nerve tissue reaction. In addition to the stereology, the area around the distal suture (bridging 1 mm distance, see Fig. 1) was evaluated with regard to the presence of activated macrophages in the regenerated nerve tissue after double-staining for the ED1-antigen and NF200-Neurofilaments (Fig. 10A–C). Whereas in nerves regenerated through DAI and DAII chitosan tubes similar amounts of ED1-immunopositive cells were found, nerves regenerated through DAIII chitosan tubes contained significantly higher numbers of these cells, i.e. activated macrophages. As expected, in all tubes the number of macrophages was significantly lower than in autologous nerve grafts where it can be attributed to myelin debris removal (Fig. 10D). On the same sections of the regenerated nerves the thickness of the perineurium was measured. Interestingly, whereas thickness of the perineurium of nerves regenerated through DAI and DAII chitosan tubes was comparable with the perineurium thickness in the autologous nerve graft group, nerves regenerated through DAIII chitosan tubes displayed a significantly thicker perineurium (Fig. 10E). The higher number of macrophages together with a thicker perineurium point to an immunological reaction in DAIII.

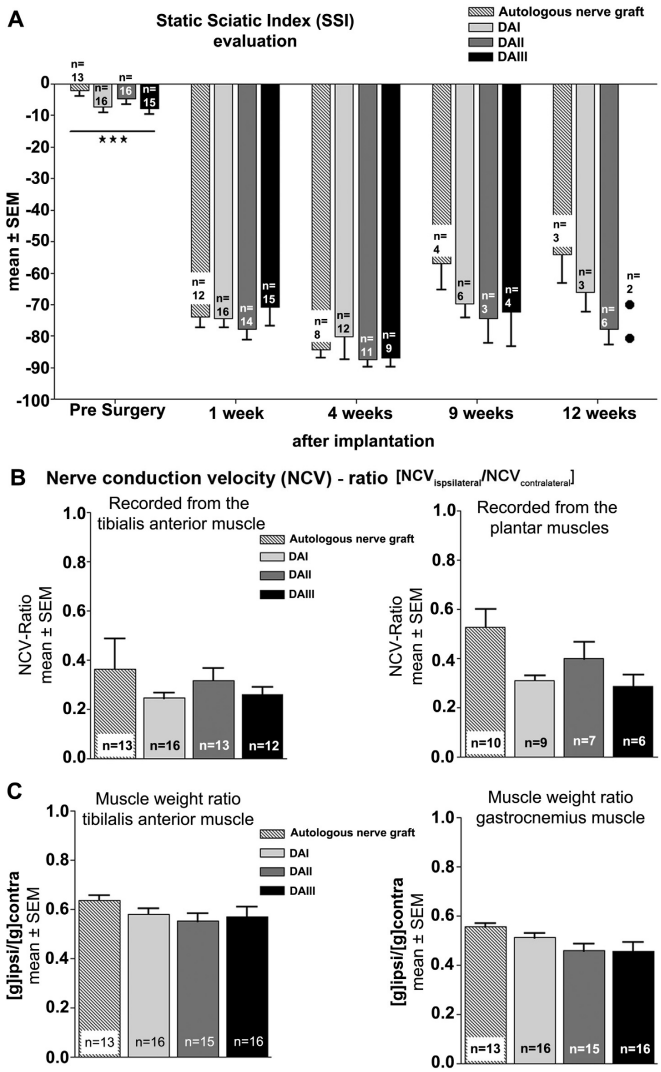

Fig. 7. Functional evaluation of motor recovery revealed no significant differences among the gold standard autologous nerve graft and the nerve reconstruction with chitosan tubes of different degree of acetylation. DAI = ~2%; DAII = ~5%; DAIII = ~20%. (A) Results of the calculation of the static sciatic index (SSI). Statistical test: two way ANOVA, Tukey's multiple comparison, triple asterix indicating difference to post nerve lesion values, $p < 0.001$. (B) Calculation of the nerve conduction velocity ratio. (C) Calculation of the lower limb muscle weight ratio.

3.2.4.3. Connective tissue evaluation. There was never a strong scar tissue formation around the chitosan tubes. Similar as performed 18 days after nerve reconstruction (Fig. 1), the connective tissue surrounding the tubes was explanted and analysed morphologically with regard to its optical density, its area and thickness, the presence of multinucleated giant cells (HE staining, Fig. 2B), and immunohistochemically for the presence of activated macrophages (ED1-immunopositive cells). Similar to the findings after short term nerve reconstruction, the optical density of the connective tissue surrounding DAIII chitosan tubes was significantly increased in

Table 2
Increasing distribution of animals per group which showed evocable compound muscle action potentials in the tibialis anterior or plantar muscles during the regeneration period after autologous nerve grafting or nerve reconstruction with chitosan tubes of different degree of acetylation (DAI = ~2%; DAII = ~5%; DAIII = ~20%).

	9 weeks			12 weeks			13 weeks (invasive)		
	Animals/group	Percentage	Significant difference	Animals/group	Percentage	Significant difference	Animals/group	Percentage	Significant difference
Tibialis anterior muscle									
Autologous nerve graft	8/13	62%		13/13	100%		13/13	100%	
DAI	1/17	6%	#	14/16	88%	#‡	16/16	100%	‡
DAII	2/16	13%	#	11/16	69%	#†	13/14	93%	#†
DAIII	5/17	29%	#†‡	13/16	82%	#†	12/15	80%	#†‡
Plantar muscles									
Autologous nerve graft	8/10	80%		10/10	100%		10/10	100%	
DAI	5/10	50%	#	8/10	80%	#‡	9/10	90%	#‡
DAII	6/12	50%	#	7/11	64%	#†	7/10	70%	#†
DAIII	4/12	33%	#†	7/11	64%	#‡	6/9	67%	#†‡

Significant differences $p < 0.05$ are indicated as follows: # versus nerve autograft, † versus DAI-chitosan tube, ‡ versus DAII-chitosan tube.

comparison to the connective tissue from the other groups (Fig. 5A). Connective tissue area and thickness displayed no significant differences among chitosan tubes of different DAs after 3 months and, in addition, no significant differences were obvious when compared with the data after 18 days (Fig. 5B). Multinucleated giant cells were only detected in two animals (DAI group) displaying a significant reduction of the foreign body reaction at 3 months after nerve reconstruction (Fig. 5C). Quantification of ED1-immunopositive cells revealed a highly significant reduction of their appearance as compared to the evaluation after short term nerve reconstruction (18 days, Fig. 5D). However, at both time points no differences in the immunological connective tissue reaction to chitosan tubes of different degrees of acetylation were obvious.

3.2.5. Assessment of chitosan tube properties after explantation

In addition to the above mentioned analyses of the connective tissue and regenerated nerve tissue peculiarities, the chitosan tubes were also macroscopically analysed upon explantation. The properties of the tubes differed substantially among the different degrees of acetylation. While 5 days after nerve reconstruction no macroscopic differences were detectable, DAIII-chitosan tubes showed signs of beginning degradation already 18 days after nerve reconstruction. In two of six DAIII-tubes small longitudinal fissures were visible through the surgery microscope and a 3rd sample displayed a rough surface. The degradation of DAIII-chitosan tubes was much further in progress three months after nerve reconstruction when these tubes displayed longitudinal fissures (4 out of 15), a fragmentary appearance that broke apart upon nerve tissue harvest (8/15) or they were already longitudinally broken and compressed (3/15). The crack-lines and sharp edged pieces appearing with progressed degeneration could have potentially damaged already regenerated nerve tissue. In contrast, DAI- and DAII-chitosan tubes mostly displayed a regular shape and firmness (13/16 and 11/15, respectively) and rarely a slightly bent shape (3 each) or a slight compression (DAII only: 1/15), both together with regular firmness. The colour of DAI and DAII tubes was changed to a serous yellow, while in DAIII tubes the change of colour was minimal. Fig. 11 shows representative samples of all chitosan tube types before and after nerve reconstruction. A cracked DAIII-chitosan tube 13 weeks after nerve reconstruction is shown in Fig. 12, demonstrating that degeneration of the tubes leads to damages that are already microscopically evident and can easily be confirmed in ultrastructural images.

Table 3
Results of the mechanical and biochemical analyses of chitosan tubes, which were explanted 13 weeks after nerve reconstruction. The degree of acetylation was determined in NMR spectrometry and the molecular weight (MW) was determined using the GPC method. With the latter no clear differences have been detected among the chitosan tubes of different DA. The symbols shown in the respective column show a tendency to most obvious reduction of MW in DAI chitosan tubes.

Chitosan tubes	Before implantation DA	13 weeks after nerve reconstruction			
		DA	Solubility	Toughness	MW degradation
DAI	~2%	1.1% ± 0.3%	− −	++	+++
DAII	~5%	3.6% ± 0.3%	−	+	++
DAIII	~20%	14.6% ± 1.1%	++	− − (brittle)	+

3.2.5.1. Biochemical characterization (Table 3).

The GPC chromatographs obtained showed an increase in the retention time for all chitosan tubes (the molecular weight distribution has shifted to the right) independently of the DA of the raw material. This evidence highlights the fact that all chitosan tubes used to bridge the nerve defects suffer depolymerisation during the time in vivo after nerve reconstruction. The DAIII-tubes showed a more symmetrical molecular weight (MW) degradation when compared with the other chitosan tubes with less DA. Nevertheless all samples analysed from the same group of chitosan tubes (DAI, DAII or DAIII) showed a similar chromatographic profile among them. This demonstrates a rather high reproducibility of the MW of the biopolymer (dispersibility of molecular weights) within the sample tubes, which suggests that both the tube production and biological activity are similar for each group. Homogeneity of the results within the three groups DAI–DAIII was quite high.

The variation of the DA among the chitosan tubes prior to nerve reconstruction and after explantation at 3 months was also investigated. Upon analytical evaluation of the NMR spectra, all sample chitosan tubes showed a rather similar DA before and after nerve reconstruction, demonstrating that there is no visible hydrolysis of the remaining acetyl groups of the chitosan main chain by biological action. Regarding solubility there was a clear tendency of chitosan tubes with higher DA to show a higher solubility when compared with other chitosan tubes of lower DA. In the case of DAI-chitosan tubes (DA ~2%) it was necessary to heat the solution in order to achieve a total dissolution of the tubes. On the other hand, the toughness of the tubes after explantation at 3 months was higher in DAI and DAII chitosan tubes when compared to DAIII-tubes, which were brittle.

4. Discussion

During the last years there has been an interest in chitosan as a suitable biomaterial for medical and pharmaceutical applications

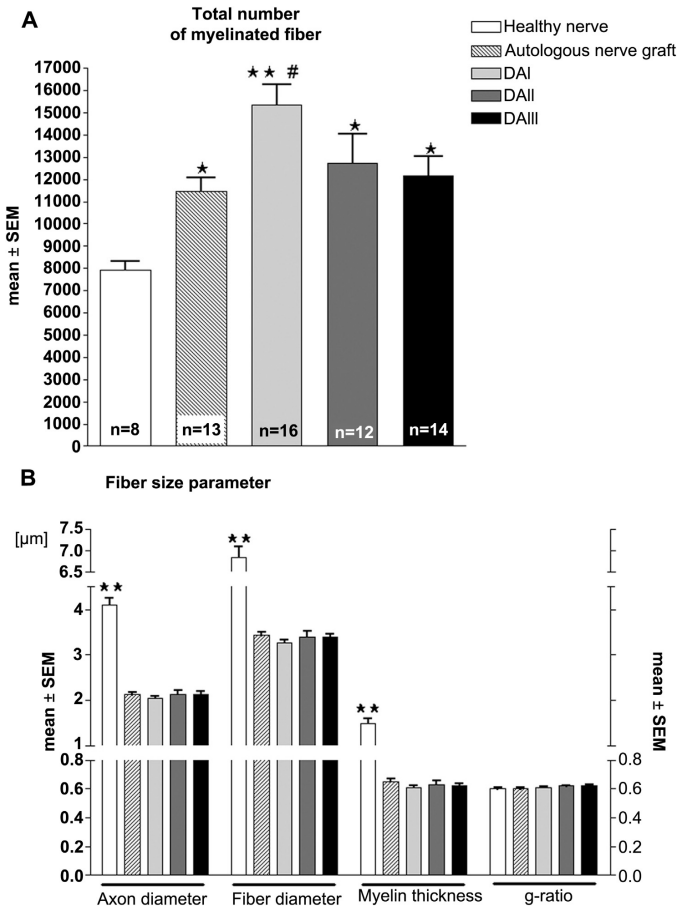

Fig. 8. The distal nerve (5 mm segment harvested 1 mm distal to the distal suture) was stereologically analysed in order to assess the myelinated fibres. (A) Result of myelinated fibre quantification. (B) Results of fibre size parameter analyses. Samples of healthy contralateral nerves were compared to nerve samples regenerated through autologous nerve grafts or chitosan tubes of different degrees of acetylation (DAI = ~2%; DAII = ~5%; DAIII = ~20%). $^{*}p \leq 0.05$ and $^{**}p \leq 0.01$: experimental groups vs healthy nerve; $\#p \leq 0.05$: DAI vs autologous nerve graft.

because of its biocompatibility, non-toxicity, and biodegradability. These properties qualified chitosan also as a putative candidate material for fabrication of peripheral nerve reconstruction devices [18,32]. However, the poor mechanical strength of chitosan conduits, along with pre-mature degradation and loss of structural integrity in vivo, were major limitations which prevented their commercial application in neural tissue engineering until now [15,18,32]. The present study, using chitosan conduits with different degrees of acetylation, indicates that fine-tuned chitosan tubes induce sufficient peripheral nerve regeneration when used to reconstruct a 10 mm nerve defect in adult rat sciatic nerves.

In vitro cytotoxicity tests with extracts from the different chitosan tubes revealed no detrimental effects on cell metabolic viability. Indeed when observing Fig. 3, it is noticeable that the values obtained are even above those obtained with the positive control extracts. As it is known chitosan withholds several structural affinities with animal/human tissues [33], however, when it degrades it can induce an increase of cell metabolic viability. Moreover, this is probably the reason why DAIII extracts disclose higher metabolic viabilities when compared to DAI or DAII extracts.

Short and long term in vivo studies demonstrated that i) mainly DAII chitosan tubes support nerve regeneration in a similar extent as the gold standard autologous nerve graft with regard to both function and morphology, while DAI and DAIII chitosan tubes demonstrated some shortcomings ii) the lesion-induced regulation of regeneration associated neurotrophic factors in the corresponding dorsal root ganglia and the secretion of BDNF and NGF into the chitosan tubes was not altered due to their different DAs,

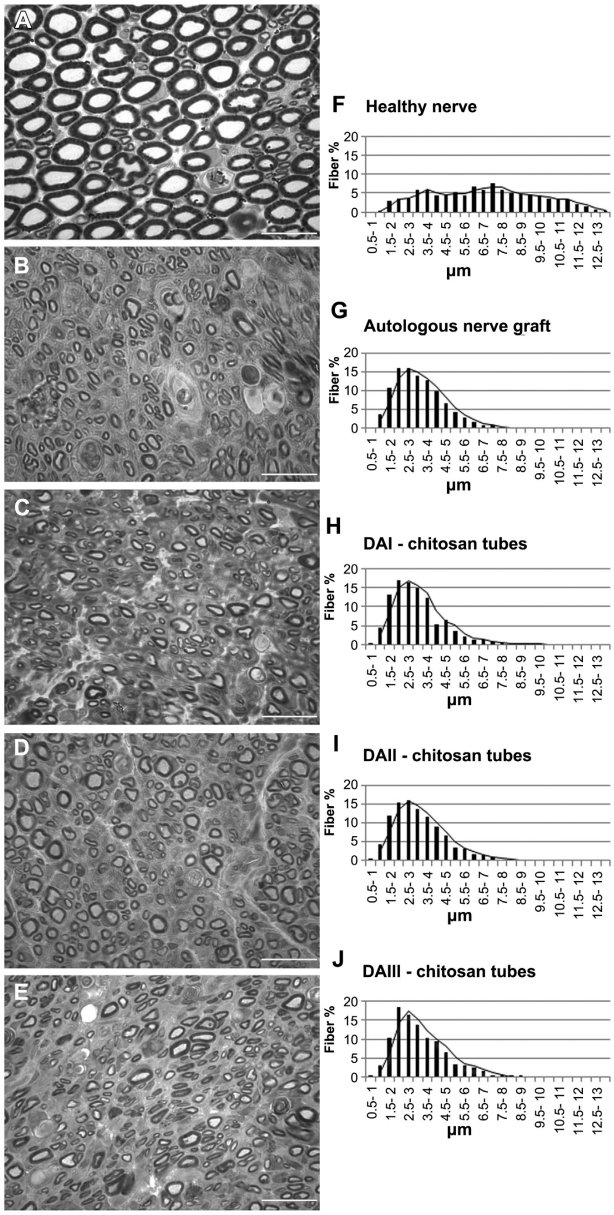

Fig. 9. High resolution images of representative semithin sections, stained with Toluidine blue, of nerve samples (A) from a healthy contralateral nerve, (B) regenerated through an autologous nerve graft, (C)–(E) regenerated through chitosan tubes (DAI = ~2%; DAII = ~5%; DAIII = ~20%). Scale bars: 20 µm. (F)–(J) fibre size distribution in the analysed groups of nerve samples.

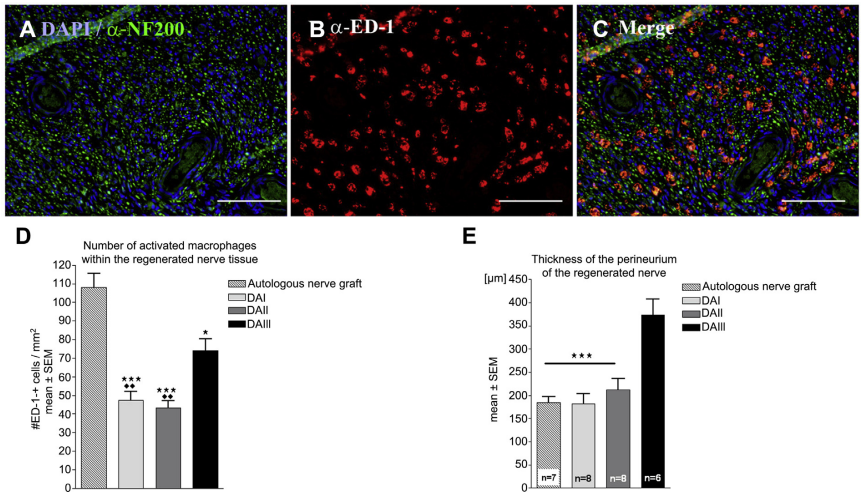

Fig. 10. (A)–(C) Representative photomicrographs of a cross-section of nerve tissue regenerated through DAIII-chitosan tubes analysed for the number of activated macrophages (ED-1-immunopositive cells), Scale bars: 100 µm. (D) Results of ED-1-cell quantification. Significantly less immunological tissue reaction was seen in nerves regenerated through DAI- or DAII-chitosan tubes compared to DAIII-group samples. (E) Measurement of the thickness of the perineurium in the regenerated nerve tissue further revealed that significantly more connective nerve tissue was formed inside of DAIII-chitosan tubes when compared to DAI- and DAII-tubes. DAI = ~2%; DAII = ~5%; DAIII = ~20%. Statistical tests used: (D) Kruskal–Wallis Test, Dunn's multiple comparison, asterix indicating inter-group differences to autologous nerve graft and solid rhombus indicating inter-group difference to DAIII-chitosan tubes $p < 0.05$; (E) One way ANOVA, Bonferroni multiple comparisons test, asterix indicating difference to DAIII-chitosan tubes, $p < 0.001$.

iii) the regenerative matrix formed in DAI and DAII chitosan tubes contained a lower number of cleaved caspase 3 stained, i.e. apoptotic, Schwann cells, as compared to DAIII chitosan tubes, iv) the number of ED1-immunopositive cells, i.e. activated macrophages, and thus the tissue reaction, in the regenerated nerve was significantly lower after nerve reconstruction with DAI and DAII chitosan tubes, and v) the material-induced immunoreaction in the connective tissue formed around the chitosan tubes was not altered by their different DA (equal numbers of multinucleated giant cells and activated macrophages) and was considerably reduced from 18 days to 3 months after nerve reconstruction.

Although the chitosan tubes with the different DAs allowed good structural and functional sciatic nerve regeneration, there were obvious differences with regard to the speed of their degradation (structural integrity), which were most evident at 3 months after nerve reconstruction. Overall, the DAIII chitosan tubes were much less stable during the observation period, which is probably the reason for the development of connective tissue with a significantly higher optical density. After explantation, tubes of the different DAs revealed differences with regard to consistency and chemical properties, which were related to the different grades of degradation. Macroscopically detectable crack lines were also obvious in SEM ultrastructures, although the electron microscopic appearance was rather similar among the three groups. However, the DAI chitosan tubes display almost no degradability.

Regarding previous chitosan devices, the main differences to the chitosan tubes presented here include their fine-tuned chemical structure which provided an optimal substrate for the formation of a regenerative matrix, where the thickness of such matrix correlated to the length of the outgrowing axons in accordance with findings from silicone tubes [34]. This goes along with the high mechanical compression strength and collapse stability. Furthermore, these chitosan tubes are completely transparent to ease the surgical procedure, and because also microneedles go through the material very easily, they seemed to be very suitable for bridging nerve defects. Moreover, the chitosan raw material and the tubes are manufactured according to ISO standard protocols for medical devices, which is a pre-requisite for regulatory approval and commercial application.

Analysis of the early regeneration phase (21 days) after nerve reconstruction with the chitosan tubes of different DAs demonstrated a higher number of activated Schwann cells in the distal segments of nerves regenerated through DAIII tubes. This may mirror that Schwann cells are stimulated and prepared to attract the outgrowing axons [26,27]. However, there was a tendency to shorter axonal outgrowth in this early regeneration phase in the same group of animals. In addition, the number of cells stained for cleaved caspase 3 was significantly higher in the regenerative matrix within DAIII chitosan tubes. The latter may be detrimental for axonal outgrowth although the number of such cells did not correlate with axonal outgrowth.

While usually not considered in studies where new materials are analysed, it is worth to consider other endogenous early events of regeneration in addition to the immunological reaction and the regenerative efficiency in the presence of the foreign material. During regeneration a distinct pattern of neurotrophic factors is produced and secreted by the nerve ends [35]. Pooled tube contents were collected at 5 and 18 days after nerve reconstruction and Western Blots were performed for BDNF and NGF, which revealed no differences among the different experimental groups. Moreover, the analysis of the corresponding dorsal root ganglia for expression of different growth factors, which are regulated during the regeneration process, did also not reveal differences among the different experimental groups. This suggests that the presence of the chitosan tubes, irrespective of their DAs, does not disturb these molecular processes.

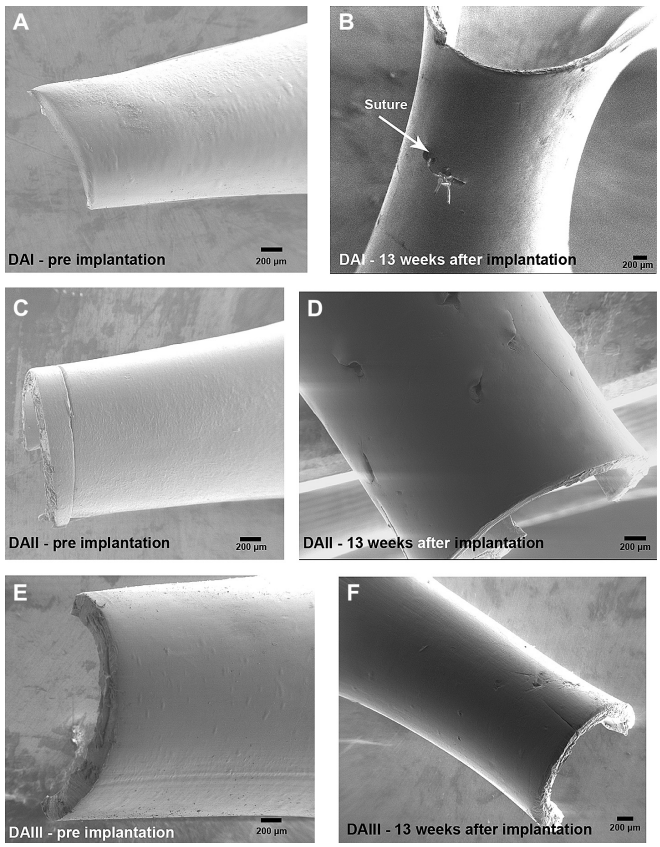

Fig. 11. Left column: representative SEM images of chitosan tubes of different degree of acetylation before nerve reconstruction. Right column: representative SEM images of example chitosan tubes explanted and analysed 13 weeks after nerve reconstruction. DAI = ~2%; DAII = ~5%; DAIII = ~20%.

Up to now the nerve reconstruction with an autologous nerve graft is the gold standard to overcome substance loss after peripheral nerve injury [1]. Thus, any nerve conduits have to be compared with this standard. With regard to the stereological parameters of the regeneration efficiency, the chitosan tubes presented in this study supported axonal regrowth to a similar extent as the autologous nerve graft. However, nerves regenerated through DAI chitosan tubes revealed a significantly higher total

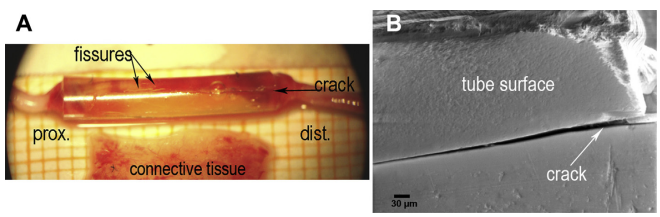

Fig. 12. (A) Chitosan tube of DAIII (~20% acetylation) upon explantation 13 weeks after nerve reconstruction, displaying several longitudinal fissures and a clear crack line. The connective tissue is opaque and the tube contains regenerated nerve tissue. (B) SEM image displaying the ultrastructure of the DAIII chitosan tube shown in (A) as well as the roughened outer surface of the tube after long term in vivo.

number of myelinated axons as compared to the gold standard. The increased number of regenerated axons after 3 months can be the morphological correlate of enhanced sprouting in the presence of DAI chitosan tubes, although fibre size under all experimental conditions was not different. Enhanced sprouting could eventually become a limiting factor for the outcome of functional recovery [36] and thus argues against the use of DAI chitosan tubes for future trials.

The good morphological regeneration in the presence of chitosan tubes is also reflected in the behavioural and functional parameters analysed. Regarding the SSI, animals of the different experimental groups displayed no significant differences compared to the gold standard. Moreover, although the electrophysiological measurements revealed a faster functional recovery in animals treated with autologous nerve grafts, after 3 months there were no significant differences with regard to the functional data among all experimental groups detectable. Interestingly, we found morphological differences with regard to non-neuronal tissue in the regenerated nerves, which have important impact on the selection of the type of chitosan tube for future applications. Three months after nerve reconstruction, the highest number of activated macrophages was present in nerves regenerated through autologous nerve grafts, which is due to the need for myelin debris removal in the autografts [35]. However, it is noteworthy that the number of activated macrophages within the regenerated nerves was significantly increased in the DAIII samples when compared to DAI and DAII samples. In addition, the thickness of the perineurium was significantly higher in nerves regenerated through DAIII chitosan tubes compared to DAI and DAII tubes and the autologous nerve graft. Both facts could reflect the acute tissue reaction to the faster degrading DAIII chitosan tubes, which argues against the use of those tubes for future trials.

Regarding the connective tissue surrounding the tube, no significant differences in thickness, area, numbers of multinucleated giant cells, and activated macrophages among the three DA groups were obvious. However, we detected a shift to a higher optical density of the unfolded connective tissue formed around DAIII chitosan tubes. Previously, it was reported that subcutaneously implanted chitosan scaffolds of different DAs induced different inflammatory responses which were more intense in the presence of materials with a DA of 15% as compared to materials with a DA of 4% [37]. In another study, chitosan membranes with different DAs were implanted under the calvarial periosteum and revealed as well different inflammation reactions [38]. Furthermore, chitosan sheets of different acetylation grades implanted into the spinal cord elicited different morphological reactions also in the nervous tissue [39]. In addition to different modes of fabrication of the chitosan devices, also the investigated implantation sites were different and could be the reason why in the present study varying reactions of the tube-surrounding connective tissue to the different DAs were minimized. Moreover, after 3 months only 1–2 remaining giant cells were found in the connective tissue preparations, which is the pattern of a reduced tissue response even seen at one year after the use of silicone tubes in nerve repair in humans, thus, the chitosan tubes can be judged as immunologically inert [5,40].

5. Conclusions

This comprehensive study provides a complex view on the suitability of fine-tuned chitosan tubes of different degree of acetylation to support peripheral nerve regeneration. With regard to the morphological and functional parameters of nerve regeneration, the chitosan tubes displayed a similar efficiency as the gold standard. However, differences were discovered regarding the immunological reaction, as well as other cellular processes, in the regenerative matrix and distal to the regenerated nerve and the chemical properties of tubes with the different DAs. While DAIII chitosan tubes (DA: ~20%) displayed a too fast degradation and induced degradation related tissue reactions, DAI tubes (DA: ~2%) induced an unintended sprouting effect in regenerating nerve fibres. Our findings point to DAII chitosan tubes (DA: ~5%) as the most supporting ones for peripheral nerve regeneration and as the first choice for ongoing applications in nerve reconstruction.

Acknowledgements

This work has received funding from the European Community's Seventh Framework Programme (FP7-HEALTH-2011) under grant agreement n° 278612 (BIOHYBRID).

We gratefully acknowledge the excellent technical assistance from the following people: members of the Institute of Neuroanatomy (Hannover Medical School): S. Fischer, N. Heidrich, K. Kuhlemann, J. Metzen and H. Streich; members of Università di Torino: S. Bompasso; and the guest researcher at Department of Clinical Sciences – Hand Surgery, Lund University, Dr A. Kodama from Hiroshima University, Hiroshima, Japan.

References

[1] Deumens R, Bozkurt A, Meek MF, Marcus MA, Joosten EA, Weis J, et al. Repairing injured peripheral nerves: bridging the gap. Prog Neurobiol 2010;92:245–76.
[2] Ray WZ, Mackinnon SE. Management of nerve gaps: autografts, allografts, nerve transfers, and end-to-side neurorrhaphy. Exp Neurol 2010;223:77–85.
[3] Battiston B, Raimondo S, Tos P, Gaidano V, Audisio C, Scevola A, et al. Chapter 11: tissue engineering of peripheral nerves. Int Rev Neurobiol 2009;87:227–49.
[4] Xu H, Yan Y, Li S. PDLLA/chondroitin sulfate/chitosan/NGF conduits for peripheral nerve regeneration. Biomaterials 2011;32:4506–16.
[5] Dahlin LB, Anagnostaki L, Lundborg G. Tissue response to silicone tubes used to repair human median and ulnar nerves. Scand J Plast Reconstr Surg Hand Surg 2001;35:29–34.
[6] Lundborg G, Rosen B, Dahlin L, Holmberg J, Rosen I. Tubular repair of the median or ulnar nerve in the human forearm: a 5-year follow-up. J Hand Surg Br 2004;29:100–7.
[7] Weber RA, Breidenbach WC, Brown RE, Jabaley ME, Mass DP. A randomized prospective study of polyglycolic acid conduits for digital nerve reconstruction in humans. Plast Reconstr Surg 2000;106:1036–45 discussion 46–8.
[8] Archibald SJ, Krarup C, Shefner J, Li ST, Madison RD. A collagen-based nerve guide conduit for peripheral nerve repair: an electrophysiological study of nerve regeneration in rodents and nonhuman primates. J Comp Neurol 1991;306:685–96.
[9] Archibald SJ, Shefner J, Krarup C, Madison RD. Monkey median nerve repaired by nerve graft or collagen nerve guide tube. J Neurosci 1995;15:4109–23.
[10] Bertleff MJ, Meek MF, Nicolai JP. A prospective clinical evaluation of biodegradable neurolac nerve guides for sensory nerve repair in the hand. J Hand Surg Am 2005;30:513–8.
[11] Hernandez-Cortes P, Garrido J, Camara M, Ravassa FO. Failed digital nerve reconstruction by foreign body reaction to Neurolac nerve conduit. Microsurgery 2010;30:414–6.
[12] Yuan Y, Zhang P, Yang Y, Wang X, Gu X. The interaction of Schwann cells with chitosan membranes and fibers in vitro. Biomaterials 2004;25:4273–8.
[13] Jiang X, Lim SH, Mao HQ, Chew SY. Current applications and future perspectives of artificial nerve conduits. Exp Neurol 2010;223:86–101.
[14] Dahlin LB, Lundborg G. Use of tubes in peripheral nerve repair. Neurosurg Clin N Am 2001;12:341–52.
[15] Freier T, Koh HS, Kazazian K, Shoichet MS. Controlling cell adhesion and degradation of chitosan films by N-acetylation. Biomaterials 2005;26:5872–8.
[16] Simoes MJ, Gartner A, Shirosaki Y, Gil da Costa RM, Cortez PP, Gartner F, et al. In vitro and in vivo chitosan membranes testing for peripheral nerve reconstruction. Acta Med Port 2011;24:43–52.
[17] Ao Q, Fung CK, Tsui AY, Cai S, Zuo HC, Chan YS, et al. The regeneration of transected sciatic nerves of adult rats using chitosan nerve conduits seeded with bone marrow stromal cell-derived Schwann cells. Biomaterials 2011;32:787–96.
[18] Freier T, Montenegro R, Shan Koh H, Shoichet MS. Chitin-based tubes for tissue engineering in the nervous system. Biomaterials 2005;26:4624–32.
[19] Hirai A, Odani H, Nakajima A. Determination of degree of deacetylation of chitosan by ^{1}H NMR spectroscopy. Polym Bull 1991;26:87–94.
[20] Salgado AJ, Coutinho OP, Reis RL. Novel starch-based scaffolds for bone tissue engineering: cytotoxicity, cell culture, and protein expression. Tissue Eng 2004;10:465–74.
[21] Salgado AJ, Gomes ME, Coutinho OP, Reis RL. Isolation and osteogenic differentiation of bone-marrow progenitor cells for application in tissue engineering. Methods Mol Biol 2004;238:123–30.

[22] Haastert-Talini K, Schmitte R, Korte N, Klode D, Ratzka A, Grothe C. Electrical stimulation accelerates axonal and functional peripheral nerve regeneration across long gaps. J Neurotrauma 2011;28:661–74.
[23] Cobianchi S, Casals-Diaz L, Jaramillo J, Navarro X. Differential effects of activity dependent treatments on axonal regeneration and neuropathic pain after peripheral nerve injury. Exp Neurol 2013;240:157–67.
[24] Rumpel R, Alam M, Klein A, Özer M, Wesemann M, Jin X, et al. Neuronal firing activity and gene expression changes in the subthalamic nucleus after transplantation of dopamine neurons in hemiparkinsonian rats. Neurobiol Dis 2013;59:230–43.
[25] Ratzka A, Kalve I, Ozer M, Nobre A, Wesemann M, Jungnickel J, et al. The co-layer method as an efficient way to genetically modify mesencephalic progenitor cells transplanted into 6-OHDA rat model of Parkinson's disease. Cell Transplant 2012;21:749–62.
[26] Saito H, Dahlin LB. Expression of ATF3 and axonal outgrowth are impaired after delayed nerve repair. BMC Neurosci 2008;9:88.
[27] Tsuda Y, Kanje M, Dahlin LB. Axonal outgrowth is associated with increased ERK 1/2 activation but decreased caspase 3 linked cell death in Schwann cells after immediate nerve repair in rats. BMC Neurosci 2011;12:12.
[28] Stenberg L, Kanje M, Dolezal K, Dahlin LB. Expression of activating transcription factor 3 (ATF 3) and caspase 3 in Schwann cells and axonal outgrowth after sciatic nerve repair in diabetic BB rats. Neurosci Lett 2012;515:34–8.
[29] Huelsenbeck SC, Rohrbeck A, Handreck A, Hellmich G, Kiaei E, Roettinger I, et al. C3 peptide promotes axonal regeneration and functional motor recovery after peripheral nerve injury. Neurotherapeutics 2012;9:185–98.
[30] Raimondo S, Fornaro M, Di Scipio F, Ronchi G, Giacobini-Robecchi MG, Geuna S. Chapter 5: methods and protocols in peripheral nerve regeneration experimental research: part II – morphological techniques. Int Rev Neurobiol 2009;87:81–103.
[31] Geuna S. Appreciating the difference between design-based and model-based sampling strategies in quantitative morphology of the nervous system. J Comp Neurol 2000;427:333–9.
[32] Yamaguchi I, Itoh S, Suzuki M, Osaka A, Tanaka J. The chitosan prepared from crab tendons: II. The chitosan/apatite composites and their application to nerve regeneration. Biomaterials 2003;24:3285–92.
[33] Costa-Pinto AR, Salgado AJ, Correlo VM, Sol P, Bhattacharya M, Charbord P, et al. Adhesion, proliferation, and osteogenic differentiation of a mouse mesenchymal stem cell line (BMC9) seeded on novel melt-based chitosan/polyester 3D porous scaffolds. Tissue Eng Part A 2008;14:1049–57.
[34] Zhao Q, Lundborg G, Danielsen N, Bjursten LM, Dahlin LB. Nerve regeneration in a 'pseudo-nerve' graft created in a silicone tube. Brain Res 1997;769:125–34.
[35] Schmidt CE, Leach JB. Neural tissue engineering: strategies for repair and regeneration. Annu Rev Biomed Eng 2003;5:293–347.
[36] Streppel M, Azzolin N, Dohm S, Guntinas-Lichius O, Haas C, Grothe C, et al. Focal application of neutralizing antibodies to soluble neurotrophic factors reduces collateral axonal branching after peripheral nerve lesion. Eur J Neurosci 2002;15:1327–42.
[37] Barbosa JN, Amaral IF, Aguas AP, Barbosa MA. Evaluation of the effect of the degree of acetylation on the inflammatory response to 3D porous chitosan scaffolds. J Biomed Mater Res A 2010;93:20–8.
[38] Hidaka Y, Ito M, Mori K, Yagasaki H, Kafrawy AH. Histopathological and immunohistochemical studies of membranes of deacetylated chitin derivatives implanted over rat calvaria. J Biomed Mater Res 1999;46:418–23.
[39] Yussof SJM, Halim AS, Saad AZM, Jaafar H. Evaluation of the biocompatibility of a bilayer chitosan skin regenerating template, human skin allograft, and integra implants in rats. ISRN Mater Sci 2011;2011:7.
[40] Brodbeck WG, Anderson JM. Giant cell formation and function. Curr Opin Hematol 2009;16:53–7.

Paper IV

EJN European Journal of Neuroscience

FENS

European Journal of Neuroscience, Vol. 43, pp. 463–473, 2016 doi:10.1111/ejn.13068

Nerve regeneration in chitosan conduits and in autologous nerve grafts in healthy and in type 2 diabetic Goto–Kakizaki rats

Lena Stenberg,[1,2] Akira Kodama,[3] Charlotta Lindwall-Blom[4] and Lars B. Dahlin[1,2]
[1]Department of Translational Medicine – Hand Surgery, Lund University, Jan Waldenströms gata 5, 205 02 Malmö, Sweden
[2]Department of Hand Surgery, Skåne University Hospital, Malmö, Sweden
[3]Department of Orthopaedic Surgery, Integrated Health Sciences, Institute of Biomedical and Health Science, Hiroshima University, Hiroshima, Japan
[4]Cellectricon AB, Mölndal, Sweden

Keywords: ATF3, cleaved caspase 3, diabetes, nerve reconstruction, Schwann cell

Edited by John Foxe
Received 4 May 2015, accepted 6 September 2015

Abstract

Knowledge about nerve regeneration after nerve injury and reconstruction in appropriate diabetic animal models is incomplete. Short-term nerve regeneration after reconstruction of a 10-mm sciatic nerve defect with either a hollow chitosan conduit or an autologous nerve graft was investigated in healthy Wistar and diabetic Goto–Kakizaki (GK) rats. After 21 days, axonal outgrowth, the presence of activated and apoptotic Schwann cells and the thickness of the formed matrix in the conduits were measured. In general, nerve regeneration was superior in autologous nerve grafts. In chitosan conduits, a matrix, which was thicker in diabetic rats, was formed and was positively correlated with length of axonal outgrowth. Axonal outgrowth in conduits and in nerve grafts extended further in diabetic rats than in healthy rats. There was a higher percentage of activating transcription factor 3 (ATF3)-immunostained cells in nerve segments from healthy rats than in diabetic rats after autologous nerve graft reconstruction. In chitosan conduits, more cleaved caspase 3-stained Schwann cells were generally observed in the matrix from the diabetic rats than in healthy rats. However, there were fewer apoptotic cells in the distal segment in diabetic rats reconstructed with a chitosan conduit. Preoperative glucose levels were positively correlated with axonal outgrowth after both reconstruction methods. Axonal regeneration was better in autologous nerve grafts than in hollow chitosan conduits and was enhanced in diabetic GK rats compared to healthy rats after reconstruction. This study provides insights into the nerve regeneration process in a clinically relevant diabetic animal model.

Introduction

In general, the incidence of diabetes mellitus is increasing globally due to both a growing number of older people developing type 2 diabetes and an increased incidence of type 1 diabetes in young people. Thus, there is an associated risk of an increased number of people with diabetic-related complications of the eyes, the kidneys and the cardiovascular system. More relevant for the present study, diabetes also affects the peripheral nervous system, i.e. neuropathy, but the detailed mechanisms behind the development of neuropathy are not understood (Callaghan & Feldman, 2013). As the world population is growing older, with a rising number of type 2 diabetic patients, there is a trend to be more active at older ages for both physical and mental reasons (Caspersen *et al.*, 2000; Keller & Lemberg, 2002; Chang *et al.*, 2014). In addition to more active older adults with diabetes, there are a growing number of younger people with diabetes who may also do manual labor. Both of these factors increase the risk that subjects with diabetes may also suffer from traumatic hand injuries, particularly injuries to their peripheral nerves (Kannus *et al.*, 2005; Keller *et al.*, 2012; Bonne & Schuerer, 2013; Kara *et al.*, 2014). From experimental studies, it has been reported that the regeneration pattern differs between healthy Wistar rats and diabetic Goto–Kakizaki (GK) rats after nerve injury and repair {i.e. direct suture; Stenberg & Dahlin, 2014). However, knowledge about the initial nerve regeneration process following reconstruction of a nerve injury with a defect in relevant diabetic rat models is insufficient, but is essential from both the clinical and neurobiological points of view. Due to reasons of animal care, evaluation of the short-term regeneration process in rats with diabetes is more feasible than the conventional long-term experiments in healthy rats.

A traumatic nerve injury causing a nerve defect between the proximal and distal nerve ends can be bridged by the gold standard technique of autologous nerve grafting, or in certain situations by various nerve conduits (Weber *et al.*, 2000; Lundborg *et al.*, 2004; Boeckstyns *et al.*, 2013; Konofaos & Ver Halen, 2013) such as

Correspondence: Lars B. Dahlin, [1]Department of Translational Medicine – Hand Surgery, as above.
E-mail: lars.dahlin@med.lu.se

© 2015 Federation of European Neuroscience Societies and John Wiley & Sons Ltd

non-degradable silicone tubes (Dahlin & Lundborg, 2001; Dahlin *et al.*, 2001), or degradable materials (i.e. polyglycolic acid tubes; Weber *et al.*, 2000; Boeckstyns *et al.*, 2013) or with processed nerve allografts (Rinker *et al.*, 2015). Recently, chitosan, produced commercially by deacetylation of chitin (the structural element in the exoskeleton of crustaceans such as crab and shrimp), has been described as an alternative for bridging nerve defects with the advantage of being absorbable (Haastert-Talini *et al.*, 2013). Whether chitosan conduits can also be used in subjects with diabetes needs to be determined. Furthermore, it is also crucial to evaluate from a neurobiological point of view the initial regeneration process, including matrix formation, axonal outgrowth, and activation and apoptosis of Schwann cells. The different components of the initial regeneration process are critical for the overall regeneration process (Zhao *et al.*, 1993; Stenberg & Dahlin, 2014) that leads to functional recovery. However, reconstruction of longer nerve defects (i.e. 15 mm compared to 10 mm) with chitosan conduits may be less successful than nerve grafts (Gonzalez-Perez *et al.*, 2015; Shapira *et al.*, 2015). Our aim was to bridge a shorter, i.e. 10 mm, sciatic nerve defect with a hollow chitosan conduit (low acetylation) or with an autologous nerve graft in healthy and genetically modified type 2 diabetic rats (i.e. GK rats; Portha *et al.*, 2009; Stenberg & Dahlin, 2014) with focus on evaluating the aforementioned components of the initial nerve regeneration process in short-term experiments.

Materials and methods

Animals

All animal experiments were approved by the ethical committee in Malmö and Lund region, Sweden (Lund University permit number 347/2011). A total of 32 female Wistar (Taconic, Denmark) and GK rats (~ 200 g each, kindly provided by Malin Fex, Lund University) were included and divided into four groups: (i) healthy Wistar rats with chitosan conduit (n = 8); (ii) healthy Wistar rats with autologous nerve graft (n = 8); (iii) diabetic GK type 2 rats with chitosan conduits (n = 8); and (iv) diabetic GK type 2 rats with autologous nerve graft (n = 8). Altakitin S.A., Portugal and Medovent GmbH, Germany, kindly provided the chitosan conduits. All animals also had a 12-h day–night cycle in the cages. The GK rats were provided with extra water. Fasting blood sugar and body weight of the rats were measured once a week in all animals. Blood glucose was measured with a blood sample from the tail vein [Ascensia contour TM (Bio health Care, USA, Bio Diagnostics Europe) and LT (Bayer AB, Diabetes Care, Solna, Sweden); test slips Microfil TM (Bio Healthcare Diabetes Care, USA)]. Before surgery the rats were anesthetized with an intraperitoneal injection of a mixture of Rompun® (20 mg/mL; Bayer Health Care, Leverkusen, Germany) and Ketalar® (10 mg/mL; Pfizer, Helsinki, Finland) with a dose of 1 mL Ketalar® and 0.25 mL Rompun® per 100 g body weight rat. For pain prevention, all rats were postoperatively injected with Temgesic® 0.01–0.05 mg/kg (0.3 mg/mL; Schering-Plough Europe, Brussels, Belgium).

Surgery

The sciatic nerve was exposed in deeply anesthetized animals at the hind-limb level. For implantation of the chitosan conduit, the sciatic nerve was transected and a 5-mm segment was removed. A low-acetylation chitosan conduit was implanted and 2 mm of the proximal and distal nerve ends were sutured within the conduit using 9–0 Ethilon (Ethicon®) epi/perineurial sutures. The length of the conduit was 14 mm, its inner diameter was 2.1 mm and the nerve defect in the rats was 10 mm (Fig. 1). After surgery, the skin was sutured and the rats were allowed to recover. For implantation of the autologous nerve graft a 10-mm nerve segment was removed from the sciatic nerve, rotated 180° and then sutured with 9–0 Ethilon (Ethicon®) epi/perineurial sutures (Fig. 1). Twenty-one days was chosen as sufficient time for matrix formation within the conduit and thus as the end-point based on pilot experiments (i.e. single rats evaluated at 10, 14 and 21 days; data not shown for 10 and 14 days).

Harvest of specimens

After 21 days, the animals (n = 8 in each group) were re-anesthetized and the sciatic nerves, together with the formed matrix inside the conduit, and the autologous nerve grafts as well as the sciatic nerves from contralateral side were removed. After removal, the animals were killed by an overdose of pure pentobarbitalnatrium (60 mg/mL; Apoteksbolaget, Malmö, Sweden). Before fixing the tissue in Stefanini solution [4% paraformaldehyde and 1.9% picric acid in 0.1M phosphate-buffered saline (PBS) pH 7.2], the chitosan conduits were carefully removed from the sciatic nerve specimens, leaving only the nerve ends and the matrix that had formed within the conduit. After 24 h of fixation, the samples were washed in 0.01M PBS, pH 7.2, three times and then placed in 20% sucrose solution overnight for cryoprotection. The samples were then embedded in OCT Cryo mount (Histolab products AB, Gothenburg, Sweden) and sectioned longitudinally at 6 μm thickness and mounted on superfrost plus glass (Thermo Scientific, Braunschweig, Germany).

Immunohistochemistry

For immunolabelling, the sections were washed for 5 min with PBS prior to incubation with primary antibodies. The following primary antibodies were used: monoclonal mouse anti-human neurofilament (1:80; Dako, Glostrup, Denmark), rabbit anti-activating transcription factor 3 (ATF3) polyclonal antibody (1:200; Santa Cruz Biotechnology, USA) and rabbit anti-cleaved caspase-3 antibody (1:200; BioNordica, Stockholm, Sweden). Antibodies were diluted in 0.25% Triton-X 100 and 0.25% BSA (bovine serum albumin) in PBS. The sections were incubated with antibodies overnight at 4 °C. The next day, the slides were washed with PBS for 3 × 5 min followed by incubation with secondary antibodies, Alexa Fluor 594-conjugated goat anti-mouse IgG or Alexa Fluor 488 conjugated goat anti-rabbit IgG (both from Invitrogen, Molecular Probes, Eugene, Oregon, USA), diluted at 1:500 in PBS. Sections were incubated with the secondary antibody solution for 1 h in the dark at room temperature. After 1 h, the slides were washed with PBS for 3 × 10 min, counterstained with 4′,6′diamidino-2-phenylindole (DAPI; Vectashield®, Vector Laboratories, Inc. Burlingame, CA 94010, USA) to visualize the nuclei (i.e. for total number of DAPI cells; expressed as no/mm^2), and then coverslipped.

Double staining: S-100 and ATF3 or cleaved caspase 3

To make sure that we only counted Schwann cells in the sciatic nerve segments, we also performed a double staining with S-100 and anti-ATF3 or anti-cleaved caspase 3. The sections were incubated with rabbit anti-ATF3 polyclonal antibody (see above), or with rabbit anti-cleaved caspase 3 antibody (see above) and on day 2 with the second antibody, Alex Fluor 488-conjugated goat anti-rabbit IgG, as described above. After 1 h the slides were incubated with mouse monoclonal IgG anti-S100 antibody α/β chain

© 2015 Federation of European Neuroscience Societies and John Wiley & Sons Ltd

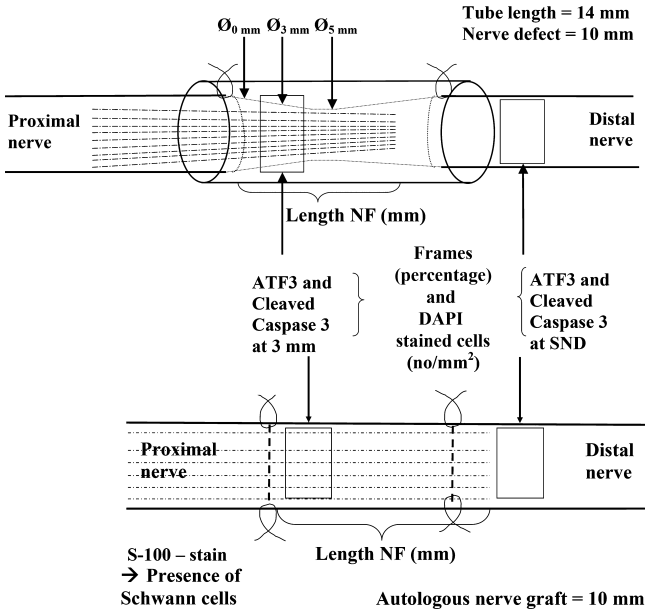

FIG. 1. Schematic drawing of surgical procedures to reconstruct nerve defects in healthy and diabetic rat sciatic nerves. In healthy and diabetic GK rats, the sciatic nerve was transected and a 10-mm nerve defect was reconstructed with a chitosan conduit (upper panel) or a 10-mm nerve segment was cut, rotated 180° and resutured as an autologous nerve graft (lower panel). Details are provided where length of axonal outgrowth and presence of ATF3 and cleaved caspase 3-stained Schwann cells are quantified. SND, distal nerve segment.

(Santa Cruz Biotechnology) diluted at 1:200 in PBS. On the final day the sections were washed in PBS 3 × 5 min and then incubated with Alexa Fluor 594-conjugated goat anti-mouse IgG as described above. After 1 h we washed the slides in PBS as described, mounted with Vectashield and cover-slipped.

Imaging and analyses

The sections were photographed using an inverted fluorescence microscope (Nikon Eclipse) equipped with a digital camera (Nikon 80i) and analysed with the Software NIS elements (Nikon). The widths (i.e. distance across) of the formed matrices inside the conduit were measured on three sections in the microscope (10 × magnification) at three levels, i.e. near lesion and 3 mm and 5 mm distal to the lesion (Fig. 1). A few sections were analysed from the contralateral side from both rats with conduits and rats with autologous nerve grafts to visualize differences between the groups (data not shown; Stenberg & Dahlin, 2014). The length of the stained neurofilament proteins were measured in three randomly selected sections (10 × magnification) from the site of lesion to the front of the longest growing axons (Stenberg & Dahlin, 2014) in both chitosan conduits and in nerve grafts (Fig. 1) with the requirement that the neurofilaments should be continuously traced from the proximal nerve segment to the front of the regenerating axons (Stenberg & Dahlin, 2014). A mean value of the length of axons from the three evaluated sections was calculated from each animal and used for statistical analyses. ATF3 and cleaved caspase 3-labelled cells were counted in sciatic nerve sections (image size 500 × 400 μm; 20 ×magnification) both at 3 mm from the proximal nerve suture and in the distal nerve segment just distal to the end of the conduit or the autologous nerve graft (Fig. 1). At these locations, squares (6 × 100 μm^2) were randomly selected and examined for presence of apoptotic cleaved caspase 3 and activated ATF3 as well as for DAPI-stained cells (i.e. total number of cells; Fig. 1). Presence of ATF3 and cleaved caspase 3-stained cells was expressed as percentage of total number of DAPI-stained cells. In all cases for the autologous nerve graft groups, mean values were calculated from the three sections. From the chitosan conduit groups only one proper section was available and used for evaluation of cleaved caspase 3 and ATF3, due to the limited number of sections that could be obtained as the matrices were thin. The number of DAPI cells (indicating total number of cells) was also evaluated from the sections stained for ATF3 and cleaved caspase 3 (mean values from these sections) and expressed as no/mm^2.

Statistical methods

The statistical analyses were performed using the software IBM SPSS Statistics, version 22. All results are presented as median values (with 25–75th percentiles) due to a non-normal distribution of data. The nonparametric Kruskal–Wallis (KW) test was used to determine whether there were any significant differences between the four groups. The Mann–Whitney *post hoc* test was used to identify differences between the four groups: healthy rats with chitosan conduit, healthy rats with autologous nerve grafts, diabetic GK rats with chitosan conduits and diabetic GK rats with autologous nerve grafts. Separate *P*-values for healthy vs. diabetic rats and chitosan conduits vs. autologous nerve grafts were then combined to a single

© 2015 Federation of European Neuroscience Societies and John Wiley & Sons Ltd

P-value by using the Fisher method for independent samples based on the χ^2 distribution (Fisher, 1948; https://en.wikipedia.org/wiki/Fisher%27s_method, courtesy of statistician Professor Jonas Björk, Lund University, Lund, Sweden; Stenberg & Dahlin, 2014). Spearman's rank correlation test was used to evaluate relationships between different parameters (expressed as *r*-values and *P*-values). A *P*-value of < 0.05 was considered significant.

Results

Fasting preoperative blood glucose and weight increase

We observed significant differences in blood glucose between the healthy and diabetic GK rats with higher blood glucose levels in the diabetic rats ($P < 0.0001$; Fisher's test; Table 1). However, no statistical differences in blood glucose levels were detected between rats treated with either the autologous nerve grafts or the chitosan conduits within the healthy or diabetic groups ($P = 0.80$). The preoperative [healthy rats 264 (244–279) g, $n = 16$; rats with diabetes 244 (227–259) g, $n = 16$] and postoperative [healthy rats 267 (253–283) g, $n = 16$; rats with diabetes 249 (236–270) g, $n = 16$] weights were higher ($P = 0.043$ and 0.021, Mann–Whitney, respectively) in the healthy rats. The weight increase [healthy rats 2.8% (0.4–6.2); rats with diabetes 3.5% (1.5–4.8)] was not different between the healthy and the diabetic rats ($P = 0.84$, Mann–Whitney).

Matrix formation in the conduit

A matrix, extending from the proximal to the distal nerve ends, was formed after 21 days in the chitosan conduits in both the healthy and the diabetic rats. The formed matrix in the chitosan conduits (Fig. 2e and f) was significantly thicker in the diabetic rats than in the healthy rats at all three measured locations (Mann–Whitney; $P = 0.007$, $P = 0.0001$; and $P = 0.0001$, respectively): near the lesion [10.4%; healthy rats 317 (305–322) μm; rats with diabetes 350 (331–378) μm]; at 3 mm [41.5%; healthy rats 236 (231–245) μm; rats with diabetes 334 (303–346) μm] and at 5 mm [21.2%; healthy rats 241 (232–244) μm; rats with diabetes 292 (286–302) μm].

Length of axonal outgrowth in conduits and autologous nerve grafts

Axons had grown into the chitosan conduits and in the autologous nerve grafts in all specimens (Fig. 2a–d). There were, however, statistical differences in length of axonal outgrowth between the various groups reconstructed with autologous nerve grafts and the chitosan conduits ($P = 0.0001$; Table 1; Figs 1 and 2a–d), with axons extending further into the autologous nerve grafts than in the chitosan conduits ($P < 0.0001$, Fisher's test). The axonal outgrowth in both types of reconstruction procedures was longer in diabetic rats than in healthy rats ($P < 0.0001$, Fisher's test; Table 1).

ATF3-stained Schwann cells in conduits and autologous nerve grafts (at 3 mm)

Only cells with characteristics of a Schwann cell, i.e. shape and location as well as double staining (Saito & Dahlin, 2008; Tsuda *et al.*, 2011), were counted as ATF3-positive cells (Fig. 3a). Significant differences at 3 mm from the proximal suture in the reconstruction models were observed between the groups (KW, $P = 0.0001$; Table 1; Fig. 3a–h). The differences were observed between the chitosan conduit and autologous nerve graft models ($P < 0.0001$; Fisher's test) as

TABLE 1. Nerve regeneration in healthy Wistar rats and in diabetic GK rats after reconstruction of a 10-mm-long sciatic nerve defect with autologous nerve grafts or hollow chitosan conduits, and evaluated after 21 days

		Healthy rats				Diabetic rats					Fisher's method†	
		Chitosan ($n = 8$)		Autologous nerve graft ($n = 8$)		Chitosan ($n = 8$)		Autologous nerve graft ($n = 8$)				
	Unit	Med	Q1–Q3	Med	Q1–Q3	Med	Q1–Q3	Med	Q1–Q3	*P* (KW)	Conduit/graft	Healthy/diabetes
Axonal outgrowth (neurofilaments)	mm	8.3	8.1–8.5	14.0	13.9–14.2	9.9	9.6–10.0	16.5	15.7–18.5	0.0001	< 0.0001	< 0.0001
ATF3												
at 3 mm	% of total	0.9	0.4–1.0	13.8	13.1–14.8	1.5	1.3–1.9	6.8	6.3–7.2	0.0001	< 0.0001	< 0.0001
SND	% of total	19.1	18.2–21.2	19.4	19.0–19.7	7.5	6.5–9.0	14.2	13.9–15.1	0.0001	0.006	< 0.0001
Cleaved caspase–3												
at 3 mm	% of total	7.0	6.6–7.3	16.3	15.3–17.0	13.0	12.6–14.3	15.5	15.2–15.8	0.0001	< 0.0001	0.002
SND	% of total	20.6	17.4–22.2	20.0	19.1–21.0	14.1	13.7–15.0	20.1	19.6–21.1	0.001	0.006	0.005
DAPI-stained cells												
at 3 mm	no/mm^2	939	916–976	815	792–833	1056	1047–1063	902	892–914	0.0001	< 0.0001	< 0.0001
SND	no/mm^2	1067	1043–1088	830	816–839	891	867–912	886	882–889	0.0001	0.0004	< 0.0001
Preoperative B-glucose	mmol/L	3.9	3.7–4.3	4.1	3.4–4.4	11.1	9.4–12.4	8.0	7.4–10.6	0.0001	0.80	< 0.0001

Values are median (Med) and 25th (Q1)–75th (Q3) percentiles. SND, distal nerve segment (see Fig. 1). †Fisher method for independent samples based on the χ^2 distribution. For details of evaluation see Fig. 1.

© 2015 Federation of European Neuroscience Societies and John Wiley & Sons Ltd

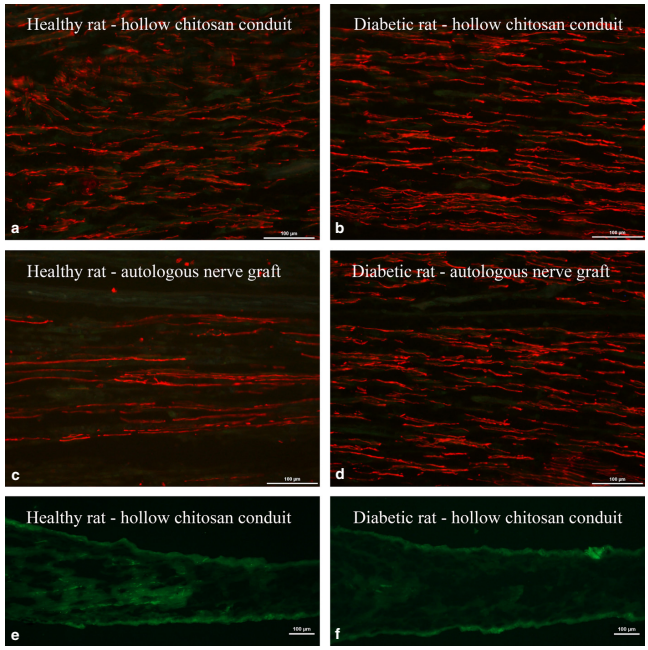

FIG. 2. Neurofilament staining in the matrix of the chitosan conduits and in autologous nerve grafts. Immunohistochemical staining of neurofilament proteins in (a and c) healthy and in (b and d) diabetic GK rats in the matrix formed in hollow chitosan conduits (a and b) and in autologous nerve grafts (c and d). The matrix was thinner in the healthy rats (e) than in the GK rats (f). For details see Fig. 1. Scale bars, 100 μm.

well as between the healthy and diabetic rats ($P < 0.0001$; Fisher's test; Table 1). There was a high percentage of ATF3-stained cells in the autologous nerve grafts, particularly in the healthy rats. In contrast, nerve segments from the contralateral, uninjured, sciatic nerve, exhibited only a few positive ATF3-stained cells (data not shown).

ATF3-stained Schwann cells in the distal nerve segment

There were also ATF3-stained cells in the distal nerve segment in all specimens (Fig. 4a–d). The KW test revealed differences between the test groups ($P = 0.0001$; Table 1). Differences were observed between healthy and diabetic rats ($P < 0.0001$; Fisher's test), where healthy rats exhibited a higher percentage of ATF3-stained cells. There were also statistical differences between autologous nerve grafts and chitosan conduits ($P = 0.006$; Fisher's test) with a higher percentage of ATF3-stained cells in those diabetic rats with autologous nerve grafts (Table 1).

Apoptotic Schwann cells within conduits and autologous nerve grafts (at 3 mm)

Statistically significant differences were also observed for the cleaved caspase 3-stained Schwann cells among the groups at 3 mm from the proximal nerve suture ($P = 0.0001$, KW; Table 1; Fig. 5a–h). Significant differences were found between healthy and diabetic rats ($P < 0.002$; Fisher's test) and also between chitosan conduit and autologous nerve graft ($P < 0.0001$; Fisher's test). There was a higher percentage of cleaved caspase-3-stained cells in the autologous nerve graft model both in diabetic and in healthy rats. The percentage was higher in diabetic rats reconstructed with chitosan conduits than in the healthy rats reconstructed with the same method (Table 1). Nerve segments from the contralateral, uninjured, sciatic nerve exhibited only single-stained cleaved caspase 3-stained cells (data not shown).

Apoptotic Schwann cells in the distal nerve segment

Cleaved caspase 3-stained cells were observed in the distal nerve segment in all specimens (Fig. 4e–h). Differences in the percentage of cleaved caspase 3-stained Schwann cells at this location were detected between the test groups (KW, $P = 0.001$). There was a significant difference between healthy and diabetic rats ($P < 0.005$; Fisher's test) with generally higher percentages of stained cells in healthy rats (Table 1). There were also differences in the number of cleaved caspase 3-stained cells between the two reconstruction models with a lower percentage in the diabetic rats reconstructed with the chitosan conduit ($P < 0.006$; Fisher's test; Table 1).

DAPI-stained cells in conduits and autologous nerve grafts at 3 mm and in distal nerve segment

The analyses of the density of the DAPI-stained cells, indicating total cell number of all cells and expressed as no/mm^2, also showed

© 2015 Federation of European Neuroscience Societies and John Wiley & Sons Ltd

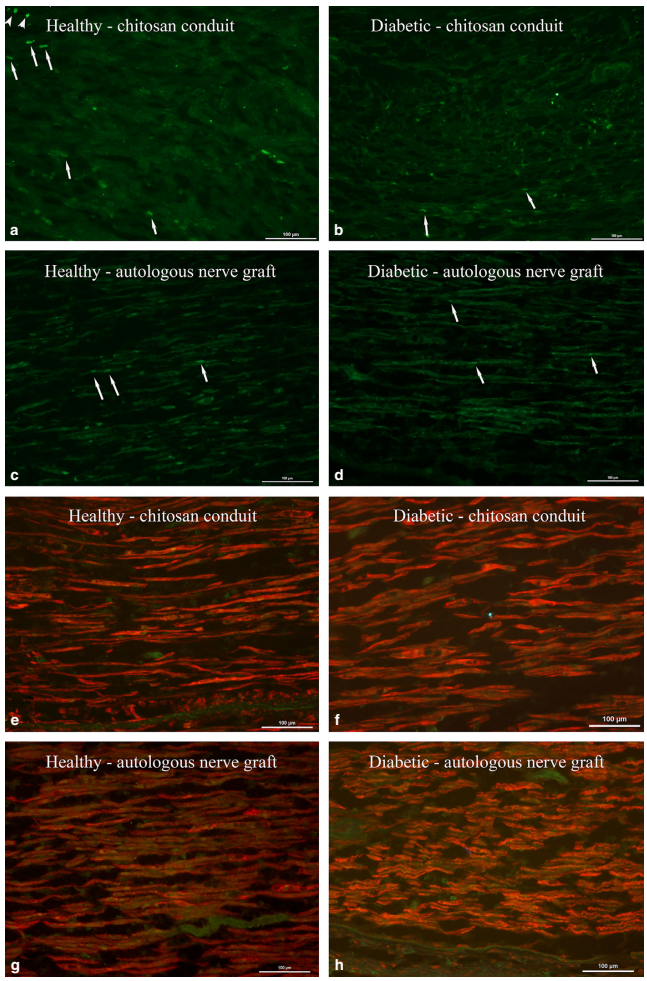

FIG. 3. ATF3 and S-100 in chitosan conduits and autologous nerve grafts. Immunohistochemical staining of (a–d) ATF3 and double staining with (e–h) S-100 in healthy (a, c, e and g) and in diabetic GK rats (b, d, f and h) in the matrix formed in hollow chitosan conduits (a, b, e and f) and in autologous nerve grafts (c, d, g and h). In the insert (upper left corner) three Schwann cells (arrows) and two inflammatory cells (arrowheads) are shown. Arrows in the other images indicate Schwann cells. For details see Fig. 1. Scale bars, 100 µm.

differences (KW, $P = 0.0001$; Table 1). The Fisher method, when analysing the cells within the conduits and the autologous nerve grafts at 3 mm, showed significant differences between the chitosan conduit and autologous nerve graft models ($P < 0.0001$; lower number in the grafts) and between the healthy and diabetic rats ($P < 0.0001$; higher in diabetic rats).

The density of DAPI-stained cells showed a different pattern in the distal nerve segment, but still with differences (KW, $P = 0.0001$; Table 1). Thus, the Fisher test showed statistical differences between the diabetic and healthy rats ($P < 0.0001$; depending on reconstruction model) and between the autologous nerve graft and the conduit models ($P = 0.0004$; somewhat lower in the autologous nerve grafts).

Correlations

Analyses of correlations were also done because previous studies (Saito & Dahlin, 2008; Tsuda *et al.*, 2011; Stenberg & Dahlin,

© 2015 Federation of European Neuroscience Societies and John Wiley & Sons Ltd

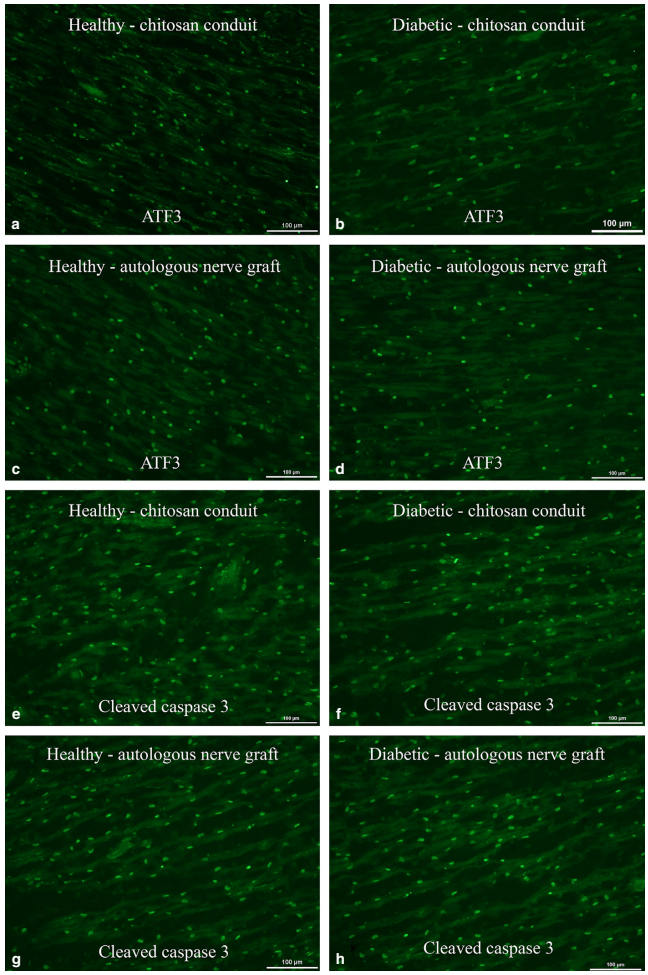

FIG. 4. ATF3 and cleaved caspase 3 in the distal nerve segment after reconstruction with chitosan conduits and autologous nerve grafts. Immunohistochemical staining of (a–d) ATF3 and (e–h) cleaved caspase 3 in healthy (a, c, e and g) and in diabetic GK (b, d, f and h) rats in the distal nerve segment from regeneration in hollow chitosan conduits (a, b, e and f) and in autologous nerve grafts (c, d, g and h). For details see Fig. 1. Scale bars, 100 µm.

2014) have shown an association between preoperative blood glucose and different variables related to nerve regeneration, and that the matrix is important for axonal outgrowth (Zhao *et al.*, 1993). Furthermore, one may also hypothesize that an association exists between the percentage of activated and apoptotic cells due to positive and negative regulators of Schwann cell differentiation (Ogata *et al.*, 2006; Heinen *et al.*, 2013). Relevant correlations were examined with the data pooled and with the data from the chitosan conduits as well as from the autologous nerve grafts. There were no significant correlations between the different evaluated variables when the four different groups were analysed individually, probably due to a limited number of observations in the individual groups.

Pooled data

When analysing all treatment groups together, i.e. regeneration in healthy and diabetic rats through conduits and autologous nerve grafts, the axonal outgrowth showed no correlation with preoperative glucose ($r = 0.256$, $P = 0.16$; Fig. 6a). However, axonal outgrowth did

© 2015 Federation of European Neuroscience Societies and John Wiley & Sons Ltd

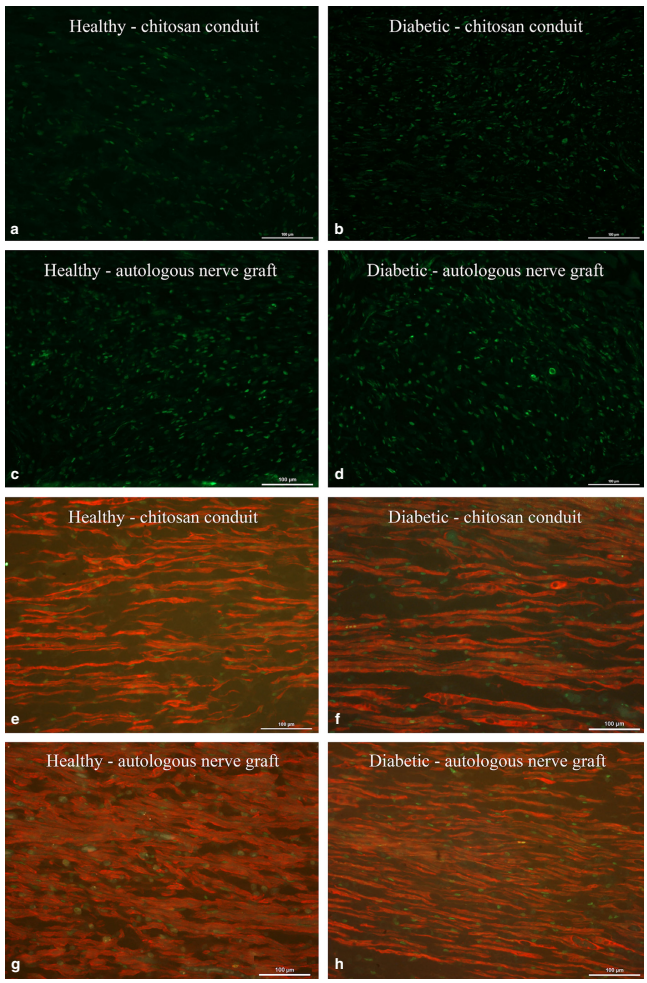

FIG. 5. Cleaved caspase 3 and S-100 in chitosan conduits and autologous nerve grafts. Immunohistochemical staining of (a–d) cleaved caspase 3 and (e–h) double staining with S-100 in healthy (a, c, e and g) and in diabetic GK (b, d, f and h) rats in the matrix formed in hollow chitosan conduits (a, b, e and f) and in autologous nerve grafts (c, d, g and h). For details see Fig. 1. Scale bars, 100 μm.

correlate with the percentage of ATF3-stained ($r = 0.703$, $P = 0.0001$) and cleaved caspase 3-stained ($r = 0.781$, $P = 0.0001$) Schwann cells at 3 mm from the site of the proximal suture. The preoperative glucose levels did not correlate with the percentage of ATF3-stained ($P = 0.60$) or cleaved caspase 3-stained ($P = 0.65$) Schwann cells at 3 mm in the reconstruction models. However, the percentage of ATF3-stained Schwann cells was positively correlated ($r = 0.841$, $P = 0.0001$; Fig. 6b) with the percentage of cleaved caspase 3-stained Schwann cells at the same location as well as in the distal nerve segment ($r = 0.65$, $P = 0.0001$; Fig. 6c).

Chitosan conduits

The axonal outgrowth in the chitosan conduits positively correlated with the diameter of the formed matrix [near lesion, $r = 0.55$, $P = 0.026$; at 3 mm, $r = 0.63$, $P = 0.009$ (Fig. 6d); and at 5 mm, $r = 0.72$, $P = 0.002$]. Length of axonal outgrowth also correlated with the preoperative glucose levels ($r = 0.82$, $P = 0.0001$; see individual data in Fig. 6a). Furthermore, axonal outgrowth positively correlated with the percentage of cleaved caspase 3-stained Schwann cells ($r = 0.78$, $P = 0.0001$) in the chitosan conduit at 3 mm,

© 2015 Federation of European Neuroscience Societies and John Wiley & Sons Ltd

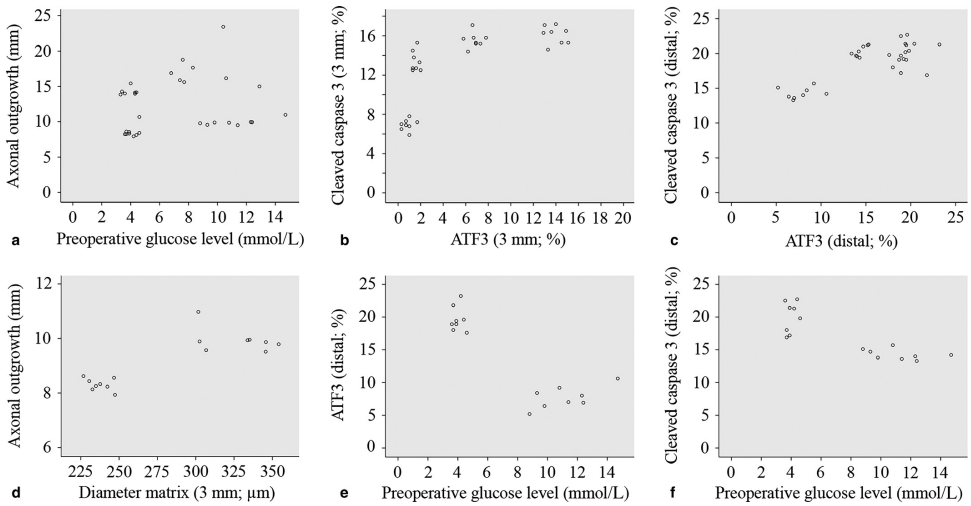

FIG. 6. Relationships in nerve regeneration in chitosan conduits and autologous nerve grafts in healthy and diabetic rats. Scatter diagrams showing correlations between preoperative glucose levels, length of axonal outgrowth, diameter of the formed matrix in chitosan conduits and presence of ATF3 and cleaved caspase 3-stained Schwann cells from all groups of rats (a–c) and from the rats in which the nerve defect was reconstructed with a chitosan conduit (d–f). For detailed correlation ρ-values and *P*-values see Results.

but not with the percentage of ATF3-stained Schwann cells at the same location (i.e. 3 mm; $P = 0.08$).

The preoperative glucose levels positively correlated with the percentages of ATF3-stained ($r = 0.64$, $P = 0.008$) and cleaved caspase 3-stained ($r = 0.84$, $P = 0.0001$) Schwann cells inside the conduit (i.e. at 3 mm), but negatively with the corresponding percentages in the distal nerve segment (respectively, $r = -0.70$, $P = 0.003$; Fig. 6e; and $r = -0.79$, $P = 0.0001$; Fig. 6f). The percentages of ATF3- and cleaved caspase 3-stained Schwann cells at 3 mm inside the chitosan conduit ($r = 0.67$, $P = 0.005$) and in the distal nerve segment ($r = 0.81$, $P = 0.0001$) positively correlated with each other.

Autologous nerve grafts

The axonal outgrowth in the autologous nerve grafts did not correlate with the percentage of cleaved caspase 3-stained Schwann cells at 3 mm in the graft ($P = 0.41$), but correlated negatively ($r = -0.79$, $P = 0.0001$) with percentage of ATF3-stained Schwann cells in the graft. The preoperative glucose levels positively correlated with the length of axonal outgrowth ($r = 0.67$, $P = 0.004$; see details in Fig. 6a). The preoperative glucose levels correlated negatively with the percentage of ATF3-stained Schwann cells inside the graft ($r = -0.76$, $P = 0.001$) as well as in the distal nerve segment ($r = -0.75$, $P = 0.001$), but did not correlate with the percentage of cleaved caspase 3-stained Schwann cells ($P = 0.29$ and 0.45, respectively). The percentages of ATF3- and cleaved caspase 3-stained Schwann cells did not correlate with each other, either at 3 mm in the autologous nerve grafts ($P = 0.37$) or in the distal nerve segment ($P = 0.45$).

Discussion

We examined short-term nerve regeneration in two different nerve reconstruction models, bridging a short (i.e. 10 mm) nerve defect (Shapira *et al.*, 2015) in healthy rats as well as in a genetically modified diabetic GK rats with clinically relevant blood glucose levels (Portha *et al.*, 2009; Stenberg & Dahlin, 2014). The advantage of the diabetic GK rats compared to other diabetic rat or mouse models, such as the Biobreeding rats and rats with streptozotocin-induced diabetes (Stenberg *et al.*, 2012), is that diabetic GK rats display only a modest, but constant, increase in blood sugar levels. They survive for longer periods of time without needing insulin treatment, as well as without the risk of severe variations in blood glucose levels or developing a catabolic condition that may severely influence the nerve regeneration process. Thus, the diabetic GK rat model is relevant in evaluating the nerve regeneration process after nerve injury and reconstruction of a nerve defect.

As expected at the early stage of the nerve regeneration process investigated here (i.e. 21 days), axonal outgrowth was longer in autologous nerve grafts than in the chitosan conduits in both healthy and diabetic rats. One reason for this could be the larger percentage of activated (i.e. ATF3-stained) Schwann cells observed in the autologous nerve grafts compared to the chitosan conduits. In a similar model, albeit with a longer nerve defect (i.e. 15 mm), the functional recovery in healthy rats evaluated at 4 months is better after reconstruction with autologous nerve grafts than with chitosan conduits (Gonzalez-Perez *et al.*, 2015). However, the functional recovery is similar when a shorter nerve defect (i.e. 10 mm; Shapira *et al.*, 2015) is bridged with chitosan conduits or autologous nerve grafts. Such observations stress the importance of the length of the defect (Zhao *et al.*, 1993) as well as the presence of Schwann cells in an

© 2015 Federation of European Neuroscience Societies and John Wiley & Sons Ltd

appropriate extracellular matrix (i.e. tissue niche; Andersson-Sjoland *et al.*, 2011). Interestingly, the length of axonal outgrowth was longer in the diabetic GK rats than in the healthy rats, which is in contrast to short-term axonal outgrowth after a nerve transection with subsequent direct end-to-end nerve repair, where the length of axonal outgrowth in healthy Wistar rats exceeded the ones in diabetic GK rats (Stenberg & Dahlin, 2014). This discrepancy may be explained by the fact that axons after a direct nerve repair (Stenberg & Dahlin, 2014) are allowed to grow into a well vascularized distal nerve segment. In the present autologous nerve graft model, the grafts bridging the 10 mm nerve defect were transected, rotated 180° and re-sutured. The implication is that the Schwann cells present in the autologous nerve graft depend initially on diffusion and later on revascularization, which modulate the tissue niche (Andersson-Sjoland *et al.*, 2011), thus mimicking the situation in clinical practice. However, the presence of activated Schwann cells (i.e. the percentage of ATF3-stained Schwann cells) cannot explain the longer axonal outgrowth in the diabetic GK rats, as the percentage of ATF3-stained Schwann cells inside the graft was higher in healthy rats. The blood glucose levels, with the modestly higher levels in the diabetic GK rats, positively correlated with length of axonal outgrowth in the autologous nerve grafts as well as in the chitosan conduits (see separate correlations and individual data in Fig. 6a), and may possibly influence the processes through diverse mechanisms, e.g. a different association with the percentage of ATF3-stained Schwann cells. There is a possibility of a direct effect of the modest blood glucose levels on the neurons and their regenerating axons or through produced AGE products (advanced glycation end products), which has been shown *in vitro* and *in vivo*, but mostly in conditions with high glucose levels (Sango *et al.*, 2006; Tosaki *et al.*, 2008; Duran-Jimenez *et al.*, 2009; Bennmann *et al.*, 2014; Tsukamoto *et al.*, 2015) and in models examining regeneration after a nerve crush injury (Ekstrom & Tomlinson, 1989, 1990). Again, high blood glucose levels in *in vitro* systems induce a number of oxidative, metabolic and apoptotic responses in Schwann cells (Cinci *et al.*, 2015) as well as an impairment of proliferation and migration of Schwann cells with subsequent diminished axonal outgrowth (Gumy *et al.*, 2008). Other authors have stressed that the age of the postnatal rat dorsal root ganglia, and not glucose levels *in vitro*, influences the number of surviving neurons as well as those that develop neurites (Sepehr *et al.*, 2009). In contrast to the present findings using the diabetic GK rat model with moderately increased blood glucose levels and evaluated at 21 days, *in vivo* experiments in a different diabetic model (i.e. streptozotocin-induced diabetes) have shown that local glucose exposure has no influence on the early outgrowth of axons or migration of Schwann cells in rats (Zochodne *et al.*, 2007). However, the 'diabetic bridges' used by Zochodne and colleagues demonstrated extensive failure of reconstruction 3 weeks after injury, with the conclusion that diabetes severely limits the success of regeneration (Zochodne *et al.*, 2007). With respect to the clinical situation, the present diabetic GK rat model, in which the sciatic nerve defect of 10 mm was reconstructed with common techniques, is relevant with its moderately increased blood glucose level.

The chitosan conduit is formed of a tissue-compatible material with several positive abilities that makes it suitable for bridging short nerve defects (Haastert-Talini *et al.*, 2013). We found that the length of axonal outgrowth was greater in the chitosan conduits in the diabetic GK rats than in the healthy Wistar rats, although shorter than in the autologous nerve grafts. At 21 days, a matrix was formed inside the hollow chitosan conduits in both healthy and diabetic animals and the matrix was thicker in the diabetic GK rats. The thickness of the matrix positively correlated with the length of the axonal outgrowth (Fig. 6d), supporting the concept of the crucial influence of matrix formation on the nerve regeneration process (Zhao *et al.*, 1993). The length of the sciatic nerve defect is relevant for nerve regeneration and functional recovery as the success of functional recovery is higher after reconstruction with chitosan conduits of a short (10 mm) than of a long (i.e. 15 mm) sciatic nerve defect in healthy rats (Gonzalez-Perez *et al.*, 2015; Shapira *et al.*, 2015). Whether the nerve regeneration process can be improved in chitosan conduits in healthy and diabetic GK rats by modulating their contents, e.g. by inserting membranes, is currently being evaluated.

There was a higher percentage of ATF3-stained cells in healthy rats than in diabetic GK rats in the distal nerve segment, where the reconstruction technique should not influence the condition of the distal nerve segment. However, the percentage of ATF3-stained Schwann cells seemed to be negatively influenced by the preoperative blood glucose levels (see e.g. Fig. 6e). Furthermore, the positive and negative regulation of Schwann cell differentiation is notably seen in the distal nerve segment where the percentages of ATF3- and cleaved caspase 3-stained Schwann cells correlated with each other (Fig. 6c; also Ogata *et al.*, 2006; Heinen *et al.*, 2013), and which explains the negative correlation also observed for the cleaved caspase 3-stained Schwann cells in the distal nerve segment (Fig. 6f). However, we did not in detail analyze these processes as our purpose was, in short-term experiments, to analyze the axonal outgrowth inside the reconstruction models.

Clinical studies have not focused on the nerve regeneration process in humans with diabetes after nerve injury and repair or reconstruction, but mechanisms have been suggested for a potential impairment of axonal outgrowth (Kennedy & Zochodne, 2005). In a clinical study of nerve regeneration and degeneration (i.e. 52-week trial of acetyl-L-carnitine), based on a change of myelinated nerve fiber density in the sural nerve of patients with diabetes, it was shown that maintaining optimal HbA1c-levels, i.e. long-term levels of blood glucose levels, were an important factor for regeneration (Hur *et al.*, 2013). Whether the regeneration process in humans is influenced by diabetes has to be determined in clinical studies defining type of diabetes, as the mechanism(s) of development of neuropathy are different between types 1 and 2 diabetes (Callaghan *et al.*, 2012). However, a potential limitation of performing such a study is the limited number of available patients with suitable nerve injury; there is an inherent statistical power problem in a clinical study.

In conclusion, short-term regeneration is improved in autologous nerve grafts compared to hollow chitosan conduits in both healthy and diabetic GK rats. In addition, axonal outgrowth in diabetic GK-rats surpasses healthy Wistar rats in both these nerve reconstruction models.

Competing interests

The authors declare that they have no competing interests.

Acknowledgements

We would like to acknowledge our close friend, colleague and mentor Professor Martin Kanje, PhD, Department of Biology, Lund University, Sweden, who died in March 2013. Martin was an important source of knowledge for the design of the present project but he was not able to see it finalized. Martin should be remembered as an outstanding scientist in the field of peripheral nerve regeneration and will continue to be an inspiration in our research. The authors gratefully acknowledge the delivery of the chitosan raw material by Altakitin S.A., Portugal, and the fabrication of chitosan conduits by Medovent GmbH, Germany. This project has received funding from the European Union's Seventh Programme for research, technological

© 2015 Federation of European Neuroscience Societies and John Wiley & Sons Ltd

development and demonstration under grant agreement No. 278612 (BIOHYBRID), the Swedish Research Council (Medicine), Lund University, Sydvästra Skånes Diabetesförening and Region Skåne (Skåne University Malmö, Lund), Sweden. We would also like to thank Professor Jonas Björk for statistical advice concerning the Fisher test.

Abbreviations

ATF3, activating transcription factor 3; DAPI, 4′,6′diamidino-2-phenylindole; GK rats, Goto–Kakizaki rats; KW, Kruskal–Wallis; PBS, phosphate-buffered saline.

References

Andersson-Sjoland, A., Nihlberg, K., Eriksson, L., Bjermer, L. & Westergren-Thorsson, G. (2011) Fibrocytes and the tissue niche in lung repair. *Respir. Res.*, **12**, 76.

Bennmann, D., Horstkorte, R., Hofmann, B., Jacobs, K., Navarrete-Santos, A., Simm, A., Bork, K. & Gnanapragassam, V.S. (2014) Advanced glycation endproducts interfere with adhesion and neurite outgrowth. *PLoS One*, **9**, e112115.

Boeckstyns, M.E., Sorensen, A.I., Vineta, J.F., Rosen, B., Navarro, X., Archibald, S.J., Valss-Sole, J., Moldovan, M. & Krarup, C. (2013) Collagen conduit versus microsurgical neurorrhaphy: 2-year follow-up of a prospective, blinded clinical and electrophysiological multicenter randomized, controlled trial. *J. Hand. Surg. Am.*, **38**, 2405–2411.

Bonne, S. & Schuerer, D.J. (2013) Trauma in the older adult: epidemiology and evolving geriatric trauma principles. *Clin. Geriatr. Med.*, **29**, 137–150.

Callaghan, B. & Feldman, E. (2013) The metabolic syndrome and neuropathy: therapeutic challenges and opportunities. *Ann. Neurol.*, **74**, 397–403.

Callaghan, B.C., Hur, J. & Feldman, E.L. (2012) Diabetic neuropathy: one disease or two? *Curr. Opin. Neurol.*, **25**, 536–541.

Caspersen, C.J., Pereira, M.A. & Curran, K.M. (2000) Changes in physical activity patterns in the United States, by sex and cross-sectional age. *Med. Sci. Sport. Exer.*, **32**, 1601–1609.

Chang, P.J., Wray, L. & Lin, Y. (2014) Social relationships, leisure activity, and health in older adults. *Health Psychol.*, **33**, 516–523.

Cinci, L., Corti, F., Di Cesare Mannelli, L., Micheli, L., Zanardelli, M. & Ghelardini, C. (2015) Oxidative, metabolic, and apoptotic responses of schwann cells to high glucose levels. *J. Biochem. Mol. Toxic.*, **29**, 274–279.

Dahlin, L.B. & Lundborg, G. (2001) Use of tubes in peripheral nerve repair. *Neurosurg. Clin. N. Am.*, **12**, 341–352.

Dahlin, L.B., Anagnostaki, L. & Lundborg, G. (2001) Tissue response to silicone tubes used to repair human median and ulnar nerves. *Scand. J. Plast. Recons.*, **35**, 29–34.

Duran-Jimenez, B., Dobler, D., Moffatt, S., Rabbani, N., Streuli, C.H., Thornalley, P.J., Tomlinson, D.R. & Gardiner, N.J. (2009) Advanced glycation end products in extracellular matrix proteins contribute to the failure of sensory nerve regeneration in diabetes. *Diabetes*, **58**, 2893–2903.

Ekstrom, A.R. & Tomlinson, D.R. (1989) Impaired nerve regeneration in streptozotocin-diabetic rats. Effects of treatment with an aldose reductase inhibitor. *J. Neurol. Sci.*, **93**, 231–237.

Ekstrom, P.A. & Tomlinson, D.R. (1990) Impaired nerve regeneration in streptozotocin-diabetic rats is improved by treatment with gangliosides. *Exp. Neurol.*, **109**, 200–203.

Fisher, R.A. (1948) Combining independent tests of significance. *Am. Stat.*, **2**, 30.

Gonzalez-Perez, F., Cobianchi, S., Geuna, S., Barwig, C., Freier, T., Udina, E. & Navarro, X. (2015) Tubulization with chitosan guides for the repair of long gap peripheral nerve injury in the rat. *Microsurgery*, **35**, 300–308.

Gumy, L.F., Bampton, E.T. & Tolkovsky, A.M. (2008) Hyperglycaemia inhibits Schwann cell proliferation and migration and restricts regeneration of axons and Schwann cells from adult murine DRG. *Mol. Cell Neurosci.*, **37**, 298–311.

Haastert-Talini, K., Geuna, S., Dahlin, L.B., Meyer, C., Stenberg, L., Freier, T., Heimann, C., Barwig, C., Pinto, L.F., Raimondo, S., Gambarotta, G., Samy, S.R., Sousa, N., Salgado, A.J., Ratzka, A., Wrobel, S. & Grothe, C. (2013) Chitosan tubes of varying degrees of acetylation for bridging peripheral nerve defects. *Biomaterials*, **34**, 9886–9904.

Heinen, A., Lehmann, H.C. & Kury, P. (2013) Negative regulators of schwann cell differentiation-novel targets for peripheral nerve therapies? *J. Clin. Immunol.*, **33**(Suppl 1), S18–S26.

Hur, J., Sullivan, K.A., Callaghan, B.C., Pop-Busui, R. & Feldman, E.L. (2013) Identification of factors associated with sural nerve regeneration and degeneration in diabetic neuropathy. *Diabetes Care*, **36**, 4043–4049.

Kannus, P., Sievanen, H., Palvanen, M., Jarvinen, T. & Parkkari, J. (2005) Prevention of falls and consequent injuries in elderly people. *Lancet*, **366**, 1885–1893.

Kara, H., Bayir, A., Ak, A., Akinci, M., Tufekci, N., Degirmenci, S. & Azap, M. (2014) Trauma in elderly patients evaluated in a hospital emergency department in Konya, Turkey: a retrospective study. *Clin. Interv. Aging*, **9**, 17–21.

Keller, K.B. & Lemberg, L. (2002) Retirement is no excuse for physical inactivity or isolation. *Am. J. Crit. Care*, **11**, 270–272.

Keller, J.M., Sciadini, M.F., Sinclair, E. & O'Toole, R.V. (2012) Geriatric trauma: demographics, injuries, and mortality. *J. Orthop. Trauma*, **26**, e161–e165.

Kennedy, J.M. & Zochodne, D.W. (2005) Impaired peripheral nerve regeneration in diabetes mellitus. *J. Peripher. Nerv. Syst.*, **10**, 144–157.

Konofaos, P. & Ver Halen, J.P. (2013) Nerve repair by means of tubulization: past, present, future. *J. Reconstr. Microsurg.*, **29**, 149–164.

Lundborg, G., Rosen, B., Dahlin, L., Holmberg, J. & Rosen, I. (2004) Tubular repair of the median or ulnar nerve in the human forearm: a 5-year follow-up. *J. Hand Surg. Brit.*, **29**, 100–107.

Ogata, T., Yamamoto, S., Nakamura, K. & Tanaka, S. (2006) Signaling axis in schwann cell proliferation and differentiation. *Mol. Neurobiol.*, **33**, 51–62.

Portha, B., Lacraz, G., Kergoat, M., Homo-Delarche, F., Giroix, M.H., Bailbe, D., Gangnerau, M.N., Dolz, M., Tourrel-Cuzin, C. & Movassat, J. (2009) The GK rat beta-cell: a prototype for the diseased human beta-cell in type 2 diabetes? *Mol. Cell. Endocrinol.*, **297**, 73–85.

Rinker, B.D., Ingari, J.V., Greenberg, J.A., Thayer, W.P., Safa, B. & Buncke, G.M. (2015) Outcomes of short-gap sensory nerve injuries reconstructed with processed nerve allografts from a multicenter registry study. *J. Reconstr. Microsurg.*, **31**, 384–390.

Saito, H. & Dahlin, L.B. (2008) Expression of ATF3 and axonal outgrowth are impaired after delayed nerve repair. *BMC Neurosci.*, **9**, 88.

Sango, K., Saito, H., Takano, M., Tokashiki, A., Inoue, S. & Horie, H. (2006) Cultured adult animal neurons and schwann cells give us new insights into diabetic neuropathy. *Curr. Diabetes Rev.*, **2**, 169–183.

Sepehr, A., Ruud, J. & Mohseni, S. (2009) Neuron survival in vitro is more influenced by the developmental age of the cells than by glucose condition. *Cytotechnology*, **61**, 73–79.

Shapira, Y., Tolmasov, M., Nissan, M., Reider, E., Koren, A., Biron, T., Bitan, Y., Livnat, M., Ronchi, G., Geuna, S. & Rochkind, S. (2015) Comparison of results between chitosan hollow tube and autologous nerve graft in reconstruction of peripheral nerve defect: an experimental study. *Microsurgery*, doi: 10.1002/micr.22418. [Epub ahead of print].

Stenberg, L. & Dahlin, L.B. (2014) Gender differences in nerve regeneration after sciatic nerve injury and repair in healthy and in type 2 diabetic Goto-Kakizaki rats. *BMC Neurosci.*, **15**, 107.

Stenberg, L., Kanje, M., Dolezal, K. & Dahlin, L.B. (2012) Expression of activating transcription factor 3 (ATF 3) and caspase 3 in Schwann cells and axonal outgrowth after sciatic nerve repair in diabetic BB rats. *Neurosci. Lett.*, **515**, 34–38.

Tosaki, T., Kamiya, H., Yasuda, Y., Naruse, K., Kato, K., Kozakae, M., Nakamura, N., Shibata, T., Hamada, Y., Nakashima, E., Oiso, Y. & Nakamura, J. (2008) Reduced NGF secretion by Schwann cells under the high glucose condition decreases neurite outgrowth of DRG neurons. *Exp. Neurol.*, **213**, 381–387.

Tsuda, Y., Kanje, M. & Dahlin, L.B. (2011) Axonal outgrowth is associated with increased ERK 1/2 activation but decreased caspase 3 linked cell death in Schwann cells after immediate nerve repair in rats. *BMC Neurosci.*, **12**, 12.

Tsukamoto, M., Sango, K., Niimi, N., Yanagisawa, H., Watabe, K. & Utsunomiya, K. (2015) Upregulation of galectin-3 in immortalized Schwann cells IFRS1 under diabetic conditions. *Neurosci. Res.*, **92**, 80–85.

Weber, R.A., Breidenbach, W.C., Brown, R.E., Jabaley, M.E. & Mass, D.P. (2000) A randomized prospective study of polyglycolic acid conduits for digital nerve reconstruction in humans. *Plast. Reconstr. Surg.*, **106**, 1036–1045; discussion 1046-1038.

Zhao, Q., Dahlin, L.B., Kanje, M. & Lundborg, G. (1993) Repair of the transected rat sciatic nerve: matrix formation within implanted silicone tubes. *Restor. Neurol. Neuros.*, **5**, 197–204.

Zochodne, D.W., Guo, G.F., Magnowski, B. & Bangash, M. (2007) Regenerative failure of diabetic nerves bridging transection injuries. *Diabetes Metab. Res.*, **23**, 490–496.

© 2015 Federation of European Neuroscience Societies and John Wiley & Sons Ltd

Paper V

Biomaterials 76 (2016) 33–51

Contents lists available at ScienceDirect

Biomaterials

journal homepage: www.elsevier.com/locate/biomaterials

Chitosan-film enhanced chitosan nerve guides for long-distance regeneration of peripheral nerves

Cora Meyer [a, 1], Lena Stenberg [b, 1], Francisco Gonzalez-Perez [c, 1], Sandra Wrobel [a], Giulia Ronchi [e], Esther Udina [c], Seigo Suganuma [d], Stefano Geuna [e], Xavier Navarro [c], Lars B. Dahlin [b], Claudia Grothe [a, *, 2], Kirsten Haastert-Talini [a, 2]

[a] Institute of Neuroanatomy, Hannover Medical School, Hannover, Germany and Center for Systems Neuroscience (ZSN), Hannover, Germany
[b] Department of Translational Medicine – Hand Surgery, Lund University, Skåne University Hospital, Malmö, Sweden
[c] Department of Cell Biology, Physiology, and Immunology, Institute of Neurosciences, Universitat Autonoma de Barcelona and CIBERNED, Bellaterra, Spain
[d] Department of Orthopaedic Surgery, Kanazawa University Hospital, Kanazawa, Japan
[e] Department of Clinical and Biological Sciences, and Cavalieri Ottolenghi Neuroscience Institute, University of Turin, Turin, Italy

ARTICLE INFO

Article history:
Received 27 August 2015
Received in revised form
13 October 2015
Accepted 18 October 2015
Available online 21 October 2015

Keywords:
Chitosan film
Chitosan nerve guide
Regenerative matrix
Functional recovery
Nerve morphometry
Diabetic condition

ABSTRACT

Biosynthetic nerve grafts are developed in order to complement or replace autologous nerve grafts for peripheral nerve reconstruction. Artificial nerve guides currently approved for clinical use are not widely applied in reconstructive surgery as they still have limitations especially when it comes to critical distance repair. Here we report a comprehensive analysis of fine-tuned chitosan nerve guides (CNGs) enhanced by introduction of a longitudinal chitosan film to reconstruct critical length 15 mm sciatic nerve defects in adult healthy Wistar or diabetic Goto-Kakizaki rats. Short and long term investigations demonstrated that the CNGs enhanced by the guiding structure of the introduced chitosan film significantly improved functional and morphological results of nerve regeneration in comparison to simple hollow CNGs. Importantly, this was detectable both in healthy and in diabetic rats (short term) and the regeneration outcome almost reached the outcome after autologous nerve grafting (long term). Hollow CNGs provide properties likely leading to a wider clinical acceptance than other artificial nerve guides and their performance can be increased by simple introduction of a chitosan film with the same advantageous properties. Therefore, the chitosan film enhanced CNGs represent a new generation medical device for peripheral nerve reconstruction.

© 2015 The Authors. Published by Elsevier Ltd. This is an open access article under the CC BY-NC-ND license (http://creativecommons.org/licenses/by-nc-nd/4.0/).

1. Introduction

Treatment of peripheral nerve transection and laceration injuries represents a major challenge in reconstructive surgery and regenerative medicine. Although peripheral nerves are featured with the intrinsic capacity to regenerate, the degree of functional recovery depends on a number of factors, such as the patient's age and general condition, the type of nerve, the delay between the accident causing the injury and the time of surgery, the skills of the surgeon as well as on the location and length of the nerve injury. Small defects (<2 cm) between the separated nerve ends in humans can be bridged by a number of marketed bioartificial hollow conduits of various origins or by processed human peripheral nerve tissue from donors [1]. Treatment of larger defects, however, is still a field of intensive research with the autologous nerve graft treatment representing the clinical gold standard [2,3]. For the latter, the grafts are harvested from less important sensory nerves. Regeneration and functional recovery across defects of >3 cm in length, however, are often incomplete due to differences in nerve architecture (e.g. size of endoneurial tubes) and mismatch in Schwann cell phenotypes (sensory vs motor nerve peripheral glia cells) [4].

* Corresponding author. Institute of Neuroanatomy, Hannover Medical School, Carl-Neuberg-Str.1, 30625, Hannover, Germany.
E-mail address: Grothe.Claudia@mh-hannover.de (C. Grothe).

[1] Cora Meyer, Lena Stenberg, and Francisco Gonzalez-Perez share first authorship as they performed substantial parts of either study III, study II, and study I. They analyzed the data. CM collected and arranged the data for the first draft of the manuscript.

[2] Kirsten Haastert-Talini and Claudia Grothe share senior authorship. KHT coordinated the experiments, outlined the manuscript and wrote its final version. CG initiated the experiments, contributed to the study concept and to drafting of the final manuscript.

http://dx.doi.org/10.1016/j.biomaterials.2015.10.040
0142-9612/© 2015 The Authors. Published by Elsevier Ltd. This is an open access article under the CC BY-NC-ND license (http://creativecommons.org/licenses/by-nc-nd/4.0/).

Furthermore, this type of treatment has several disadvantages, including donor site morbidity, need of additional surgery and limited number of available grafts [3,5]. Another condition that can limit the outcome of any chosen reconstructive therapy for injured peripheral nerves is generalized peripheral neuropathy, such as that occurring in diabetes [6]. The number of patients with diabetes is increasing globally and any innovative technique for peripheral nerve repair and reconstruction needs to be evaluated not only for the use in subjects with healthy general conditions, but also for those with diabetes [6,7]. Current research and development attempts aim therefore to overcome the present obstacles that prevent a widespread use of bioartificial nerve guides, to significantly increase the length limit that can currently be successfully bridged with them (max 2.5 cm) [8], and to significantly improve the achievable level of functional recovery both in generally healthy and diabetic subjects suffering from traumatic nerve injuries. The usually accepted maximal defect length for nerve guide repair in the clinic is 2.5 cm because the surgeon needs to ensure that regeneration will occur also without the use of autologous nerve transplantation. The clinical use of nerve guides, however, depends also on the type of nerve that has to be reconstructed, e.g., small digital nerves or the larger median or ulnar nerves [9–11]. To overcome the critical gap lengths, many different attempts have been evaluated experimentally also in larger animal models like Beagle dogs with a defect lengths of 3–6 cm [12–14].

We have previously demonstrated that hollow nerve guides produced from a fine-tuned form of the natural biopolymer chitosan are as effective in peripheral nerve repair as autologous nerve grafts when bridging 10 mm sciatic nerve gaps in rat experimental models [15–17]. These nerve guides did further qualify for functional repair of critical length, 15 mm, sciatic nerve defects in a considerably high percentage of the evaluated rats [18]. In order to further increase the regeneration outcome, the chitosan nerve guides have been filled with a neural and vascular regenerative hydrogel (NVR-Gel) in a non-modified form or additionally enriched with primary, naïve or genetically modified Schwann cells overexpressing selected neurotrophic factors. Although supporting neurite outgrowth in vitro, the NVR-Gel did not provide a growth-permissive environment in vivo, but rather impaired the regeneration process across a 15 mm critical defect. Supplementation of fibroblast growth factor 2 (FGF-2) overexpressing Schwann cells was able to partially overcome this obstacle [19].

The aim of the present study was to apply a simpler intraluminal modification to the chitosan nerve guides in order to increase the success of axonal regeneration and enhance functional recovery across the critical defect length of 15 mm in rat sciatic nerves in healthy and diabetic rats; the latter with moderate and clinically relevant blood glucose levels and with a profile resembling type 2 diabetes [6]. We enhanced the chitosan nerve guides by introducing a longitudinal film made out of the same fine-tuned chitosan. That a longitudinal guidance structure can increase peripheral nerve regeneration has earlier been demonstrated [20]. The chitosan film that we used for the purpose of chitosan tube enhancement has previously demonstrated to be a suitable biomaterial for Schwann cell attachment and support of sensory dorsal root ganglion neurite outgrowth in vitro [21].

The potential of chitosan film enhanced chitosan nerve guides (CFeCNG) to increase peripheral nerve regeneration was evaluated in three coordinated successive sub-studies. Study I compared the functional and morphological outcome of peripheral nerve regeneration after 15 mm sciatic nerve defect reconstruction with hollow chitosan nerve guides (hCNG) or 1st generation CFeCNG (continuous chitosan films). In the next step the chitosan films were modified by introducing holes allowing exchange between the two compartments of 2nd generation CFeCNG and comprehensive short (Study II) and long-term (Study III) studies were conducted. Study II evaluated the initially formed regenerated matrix within hCNGs or CFeCNGs and the regeneration related processes within the dorsal root ganglia at 56 days after surgery with immunohistochemical methods. These crucial early events of regeneration were additionally addressed regarding the differences between generally healthy and diabetic rats. Study III finally evaluated comprehensively the functional and morphological outcome of peripheral nerve regeneration in experimental groups including implantation of (i) hCNG and (ii) 2nd generation CFeCNG, additionally compared to (iii) autologous nerve grafts (ANGs) and (iv) CFeCNG enriched with FGF-2 overexpressing Schwann cells (SC-FGF-2^{18kDa}). Two very important results were achieved in our comprehensive analyses. First, motor recovery was detectable in significantly more animals in CFeCNG groups than in hCNG groups and the 2nd generation CFeCNG group demonstrated a significantly better outcome in this respect than the 1st generation CFeCNG group. While in the ANG group 100% of the animals demonstrated reinnervation of proximal as well as distal target muscles this was reached in the remarkable amount of 86% and 67% of the CFeCNG^{2nd} group. Second, and similarly important, 2nd generation CFeCNGs supported the early regenerative process more than hCNGs and this was particularly relevant in diabetic rats.

2. Materials and methods

2.1. Manufacturing of chitosan film enhanced chitosan nerve guides (CFeCNG)

Pandalus borealis shrimp shells served as a source for certified medical grade chitosan (Altakitin S.A., Lisboa, Portugal). Hollow chitosan nerve guides (hCNG) with an inner diameter of 2.1 mm and a length of 19 mm as well as chitosan films (CF) were manufactured as described before (Chitosan degree of acetylation ~ 5%; [15,21]) at Medovent GmbH (Mainz, Germany). ISO 13485 requirements and specifications were applied for all production steps.

The CFs were cut into a rectangular shape of 15 mm length and 5 mm width. To allow insertion into the conduits, CFs were folded into a Z-form along their longitudinal axis resulting in kinked edges of 1.5 mm width pointing into opposite directions (Fig. 1A). Before being sterilized by electron beam, these films were placed in the center of chitosan nerve guides leaving 2 mm on each side for nerve end insertion and suturing (Fig. 1B, 1st generation of CFeCNG). For production of 2nd generation CFeCNGs (Fig. 1C–D), six holes were introduced along the middle line of the CFs at a distance of 2 mm between each other by using a sharp needle (0.30 × 12 mm). Introduction of the holes was performed in an alternating manner from both sides to provide similar surface properties at the two compartments of the CFeCNG.

2.2. Experimental design

Table 1 summarizes the three coordinated successive sub-studies performed and provides an overview regarding the respective experimental groups as well as accomplished analyses after 15 mm rat sciatic nerve defect reconstruction. Study I was conducted at the Universitat Autònoma de Barcelona (UAB, Spain) and included two reconstruction conditions: basic hCNGs (group hCNG-I) or 1st generation CFeCNGs (group CFeCNG^{1st}). The observation period was 122 days in which functional recovery was periodically assessed. Study II was executed at University of Lund (ULUND, Sweden) and included two reconstruction conditions in generally healthy or diabetic Goto-Kakizaki rats [6]: basic hCNGs or 2nd generation CFeCNGs (groups: hCNG-II^{healthy}, hCNG-II^{diabetic};

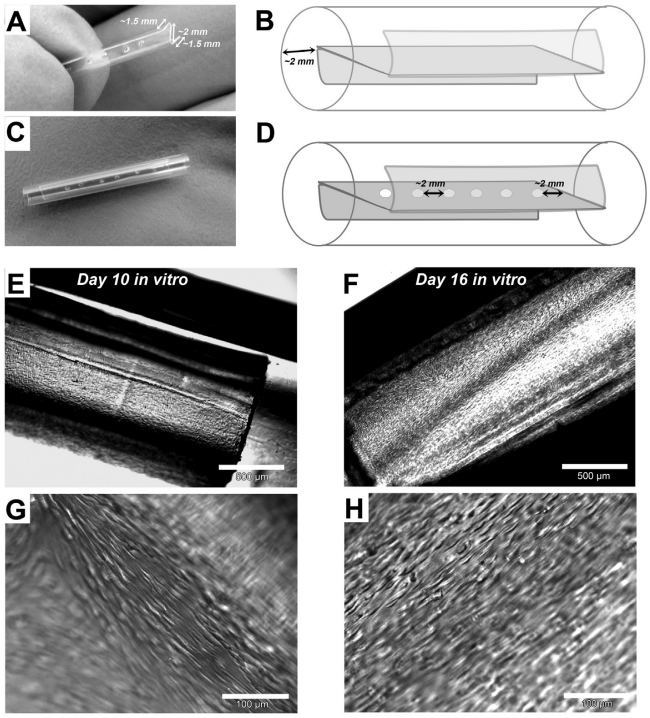

Fig. 1. Preparation of the different types of nerve guides used. (A) Chitosan films were cut into rectangular shape (length: 15 mm, width: 5 mm) and manually folded into a Z-form. (B–D) Film placement within basic chitosan conduits (length: 19 mm, inner diameter: 2.1 mm) left about 2 mm space at both ends to allow nerve end insertion and suturing. (B) 1st generation chitosan film enhanced chitosan nerve guide (CFeCNG) as used in study I. (C–D) 2nd generation CFeCNGs as used in study II and study III with six holes 2 mm distant from each other. (E–F) Representative photomicrographs taken from CFeCNG^{2nd} seeded with neonatal rat Schwann cells. Top views on a nerve guide after 10 days in vitro (E) or after 16 days in vitro (F). (G–H) Detail of the Schwann cell seeded chitosan films within the nerve guides illustrating the fish-swarm like growth of the Schwann cells on both surfaces of the films after 10 days in vitro (G) or 16 days in vitro (H).

CFeCNG$^{2nd\text{-}healthy}$; CFeCNG$^{2nd\text{-}diabetic}$). The observation period, based on pilot experiments, was 56 days in order to assess the formed regenerative matrix, axonal outgrowth, Schwann cell activation and apoptosis, as well as activation and neuroprotection of sensory dorsal root ganglion neurons with immunohistological techniques. Study III was performed at Hannover Medical School (MHH, Germany) and included four reconstruction conditions: autologous nerve grafts (group ANG), basic hCNGs (group hCNG-III), 2nd generation CFeCNGs (group CFeCNG^{2nd}), and 2nd generation CFeCNGs enriched with FGF-2^{18kDa} overexpressing Schwann cells (SCs) seeded on both sides of the CF (group CFeCNG^{2nd}-SC-FGF-2^{18kDa}). The observation period was 120 days in which functional recovery was periodically assessed. Study I and Study III were completed by endpoint histomorphometrical analysis of axonal regeneration.

2.3. Animals and surgery

The in vivo studies were performed in three different laboratories as stated above with different animal breeders and regimes for anesthesia and analgesia due to different local animal care rules. All animal experiments were approved by the local animal ethical committees (animal ethics committee in Malmö [ULUND, Sweden], Barcelona [UAB, Spain], and Lower-Saxony [MHH, Germany]). In common, female Wistar rats (225–250 g) and Goto-Kakizaki rats (GK-rats: kindly provided by Malin Fex, Lund University; around 250 g) were subjected to the experiments and housed in groups of four animals under standard conditions, with food and water ad libitum (the diabetic GK rats were provided with extra water). Fasting blood sugar was measured once a week in the rats at ULUND from the tail vein (Ascensia contour TM [Bio health Care, USA, Bio Diagnostics Europe] and LT [Bayer AB, Diabetes Care, Solna, Sweden]; test slips Microfil TM [Bio Healthcare Diabetes Care, USA]).

Aseptic conditions, sufficient anesthesia and analgesia were applied for all surgical procedures and postoperative analgesia was ensured by appropriate drug application. Animals were prepared and underwent surgery as described before [15,18]. Briefly, following exposure at midthigh level, the left sciatic nerve was transected by a single microscissor cut at a constant point (6 mm distal to its exit from the gluteus muscle) and a 6 mm segment removed from the distal nerve end in study I. In studies II and III

Table 1
Overview of the experimental design of the three coordinated successive sub-studies.

	Observation time	Experimental groups	N	Group name	Performed experiments
Study I (UAB)	120 days	Hollow chitosan nerve guide 1st generation chitosan film enhanced chitosan nerve guide	10 7	hCNG-I $CFeCNG^{1st}$	*Motor recovery:* electrophysiology non-invasive (60, 90, 120 days); *Sensory recovery:* von Frey algesimetry (7, 60, 90, 120 days); *Histomorphometry*
Study II (ULUND)	56 days	Healthy rats: Hollow chitosan nerve guide Diabetic GK rats: Hollow chitosan nerve guide Healthy rats: 2nd generation chitosan film enhanced chitosan nerve guide Diabetic GK rats: 2nd generation chitosan film enhanced chitosan nerve guide	8 8 8 8	$hCNG\text{-}II^{healthy}$ $hCNG\text{-}II^{diabetic}$ $CFeCNG^{2nd\text{-}healthy}$ $CFeCNG^{2nd\text{-}diabetic}$	*Analysis of regenerative matrix*: presence of axons and activated and apoptotic Schwann cells by immunhohistochemistry; *Analysis of sensory dorsal root ganglion activation* by immunohistochemistry
Study III (MHH)	120 days	Autologous nerve graft Hollow chitosan nerve guide 2nd generation chitosan film enhanced chitosan nerve guide 2nd generation chitosan film enhanced chitosan nerve guide with FGF-2 overexpressing Schwann cells	8 8 8 8	ANG hCNG-III $CFeCNG^{2nd}$ $CFeCNG^{2nd}\text{-}SC\text{-}FGF\text{-}2^{18kDa}$	*Motor recovery:* electrophysiology non-invasive (60, 90 days) and finally invasive (120 days) and Muscle weight ratio; *Sensory recovery:* von Frey algesimetry (7, 60, 90, 120 days); *Histomorphometry; Immunohistochemistry*

only a 5 mm segment was removed providing an increased length of the distal nerve end. For nerve reconstruction using the different types of chitosan nerve guides, the liquid-soaked guides (>30 min in 0.9% NaCl solution or Schwann cell medium) had a length of 19 mm and bridged a 15 mm defect between the two nerve ends. The nerve guides were sutured with one epineurial stitch at each end (9–0, EH7981G, Ethilon, Ethicon, Scotland). For transplantation of reversed autologous nerve grafts (ANGs) no nerve tissue was removed, but the distal nerve end again transected 15 mm distal to the first transection point, flipped (proximal-distal direction) and turned 180° around its longitudinal axis before three epineurial sutures were placed with a spacing of 120° from each other.

2.4. Preparation of FGF-2 overexpressing Schwann cells for enrichment of CFeCNGs

Neonatal rat Schwann cells (neoSC) were obtained, cultured and genetically modified as described before [19,21]. Briefly, sciatic nerves were harvested from Hannover Wistar rat pups (p1-3) and neoSC isolated and purified by immunopanning until >90% pure neoSCs cultures were achieved.

Three days prior to transplantation, neoSCs (passage 8–9) were genetically modified using the nucleofection technique (Basic glial cell nucleofection kit and program T-20 of AMAXA II device, LONZA, Cologne, Germany) to introduce the non-viral plasmid encoding for $FGF\text{-}2^{18kDa}$ (pCAGGS-FGF-2-18 kDa-Flag, NCBI GenBank accession NM_019305.2, 533–994 bp) as described before [19]. Afterwards, cells were cultured for 24 h on poly-L-lysine-coated 6 well-plates (Sigma–Aldrich, Munich, Germany) with neoSC-specific culture medium (DMEM, 1% Penicillin/streptomycin, 2 mM L-glutamine, 1 mM sodium pyruvate and 10% fetal calf serum [all PAA Laboratories, Coelbe, Germany]) to recover from transfection. On the following day, the genetically modified neoSCs were seeded on the central part of CFs within 2nd generation CFeCNGs ($CFeCNG^{2nd}\text{-}SC\text{-}FGF\text{-}2^{18kDa}$). Therefore, 5×10^5 cells were suspended in a volume of 30 µl culture medium and 15 µl applied on both sides of the CF. After 30 min to allow cell adhesion, the scaffolds were covered with culture medium to avoid drying of the nerve guides and incubated at 37 °C in humidified atmosphere with 5% (v/v) CO_2 for another 24 h. On the next day, the medium was changed to serum free-N2 medium and the cell-seeded nerve guides were again incubated overnight in preparation for surgery.

5×10^4 cells were seeded into 24-well plates for analyses of cell purity and transfection efficiency in corresponding sister cultures after immunostaining with SC specific α-S100 antibody 1:200 (Dako, Denmark) in phosphate buffered salt solution (PBS)/0.3% Triton-X-100/5% BSA solution or anti-Flag antibody 1:200 (all Sigma–Aldrich, Germany) and Alexa 488-labelled goat α-rabbit secondary (Invitrogen, Germany) antibody or Alexa-555-labelled goat α-mouse IgG secondary antibody 1:500 (Invitrogen, Germany), respectively [19]. All cell nuclei were counterstained with DAPI (1:1000 in PBS, Sigma–Aldrich, Germany). The transplanted cells had a purity of 90.2% S100-+ SCs and 90.1% of the cells were Flag-+ after nucleofection.

In order to proof that the neoSCs successfully adhered to the chitosan surfaces and populated the CFs within the nerve guides, sample $CFeCNG^{2nd}$ were seeded with 5×10^5 neoSCs and kept in culture for up to 16 days. Fig. 1E–F shows representative photomicrographs taken at day 10 and day 16 in vitro, which clearly demonstrate that the cells densely populated both surfaces of the CF in the SC-typical fish-swarm like manner.

2.5. Assessment of the regenerative matrix at day 56 after surgery (study II)

At 56 days after surgery a regenerative matrix, sufficient for immunohistochemical analyses, was formed in the 15 mm long nerve defect within the nerve guides. The contents of the conduits together with the respective proximal and distal nerve ends were harvested as described before [6,15,17]. Briefly, the tube content was processed for sectioning using a cryostat and longitudinal sections at 4 µm thickness were collected on Super Frost® plus glass slides (Menzel-Gläser, Germany). On these sections, immunohistochemistry was performed to evaluate (1) presence of axons by neurofilament staining (anti-human neurofilament protein, 70 kDa NF-L [DAKO Glostrup, Denmark], 1:80 in 0.25% Triton-X 100 and 0.25% FCS in phosphate buffered salt solution [PBS]/Alexa Fluor 594 conjugated goat anti-mouse IgG [Invitrogen, Molecular Probes,

USA], diluted in 1:500 in PBS), and (2) activated Schwann cells and apoptotic Schwann cells, respectively, by anti-activating transcription factor 3 (ATF3) and anti-cleaved caspase 3 staining (rabbit anti-ATF-3 polyclonal antibody [1:200; Santa Cruz Biotechnology, USA] or anti-cleaved caspase-3 antibody [1:200; *Invitro* Sweden AB, Stockholm, Sweden]; both diluted in 0.25% Triton-X 100 and 0.25% FCS in PBS/Alexa Fluor 488 conjugated goat anti-rabbit IgG [Invitrogen, Molecular Probes, USA], diluted in 1:500 in PBS). The Schwann cells were identified on their location and the oval shaped nuclei [6,22]. Furthermore, double staining for ATF3 or cleaved caspase 3 and S-100 was additionally performed as earlier described and mounted in Vectashield® (Vector Laboratories, Inc. Burlingame, USA) [17,22]. Finally, the slides were mounted with 4′,6′-diamino-2-phenylindole DAPI to visualize the nuclei (i.e. for counting the total number of the cells) and cover slipped.

For analysis, as earlier described [6,15,17], blind-coded sections were digitized and the presence of outgrowing axons in the formed matrix inside the conduits was evaluated (i.e. present or non-present) in three randomly selected sections at two different locations: in the center of the formed matrix as well as in the distal nerve segment just distal to the distal suture line. The stained cells for cleaved caspase-3 and ATF-3 were also counted in three sections (image size 500 × 400 μm; mean of the three sections calculated for each rat) at two different levels in the matrix and in the adjacent sciatic nerve: at 3 mm distal to the proximal nerve suture, in the center of the formed matrix in the nerve guides and in the distal segment (see above). The same squares were also used for counting the total number of DAPI stained cells (no/mm^2). The images (20× magnification) were analyzed with NIS elements (Nikon, Japan).

2.6. Assessment of sensory dorsal root ganglia at day 56 after surgery (study II)

At the same time as the content of the nerve guides was harvested, the dorsal root ganglia (DRG) L4 and L5 were collected bilaterally and processed for cryostat sectioning. Longitudinal sections (8 μm thickness) were collected on Super Frost® plus glass slides (Menzel-Gläser, Germany) for evaluation of cell activation (i.e. ATF3) and presence of the neuroprotective substance Heat Shock Protein 27 (HSP27; [6,23]). The DRG sections were air dried, washed in PBS for 15 min, and thereafter incubated for ATF-3 immunohistochemistry as described above or incubated with a primary goat-anti-HSP27 antibody [sc-1048, Santa Cruiz Biotechnology, USA; dilution 1:200 in 0.25% Triton-X-100 (Sigma–Aldrich, USA) and 0.25% bovine serum albumin (BSA; Sigma–Aldrich, USA) in PBS overnight at 4 °C. The anti-HSP27 antibody was detected with the secondary Alexa flour 488 donkey anti-goat antibody (Molecular Probes, Eugene, Oregon, USA; dilution 1:500) in PBS for 2 h at room temperature followed by a further wash with PBS for 3 × 5 min. Finally, theses sections were cover-slipped with Vectashield® (Vector Laboratories, CA, USA) containing DAPI for counterstaining of the nuclei. Three sections from each DRG were analyzed for ATF3 and HSP27 staining, respectively, and mean values were calculated from each rat.

To analyze the presence of ATF3 activated sensory neurons and the expression of HSP27 in the DRGs, images were captured at 10× magnification with the same equipment and processed as above followed by import into Image J. ATF3 stained sensory neurons were quantified as described [24] and expressed as percent of total number of sensory neurons (i.e. DAPI stained cells). A region of interest (ROI) covering 75x75 pixels was determined to analyze HSP27 expression. The tool threshold was used to determine the immunolabelling with the intensity threshold decided by adding three times the standard deviation of the background to the mean intensity ($\bar{x} + 3 \times SD$). Measurement of the immunostained area was performed across the entire section and expressed in percent of the total area of the section; thus, both intensity of neurons and their satellite cells were included. Furthermore, the HSP27 expression was also expressed as a ratio; i.e. percent HSP27 at the experimental side divided by the expression on the control side.

2.7. Assessment of functional motor and sensory recovery

2.7.1. Motor recovery: electrophysiological tests

The tests were performed according to previous description [15,18]. Briefly, the animals were anesthetized and monopolar needle stimulation electrodes were transcutaneously placed at the sciatic notch. Single electrical impulses (100 μs duration, supramaximal intensity) were applied and the compound muscle action potentials (CMAPs) were recorded from the tibialis anterior muscle (TA) and the plantar interosseus muscles (PL). The active recording electrode was located in the respective muscle belly, the reference electrode in the second or fourth toe and the ground needle electrode was inserted in the skin at the knee. To ensure a steady body temperature the animals were placed in a prone position on a thermostatic blanket. For invasive recordings (final examination in study III), the sciatic nerves were exposed consecutively on the lesioned and non-lesioned side and stimulated proximal to the lesion site using a bipolar steel hook electrode (single electrical pulses, 100 μs duration, supramaximal, but not exceeding 8 mA). Recording sites remained as described above. The CMAPs were recorded and displayed in an EMG apparatus (Sapphyre 4ME, Vickers Healthcare Co, United Kingdom, at UAB (study I) or Keypoint Portable, Medtronic Functional Diagnostics A/S, Denmark, at MHH (study III)).

Evaluation parameters included the latency of the arriving signals and the amplitude ratio (amplitude [mV] recorded from lesioned side divided by non-lesioned side values). For latency evaluation all values obtained from animals showing distal muscle reinnervation were taken into account for statistical tests. If no evoked CMAP was detected a 0.00 value was noted and included for statistical analysis in case of the amplitude ratio.

2.7.2. Sensory recovery: mechanical pain threshold assessment (von Frey algesimetry)

Sensory recovery was determined via von Frey test as previously described [18,19,25]. In brief, animals were placed into plastic compartments located on a metallic mesh grid 15–30 min before starting the experimental session for habituation. Then, the probe of a von Frey algesimeter (UAB (study I): Bioseb, Chaville, France; MHH (study III): IITC Inc, Life Science, USA) was applied for stimulation of the lateral paw area innervated by the tibial and sural nerve branches of the sciatic nerve. The stimulation force required to elicit a withdrawal response from the animals was noted in grams [g] and three measurements per stimulation site were used to determine a mean value. A cut-off force was set to 40 g, when either no withdrawal was observed or no active response occurred. To minimize variations between days, the values are stated in % compared to data obtained from the non-lesioned, healthy side calculated by the following formula: lesioned side [g]/non-lesioned side [g] *100.

In Study I the test was performed 7 days, 21 days, 30 days, 60 days, 90 days, and 120 days after nerve guide implantation. Subsequently, the saphenous nerve was cut and the test was conducted once more on day 122. In Study III the test was performed 7 days, 60 days, 90 days, and 120 days after nerve reconstruction.

For statistical analysis all measured values were used and in case of no response the cut-off force was included. In the course of Study I successful recordings from the PL muscle positively correlated with withdrawal responses seen in von Frey test only after deletion

of the saphenous nerve function on day 122. This additional surgery was avoided in Study III and only values obtained from animals showing PL CMAPs were used for final calculation of sensory recovery level, while cut-off forces (40 g) were included for animals that did not show CMAP.

2.8. Nerve immunohistochemistry and morphometry

2.8.1. Nerve immunohistochemistry

After completion of the final functional tests, animals were sacrificed and the regenerated nerve tissues with the surrounding chitosan nerve guides were harvested for further analysis. In study I the complete nerve guide was removed from the regenerated nerve tissue and the macroscopic appearance assessed. In study III, the entire samples (nerve tissue together with nerve guides) were fixed in 4% PFA overnight (4 °C) for subsequent paraffin-embedding and (immuno-) histological analysis. Serial 7 μm sections were obtained (two series of 20 blind-coded sections each, one in the region without CF and one with CF, each covering a distance of about 630 μm). Sample sections were processed for hematoxylin eosin (HE) and trichrome (collagen) staining in order to visualize the tissue within the nerve guides. For the trichrome-staining, sections were subjected to hematoxylin (Roth, Germany), before being washed-offed under tap water. Afterwards the slides were incubated in 20 ml staining solution containing acetic acid (1 ml in 99 mlH_2O, Merck, Germany) and acetic fuchsin (0.5 g, in 100 ml 1% acetic acid, Merck, Germany) mixed with 10 ml light green (1 g in 100 ml 1% acetic acid, Chroma Gesellschaft, Schmidt & Co., Germany) and 10 ml wolframate phosphoric acid (1 g in 100 ml H_2O, Merck, Germany). Following a washing step in distilled water, the slides were subjected to 1% acetic acid, before being pressed with filter paper, dehydrated, and mounted with corbit-balsam (Hecht, Germany).

Immunohistology was performed on sections consecutive to the ones processed for HE or trichrome staining by double-staining for neurofilament and choline acetyltransferase (ChAT). Therefore, the sections were incubated in 5% horse serum in PBS for blocking before incubation with primary goat α-ChAT antibody (1:50, in blocking solution, AB144P, Millipore, Germany) at 4 °C overnight. Following three washing steps in PBS, incubation with Alexa 555-conjugated secondary donkey α-goat antibody (1:500, in blocking solution, A21422, Invitrogen, Germany) for 1 h at RT was performed and succeeded by another washing round. After a second blocking step (3% milk powder/0.5% triton X-100 in PBS) overnight incubation with primary rabbit α-NF200 antibody (against phosphorylated NF–H, 1:500, in blocking solution, N4142, Sigma–Aldrich, Germany) was conducted. Three washing steps followed, before incubation with Alexa 488-conjugated secondary goat α-rabbit antibody (1:1000, in blocking solution, A11034, Invitrogen, Germany) for 1 h at RT and counterstaining with DAPI (1:2000, in PBS, Sigma–Aldrich, Germany) was performed. Finally, sections were mounted using Mowiol (Calbiochem, Germany).

For qualitative analysis, representative photomicrographs of HE and trichrome stained sections were taken with the help of BX53 and BX51 microscopes and the programs CellSense Dimension and CellSense Entry (all Olympus, Germany). Immunohistochemistry images were digitized with the help of a fluorescence microscope (BX60, Olympus, Germany) and cellP software (Olympus, Germany).

2.8.2. Nerve morphometry

Together with the harvest of the regenerated nerve tissue and nerve conduits for nerve histology, distal nerve segments (5 mm segments from distal nerve guide end into distal direction) were harvested and processed as described before [15,18]. In short, the tissue was subjected to an initial fixation based on glutaraldehyde containing fixatives and post-fixed in 1% OsO_4. Following dehydration samples were processed for epoxy resin embedding and semi-thin (2.5 μm) transverse sections were cut in proximal direction using an Ultracut UCT ultramicrotome (Leica Microsystems, Germany) and stained with toluidine blue. Finally, total myelinated fiber number, cross sectional area, nerve fiber density, axon diameter, fiber diameter, g-ratio, and myelin thickness were determined for all experimental groups of study I and study III in addition to values obtained from healthy control samples. All histomorphometry was performed at the University of Turin (UNITO, Italy) with the help of systematic random sampling as described before [15].

2.9. Muscle weight ratio

Upon harvest of the nerve tissue samples also the tibialis anterior and gastrocnemius muscles were explanted from study III animals. The fresh muscle weight from the ipsilateral lesioned side was then compared to the weight measured from contralateral healthy muscles to calculate the muscle weight ratio ([g] ipsilateral/[g] contralateral). The ratios from all animals were included into statistical analysis irrespectively of the electrodiagnostic or macroscopic outcome of the nerve regeneration process.

2.10. Statistics

The data obtained in the different experimental settings were subjected to statistical analysis using Kruskal–Wallis test or two-way ANOVA (Analysis of Variance) followed by Dunn's or Tukey's multiple comparison test or by Mann–Whitney U-test (with subsequent Fisher's test; [6]) as specifically indicated in the results section. Differences concerning expression of HSP27 in DRGs on the control and experimental sides were examined with the Wilcoxon signed rank test. The proportion of animals per group that displayed a predefined qualitative parameter (evoked CMAP) was calculated as percentage (0–100%) and analyzed with the Chi-Square-Test. The p-value was set at < 0.05 as level of significance. For statistical analysis either the statistical package SPSS (version 17.0 or 20.0, IBM, USA) or GraphPad InStat software, version 5.0.3.0 & 6.00 (Graphpad Software, CA, USA) were used.

3. Results

In the first part of the results section long term study results obtained from Study I and Study III will be presented. In both studies, examination of motor and sensory functional recovery and histo-morphometry were performed over a period of 120 days after reconstruction of 15 mm rat sciatic nerve defects. In the second part of the results section short term results obtained from Study II will be presented. Here, the regenerative matrix formed after nerve guide grafting and the activation of sensory DRG neurons were immunohistologically analyzed 56 days after reconstruction of 15 mm rat sciatic nerve defects in healthy and diabetic rats. Diabetic Goto-Kakizaki rats could not be subjected to long-term studies because of their expected limited life-span and ethical approval.

3.1. Long term evaluation of the effects of different reconstruction approaches on functional recovery and axonal regeneration

The long term evaluations were performed to elucidate the potential of chitosan film enhanced chitosan nerve guides of the first ($CFeCNG^{1st}$, continuous chitosan film, study I) and second ($CFeCNG^{2nd}$, chitosan film with holes, study III) generation to support peripheral nerve regeneration across critical length defects. In an additional experimental group, $CFeCNG^{2nd}$ were enriched with

FGF-2^{18kDa} overexpressing Schwann cells (CFeCNG^{2nd}-SC-FGF-2^{18kDa}). Control animals received either nerve reconstruction with hollow chitosan nerve guides (hCNG-I or hCNG-III, respectively) or with autologous nerve grafts (ANG).

3.1.1. Electrophysiological assessment

The qualitative results are summarized in Table 2. Non-invasive electrophysiological recordings did not detect evoked CMAPs before day 60 after nerve repair.

At this time point, regenerating fibers had reached the TA muscle in 3 out of 10 hCNG-I animals and in 2 out of 7 CFeCNG^{1st} animals in study I. At the same examination time point in study III, reinnervation of the TA muscle did already occur in 7 out of 8 ANG animals and in none of the other experimental groups. Recordings from the more distal PL muscle in study I also detected reinnervation in the same 3 hCNG-I animals but only in one of the TA-positive CFeCNG^{1st} animals. In study III, PL muscle reinnervation was already detectable in 7 out of 7 examinable ANG animals (one drop out due to events of autotomy), but not in the other groups.

Upon the next examination at day 90 after nerve reconstruction, additional 1 or 2 animals, respectively, displayed reinnervation of the TA muscle in study I (Table 2), increasing the percentage of animals with muscle reinnervation to 40% in hCNG-I group and 57% in CFeCNG^{1st} group. In study III (Table 2), 100% of ANG animals displayed TA muscle reinnervation and a gain of motor function was detectable in hCNG-II animals while CFeCNG^{2nd} caught up with the CFeCNG^{1st} animals. In contrast, the number of animals with detectable reinnervation of PL muscles did not increase in study I in the hCNG-I group, but a higher percentage of animals demonstrated motor recovery in the CFeCNG^{1st} group. In study III, PL muscle reinnervation was started in nerve guide repaired groups, displaying a slightly better result in the CFeCNG^{2nd} group than in the hCNG-III group.

At the final examination 120 days after nerve reconstruction (Table 2), TA and PL CMAPs increased in amplitude but muscle reinnervation was not found in further animals in study I. In contrast, TA muscle reinnervation was detected, in final invasive testing, in an increased number of study III animals of the CFeCNG^{2nd} as well as the CFeCNG^{2nd}-SC-FGF-2^{18kDa} group. Reinnervation of PL muscle was detectable in one additional animal of the CFeCNG^{2nd} group.

When comparing the performance of CFeCNG^{1st} and CFeCNG^{2nd}, while at 60 days after nerve repair CFeCNG^{1st} performed better than CFeCNG^{2nd}, at 120 days CFeCNG^{2nd} supported functional motor recovery in a higher percentage of animals. Additional enrichment of the CFeCNG^{2nd} with FGF-2^{18kDa} overexpressing Schwann cells did not allow for the level of distal target reinnervation displayed in the hCNG and CFeCNG groups.

Quantitative results were calculated for the latencies and amplitude ratios of the recorded CMAPs at day 120 after nerve reconstruction and no significant differences between the groups were detected in study I (non-invasive measurements, mean ± SEM): TA muscle latency hCNG-I = 4.50 ± 0.82 ms; CFeCNG^{1st} = 4.05 ± 0.17 ms; TA muscle amplitude ratio hCNG-I = 16.52 ± 8.10%; CFeCNG^{1st} = 24.80 ± 10.41%; PL muscle latency hCNG-I = 5.19 ± 0.16 ms; CFeCNG^{1st} = 5.43 ± 0.36 ms; PL muscle amplitude ratio hCNG-I = 12.86 ± 7.87%; CFeCNG^{1st} = 7.75 ± 4.55%. Fig. 2 summarizes the quantitative results obtained from study III at day 120 after nerve reconstruction (invasive measurements). Latencies (Fig. 2A) were significantly increased in comparison to healthy nerve values in the CFeCNG^{2nd} and CFeCNG^{2nd}-SC-FGF-2^{18kDa} groups when CAMPs were recorded from the TA muscle. This was also the case for all groups, including ANG and hCNG-III, when CAMPs were recorded from the PL muscle. TA CMAP amplitude ratios (Fig. 2B) were decreased in comparison to ANG values in all nerve guide groups but this difference was significant only for the hCNG-III and the CFeCNG^{2nd}-SC-FGF-2^{18kDa} groups. Due to high variance, PL CMAP amplitude ratios were significantly lower in comparison to ANG values only in the CFeCNG^{2nd}-SC-FGF-2^{18kDa} group (Fig. 2B). These quantitative results indicate that not only muscle reinnervation in general but also the amount of recruited regenerated fibers in the CFeCNG^{2nd} group approximated that in the ANG group.

3.1.2. Muscle weight ratio

As an additional indicator for motor recovery, the hindlimb TA and gastrocnemius (GA) muscles wet weight ratios were determined in study III. As depicted in Fig. 2C, statistical analysis revealed again that CFeCNG^{2nd} and ANG group values were not significantly different from each other, although ANG group had the highest ratios. Significantly lower muscle weight ratios compared to ANG group values were detected for the TA muscle and the GA muscle in the CFeCNG^{2nd}-SC-FGF-2^{18kDa}group, and for the GA muscle additionally in the hCNG-III group. These results underscore the relatively good performance of the CFeCNG^{2nd} already detected in the electrophysiological tests.

Table 2
Overview of the gain in electrophysiologically detectable motor recovery (evocable compound muscle action potentials) during the observation in sub study I and sub study III. Significant differences ($p < 0.05$) are indicated as follows: + versus ANG,# hCNG-I versus CFeCNG^{1st},§ versus CFeCNG^{2nd}, **$** versus CFeCNG^{2nd}-SC-FGF-2^{18kDa},* CFeCNG^{1st} versus CFeCNG^{2nd}.

		60 days			90 days			120 days		
		Animals/ group	Percentage	Significant difference	Animals/ group	Percentage	Significant difference	Animals/ group	Percentage	Significant difference
Tibialis anterior muscle										
Study I	hCNG-I	3/10	33%	+	4/10	40%	+	4/10	40%	+
	CFeCNG^{1st}	2/7	29%	+	4/7	58%	+#	4/7	58%	+#
Study III	ANG	7/8	88%		8/8	100%		8/8	100%	
	hCNG-III	0/8	0%	+	2/7	29%	+§ **$**	3/7	43%	+§ **$**
	CFeCNG^{2nd}	0/8	0%	+*	4/7	58%	+	6/7	86%	+*
	CFeCNG^{2nd}-SC-FGF-2^{18kDa}	0/8	0%	+	0/8	0%	+§	5/7	71%	+§
Plantar muscle										
Study I	hCNG-I	3/10	33%	+	3/10	33%	+	3/10	33%	+
	CFeCNG^{1st}	1/7	14%	+	3/7	43%	+	3/7	43%	+
Study III	ANG	7/7	100%		7/7	100%		7/7	100%	
	hCNG-III	0/8	0%	+	3/7	43%	+ **$**	3/7	43%	+§ **$**
	CFeCNG^{2nd}	0/7	0%	+*	3/6	50%	+	4/6	67%	+*
	CFeCNG^{2nd}-SC-FGF-2^{18kDa}	0/6	0%	+	1/6	17%	+§	1/6	17%	+§

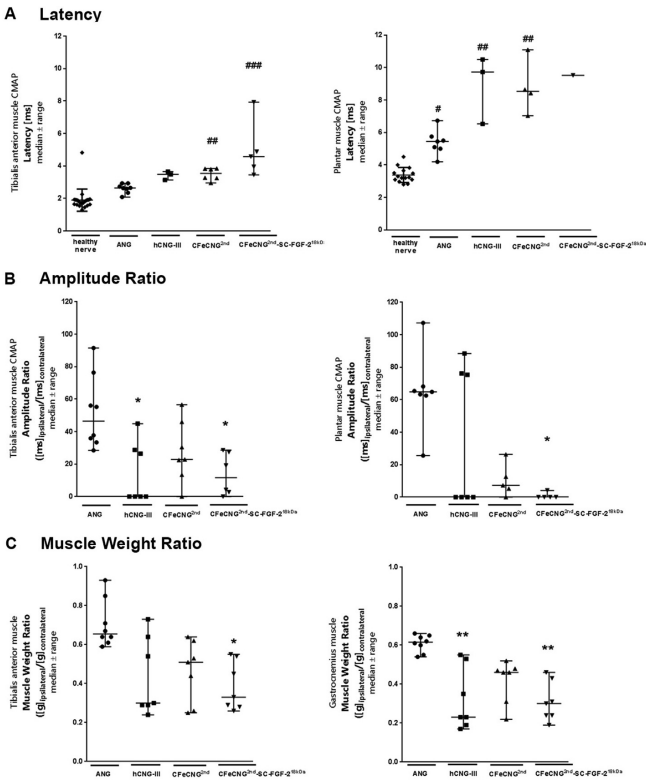

Fig. 2. Dot plot depicting the latency (A) and amplitude ratio (B) of compound muscle action potentials (CMAPs) recorded during final electrophysiological tests performed 120 days after nerve surgery in the tibialis anterior muscle (left column) and plantar muscles (right column). (C) Dot plot depicting tibialis anterior muscle (left column) and gastrocnemius muscle (right column) muscle weight ratios calculated after final electrophysiological measurements. Results were tested for significance ($p < 0.05$) by Kruskal–Wallis test, followed by Dunn's multiple comparison. #$p < 0.05$, ##$p < 0.01$, ###$p < 0.001$ vs healthy control values; *$p < 0.05$, **$p < 0.01$ vs ANG group.

3.1.3. Von Frey algesimetry

The results obtained for evaluation of sensory recovery using the von Frey test are summarized in Fig. 3. The withdrawal response obtained at the healthy contralateral paw was calculated as 100%. From the injured/regenerating paw two types of withdrawal response have been recorded, a response at lower force compared to the contralateral paw (<100%, higher or maladaptive mechanosensitivity than normal) or a response at higher force compared to the contralateral paw (>100%, less mechanosensitivity than normal).

Study I (Fig. 3A) revealed no withdrawal responses within the first 21 days following sciatic nerve transection indicating complete denervation of the animals plantar surface. However, after 30 days, some animals of both groups (hCNG-I and CFeCNG^{1st}) demonstrated a withdrawal of the lesioned paw at lower stimulus intensities than seen for the contralateral, intact side. At 60 days after nerve reconstruction, 7 out of 10 animals from the hCNG-I group and all animals of the CFeCNG^{1st} displayed withdrawal responses at low stimulus intensities. During the next examination at 90 days and 120 days after nerve reconstruction, all animals regardless of the received treatment responded to the stimulation at low stimulation intensities. To exclude false positive responses due to sprouting events from branches of the saphenous nerve [25], this nerve was then cut and the von Frey test conducted once more on day 122. At this time point, 4 out of 10 animals (40%) in the hCNG-I group showed withdrawal responses, resulting in 103 ± 6.57% response compared to contralateral, and 3 out of 7 animals (43%) demonstrated a withdrawal response in the CFeCNG^{1st} group, resulting 117 ± 8.20% response compared to contralateral. These latter results indicate that the withdrawal responses in previous test days were in part due to hypersensitivity caused by collateral spouting of the saphenous nerve and not fully attributable to sciatic nerve regeneration.

Study III (Fig. 3B) also revealed a gain in mechanosensitivitiy over time after nerve reconstruction. At 60 days the following numbers of animals withdrew their paws following lower stimulation intensities than recorded for the contralateral, healthy side: ANG group: 6 out of 7, hCNG-III group: 4 out of 7, CFeCNG^{2nd} group: 3 out of 6, and none in the other groups. In the course of the study, additional animals responded to the stimulation. To avoid an

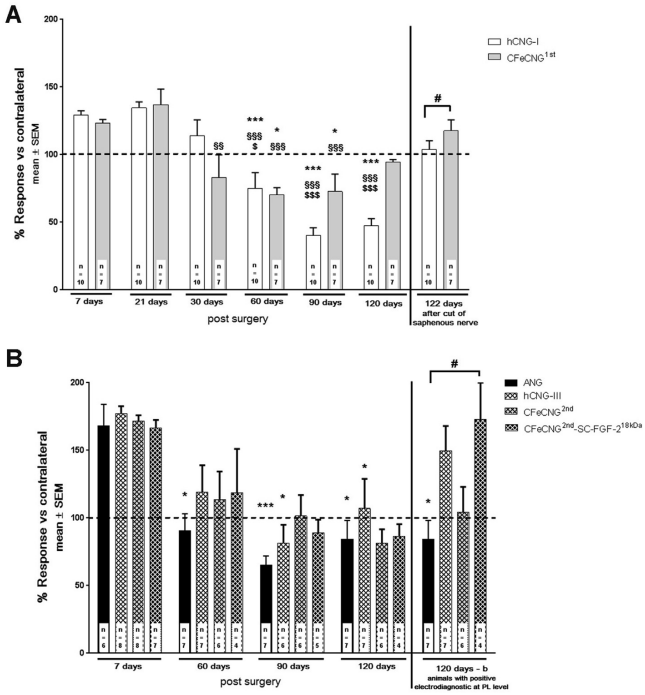

Fig. 3. Results of mechanical pain threshold assessment in the course of Study I and Study III expressed as percentage of values obtained from the contralateral, non-lesioned side. (A) Results obtained during Study I at various time points. Following 120 days of observation, the saphenous nerve was cut to exclude false positive responses due to saphenous nerve collateral reinnervation. This resulted in a withdrawal response only from animals that also displayed reinnervation of PL muscles in electrophysiological tests. Results of the final mechanical pain threshold evaluation are depicted in the last pair of columns (122 days). (B) Results obtained during Study III. The last set of columns (120 days-b) depicts the calculation corrected according to electrodiagnostic results at the PL muscle level (determined values included for animals with positive CMAP and cut-off values included for animals without recordable CMAP). Variations in animal numbers are due to exclusions because of autotomy events. Significant differences ($p < 0.05$) were determined by Two-Way ANOVA, followed by Tukey's multiple comparisons tests. #$p < 0.05$; *$p < 0.05$, **$p < 0.01$, ***$p < 0.001$ vs 7 day results within same group; §§$p < 0.01$, §§§$p < 0.001$ vs 21 day results within same group; $ $p < 0.05$, $$$ $p < 0.001$ vs 30 day results within same group.

additional surgery (cutting of the saphenous nerve), only values from animals that showed recordable CMAPs at the PL muscle during final electrophysiological tests were accepted for the 120 days-b calculation (Fig. 3B last set of columns), while the cut-off force (40 g, see Section 2.7.2) was included for animals demonstrating no reinnervation of the PL muscle. Thereby, no significant differences were detected between the ANG group (84.40 ± 13.70% response compared to contralateral) and the hCNG-III (149.50 ± 18.52%) or CFeCNG^{2nd} (104.04 ± 18.87%) groups. The CFeCNG^{2nd}-SC-FGF-2^{18kDa} group (172.90 ± 26.99%) did not display successful sensory recovery. Overall the values indicate that recovery of the mechanosensitivity approximated normal values most closely in the CFeCNG^{2nd} group.

3.1.4. Macroscopic inspection upon explantation

Prior to nerve tissue harvest for histomorphometrical evaluation, macroscopic observation of the reconstructed nerves in study I visualized in the hCNG-I group a nerve cable bridging the 15 mm gap in 5 out of 10 (50%) animals (Fig. 4A). In the CFeCNG^{1st} group, the bridging tissue was split into two cables and visible in 5 out of 7 (71%) animals (Fig. 4B). The two regenerated tissue cables were separated from each other closely proximal to the central CF and fused again distal to it (Fig. 4B).

In study III all animals of the ANG group showed bridged nerve ends. Nerve guide repair resulted in the following macroscopically visible tissue regeneration outcome: hCNG-III group single tissue cables in 4 out of 7 seven animals (57%); CFeCNG^{2nd} group: two tissue cables, one in each compartment of the nerve guide, in 7 out of 7 (100%) animals; CFeCNG^{2nd}-SC-FGF-2^{18kDa} group: two tissue cables, one in each compartment of the nerve guide, in 6 out of 7 animals plus a single cable (in one compartment only) in the last animal.

The macroscopic inspection demonstrated that nerve regeneration through chitosan guides was increased by introducing into these guides continuous chitosan films (CFeCNG^{1st}) and further improved by the perforated chitosan films (CFeCNG^{2nd}), while additional enrichment with FGF-2^{18kDa} overexpressing Schwann cells (CFeCNG^{2nd}-SC-FGF-2^{18kDa}) did not provide a synergistic effect.

3.1.5. Nerve histology

To reveal differences in regenerated tissue organization in study

III, histological cross-sections were prepared from whole nerve guide/nerve tissue samples at mid-graft level (with visible CF in the respective groups) and at ~1 mm proximal to the distal suture side (without CF in the respective groups). As shown in Fig. 5, the two regenerated tissue cables in the CFeCNG^{2nd} and CFeCNG^{2nd}-SC-FGF-2^{18kDa} groups appeared to be connected to each other through the holes inside the CF. In some cases also small vessels traveling through the holes were visible with the help of the microsurgical microscope (Fig. 5A–B). Single histological cross-sections taken from the mid-graft level and stained for collagen (trichrome staining) also displayed these connections (Fig. 5C–F), although the staining procedures partly caused the dissolution of CF out of the sections. Interestingly, no axons traveling with these tissue bridges could be detected in neurofilament staining (see below).

Fig. 6 shows representative photomicrographs of HE stained sections from the ANG group (Fig. 6A–B) or of a regenerated nerve inside hCNG-III grafts (Fig. 6C–D). Fig. 6E–F demonstrates that two tissue cables, which were separated by the z-shaped CF regenerated in CFeCNG^{2nd} grafts (Fig. 6E) and fused again prior to reconnecting to the distal nerve end (Fig. 6F).

Furthermore, consecutive sections were double-stained for NF200-neurofilament and ChAT to demonstrate the presence of motor fibers within the regenerated nerve cables. Fig. 7 shows representative photomicrographs from the ANG group (Fig. 7A–C), the hCNG-III group (Fig. 7D–F), and the CFeCNG^{2nd} group (Fig. 7G–H).

3.1.6. Nerve morphometry

Fig. 8 depicts the results of the stereological assessment of the regenerated myelinated axons in a segment 5 mm distal to the nerve grafts. The total numbers of myelinated fibers (Fig. 8A) are significantly different in the ANG group compared to the healthy nerve, but no differences are detectable between the experimental groups.

With regard to axon and fiber diameters and myelin thickness (Fig. 8B), single significant differences from healthy nerve values could be detected, but again no differences are detectable among the experimental groups.

These results indicate that once regeneration occurred through any of the used graft types, axonal regeneration at a short distance from the graft or guide (in contrast to functional recovery of more distal targets) follows a similar course in all the reconstruction conditions assayed.

3.2. Short term evaluation of the regenerative matrix and dorsal root ganglia

The pre- and postoperative (at 56 days post surgery) blood glucose levels in the healthy and diabetic GK rats were measured and are presented in Table 3, with significantly higher values in the diabetic GK rats. Furthermore it can be revisited in Table 3 that in contrast to other diabetic animal models these rats developed a moderate and therefore clinically relevant increase of blood glucose levels resembling type 2 diabetes in human patients.

3.2.1. Regenerative matrix and distal nerve segment

In single animals we examined the regenerative matrices formed at earlier time points before 56 days post surgery and found that then those were not developed enough to allow comprehensive histological analyses (results not shown).

Table 4 summarizes the qualitative and quantitative data as well as the statistical correlations. At 56 days post surgery, macroscopically, a regenerative matrix was formed completely extending between the proximal and distal nerve stumps in 6 of 8 animals (75%) in the hCNG-II^{healthy} group and in 4 of 8 animals (50%) in the hCNG-II^{diabetic} group. In groups where CFeCNG^{2nd} had been implanted, a complete (i.e. connecting the proximal and distal nerve segments) matrix was formed in 8/8 animals (100%) of both the CFeCNG$^{2nd\text{-}healthy}$ and the CFeCNG$^{2nd\text{-}diabetic}$ groups. In these animals, 6 of 8 (75%) of the CFeCNG$^{2nd\text{-}healthy}$ and 7 of 8 (88%) CFeCNG$^{2nd\text{-}diabetic}$ showed a matrix composed of two cables, extending on each side of the chitosan film, instead of one single cable as in the hCNG-II samples. Notably, in the CFeCNG^{2nd} guides, especially in the GK diabetic rats neovascularisation inside and outside the nerve guides was macroscopically observed.

3.2.1.1. Axonal outgrowth (neurofilament staining). The presence of axons in the formed matrices was evaluated by neurofilament staining (Fig. 9). Due to the thin matrix the exact length of axonal outgrowth was not possible to calculate as previously described [17]. Axons were present in the center of the formed matrices in 6/8 (75%) of hCNG-II^{healthy}and hCNG-II^{diabetic} rats (i.e. axons were also present in two of the incomplete matrices in the diabetic GK rats; Table 4). In all rats, where CFeCNG^{2nd} had been implanted, axons (i.e. 8/8 CFeCNG$^{2nd\text{-}healthy}$ and CFeCNG$^{2nd\text{-}diabetic}$ rats; i.e. 100%) were observed in the center of the matrix (Table 4; Fig. 9). The Chi-squared test did not reveal any differences in presence of neurofilaments in the nerve guide among the groups ($p = 0.21$; Table 4).

Neurofilament staining of the nerve segment distal to the nerve guides revealed axons in 3/8 (38%) hCNG-II^{healthy} rats and in 4/8 (50%) hCNG-II^{diabetic} rats, while all rats (100%) in which CFeCNG^{2nd} had been implanted exhibited axons in the segment just distal to the nerve guides (Table 4), irrespective of the healthy or diabetic condition. Thus, the chi-squared test showed a statistical significant difference in presence of neurofilaments in the distal nerve segment between the groups ($p = 0.005$), with differences observed between reconstructions using the hCNG-II and the CFeCNG^{2nd} ($p = 0.01$; Fisher's method; Table 4), but with no differences between healthy and diabetic rats.

3.2.1.2. Activated Schwann cells (ATF3-staining). The percentage of ATF3 stained Schwann cells was evaluated at three locations: 3 mm from the proximal suture line, at the center of the matrix formed in the nerve guide and at the distal nerve segment just distal to the nerve guide [17]. Double staining with S-100 has revealed that the evaluated cells were Schwann cells [6,17]. In general, few ATF3

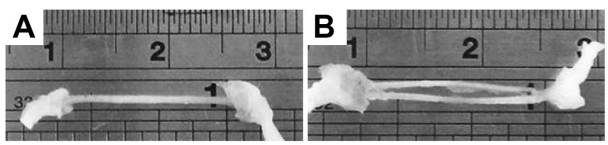

Fig. 4. Harvested regenerated nerve cable 4 months after nerve reconstruction with hollow (hCNG-I) or 1st generation chitosan film enhanced chitosan nerve guides (CFeCNG^{1st}). (A) A single nerve cable bridging the gap was seen when a hCNG-I had been used for nerve reconstruction, while (B) two bridging tissue cables (one in each compartment) were found after implantation of CFeCNG^{1st}.

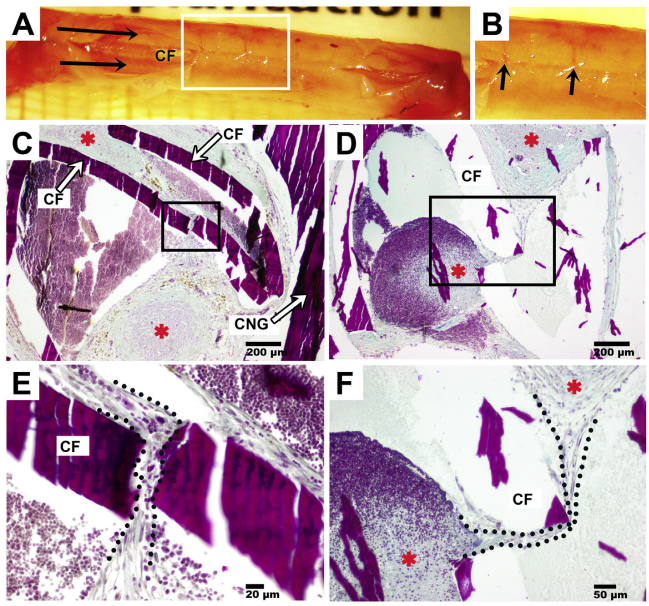

Fig. 5. (A) Photograph showing an explanted nerve guide from the CFeCNG^{2nd} group. The nerve guide is surrounded by a thin layer of connective tissue and a window has been cut to visualize two regenerated vascularized tissue cables (black arrows) separated by the chitosan film (CF). (B) The magnification of the white insert drawn in (A), clearly demonstrates the tissue growth (connective tissue and small vessels, black arrows) through the holes in the CF connecting the two regenerated tissue cables. (C, D) Sections subjected to trichrome-staining (light green) visualizing collagen. Red asterisks mark the regenerated tissue cables that are connected through the holes in the CF. The black inserts have been further magnified in (E) and (F), respectively. (E) Magnification from insert in (C), the dotted line outlines the tissue bridge between the regenerated cables. (F) Magnification from insert in (D), the dotted line outlines the tissue bridge between the regenerated cables (marked with red asterisks). CNG: chitosan nerve guide.

stained Schwann cells were observed (Fig. 10), but with differences detected between the groups (Table 4) at the three sites. There was a higher percentage of stained cells in the CFeCNG^{2nd} than in the hCNG-II samples as well as in the distal nerve segment. Furthermore, there was also higher percentage of stained cells in diabetic GK rats, except at 3 mm from the proximal suture line.

3.2.1.3. Apoptotic Schwann cells (cleaved caspase 3- staining). The percentage of cleaved caspase 3 stained Schwann cells (double staining with S-100; [17]) was evaluated at the same locations as for the ATF3 labeling (Table 4; Fig. 10) and showed differences between the groups at all the locations (Kruskal–Wallis $p = 0.0001$; 0.0001; 0.0001, respectively). At 3 mm in the matrix formed in the nerve guides, there was higher percentage of stained Schwann cells in the CFeCNG^{2nd} samples and higher percentage also in the diabetic GK rats (Table 4). At the center of the nerve guides there were no differences between hCNG-II and CFeCNG^{2nd} samples, although the diabetic GK rats exhibited a higher percentage of apoptotic Schwann cells. In contrast, the percentages in the distal nerve segment were lower in the CFeCNG^{2nd} groups as well as lower in the diabetic GK rats (Table 4; Fisher's test values).

3.2.1.4. Total number of cells (DAPI-staining). The total number of DAPI labeled cells was also assessed at the three mentioned locations and showed differences only inside the nerve guides. The number of DAPI stained cells (i.e. total number of cells) inside the nerve guides was generally higher in CFeCNG^{2nd} samples as well as higher in diabetic GK than in healthy rats. No differences between groups were observed, however, in the distal nerve segment.

3.2.2. Dorsal root ganglia (L4, L5)

Table 5 summarizes the quantitative data as well as the statistical analyses.

3.2.2.1. Activated sensory neurons (ATF3-staining). The sensory neurons from the control side did not show any staining for ATF3, while the experimental side showed ATF3 staining to a variable, but low extent (Table 5), with differences between the groups ($p = 0.002$; Kruskal–Wallis; for details of analysis see Ref. [24]). A significantly higher percentage of ATF3 labeled sensory neurons were observed in DRGs from CFeCNG^{2nd} rats, particularly in diabetic rats (Table 5).

3.2.2.2. Degree of neuroprotection (HSP27-staining). Accordingly, HSP27 was observed in DRG from the control side with around 18.0–22.4% of the area stained without any difference between the groups (Table 5), while the staining on the experimental side was significantly higher ($p = 0.0001$ Wilcoxon). Furthermore, a significant difference between the experimental groups was observed concerning the HSP27 staining (Table 5); the expression of HSP27 on the experimental side was again higher in the DRGs from the diabetic GK rats (Fisher test values; Table 5), without a general difference between the two types of nerve guides. Accordingly, the HSP27 expression ratio (i.e. experimental/control) revealed also differences

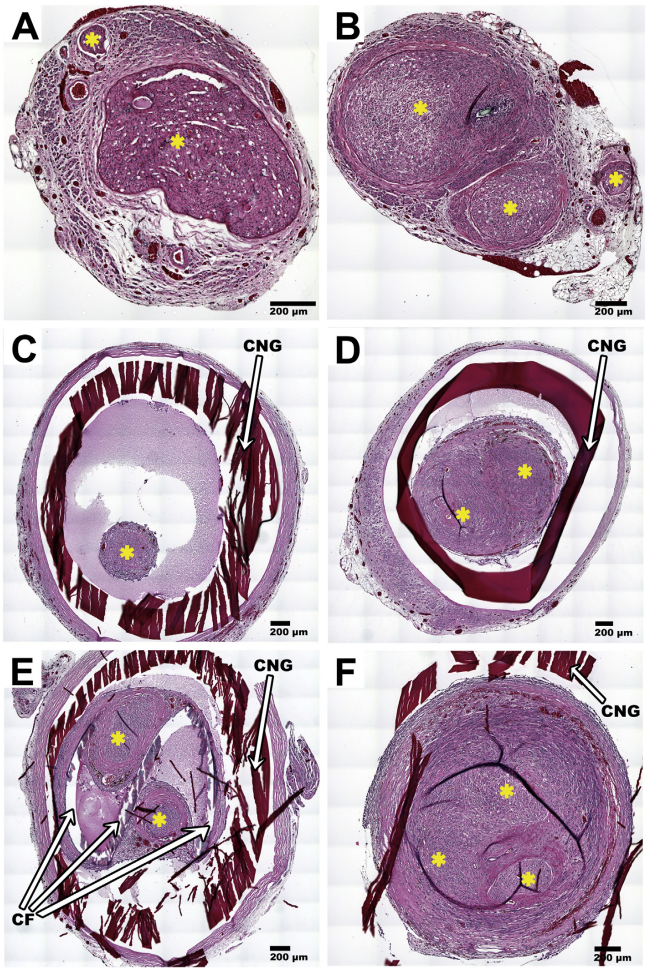

Fig. 6. Representative photomicrographs acquired from histological cross sections obtained at mid-graft level (A,C,E) or at ~1 mm proximal to the distal suture (B,D,F). Sections have been taken from samples of the ANG group (A,B), the hCNG-III group (C,D), and the CFeCNG^{2nd} group (E,F). Nerve fascicles identified in the HE staining are marked with yellow asterisks. (A) At mid-graft level an ANG is comprised of one large and one small nerve fascicle, (B) while it is separated into three fascicles in the distal region. (C) At mid-graft level a thin free floating tissue cable is detectable in hCNG-III, (D) which becomes thicker and separated into more than one fascicle at the distal region. (E) Two tissue cables separated by a z-shaped CF are visible at the mid-graft region of CFeCNG^{2nd} grafts. (F) The separate tissue cables then fuse to form a single bigger cable containing several nerve fascicles. CNG: chitosan nerve guide, CF: chitosan film.

between the groups ($p = 0.013$; Kruskal–Wallis) and with significantly higher values in the CFeCNG^{2nd} and in the diabetic GK rats (Fisher's test values; Table 5).

4. Discussion

Various conduit designs considering different intraluminal guidance structures have been experimentally examined for reconstruction of peripheral nerve defects [1]. Despite the diversity of these designs, however, little progress has been made in approving a product for clinical use that is able to reach the level of recovery seen when using the clinical standard treatment (autologous nerve grafting), especially if the nerve defect exceeds a critical length of 3 cm in humans [2,4,8]. Consequently, autologous nerve grafting still remains the surgeons preferred choice for bridging extended defects between two nerve ends, because this method gives at least a minimum chance for some functional recovery depending on the reconstructed nerve trunk [3]. Several

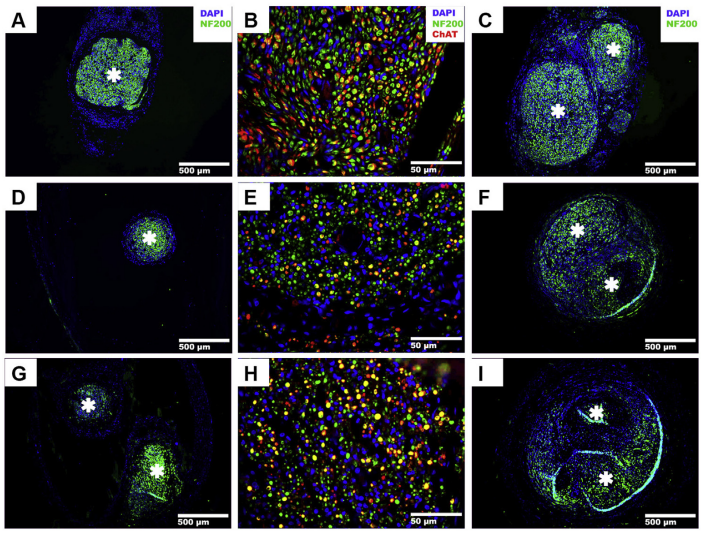

Fig. 7. Representative photomicrographs acquired from histological cross sections double-stained for neurofilament (NF200, green) and acetylcholine transferase (ChAT, red) and counterstained with DAPI (blue). The sections have been taken from samples of the ANG group (A–C), the hCNG-III group (D–F), and the CFeCNG^{2nd} group (G–I) at mid-graft level (A,D,G) or at ~1 mm proximal to the distal suture (C,F,I). White asterisks mark NF-200 immunopositive areas (nerve fascicles). (B,E,H) Merge and magnifications of the three immunostainings demonstrating nerve fascicle details and the contained regenerated motor axons (yellow).

attempts have been made to develop effective alternatives for autologous nerve grafting and promising results have been achieved experimentally and some even applied clinically, such as processed nerve allografts [26–28]. For example, non-biodegradable poly-sulfon nerve guides enhanced with one electrospun aligned thin film (poly-acrylonitril-co-methylacrylate) within their lumen were reported to significantly increase peripheral nerve regeneration across a 14 mm rat sciatic nerve defect [20]. While these nerve guides have not yet been further advanced for a possible clinical application, other attempts were made to enhance already approved nerve guide devices with engineered neural tissue [29]. For the latter, approved NeuraWrap™ nerve guides were filled with engineered neural tissue containing adipose derived stem cells and demonstrated to support axonal regeneration across a 15 mm rat sciatic nerve defect in a short-term period of 8 weeks after reconstruction to a similar extent than autologous nerve grafts [29]. Although promising, the neural engineered tissue and the use of stem cells are not likely to overcome the regulatory burden for clinical use in the near future and also the functional outcome of regeneration remains to be investigated for this type of bioartificial graft. In the recent years only one engineered nerve guide with intraluminal structures has been translated into a clinical investigation, the Neuromaix nerve guide [30] but results are not yet published. This nerve guide is collagen based and composed of an outer shell conduit filled with an inner sponge-like conduit, for which the support of functional recovery across a 2 cm rat sciatic nerve defect has already been demonstrated [31].

In the present study we evaluated chitosan films as alternative guidance substrate for regenerating axons within chitosan nerve guides across an extended rat sciatic nerve defect (15 mm). The basic chitosan nerve guides have already been approved for clinical use in Europe (CE mark, Reaxon® Nerve Guide). This was achieved after demonstrating their very good pro-regenerative properties in rat models evaluating standard and critical length nerve defect reconstruction [15–18]. These nerve guides further provide a high mechanical strength and collapse stability combined with transparency and easiness to suture them with microneedles [15], thus making it very likely that these off-the-shelve nerve guides will be widely accepted when autologous nerve grafting is not the first option for the surgeon or the patient. The chitosan films used in the present study to enhance the hollow chitosan nerve guides (hCNGs) are made under equal ISO standard protocols and out of the same certified medical grade chitosan. Therefore, only a short period will be needed until the equally transparent and collapse stable chitosan film enhanced chitosan nerve guides (CFeCNGs) may be available for clinical use. With the present results, we show that CFeCNGs significantly improved nerve regeneration for critical length defect reconstruction compared to hCNGs. Furthermore, this higher pro-regenerative effect has been demonstrated not only in healthy, but also in diabetic rats in which clinically relevant blood glucose profiles were measured.

The chitosan films were thought to support the fibrin matrix, which is initially formed upon injury and nerve guide aided nerve repair [32–34]. Importantly, it is most likely that the incomplete formation of this fibrin-based cable, or even the lack of formation, causes failure of regeneration across large defects [2,35]. Within one week after bridging a 10 mm defect, the fibrin-based cable connects the two nerve stumps and Schwann cells start to migrate along it and proliferate to form the bands of Büngner before axonal sprouts can cross the defect in the axonal phase [2,15,32,34]; again with a successful axonal outgrowth in diabetic GK rats [17].

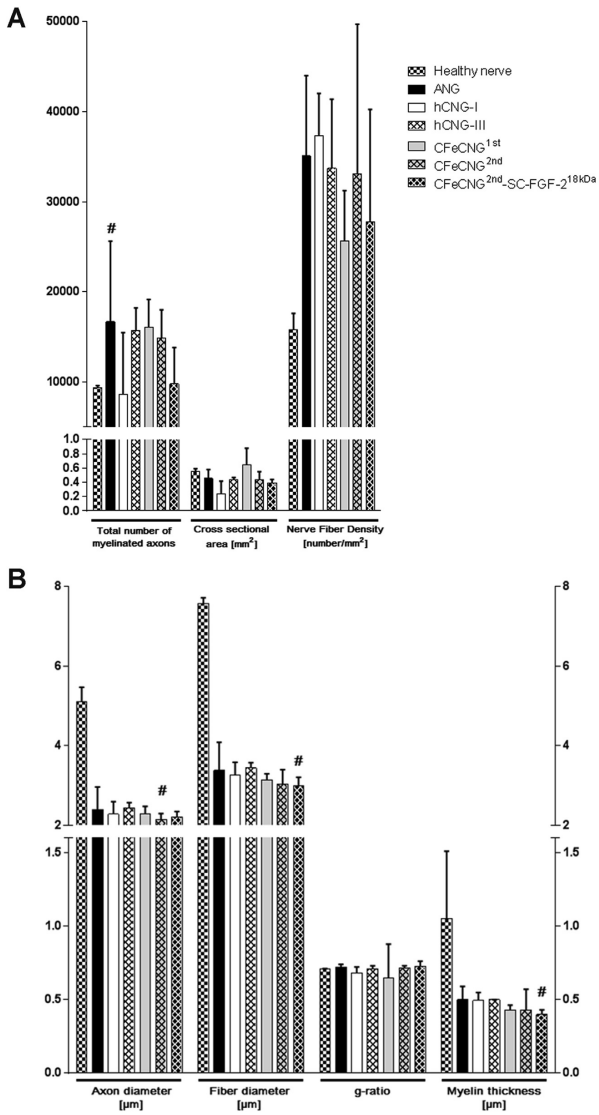

Fig. 8. Results of the morphometric analysis of the distal nerve, 5 mm distal to the nerve guide or graft, from Study I and Study III. (A) Total number of regenerated myelinated axons, total cross sectional area [mm^2], and calculated nerve fiber density. (B) Parameters related to axonal maturation: axon diameter, fiber diameter, g-ratio, and myelin thickness. Data are given in median ± range. Number of analyzed specimens: n = 3: healthy nerve and hCNG-III; n = 4: hCNG-I and $CFeCNG^{1st}$; n = 6: $CFeCNG^{2nd}$ and $CFeCNG^{2nd}$-SC-FGF-2^{18kDa}; n = 8: ANG. Results were tested for significance ($p < 0.05$) using Kruskal–Wallis test, followed by Dunn's multiple comparison. #$p < 0.05$ vs contralateral healthy nerve.

Importantly, it is considered that the absent or incomplete formation of this fibrin-based cable causes failure of regeneration across long defects [2,35]. Within one week after bridging a 10 mm defect in the rat sciatic nerve, the fibrin-based cable connects the two nerve stumps, providing physical support to the migration of fibroblasts and Schwann cells along it before axonal sprouts can cross the gap in the axonal phase [2,15,32]. In the present study where a 15 mm sciatic nerve defect was bridged with hCNGs or

Table 3
Blood glucose levels in healthy and diabetic Goto-Kakizaki (GK) rats evaluated for up to 56 days post surgery in study II. Values are median [25th (Q1) – 75th (Q3) percentiles].

		hCNG-II^{healthy}	CFeCNG$^{2nd\text{-}healthy}$	hCNG-II^{diabetic}	CFeCNG$^{2nd\text{-}diabetic}$	p-values (KW[a])	Fisher's method[b]	
							hCNG-II/CFeCNG^{2nd}	Healthy rats/ Diabetic rats
B-glucose (mmol/l)	preoperative	4.0 [3.6–4.4]	3.6 [3.3–4.0]	8.7 [8.1–1.2]	7.9 [7.4–8.4]	0.0001	0.68	<0.0001
	postoperative	4.1 [3.8–4.49]	4.3 [4.0–4.6]	9.0 [7.7–11.2]	7.7 [7.5–8.7]	0.0001	0.27	<0.0001

[a] KW = Kruskal–Wallis.
[b] Fisher method for independent samples based on the chi square distribution.

Table 4
Nerve regeneration in healthy and diabetic Goto-Kakizaki (GK) rats evaluated 56 days post surgery in study II. Values are median [25th (Q1) –75th (Q3) percentiles].

		hCNG-II^{healthy}	CFeCNG$^{2nd\text{-}healthy}$	hCNG-II^{diabetic}	CFeCNG$^{2nd\text{-}diabetic}$	p-values (KW[a])	Fisher's method[b]	
							hCNG-II/ CFeCNG^{2nd}	Healthy rats/ Diabetic rats
Presence of axons (neurofilament staining; animals/group)	In nerve guide	6/8	8/8	6/8	8/8	0.21[#]	NA	NA
	In distal nerve	3/8	8/8	4/8	8/8	0.005[#]	0.01	1.00
ATF3 - + Schwann cells (% of total)	At 3 mm	0.9 [0.5–1.5]	1.5 [1.4–2.7]	0.9 [0.4–1.9]	2.7 [2.3–3.0]	**0.004**	**0.008**	0.19
	In nerve guide	0.8 [0.7–1.2]	2.8 [2.1–3.0]	1.7 [1.5–2.0]	3.7 [3.0–4.3]	**0.0001**	**<0.0001**	**0.0002**
	In distal nerve	1.8 [1.2–3.3]	5.0 [3.9–5.3]	5.4 [4.2–6.3]	7.6 [7.0–10.5]	**0.0001**	**<0.0001**	**<0.0001**
Cleaved caspase-3 - + Schwann cells (% of total)	At 3 mm	2.6 [1.8–2.8]	4.6 [4.3–5.4]	3.9 [3.4–4.4]	4.8 [4.6–5.4]	**0.0001**	**0.0001**	**0.0006**
	In nerve guide	1.6 [1.3–2.3]	2.2 [1.9–2.6]	3.8 [3.5–4.5]	3.6 [3.3–3.9]	**0.0001**	0.094	**<0.0001**
	In distal nerve	8.7 [8.2–9.3]	7.6 [7.0–8.1]	7.9 [7.6–8.5]	6.9 [6.4–7.4]	**0.0001**	**0.0002**	**0.013**
DAPI stained cells (no/mm^2)	At 3 mm	862 [806–903]	1016 [999–1063]	1090 [1072–1106]	1070 [1062–1130]	**0.0001**	**<0.0001**	**<0.0001**
	In nerve guide	775 [759–796]	923 [904–988]	871 [852–885]	966 [951–987]	**0.0001**	**<0.0001**	**<0.0001**
	In distal nerve	1038 [1023–1107]	1051 [1035–1078]	1069 [1057–1089]	1010 [940–1204]	0.57	NA	NA

+ = Immunopositive.
NA = Not applicable.
At 3 mm = 3 mm distal to the proximal suture line. In nerve guide = in center of nerve guide. [#] indicates overall Chi-squared test (Pearson Chi-squared, cross tabulation > 2 × 2). The Fishers's method for neurofilament staining is based on subsequent 2 × 2 cross tabulation Fisher's exact test.
p-values indicating significant differences are set in bold.
[a] KW = Kruskal–Wallis.
[b] Fisher method for independent samples based on the chi square distribution.

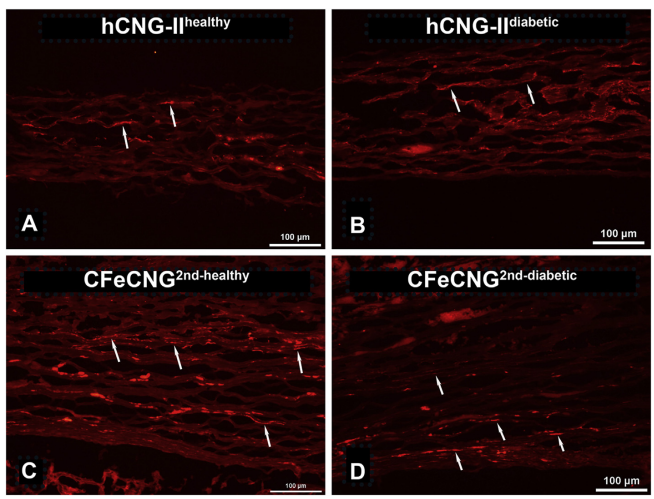

Fig. 9. Neurofilament staining in the formed matrix in healthy (A,C) and diabetic GK (B, D) rats repaired with hCNG (A, B) and with CFeCNG^{2nd} (C,D) nerve guides at 56 days post surgery. Axons (arrows) were present in all CFeCNG^{2nd} nerve guides (8/8 healthy and 8/8 GK rats) as well as in nerve guides of 6/8 hCNG-II^{healthy} and 6/8 hCNG-II^{diabetic} rats. Scale bar = 100 µm.

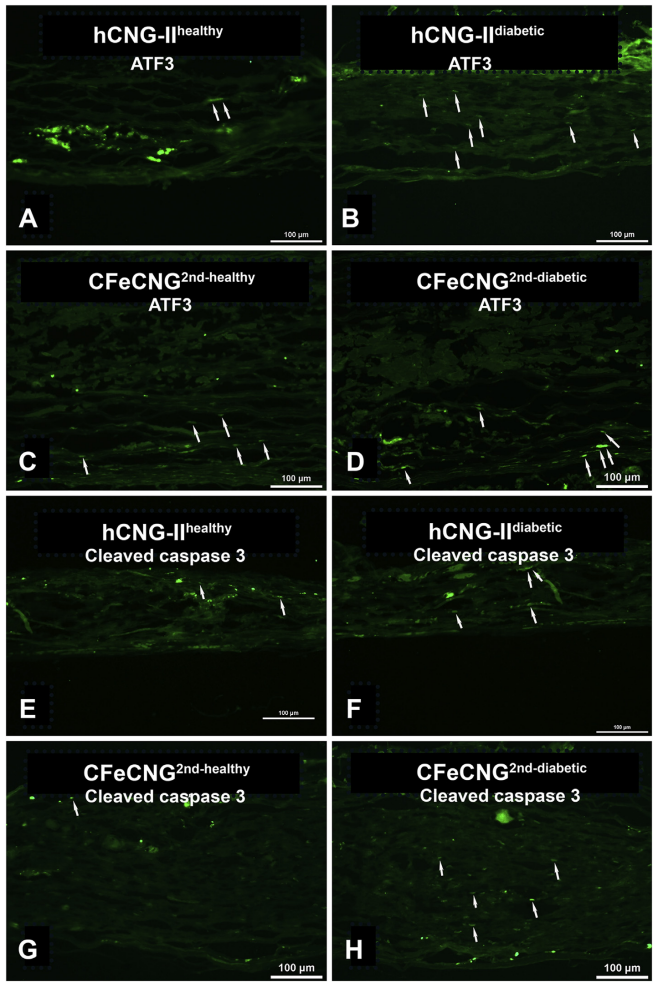

Fig. 10. Staining for activating transcription factor 3 (ATF3) (A–D) and cleaved caspase 3 (E–H) in the formed matrix in healthy (A, C, E, G) and diabetic GK (B, D, F, H) rats reconstructed with hCNG (A, B, E, F) or CFeCNG^{2nd} (C, D, G, H) at 56 days post surgery. Arrows indicate stained oval shaped Schwann cells. Scale bar = 100 µm.

CFeCNGs, a substantial regenerative matrix was found in the samples taken at 56 days after surgery in both healthy and diabetic rats. Importantly, the quality of the formed matrix was improved in the CFeCNG treated animals, and regenerating axons had already reached the distal nerve segment in a significantly higher proportion at 56 days after surgery, allowing muscle reinnervation detectable in some cases at 60 days. Furthermore, the regenerative matrix as well as the nerve segment just distal to the implanted CFeCNG displayed significantly increased numbers of activated Schwan cells (ATF3-immunopositive), which are likely to attract regrowing axons [7,15,24]. Simultaneously, the apoptotic events, as indicated by cleaved caspase 3 immunopositive Schwann cells, were reduced in nerve segments distal to CFeCNG implants, indicating that also events potentially deleterious for axonal regeneration [15] are reduced. The support of axonal regeneration by CFeCNG is further strengthened by the interesting finding that a higher number of sensory DRG neurons were found, i.e. ATF3 stained, as well as a larger area was stained for HSP27, as an indicator for increased neuroprotection [6], particularly in the diabetic GK rats with a moderately increased blood glucose level. It is conclusive that a higher degree of neuronal protection and activation together with a higher degree of Schwann cell activation and

Table 5
Analysis of sensory dorsal root ganglia (L4-L5) in healthy and diabetic Goto-Kakizaki (GK) rats evaluated 56 days post surgery in study II. Values are median [25th (Q1) – 75th (Q3) percentiles].

		hCNG-II^{healthy}	CFeCNG$^{2nd-healthy}$	hCNG-II^{diabetic}	CFeCNG$^{2nd-diabetic}$	p-values (KW[a])	Fisher's method[b]	
							hCNG-II/ CFeCNG^{2nd}	Healthy rats/ Diabetic rats
ATF3- + - cells (% of total)	Experimental	6.4 [3.9–7.1]	6.9 [5.8–11.9]	6.5 [5.5–8.7]	14.4 [13.3–20.0]	**0.002**	**0.003**	**0.01**
HSP27 expression (% of area)	Control	21.3 [18.4–22.8]	18.1 [16.8–20.4]	22.4 [19.0–23.9]	18.0 [16.6–19.7]	0.13	NA	NA
	Experimental	27.4 [24.8–29.4]	27.3 [25.5–30.5]	30.2 [24.5–32.3]	34.1 [32.1–35.9]	**0.023**	0.17	**0.03**
HSP27 Ratio (experimental/control)		1.35 [1.27–1.54]	1.62 [1.28–1.79]	1.25 [1.10–1.61]	1.83 [1.61–2.13]	**0.013**	**0.003**	**0.01**

+ = Immunopositive.
NA = Not applied.
p-values indicating significant differences are set in bold.
[a] KW = Kruskal–Wallis.
[b] Fisher method for independent samples based on the chi square distribution.

reduced apoptosis during the early phase of regeneration can lead to better functional recovery in the long term.

Usually, when new types of nerve guides or tissue engineered nerve prostheses are developed, the general health condition of the tested animals is not considered. The globally increasing number of patients with diabetes, however, makes it crucial to develop peripheral nerve reconstruction treatment strategies also suitable for patients in which neuropathies often occur [7]. Here, we demonstrate that during the matrix phase axonal regeneration is equally supported in healthy and diabetic GK rats after critical nerve defect reconstructed with CFeCNG^{2nd}. With regard to the processes undergoing in the corresponding DRGs, it has been demonstrated earlier that HSP27 is an important factor preserving nerve function in diabetic patients [23]. Here we also demonstrate that the HSP27 expression together with that of ATF3 has been found to be increased in DRGs from diabetic GK rats. In diabetic GK rats, the regenerative matrix within the nerve guides contained higher numbers of cells in general and of activated (ATF3-immunopositive) Schwann cells in particular. With regard to apoptotic events in Schwann cells we found that those are increased within the regenerative matrix but not in the distal nerve segments in diabetic GK rats. In contrast, it has been demonstrated earlier that Schwann cells in diabetic animals are less responsive to a nerve injury [36] and that nerves in diabetic animals have a slower regeneration after end-to-end repair [6]. Therefore the results obtained in the present study notably indicate that peripheral nerve reconstruction by means of basic or enhanced chitosan nerve guides represents a promising alternative to standard treatments in diabetic rats with clinically relevant blood glucose levels.

The pro-regenerative properties of chitosan are well documented not only for the peripheral and the central nervous system but also for other applications in regenerative medicine and wound healing [37–39]. Beside its antimicrobial properties also the angiogenic properties of chitosan materials are important in the context of regenerative medicine. Indeed, we observed robust neovascularization not only in the short term, being even more evident in the diabetic animals, but also on the long term, where exclusively in the second generation CFeCNGs (with perforated chitosan films) small blood vessels traveling through the holes in the chitosan films were visible. Angiogenesis is important for the survival of cells and tissue and crucial for the success of peripheral nerve regeneration across a critical length [40]. In the present study, long term axonal regeneration, as determined by nerve morphometry, was similar among all nerve guide conditions examined. When it comes to functional nerve recovery, however, the introduction of perforated chitosan films in CFeCNGs was sufficient to further increase the functional outcome compared to hCNGs. The latter was clearly demonstrated by electrophysiological recording of muscle reinnervation at 120 days after surgery. Implantation of CFeCNGs to bridge the 15 mm sciatic nerve defect induced higher reinnervation rates of the TA and PL muscles. The success rates increased by 20–30% in the CFeCNG^{2nd} group (perforated chitosan film) compared to the CFeCNG^{1st} group (continuous chitosan film). Regarding the outcome of sensory recovery in the present study at 120 days after surgery, study I revealed less efficiency of implantation of CFeCNG^{1st} compared to that of hCNG. In contrast, study III revealed the opposite and most similar recovery in comparison to autologous nerve grafting for the CFeCNG^{2nd} group. Thus, it can be hypothesized that the perforations within the chitosan films allowed nutrient interchange between the two sub-compartments within the second generation CFeCNGs (also via capillaries connecting the regenerative tissue along both sides of the chitosan films). This condition probably supported cell migration and survival across the nerve defect and formation of the regenerative fibrin matrix to a higher extent than non-perforated chitosan films used in first generation CFeCNG. Subsequently 15 mm nerve defect reconstruction with second generation CFeCNGs resulted in even increased functional recovery.

In study III we included an additional condition, the enrichment of CFeCNG^{2nd} with FGF-2^{18kDa} overexpressing Schwann cells (SC-FGF-2^{18kDa}). It was earlier demonstrated that these cells increase functional recovery across 15 mm sciatic nerve defects [41] and even support it when the regeneration process is impaired by local obstacles such as a too dense hydrogel within chitosan nerve guides [19]. In the present study CFeCNG^{2nd}-SC-FGF-2^{18kDa}did not further increase the regeneration outcome. The functional recovery was rather less in comparison to the implantation of cell free CFeCNG^{2nd}. This indicates that although Schwann cell survival within the nerve guides previously has been proven in vitro and neovascularization for nutrient supply in vivo was detectable, the implanted Schwann cells did not likely survive in vivo and their debris and metabolites might also interfere with the regrowth of axons. The Schwann cells have been seeded on non-coated chitosan films because this has been evaluated previously in vitro [21]. However, in previous studies, where they demonstrated to be effective, the cells had been suspended in different types of hydrogels [19,41,42]. Future attempts have to be made to ensure survival of Schwann cells seeded into CFeCNGs.

5. Conclusions

In the present study, hollow chitosan nerve guides were enhanced by introduction of chitosan films to increase the regeneration outcome across peripheral sciatic nerve defects of critical length, i.e. 15 mm, in healthy and diabetic rats. This enhanced chitosan nerve guides not only supported robust axonal

regeneration and functional recovery in healthy animals but also demonstrated to be beneficial for the regeneration process in diabetic rats with relevant blood glucose levels. Thus, we have an effective peripheral nerve regenerative device at hand, which represents an ideal candidate for the translation into the clinic. All components of the enhanced nerve guides can be produced under ISO standards. Furthermore, the maintained transparency and the easiness to suture the device between the nerve ends are likely to facilitate its wide acceptance among nerve surgeons. Based on the results presented here, future experiments can now proceed to address even more complex and challenging conditions for peripheral nerve reconstruction and recovery, such as the common conditions of delayed repair or the reconstruction across joints, e.g. in digital nerve repair.

Acknowledgments

This study was supported by the European Community's Seventh Framework Programme (FP7-HEALTH-2011) under grant agreement n° 278612 (BIOHYBRID). Medical grade chitosan for manufacturing the chitosan films and nerve guides was supplied by Altakitin SA (Lisbon, Portugal). The chitosan materials were supplied by Medovent GmbH (Mainz, Germany). The authors thank Dr. Andreas Ratzka, Institute of Neuroanatomy, for the construction of the plasmids used in this study. We thank Professor Jonas Björk, Lund University, Lund, Sweden for statistical advice of the Fisher's method. We are further thankful to Silke Fischer, Natascha Heidrich, Jennifer Metzen, Hildegard Streich, Maike Wesemann (all Institute of Neuroanatomy, Hannover Medical School), to Monica Espejo, Jessica Jaramillo and Marta Morell (Universitat Autonoma de Barcelona) for their technical support.

References

[1] X. Gu, F. Ding, D.F. Williams, Neural tissue engineering options for peripheral nerve regeneration, Biomaterials 35 (2014) 6143–6156.
[2] W. Daly, L. Yao, D. Zeugolis, A. Windebank, A. Pandit, A biomaterials approach to peripheral nerve regeneration: bridging the peripheral nerve gap and enhancing functional recovery, J. R. Soc. Interface 9 (2012) 202–221.
[3] R. Deumens, A. Bozkurt, M.F. Meek, M.A. Marcus, E.A. Joosten, J. Weis, et al., Repairing injured peripheral nerves: bridging the gap, Prog. Neurobiol. 92 (2010) 245–276.
[4] R.A. Weber, W.C. Breidenbach, R.E. Brown, M.E. Jabaley, D.P. Mass, A randomized prospective study of polyglycolic acid conduits for digital nerve reconstruction in humans, Plast. Reconstr. Surg. 106 (2000) 1036–1045 discussion 46–8.
[5] A. Faroni, S.A. Mobasseri, P.J. Kingham, A.J. Reid, Peripheral nerve regeneration: experimental strategies and future perspectives, Adv. Drug Deliv. Rev. 82–83 (2015) 160–167.
[6] L. Stenberg, L.B. Dahlin, Gender differences in nerve regeneration after sciatic nerve injury and repair in healthy and in type 2 diabetic Goto-Kakizaki rats, BMC Neurosci. 15 (2014) 107.
[7] L. Stenberg, M. Kanje, K. Dolezal, L.B. Dahlin, Expression of activating transcription factor 3 (ATF 3) and caspase 3 in Schwann cells and axonal outgrowth after sciatic nerve repair in diabetic BB rats, Neurosci. Lett. 515 (2012) 34–38.
[8] J.H. Bell, J.W. Haycock, Next generation nerve guides: materials, fabrication, growth factors, and cell delivery, Tissue Eng. Part B Rev. 18 (2012) 116–128.
[9] M.E. Boeckstyns, A.I. Sorensen, J.F. Vineta, B. Rosen, X. Navarro, S.J. Archibald, et al., Collagen conduit versus microsurgical neurorrhaphy: 2-year follow-up of a prospective, blinded clinical and electrophysiological multicenter randomized, controlled trial, J. Hand Surg. Am. 38 (2013) 2405–2411.
[10] G. Lundborg, B. Rosen, S.O. Abrahamson, L. Dahlin, N. Danielsen, Tubular repair of the median nerve in the human forearm. Preliminary findings, J. Hand Surg. Br. 19 (1994) 273–276.
[11] G. Lundborg, B. Rosen, L. Dahlin, J. Holmberg, I. Rosen, Tubular repair of the median or ulnar nerve in the human forearm: a 5-year follow-up, J. Hand Surg. Br. 29 (2004) 100–107.
[12] X. Wang, W. Hu, Y. Cao, J. Yao, J. Wu, X. Gu, Dog sciatic nerve regeneration across a 30-mm defect bridged by a chitosan/PGA artificial nerve graft, Brain 128 (2005) 1897–1910.
[13] C. Xue, N. Hu, Y. Gu, Y. Yang, Y. Liu, J. Liu, et al., Joint use of a Chitosan/PLGA scaffold and MSCs to bridge an extra large gap in dog sciatic nerve, Neurorehabil Neural Repair 26 (2012) 96–106.
[14] F. Ding, J. Wu, Y. Yang, W. Hu, Q. Zhu, X. Tang, et al., Use of tissue-engineered nerve grafts consisting of a Chitosan/Poly(lactic-co-glycolic acid)-based scaffold included with bone marrow mesenchymal cells for bridging 50-mm dog sciatic nerve gaps, Tissue Eng. Part A 16 (2010) 3779–3790.
[15] K. Haastert-Talini, S. Geuna, L.B. Dahlin, C. Meyer, L. Stenberg, T. Freier, et al., Chitosan tubes of varying degrees of acetylation for bridging peripheral nerve defects, Biomaterials 34 (2013) 9886–9904.
[16] Y. Shapira, M. Tolmasov, M. Nissan, E. Reider, A. Koren, T. Biron, et al., Comparison of results between chitosan hollow tube and autologous nerve graft in reconstruction of peripheral nerve defect: an experimental study, Microsurgery (2015 Apr 22), http://dx.doi.org/10.1002/micr.22418 (EPub ahead of print).
[17] L. Stenberg, A. Kodama, C. Lindwall-Blom, L.B. Dahlin, Special issue in the European journal of neuroscience nerve regeneration in chitosan conduits and in autologous nerve grafts in healthy and in type 2 diabetic Goto-Kakizaki rats, Eur. J. Neurosci. (2015), http://dx.doi.org/10.1111/ejn.13068. Epub ahead of print.
[18] F. Gonzalez-Perez, S. Cobianchi, S. Geuna, C. Barwig, T. Freier, E. Udina, et al., Tubulization with chitosan guides for the repair of long gap peripheral nerve injury in the rat, Microsurgery 35 (2015) 300–308.
[19] C. Meyer, S. Wrobel, S. Raimondo, S. Rochkind, C. Heimann, A. Shahar, et al., Peripheral nerve regeneration through hydrogel enriched chitosan conduits containing engineered Schwann cells for drug delivery, Cell Transpl. (2015 Apr 14), http://dx.doi.org/10.3727/096368915X688010 (EPub ahead of print).
[20] I.P. Clements, Y.T. Kim, A.W. English, X. Lu, A. Chung, R.V. Bellamkonda, Thin-film enhanced nerve guidance channels for peripheral nerve repair, Biomaterials 30 (2009) 3834–3846.
[21] S. Wrobel, S.C. Serra, S. Ribeiro-Samy, N. Sousa, C. Heimann, C. Barwig, et al., In vitro evaluation of cell-seeded chitosan films for peripheral nerve tissue engineering, Tissue Eng. Part A 20 (2014) 2339–2349.
[22] Y. Tsuda, M. Kanje, L.B. Dahlin, Axonal outgrowth is associated with increased ERK 1/2 activation but decreased caspase 3 linked cell death in Schwann cells after immediate nerve repair in rats, BMC Neurosci. 12 (2011) 12.
[23] K. Pourhamidi, H. Skarstrand, L.B. Dahlin, O. Rolandsson, HSP27 concentrations are lower in patients with type 1 diabetes and correlate with large nerve fiber dysfunction, Diabetes Care 37 (2014) e49–50.
[24] H. Saito, L.B. Dahlin, Expression of ATF3 and axonal outgrowth are impaired after delayed nerve repair, BMC Neurosci. 9 (2008) 88.
[25] S. Cobianchi, J. de Cruz, X. Navarro, Assessment of sensory thresholds and nociceptive fiber growth after sciatic nerve injury reveals the differential contribution of collateral reinnervation and nerve regeneration to neuropathic pain, Exp. Neurol. 255 (2014) 1–11.
[26] B.D. Rinker, J.V. Ingari, J.A. Greenberg, W.P. Thayer, B. Safa, G.M. Buncke, Outcomes of short-gap sensory nerve injuries reconstructed with processed nerve allografts from a multicenter registry study, J. Reconstr. Microsurg 31 (2015) 384–390.
[27] M.S. Cho, B.D. Rinker, R.V. Weber, J.D. Chao, J.V. Ingari, D. Brooks, et al., Functional outcome following nerve repair in the upper extremity using processed nerve allograft, J. Hand Surg. Am. 37 (2012) 2340–2349.
[28] D.N. Brooks, R.V. Weber, J.D. Chao, B.D. Rinker, J. Zoldos, M.R. Robichaux, et al., Processed nerve allografts for peripheral nerve reconstruction: a multicenter study of utilization and outcomes in sensory, mixed, and motor nerve reconstructions, Microsurgery 32 (2012) 1–14.
[29] M. Georgiou, J.P. Golding, A.J. Loughlin, P.J. Kingham, J.B. Phillips, Engineered neural tissue with aligned, differentiated adipose-derived stem cells promotes peripheral nerve regeneration across a critical sized defect in rat sciatic nerve, Biomaterials 37 (2015) 242–251.
[30] A. Bozkurt, S.G. van Neerven, K.G. Claeys, D.M. O'Dey, A. Sudhoff, G.A. Brook, et al., The proximal medial sural nerve biopsy model: a standardised and reproducible baseline clinical model for the translational evaluation of bioengineered nerve guides, Biomed. Res. Int. 2014 (2014) 121452.
[31] A. Bozkurt, F. Lassner, D. O'Dey, R. Deumens, A. Bocker, T. Schwendt, et al., The role of microstructured and interconnected pore channels in a collagen-based nerve guide on axonal regeneration in peripheral nerves, Biomaterials 33 (2012) 1363–1375.
[32] J.S. Belkas, M.S. Shoichet, R. Midha, Peripheral nerve regeneration through guidance tubes, Neurol. Res. 26 (2004) 151–160.
[33] L.R. Williams, F.M. Longo, H.C. Powell, G. Lundborg, S. Varon, Spatial-temporal progress of peripheral nerve regeneration within a silicone chamber: parameters for a bioassay, J. Comp. Neurol. 218 (1983) 460–470.
[34] Q. Zhao, L.B. Dahlin, M. Kanje, G. Lundborg, Repair of the transected rat sciatic nerve: matrix formation within implanted silicone tubes, Restor. Neurol. Neurosci. 5 (1993) 197–204.
[35] Y.T. Kim, V.K. Haftel, S. Kumar, R.V. Bellamkonda, The role of aligned polymer fiber-based constructs in the bridging of long peripheral nerve gaps, Biomaterials 29 (2008) 3117–3127.
[36] L. Stenberg, M. Kanje, L. Martensson, L.B. Dahlin, Injury-induced activation of ERK 1/2 in the sciatic nerve of healthy and diabetic rats, Neuroreport 22 (2010) 73–77.
[37] K. Azuma, S. Ifuku, T. Osaki, Y. Okamoto, S. Minami, Preparation and biomedical applications of chitin and chitosan nanofibers, J. Biomed. Nanotechnol. 10 (2014) 2891–2920.
[38] M.B. Dreifke, A.A. Jayasuriya, A.C. Jayasuriya, Current wound healing procedures and potential care, Mater Sci. Eng. C Mater Biol. Appl. 48 (2015) 651–662.

[39] S. Gnavi, C. Barwig, T. Freier, K. Haastert-Talini, C. Grothe, S. Geuna, The use of Chitosan-based scaffolds to enhance regeneration in the nervous system, Int. Rev. Neurobiol. 109C (2013) 1–62.
[40] G. Penkert, W. Bini, M. Samii, Revascularization of nerve grafts: an experimental study, J. Reconstr. Microsurg 4 (1988) 319–325.
[41] K. Haastert, E. Lipokatic, M. Fischer, M. Timmer, C. Grothe, Differentially promoted peripheral nerve regeneration by grafted Schwann cells overexpressing different FGF-2 isoforms, Neurobiol. Dis. 21 (2006) 138–153.
[42] K. Haastert-Talini, J. Schaper-Rinkel, R. Schmitte, R. Bastian, M. Muhlenhoff, D. Schwarzer, et al., In vivo evaluation of polysialic acid as part of tissue-engineered nerve transplants, Tissue Eng. Part A 16 (2010) 3085–3098.